

University of Alberta

**A BIOPHYSICAL STUDY OF INTRANUCLEAR HERPES SIMPLEX
VIRUS TYPE 1 DNA DURING LYTIC INFECTION**

by

Jonathan Jacques Lacasse

A thesis submitted to the Faculty of Graduate Studies and Research
in partial fulfillment of the requirements for the degree of

Doctor of Philosophy

Department of Biochemistry

©Jonathan Jacques Lacasse

Fall 2010

Edmonton, Alberta

Permission is hereby granted to the University of Alberta Libraries to reproduce single copies of this thesis and to lend or sell such copies for private, scholarly or scientific research purposes only. Where the thesis is converted to, or otherwise made available in digital form, the University of Alberta will advise potential users of the thesis of these terms.

The author reserves all other publication and other rights in association with the copyright in the thesis and, except as herein before provided, neither the thesis nor any substantial portion thereof may be printed or otherwise reproduced in any material form whatsoever without the author's prior written permission.

Examining Committee

Luis Schang, Biochemistry and Medical Microbiology and Immunology

Michael Schultz, Biochemistry

Tom Hobman, Cell Biology

Michael Hendzel, Oncology

Thomas Kristie, Laboratory of Viral Diseases, NIAID

ABSTRACT

Herpes Simplex Virus Type 1 (HSV-1) establishes latent infections in neurons *in vivo* and lytic infections in epithelial cells and fibroblasts. During latent infections, HSV-1 transcription is restricted and the genomes are not replicated. Latent HSV-1 genomes are chromatinized, such that digestion with micrococcal nuclease (MCN) releases DNA fragments with sizes characteristic of nucleosomal DNA. During lytic infections, in contrast, all HSV-1 genes are expressed, the genomes are replicated, and their digestion produces primarily heterogeneously sized fragments. However, as evaluated by ChIP assays, HSV-1 DNA interacts with histones during lytic infections, although in most cases only a small percentage of HSV-1 DNA co-immunoprecipitates with histones (or is cleaved to nucleosome sizes following MCN digestion). Therefore, although current models propose that chromatin regulates HSV-1 transcription, it remains unclear how the association of histones with only a small percentage of HSV-1 DNA can globally regulate viral transcription. Moreover, the physical properties of the complexes containing histones and HSV-1 DNA are unknown. My objective was therefore to evaluate the biophysical properties of the HSV-1 DNA-containing complexes during lytic infection. Differing from previous studies, however, I used classical chromatin purification techniques. I show that most HSV-1 DNA is in unstable nucleoprotein complexes and, consequently, more accessible to MCN than DNA in cellular chromatin. This HSV-1 DNA is protected from MCN redigestion only after crosslinking, similar to unstable cellular nucleosomes. HSV-1 DNA is in such complexes throughout lytic infection. Using unrelated small-molecule

inhibitors, I further show that inhibition of HSV-1 transcription is associated with a decrease in MCN accessibility of HSV-1 DNA. Roscovitine, a cyclin-dependent kinase inhibitor, prevents activation but not elongation of IE, E, and L HSV-1 transcription. Consistent with a functional association between accessibility and transcription, roscovitine only decreases the accessibility of DNA templates of which it also inhibits transcription, independent of specific promoter sequences. In summary, I show that most HSV-1 DNA is in unstable nucleosome-like complexes during lytic infection and that accessibility to HSV-1 DNA likely plays a key role in regulating HSV-1 transcription.

TABLE OF CONTENTS

| | |
|---|-----|
| CHAPTER 1: INTRODUCTION..... | 1 |
| 1.1. Herpesviridae | 1 |
| 1.2. Herpes simplex virus type 1 (HSV-1)..... | 5 |
| 1.2.1. HSV-1 Envelope | 6 |
| 1.2.2. HSV-1 Tegument | 7 |
| 1.2.3. HSV-1 Capsid | 8 |
| 1.2.4. HSV-1 Genome..... | 9 |
| 1.3. HSV-1 lifecycle | 9 |
| 1.3.1. Entry..... | 9 |
| 1.3.2. Release of tegument proteins and delivery of genome to the nucleus | 10 |
| 1.3.3. Lytic HSV-1 infection..... | 11 |
| 1.3.4. Regulation of HSV-1 gene expression..... | 13 |
| 1.3.5. Activation of IE transcription | 13 |
| 1.3.6. HSV-1 IE, E, and L promoters..... | 16 |
| 1.3.7. RNA polymerase II (RNAPII) transcription..... | 17 |
| 1.3.8. Cyclin-dependent kinases (CDKs)..... | 22 |
| 1.3.9. Pharmacological cyclin-dependent kinase inhibitors (PCIs) | 28 |
| 1.4. Chromatin | 33 |
| 1.4.1. Histone octamer and the nucleosome core particle..... | 33 |
| 1.4.2. Micrococcal nuclease as a tool to study chromatin | 36 |
| 1.4.3. Linker histone (H1)..... | 39 |
| 1.4.4. Higher order chromatin folding | 42 |
| 1.4.5. Histone post-translational modifications (PTMs)..... | 45 |
| 1.4.6. Histone variants | 47 |
| 1.5. Viruses and chromatin | 49 |
| 1.5.1. Chromatinization of polyoma and papilloma viruses | 49 |
| 1.5.2. Chromatinization of adenovirus..... | 50 |
| 1.5.3. Chromatinization of herpesviruses | 50 |
| 1.6. Rationale and hypothesis | 63 |
| 1.7. References..... | 65 |
| CHAPTER 2: MATERIALS AND METHODS | 86 |
| CHAPTER 3: DURING LYTIC INFECTIONS, HERPES SIMPLEX VIRUS TYPE 1 DNA IS IN COMPLEXES WITH THE PROPERTIES OF UNSTABLE NUCLEOSOMES | 108 |
| 3.1. Introduction..... | 108 |
| 3.2. Results..... | 109 |
| 3.2.1. <i>At 5h after infection, HSV-1 DNA is in complexes that do not fractionate as protein-free DNA.</i> | 109 |

| | |
|--|-----|
| 3.2.2. MCN digestion releases HSV-1 DNA in complexes that fractionate as cellular nucleosomes..... | 111 |
| 3.2.3. Nuclear HSV-1 DNA is more accessible to MCN than DNA in most cellular chromatin..... | 113 |
| 3.2.4. HSV-1 DNA released as soluble chromatin is mostly in complexes that fractionate as mono- to di- nucleosomes. | 115 |
| 3.2.5. Complexes containing HSV-1 or cellular DNA resolve to different fractions at low salt concentrations..... | 117 |
| 3.2.6. Nuclear HSV-1 DNA is in unstable nucleoprotein complexes..... | 119 |
| 3.2.7. HSV-1 nucleosome-like complexes are stabilized by crosslinking. .. | 121 |
| 3.3. References..... | 124 |

CHAPTER 4: THE ACCESSIBILITY OF LYTIC HSV-1 GENOMES
DEPENDS ON THE TRANSCRIPTIONAL ACTIVATION STATE 141

| | |
|--|-----|
| 4.1. Introduction..... | 141 |
| 4.2 Results..... | 142 |
| 4.2.1. The accessibility of HSV-1 DNA changes throughout the lytic infection cycle | 142 |
| 4.2.2. HSV-1 IE and L DNA is in nucleosome-like complexes throughout the lytic infection cycle | 145 |
| 4.2.3. Inhibition of HSV-1 replication at different stages changes the accessibility of HSV-1 DNA to MCN digestion..... | 148 |
| 4.2.4. HSV-1 DNA is in nucleosome-like complexes when the HSV-1 replication cycle is inhibited at different stages | 150 |
| 4.3 References..... | 154 |

CHAPTER 5: ROSCOVITINE INHIBITS ACTIVATION OF PROMOTERS IN
HERPES SIMPLEX VIRUS TYPE 1 GENOMES INDEPENDENTLY OF
PROMOTER-SPECIFIC FACTORS 167

| | |
|---|-----|
| 5.1. Introduction..... | 167 |
| 5.2. Results..... | 168 |
| 5.2.1. Rosco prevents initiation, but does not inhibit ongoing, HSV-1 transcription..... | 168 |
| 5.2.2. Rosco prevents initiation of HSV-1, but not cellular, transcription . | 171 |
| 5.2.3. Cellular transcription in the presence of Rosco is performed by RNA Pol II | 172 |
| 5.2.5. Inhibition of transcription by Rosco depends on genome but not on promoter specific factors. | 176 |
| 5.2.6. The effects of Rosco on MCN accessibility have the same genome and promoter dependence as its effects on transcription | 178 |
| 5.2.7. The effects of Rosco on accessibility are specific for the HSV-1 genome | 181 |
| 5.3 References..... | 184 |

| | |
|--|-----|
| CHAPTER 6: PURINE AND NONPURINE PHARMACOLOGICAL CYCLIN-DEPENDENT KINASE INHIBITORS PREVENT INITIATION OF HSV-1 TRANSCRIPTION | 197 |
| 6.1 Introduction..... | 197 |
| 6.2. Results..... | 198 |
| 6.2.1. <i>Less specific PCIs inhibit transcription directed by the ICP0 promoter in either HSV-1 or cellular genomes.</i> | 198 |
| 6.2.2. <i>Unrelated PCIs inhibit initiation of HSV-1 transcription</i> | 199 |
| 6.3. References..... | 202 |
| CHAPTER 7: DISCUSSION..... | 205 |
| References..... | 226 |
| APPENDICES | 233 |
| Appendix 1. Specificity profile of selected oligo- or pan-specific PCIs. | 233 |
| References..... | 246 |

LIST OF TABLES

| | |
|--|-----|
| Table 3.1. HSV-1 DNA in nuclei of lytically infected cells does not fractionate as protein-free DNA | 126 |
| Table 3.2. Nuclear HSV-1 DNA is more accessible to MCN than DNA in most cellular chromatin | 127 |
| Table 3.3. HSV-1 DNA is quantitatively recovered as poly-nucleosomes after the modified MCN digestion | 128 |
| Table 3.4. Unstable HSV-1 nucleosomes are partially stabilized by crosslinking..... | 129 |
| Table 4.1. The accessibility of HSV-1 DNA changes during lytic infection. | 155 |
| Table 4.2. Inhibition of HSV-1 transcription changes the accessibility of HSV-1 IE or L DNA to MCN digestion | 156 |
| Table 4.3. HSV-1 IE and L DNA is in nucleosome-like complexes throughout the lytic infection cycle | 157 |
| Table 4.4. HSV-1 DNA fractionates as nucleosome-like complexes when HSV-1 replication is inhibited | 158 |
| Table 5.5. Rosco specifically inhibits the accessibility of HSV-1 loci in the viral genome, but HSV-1 loci recombined into the cellular genome | 186 |

LIST OF FIGURES

| | |
|--|-----|
| Figure 3.1. HSV-1 DNA in nuclei of lytically infected cells does not fractionate as protein-free DNA | 130 |
| Figure 3.2. MCN digestion releases HSV-1 DNA in complexes that fractionate as cellular mono- to di- nucleosomes | 131 |
| Figure 3.3. Nuclear HSV-1 DNA is more accessible to MCN than DNA in most cellular chromatin | 132 |
| Figure 3.4. Most HSV-1 DNA released by MCN as soluble chromatin is in complexes that fractionate as mono- to di- nucleosomes | 134 |
| Figure 3.5. HSV-1 or cellular DNA-containing complexes resolve to different fractions at low salt concentrations | 135 |
| Figure 3.6. Potential types of HSV-1 nucleoprotein complexes | 136 |
| Figure 3.7. Modified MCN digestion protocol | 137 |
| Figure 3.8. HSV-1 DNA fractionates as poly-nucleosomes after the modified MCN digestion | 138 |
| Figure 3.9. Unstable HSV-1 nucleosome-like complexes are partially stabilized by crosslinking | 139 |
| Figure 4.1. The accessibility of HSV-1 DNA changes during lytic infection... | 159 |
| Figure 4.2. HSV-1 IE and L DNA is in nucleosome-like complexes throughout the lytic infection cycle | 161 |
| Figure 4.3. Inhibition of HSV-1 replication at different stages changes the accessibility of HSV-1 DNA to MCN digestion | 163 |

| | |
|---|-----|
| Figure 4.4. HSV-1 DNA is in nucleosome-like complexes when HSV-1 replication is inhibited at different stages | 165 |
| Figure 5.1. Rosco prevents initiation, but does not inhibit ongoing, HSV-1 transcription | 187 |
| Figure 5.2. Rosco prevents initiation of HSV-1, but not cellular, transcription..... | 188 |
| Figure 5.3. Cellular transcription in the presence of Rosco is performed by RNA Pol II | 189 |
| Figure 5.4. Characterization of Vero clones stably transfected with ICP0-driven RFP (pICP0-RFP) | 190 |
| Figure 5.5. Inhibition of transcription by Rosco is specific for the HSV-1 genome..... | 191 |
| Figure 5.6. Inhibition of transcription by Rosco depends on genome but not promoter specific factors | 192 |
| Figure 5.7. The effects of Rosco on MCN accessibility correlate with its effects on transcription | 194 |
| Figure 5.8. The effects of Rosco on accessibility are specific for the HSV-1 genome | 195 |
| Figure 6.1. Less-specific PCIs, inhibit transcription directed by the ICP0 promoter in either the HSV-1 or cellular genomes | 203 |
| Figure 6.2. Unrelated PCIs inhibit initiation of HSV-1 transcription | 204 |
| Figure 7.1. Model for the role of chromatin in the regulation of HSV-1 gene expression during lytic infections | 231 |

LIST OF APPENDICES

| | |
|---|-----|
| Appendix 1. Specificity profile of selected oligo- or pan-specific PCIs | 233 |
|---|-----|

LIST OF ABBREVIATIONS

| | |
|---------------|--|
| 3-OS HS | 3-O-sulfated heparan sulfate |
| α -Ama | α -Amanitin |
| α -IFN | Interferon alpha |
| α -TIF | α -traninducing factor |
| ac | Acetyl |
| ActD | Actinomycin D |
| AD | Activation domain |
| ADP | Adenosine diphosphate |
| ATP | Adenosine triphosphate |
| BHV | Bovine herpesvirus |
| bp | Base pair |
| CAK | CDK activating kinase |
| CDK | Cyclin-dependent kinase |
| CEB | Chromatin extraction buffer |
| CENP | Centromere protein |
| ChIP | Chromatin immunoprecipitation |
| CHX | Cylcohexamide |
| CoA | Coenzyme A |
| CPE | Cytopathic effect |
| CSB | Cell swelling buffer |
| CTD | Carboxy-terminal domain |
| DAS | Downstream activating sequence |
| DMEM | Dulbecco's modified Minimum eagle's medium |
| DMSO | Dimethyl sulfoxide |
| DNA | Deoxyribonucleic acid |
| DNA-PK | DNA-dependent protein kinase |
| DNase | Deoxyribonuclease |
| dNTP | Deoxynucleotide triphosphate |
| DRB | 5,6-dichloro-1-beta-D-ribofuranosylbenzimidazole |
| dsDNA | Double stranded DNA |
| DSIF | DRB sensitivity-inducing factor |
| DTT | Dithiothreitol |
| E | Early |
| E2F | Elongation factor 2 |
| EBV | Epstein-Barr virus |
| EDTA | Ethylene diamine tetra-acetic acid |
| EGTA | Ethylene glycol tetra-acetic acid |

| | |
|---------|---|
| EHV | Equine herpesvirus |
| ER | Eppendorf rotor |
| FAR | Fixed angle rotor |
| Flavo | Flavopiridol |
| G | Gap |
| GABP | GA-binding protein |
| GaHV-1 | Gallid herpesvirus 1 |
| GFB | Gel filtration buffer |
| GST | Glutathione-S-transferase |
| GTF | General transcription factor |
| H | histone |
| HAT/KAT | Histone acetyltransferase |
| HCF-1 | Host cell factor 1 |
| HCMV | Human cytomegalovirus |
| HDAC | Histone deactylase |
| HFD | Histone fold domain |
| HFF | Human foreskin fibroblast |
| HHV | Human herpes virus |
| HIV | Human immunodeficiency virus |
| HP1 | Heterochromatin protein 1 |
| hpi | hours post-infection |
| HPV | Human papilloma virus |
| HSV-1 | Herpes simplex virus type 1 |
| HSV-2 | Herpes simplex virus type 2 |
| HTLV | Human T-lymphotropic virus |
| HVEM | Herpes virus entry mediator |
| IC | Inhibitory concentration |
| ICP | Infected cell protein |
| IE | Immediate early |
| INR | Initiator element |
| IR | Internal repeat |
| ISH | <i>In situ</i> hybridization |
| K | Lysine |
| KDM | Lysine demethylase |
| KMT | Lysine methyltransferase |
| KSHV | Kaposi's sarcoma associated herpesvirus |
| L | Late |
| LAT | Latency associated transcript |
| M | Mitosis |
| MCMV | Murine cytomegalovirus |
| MCN | Micrococcal nuclease |

| | |
|-------------|--|
| MDV | Marek's disease virus |
| me | Methyl |
| Me3psoralen | 4, 5', 8-trimethylpsoralen |
| MEF | Mouse embryonic fibroblast |
| MHV68 | Murine gammaherpesvirus 68 |
| MLL | Mixed lineage leukemia |
| MOI | Multiplicity of infection |
| mRNA | messenger RNA |
| MRP1 | Multidrug resistance protein 1 |
| MTA | 5'-deoxy-5'-methylthioadenosine |
| NaCl | Sodium chloride |
| ND10 | Nuclear dot 10 |
| NELF | Negative elongation factor |
| NLS | Nuclear localization signal |
| Oct-1 | Octamer binding protein 1 |
| ORF | Open reading frame |
| PAA | Phosphonoacetic acid |
| PBS | Phosphate buffered saline |
| PCI | Pharmacological CDK inhibitor |
| PCR | Polymerase chain reaction |
| PEG | Polyethylene glycol |
| PFU | Plaque forming unit |
| PIC | Pre-initiation complex |
| PKB | Proteinase K buffer |
| PML | Promyelocytic leukemia |
| pRb | Retinoblastoma protein |
| PRV | Pseudorabies virus |
| P-TEFb | Positive transcription elongation factor b |
| Purv | Purvalanol |
| R | Arginine |
| RCC1 | Regulator of chromatin condensation 1 |
| RCMV | Rat cytomegalovirus |
| RFP | Red fluorescent protein |
| RNA | Ribonucleic acid |
| RNAPII | RNA polymerase II |
| RNase | Ribonuclease |
| Rosco | Roscovitine |
| RRV | Rhesus monkey rhadinovirus |
| RT-PCR | Reverse transcriptase PCR |
| S | Synthesis |
| SaHV-2 | Herpesvirus saimiri |

| | |
|-----------|---|
| SBR | Swinging bucket rotor |
| SDS-PAGE | Sodium dodecyl sulphate polyacrylamide gel eletrophoresis |
| SEC | Size exclusion chromatography |
| SELEX | Systematic evolution of ligands by exponential enrichment |
| SFM | Serum free medium |
| siRNA | Small interfering RNA |
| Sp | Promoter specific protein |
| ssDNA | Single-standed DNA |
| SV-40 | Simiam virus 40 |
| TAF | TBP-associated factor |
| TAR | Transactivation response element |
| Tat | Transactivator of transcription |
| TBP | TATA binding protein |
| TCA | Trichloroacetic acid |
| TFII | Transcription factor II |
| TG | Trigeminal ganglia |
| TK | Thymidine kinase |
| TR | Terminal repeat |
| <i>ts</i> | Temperature sensitive |
| U | units |
| UL | Unique long |
| US | Unique short |
| vhs | Virion host shutoff |
| VP | Virion protein |
| VZV | Varicella-zoster virus |

CHAPTER 1: INTRODUCTION

1.1. Herpesviridae

Herpesviridae is a large virus family that includes more than 200 members infecting a broad range of hosts, from bivalves to humans. Herpesviruses are classified based on morphological, genomic, and biological criteria.

Virion morphology is the primary criteria for inclusion in the *Herpesviridae* family. A typical spherical herpesvirus virion is approximately 200nm in diameter, and composed of four components, the core, capsid, tegument, and envelope.

The core contains a single copy of the linear double stranded DNA genome packaged at high density within the capsid. The genomes range from 124,000 to 241,000 base pairs and encode anywhere from 70 to 165 genes, depending on the species. The G+C content is also largely variable, ranging from 31% to 77% (Honest 1984). Based on the sequence arrangements of their genomes, herpesvirus genomes are classified into six classes (A through F). Class A genomes, exemplified by human herpesvirus 6 (HHV-6), contain one large unique sequence with a direct repeat at both ends. Class B genomes, exemplified by herpesvirus saimiri (SaHV-2), contain one large unique sequence flanked by multiple direct repeats at the ends. Class C genomes, exemplified by Epstein-Barr virus (EBV), contain multiple terminal repeats (similar to Class B), and unrelated internal repeats subdividing the unique sequences. Class D genomes, exemplified by varicella-zoster virus (VZV), contain two unique sequences of which only the shorter one is flanked by inverted repeats. Class E genomes, exemplified by

herpes simplex virus type 1 (HSV-1), are discussed in detail in section 1.2.4.

Class F genomes, like tupaia herpesvirus, are composed of a single unique sequence without repeated regions.

The capsid is an icosahedron composed of 162 capsomeres (150 hexon and 12 pentons) with a triangulation number $T=16$.

Surrounding the capsid is an amorphous proteinaceous layer called the tegument. Proteomic analysis has identified from 9 to 30 viral proteins in the teguments of HSV-1 and herpes simplex virus type 2 (HSV-2), human cytomegalovirus (HCMV), murine cytomegalovirus (MCMV), EBV, Kaposi's sarcoma associated herpesvirus (KSHV), rhesus monkey rhadinovirus (RRV), and murine gammaherpesvirus 68 (MHV68) (Gibson and Roizman 1971; Cohen, Ponce de Leon et al. 1980; Pignatti and Cassai 1980; Hall, Aghili et al. 1982; Baldick and Shenk 1996; Bortz, Whitelegge et al. 2003; Johannsen, Luftig et al. 2004; Kattenhorn, Mills et al. 2004; Varnum, Streblow et al. 2004; Bechtel, Winant et al. 2005; Zhu, Chong et al. 2005; O'Connor and Kedes 2006; Loret, Guay et al. 2008; Oh and Fraser 2008). The tegument makes up approximately 40% of the herpesvirus virion protein mass (Gibson 1996).

The tegument is enveloped by a lipid bilayer derived from the host membranes, which contains cellular and viral glycoproteins. Herpesviruses encode a set of 20 to 80 glycoproteins. Five glycoproteins (gB, gH, gL, gM, and gN) are conserved among all family members. HSV-1 encodes at least 20 glycoproteins, of which 11 are found in virions. HCMV potentially encodes more than 75 membrane-associated proteins, of which at least 15 are found in the

virion. Although the exact arrangement of surface glycoproteins in the envelope is not known, it appears to be non-random. For example, glycoproteins gH and gL are arranged in a complex on the surface on the virion. Together with gD and gB, they facilitate membrane fusion and viral entry (Campadelli-Fiume, Amasio et al. 2007; Subramanian and Geraghty 2007; Heldwein and Krumpfenner 2008).

All herpesviruses share several biological properties. They encode a large array of enzymes involved in nucleic acid metabolism, DNA synthesis, and processing of proteins. The DNA replication and encapsidation stages of the viral life cycle occur in the nuclei of infected cells, whereas the final processing of the virion takes place in the cytoplasm. Productive infection results in the destruction of the host cell. All herpesviruses also establish life-long latent infections within their hosts. These latent genomes retain the capacity to replicate and cause disease upon reactivation.

Based on host range, growth characteristics, and tissue tropism, herpesviruses are further classified into three sub-families, *Alphaherpesvirinae*, *Betaherpesvirinae*, and *Gammavirinae*.

Alphaherpesviruses infect a wide range of hosts and are characterized by a relatively short reproduction cycle resulting in rapid spread in cultured cells and efficient destruction of infected cells. *In vivo*, they establish latent infections primarily in sensory ganglia. The alphaherpesvirus subfamily is further subdivided into three major genera, the Mardiviruses, the Varicelloviruses, and the Simplexviruses. There is also a fourth alphaherpesvirus genus, the Iltoviruses,

which currently has only one member, Gallid herpesvirus 1 (GaHV-1).

Mardiviruses infect chickens and turkeys and include the chicken pathogen Marek's disease virus (MDV). Varicelloviruses infect large animals, including humans, and include pseudorabies virus (PRV), equine herpesvirus types 1, 2, 3, and 4 (EHV-1, EHV-2, EHV-3, and EHV-4), bovine herpesvirus types 1, 2, and 5 (BHV-1, BHV-2, and BHV-5) and VZV. Finally, Simplexviruses infect humans and non-human primates and include the important human pathogens HSV-1 and HSV-2.

HSV-1 and HSV-2 predominantly cause oral and genital herpetic lesions, respectively. HSV-1 can also infect the skin, resulting in herpetic whitlow or more seriously eczema herpeticorum. HSV-1 infections of the eye can result in herpetic stromal keratitis, the leading cause of infectious corneal blindness. HSV-1 replication in the brain causes encephalitis, a life-threatening disease of high mortality, which also commonly causes permanent neurological damage in survivors. VZV is the causative agent of chickenpox (varicella) and shingles (zoster) (Fields 2007).

Betaherpesviruses are characterized by a very restricted host range and a longer reproductive cycle than α -herpesviruses. *In vivo*, they establish latent infections in progenitor cells of the bone marrow, monocytes, secretory glands, and kidneys. The betaherpesvirus subfamily is further divided into three major genera, the Cytomegaloviruses, the Muromegaloviruses, and the Roseolaviruses. Cytomegaloviruses infect humans and non-human primates and include the important human pathogen, HCMV. The Muromegaloviruses contains two

members, mouse and rat cytomegaloviruses (MCMV and RCMV, respectively). The Roseoloviruses also contains only two members, human herpesviruses 6 and 7 (HHV-6 and HHV-7, respectively) (Fields 2007).

Finally, gammaherpesviruses infect both small and large mammals including humans. They establish latency in lymphocytes. Unlike other human herpesviruses, the human γ -herpesviruses, EBV and Kaposi's sarcoma associated herpesvirus (KSHV), establish latency *in vitro* and therefore provide an important experimental system that is unavailable for other herpesviruses. These viruses also have the propensity to cause lymphoproliferative diseases. The gammaherpesvirus subfamily is further divided into two genera, the Lymphocryptoviruses and the Rhadinoviruses. Lymphocryptoviruses infect humans and non-human primates and includes the important human pathogen, EBV. Rhadinoviruses infect large animals, including humans, and include MHV-68, herpesvirus saimiri (HVS), and the important human pathogen KSHV (Fields 2007).

1.2. Herpes simplex virus type 1 (HSV-1)

HSV-1 is the archetype α -herpesvirus. HSV-1 has served as an excellent model and tool to study host-pathogen interactions as well as general eukaryotic processes. HSV-1 has been instrumental in our understanding of gene regulation, synaptic connections in the nervous system, membrane structure, translocation of proteins, cancer therapy and gene therapy, among others.

1.2.1. HSV-1 Envelope

HSV-1 virions are on average 186nm in diameter, extending to 225nm with the glycoprotein spikes, as evaluated by cryo-electron tomography (Grunewald et al 2003). Twelve HSV-1 envelope glycoproteins have been identified gB, gC, gD, gE, gG, gH, gI, gK, gJ, gL, gM, and gN. The soluble glycoprotein gL associates with the virion through interactions with gH. All other HSV-1 glycoproteins are anchored to the lipid membrane and protrude as spikes on the surface of the envelope. They mediate viral attachment and entry.

The lipid envelope is derived from the host cell membrane. However, the precise cellular compartment from which the envelope derives is still controversial. The two alternative models are the single envelopment pathway and the double envelopment pathway (also called the de-envelopment-re-envelopment pathway). The single envelopment pathway involves the budding of capsids into the perinuclear space and the maintenance of that same lipid bilayer right through to exocytosis into the extracellular space. In this pathway, the virions acquire the full complement of tegument proteins and envelope glycoproteins at the inner nuclear membrane. The double envelopment or de-envelopment re-envelopment pathway involves the budding into, and fusion out of, the nuclear membrane, resulting in the release of the nucleocapsid into the cytoplasm. The nucleocapsid then acquires the tegument in the cytoplasm before budding into the *trans*-Golgi network or an endosomal compartment to acquire the lipid envelope. Both pathways involve the fusion of a vesicle with the plasma membrane releasing the virion. Although both models have supporting evidence,

in recent years the double envelopment pathway has been favored based on better supporting evidence. These include numerous genetic, biochemical, and cell biology experiments as well as microscopy data (reviewed in Campadelli-Fiume 2007)

1.2.2. HSV-1 Tegument

The tegument of HSV-1 contains more than 20 virus encoded proteins. In addition to their structural roles, tegument proteins are involved in altering the host cell environment, likely to promote HSV-1 infection. For example, the tegument proteins VP16 (also known as α -trans inducing factor; α -TIF or Vmw65), virion host shutoff (vhs) protein, and VP22 are involved in the regulation of HSV-1 gene expression. Vhs and the IE protein ICP27 coordinate the host cell shutoff characteristically observed in during HSV-1 infection.

ICP27 suppresses host mRNA synthesis through repression of transcription (Spencer, Dahmus et al. 1997) and pre-mRNA splicing (Hardy and Sandri-Goldin 1994). Vhs, on the other hand, contributes to host shut off through mRNA degradation (Fenwick and McMenamin 1984; Schek and Bachenheimer 1985; Strom and Frenkel 1987). Vhs cleaves cellular mRNA upon its entry into the cytoplasm. Vhs shares amino acid sequence homology with a large family of human, yeast, bacterial and phage nucleases. Mutation of the highly conserved residues essential for the catalytic activity of cellular nucleases abolishes the activity of *vhs* (Everly and Read 1999; Everly, Feng et al. 2002). Many efforts over the years have investigated whether *vhs* is a *bona fide* RNase (Jones, Smibert

et al. 1995; Zelus, Stewart et al. 1996; Elgadi, Hayes et al. 1999). *Vhs*, expressed as GST-fusion protein exhibits endoribonuclease activity in the absence of other viral or cellular proteins (Taddeo, Zhang et al. 2006). At later times, *vhs* also plays a role in regulating the transition from IE to E and L gene expression through degradation of IE mRNAs (Read and Frenkel 1983).

VP16 is present in ~1000 copies per virion and functions to activate IE gene expression (see section 1.3.5). VP22 is one of the most abundant tegument proteins, at 2000 copies per virion. VP22 interacts with VP16 (Elliott, Mouzakitidis et al. 1995) and has been implicated in the reorganization of microtubules in infected and uninfected cells (Elliott and O'Hare 1998; Kotsakis, Pomeranz et al. 2001). In addition, VP22 has also been shown to inhibit template activating factor 1 (TAF-1)-dependent deposition of histones on DNA templates (van Leeuwen, Okuwaki et al. 2003).

1.2.3. HSV-1 Capsid

The icosahedral HSV-1 capsid is composed of 162 capsomeres. The major capsid component is the major capsid protein VP5 (U_L19). VP5 is present in 960 copies per capsid, 6 copies per hexon and 5 copies per penton. The capsomeres are joined by the triplexes composed of one copy of the triplex monomer VP19C (U_L38) and two copies of the triplex dimer VP23 (U_L18).

Encapsidated HSV-1 DNA appears to be packaged in a liquid crystalline state, closely resembling that in bacteriophage T4 and Lambda (Booy, Newcomb et al. 1991; Zhou, Chen et al. 1999). HSV-1 capsids contain the polyamine

spermine, which at physiological pH is a polycation that neutralizes approximately 40% of the HSV-1 DNA phosphate backbone (Gibson and Roizman 1971).

1.2.4. HSV-1 Genome

Depending on the strain, the HSV-1 genome is approximately 152 kbp long with a G+C content of 68%. It encodes more than 80 proteins. The HSV-1 genome belongs to the class E family of genomes, a class that was actually defined by HSV-1. This is the most complex of all herpesvirus genomes, consisting of two covalently joined segments, L (long) and S (short). Each segment contains a unique region, U_L (108kbp) and U_S (13kbp). These segments are flanked by terminal (TR) and internal (IR) repeats TR_L and IR_L (~9.2kbp each) and TR_S and IR_S (~ 6.6kbp each).

1.3. HSV-1 lifecycle

1.3.1. Entry

HSV-1 enters cells by fusing with the plasma membrane. The first step involves reversible attachment of the virion to cell surface through weak affinity binding of glycoproteins C and B (gC, gB) to glycosaminoglycans. These interactions serve to bring gD within close proximity to one of its three identified cell surface receptors, nectins, herpes virus entry mediator (HVEM), or 3-O-sulfated heparan sulfate (3-OS HS). Following receptor binding, gD undergoes a conformational change and together with gB, gH, and gL enables fusion of the envelope with the

plasma membrane (Subramanian and Geraghty 2007). Both gH and gB are candidate fusion proteins. Molecular and biochemical analysis support gH being a class 1 fusion glycoprotein, although the structure of gH has yet to be solved. On the other hand, the crystal structure of gB has been solved and revealed similarities to the vesicular stomatitis G protein (Heldwein, Lou et al. 2006; Roche, Bressanelli et al. 2006). Therefore, both gB and gH/gL may execute HSV-1 membrane fusion (Campadelli-Fiume, Amasio et al. 2007; Heldwein and Krummenacher 2008; Gianni, Amasio et al. 2009).

1.3.2. Release of tegument proteins and delivery of genome to the nucleus

Following fusion with the cell membrane, the capsid and tegument proteins are released into the cytoplasm. The capsid is then transported to the nuclear membrane along the host cell microtubular network (Sodeik, Ebersold et al. 1997). The capsid docks at the nuclear pore and the viral genome is delivered into the nucleus (Miyamoto and Morgan 1971; Knipe, Batterson et al. 1981; Batterson, Furlong et al. 1983).

Inside the nucleus, the viral genome is rapidly circularized (Poffenberger and Roizman 1985; Garber, Beverley et al. 1993; Strang and Stow 2005).

Circularization has been proposed to occur by direct ligation of the termini (Davison and Wilkie 1981; Mocarski and Roizman 1982; Strang and Stow 2005), homologous recombination (Yao, Matecic et al. 1997; Yao and Elias 2001), and, more recently, by the activity of a cellular protein, regulator of chromatin condensation 1 (RCC1) (Umene and Nishimoto 1996; Strang and Stow 2007).

Following circularization, the HSV-1 genomes are deposited next to PML bodies (Ishov and Maul 1996; Maul, Ishov et al. 1996; Everett and Murray 2005).

Concomitant with the transport of the capsid to the nucleus, the tegument proteins are released into the cytoplasm and begin to alter the cell environment to promote viral infection, as discussed in section 1.2.2.

1.3.3. Lytic HSV-1 infection

Lytic HSV-1 infection (also called acute or productive infection) is characterized by the expression of the more than 80 proteins encoded by the HSV-1 genome.

HSV-1 gene expression follows a highly regulated temporal cascade. HSV-1 genes are classified as immediate-early (IE), early (E), and late (L) based on the requirements for their expression (Hones and Roizman 1973; Hones and Roizman 1974).

The rate of progression of HSV-1 infection is highly variable and depends on factors such as cell type, virus strain, and multiplicity of infection (MOI). IE genes are the first to be transcribed. During infection of African green monkey kidney fibroblasts (Vero cells) with a wild type virus (KOS) at an MOI of 3, IE transcripts accumulate during the first 2 hours post infection. IE gene expression does not require previous protein synthesis. As such, IE transcripts accumulate in the presence of the translation inhibitor cycloheximide (CHX). HSV-1 encodes five IE genes, infected cell proteins (ICP) 0, 4, 22, 27, and 47. These proteins are involved in transcriptional regulation (ICP0, ICP4, ICP27, possibly ICP22), RNAPII modification (ICP22), or immune evasion (ICP47).

IE proteins are required for the subsequent expression of E genes, which occurs between 5 and 9hpi under the conditions specified above. E genes encode proteins required for viral DNA replication and nucleotide metabolism, such as the viral DNA polymerase, ssDNA binding protein (ICP8), thymidine kinase, and ribonucleotide reductase, as well as an alkaline nuclease, among others. Therefore, HSV-1 DNA replication starts after E genes are expressed. CHX indirectly inhibits E gene transcription because IE proteins are required for the activation of E gene expression.

L genes can be divided into two subclasses, “leaky-late” and “true” late, based on their requirement for HSV-1 DNA replication. Leaky-late genes are transcribed at low levels before HSV-1 DNA replication, and peak after the onset of DNA replication. In contrast, true late genes are not transcribed until after HSV-1 DNA replication has begun. The mechanisms that control the temporal regulation of L gene expression are still unclear. Cellular DNA-PK has been shown to activate transcription driven by promoter elements from true late genes (Petroski and Wagner 1998). Considering the requirement for HSV-1 DNA replication, it also appears that template amplification is at least one of the factors required for optimal expression of both leaky-late and true late genes. In the conditions described, L genes are typically transcribed around 6hpi, which correspond with the accumulation of replicated HSV-1 DNA. In general, L genes encode the structural proteins required for encapsidation, tegument formation, and envelopment of newly synthesized genomes. Transcription of most late genes requires HSV-1 DNA replication. Therefore, late gene expression is inhibited in

the presence of the HSV-1 DNA polymerase inhibitor phosphonoacetic acid (PAA).

1.3.4. Regulation of HSV-1 gene expression

Expression of HSV-1 genes is regulated primarily at the level of transcription. However RNA processing, translational, and post-transcriptional regulation also play major roles (Hones and Roizman 1974; Johnson and Spear 1984; Harris-Hamilton and Bachenheimer 1985; Godowski and Knipe 1986; Weinheimer and McKnight 1987).

1.3.5. Activation of IE transcription

The presence of one to several copies of the ATGCTAATGARATTCTTT enhancer sequence upstream of the transcription start site of the IE promoters is their major difference with E or L promoters (Mackem and Roizman 1982; Whitton, Rixon et al. 1983; Whitton and Clements 1984). This consensus sequence nucleates the assembly of the VP16/Oct-1/HCF-1 complex, which is responsible for activating IE gene transcription. IE promoters also contain binding sites for other cellular transcription factors, such as Sp1 and GA-binding protein. These transcription factors contribute the level of IE gene transcription (Jones and Tjian 1985; Triezenberg, LaMarco et al. 1988; LaMarco and McKnight 1989).

VP16, the virally encoded component of the complex, is a 490 amino acid (aa) protein. It contains two domains which mediate various protein-protein and

protein-DNA interactions, the structural core domain (aa 49-403) and the transcription activation domain (AD) (aa 412-490).

The structural core domain is responsible for mediating interactions with HCF-1, Oct-1, and DNA, as follows. VP16 associates with HCF-1 in the cytoplasm. The VP16/HCF-1 complex then translocates to the nucleus (La Boissiere, Hughes et al. 1999). Meanwhile, the cellular transcription factor Oct-1 recognizes its target sequence (ATGC T/A AAT) within the HSV-1 IE enhancers, through a bi-partite POU-homeo domain (Sturm and Herr 1988; Kristie and Sharp 1990). Bound to the ATGCTAAT sequence, Oct-1 adopts a slightly different conformation than when bound to its consensus octamer sequence (ATGCAAAT) in cellular promoters (Walker, Hayes et al. 1994). This change in conformation, in conjunction with the downstream GARAT sequence, enables the binding of the VP16/HCF-1 complex to Oct-1 (Stern, Tanaka et al. 1989; Kristie and Sharp 1990; Stern and Herr 1991).

HCF-1 is a cellular transcriptional coactivator, which interacts with members of numerous transcription factors and other transcription coactivators. HCF-1 is also a component of multiple chromatin modification complexes (recently reviewed in Kristie 2007; Kristie, Liang et al. 2010). HCF-1 was originally identified and purified as a protein required for the stable formation of the VP16/Oct-1/HCF-1 complex (Kristie and Sharp 1993). It has since been shown to be essential for IE gene expression in HSV-1 and VZV (Narayanan, Nogueira et al. 2005).

Among other functions, HCF-1 acts as an adapter between transcription factors and chromatin modifying complexes. The lysine methyltransferase (KMTs), Set1 and MLL, for example, are recruited in a HCF-dependent manner to IE promoters (Wysocka, Myers et al. 2003; Narayanan, Ruyechan et al. 2007), where they catalyze trimethylation of histone H3 lysine 4 (H3K4me3). Therefore, recruitment of HCF-1 along with Set1 and MLL results in the accumulation of active (H3K4me3) chromatin marks, and subsequent loss of repressive ones (H3K9me3; histone H3 trimethyl lysine 9) (Huang, Kent et al. 2006; Narayanan, Ruyechan et al. 2007). More recently, HCF-1-dependent recruitment of the lysine demethylase (KDM) LSD1 was shown to be required for efficient IE gene expression (Liang, Vogel et al. 2009). Together, these results suggest that the VP16/Oct-1/HCF complexes assembled on IE promoters recruit chromatin modifying proteins that remove repressive (eg. LSD1) and add activating (eg. Set1, MLL) chromatin marks, to promote activation of IE transcription.

In addition to the structural core domain that interacts with HCF-1, VP16 contains a highly studied transcriptional activation domain (AD). This acidic carboxy-terminal domain activates transcription through multiple interactions with basal transcription factors, such as TBP/TFIID (Stringer, Ingles et al. 1990; Ingles, Shales et al. 1991; Klemm, Goodrich et al. 1995; Nishikawa, Kokubo et al. 1997; Hall and Struhl 2002), TFIIA (Kobayashi, Boyer et al. 1995), TFIIB (Lin and Green 1991; Lin, Ha et al. 1991; Goodrich, Hoey et al. 1993; Hall and Struhl 2002), and TFIIH (Xiao, Pearson et al. 1994; Gold, Tassan et al. 1996; Herrmann, Gold et al. 1996). The VP16 AD also interacts with the mediator complex

(Mittler, Kremmer et al. 2001; Ikeda, Stuehler et al. 2002), histone acetyltransferases (for example CBP and p300), and other chromatin remodelers (for example Brg-1 and BRM) (Utley, Ikeda et al. 1998; Neely, Hassan et al. 1999; Vignali, Steger et al. 2000; Hall and Struhl 2002; Memedula and Belmont 2003; Herrera and Triezenberg 2004). VP16 promotes decondensation of a large (90Mbp) highly compacted heterochromatic chromosome arms, independent of transcriptional activation (Tumbar, Sudlow et al. 1999). VP16 most likely activates transcription through the coordinated recruitment of cellular RNAPII pre-initiation complexes and chromatin modifying proteins.

1.3.6. HSV-1 IE, E, and L promoters

IE, E, and L genes differ in their promoter-specific sequences and transcription factor requirements. IE promoters contain one or more TAATGARAT sequences along with binding sites for Sp1 and GABP (as discussed in section 1.3.4.1). E promoters are representative of a large class of cellular TATA-box containing promoters which contain, in addition to a TATA-box, upstream cellular transcription factor binding sites (such as Sp1 and CCAAT). L gene promoters are characterized by the presence of an initiator element (Inr) in addition to a functional TATA-box. Interestingly, leaky-late promoters partially resemble E promoters in that they generally contain upstream cellular transcription factor binding sites (such as Sp1 and CCAAT). In contrast, true late promoters lack upstream elements and instead contain a downstream activation sequence (DAS).

Transcription of HSV-1 IE, E, and L genes share the requirement for the cellular RNAPII transcription machinery.

1.3.7. RNA polymerase II (RNAPII) transcription

Transcription by RNAPII is regulated at the stages of pre-initiation, initiation, elongation and termination.

Pre-initiation involves the binding of promoter specific transcription factors to promoter-specific sequences of DNA, found directly upstream from the transcriptional start site. For HSV-1 IE genes, pre-initiation involves the binding of the VP16/Oct-1/HCF-1 complex to TAATGARAT sequences within IE promoters.

Once bound to the promoter, the promoter specific transcription factors either nucleate the stepwise assembly of pre-initiation complexes (PICs), or recruit pre-formed PIC holoenzymes to the transcriptional start site (reviewed by (Thomas and Chiang 2006). The end result of either process is the assembly of a transcription-competent complex composed of RNAPII, general transcription factors (GTFs), and an ever-growing number of proteins involved in transcriptional activation and repression, chromatin remodeling, DNA repair, and mRNA processing (Buratowski 2009).

The GTFs TFIIA, TFIIB, TFIID, TFIIE, TFIIIF, and TFIIH were originally identified as accessory factors required for accurate initiation of transcription driven by the adenovirus major late promoter *in vitro* (Sawadogo and Roeder

1985; Reinberg and Roeder 1987; Flores, Maldonado et al. 1989; Flores, Lu et al. 1992; Ge, Martinez et al. 1996).

Following the establishment of PICs at the promoter, the initiation and elongation stages of transcription are controlled primarily by sequential phosphorylation of the carboxy-terminal domain (CTD) of the large subunit of RNAPII, Rpb1 (described in section 13.4.2.1). Sequential modification of the elongating RNAPII complexes allows for dynamic association of protein complexes involved in co-transcriptional processes such as 5' capping (coupled to transcription initiation), splicing (coupled to transcription elongation), and 3' end formation (coupled to transcription termination) (reviewed in Hirose and Ohkuma 2007). Throughout the transcription cycle, CTD phosphatases are also recruited to the RNAPII complexes and are involved in the recycling of RNAPII complexes. They are also involved in preparing them for reinitiation. Therefore, RNAPII relies on reversible phosphorylation in order to regulate transcription.

1.3.7.1. Regulation of RNAPII transcription by phosphorylation

RNAPII is a large complex (~0.5 MDa) composed of 12-subunits, named Rpb1-Rpb12. The largest subunit, Rpb1, contains a carboxy-terminal domain (CTD) composed of multiple repeats of the heptapeptide: Tyr-Ser-Pro-Thr-Ser-Pro-Ser (YSPTSPS) (Allison, Moyle et al. 1985; Corden, Cadena et al. 1985).

Interestingly, the number of CTD heptapeptide repeats increases with genome complexity, at least in yeast and animals, varying from 26, 32, 45, and 52 copies in yeast, nematodes, *Drosophila*, and mammals, respectively (Egloff and

Murphy 2008). This relationship is lost in plants, *Arabidopsis thaliana* and the soybean (*Glycine max*), which have 34-39 repeats (Dietrich, Prenger et al. 1990). The CTD serves as a scaffold for interactions with numerous RNAPII associated complexes.

Regulation of RNAPII transcription is achieved in part by the reversible phosphorylation of the CTD by a subset of cyclin dependent kinases (CDKs). CDKs phosphorylate serines 2 (Ser-2) and 5 (Ser-5) of the CTD, which in turn modulate the association of RNAPII with other proteins.

Only PICs containing a hypophosphorylated form of RNA polymerase II (RNAPII_a) bind to promoter DNA (Koleske and Young 1995; Ossipow, Tassan et al. 1995). Initiation of transcription coincides with the phosphorylation of serine 5 (Ser-5) of the CTD by the cyclin dependent kinase 7 (CDK7) subunit of transcription factor IIIH (TFIIH) (Lu, Zawel et al. 1992). This phosphorylation decreases the affinity of RNAPII for the GTFs bound to the promoter, therefore allowing RNAPII to be released from the promoter. This event is referred to as “promoter release” (Roy, Adamczewski et al. 1994; Akoulitchev, Makela et al. 1995; Serizawa, Makela et al. 1995; Shiekhattar, Mermelstein et al. 1995).

RNAPII often stalls shortly after transcription initiates, mainly through the inhibitory actions of 5,6-dichloro-1-beta-D-ribofuranosylbenzimidazole (DRB) sensitivity-inducing factor (DSIF) and negative elongation factor (NELF) (Wada, Takagi et al. 1998; Yamaguchi, Takagi et al. 1999). The DSIF/NELF complex is also responsible for recruiting the proteins involved in catalyzing the addition of the m⁷GpppN cap structure to the 5' end of the nascent mRNA (Mandal, Chu et

al. 2004). Promoter proximal pausing has therefore been proposed as a mechanism to allow enough time for proper capping of nascent mRNAs.

Transcription pausing is then relieved by the recruitment of positive transcriptional elongation factor b (p-TEFb), and subsequent phosphorylation of Ser-2 of the CTD by the CDK9 subunit of p-TEFb. CDK9 activity results in the hyperphosphorylation of RNAPII (RNAPII_o) (Wada, Takagi et al. 1998).

P-TEFb is probably best characterized in its requirement for overcoming the stalling caused by the transactivation response element (TAR) RNA encoded by human immunodeficiency virus (HIV) (Marshall and Price 1995; Yang, Herrmann et al. 1996; Yang, Gold et al. 1997; Gold, Yang et al. 1998; Peng, Zhu et al. 1998; Zhou, Halanski et al. 2000; Kim and Sharp 2001).

CDK2 has also been suggested to be involved in overcoming RNAPII stalling (Deng, Ammosova et al. 2002; Nekhai, Zhou et al. 2002; Ammosova, Berro et al. 2006).

In addition to CDK 2, 7, and 9, CDK 8 is also involved in the regulation of cellular transcription. CDK8 associates with the mediator complex (Rickert, Seghezzi et al. 1996; Hengartner, Myer et al. 1998). Like CDK7, CKD8 phosphorylates Ser-5 of the CTD. However, CDK8 does so prior to the assembly of the PIC and thus appears to prevent transcription (Hengartner, Myer et al. 1998)

1.3.7.2. HSV-1 modulation of cellular RNAPII

In uninfected cells, the large subunit of RNAPII exist is in two phosphorylation states, hypo- (II_a) and hyper- (II_o) phosphorylated. The II_a and II_o forms can be distinguished either by antibodies that specifically recognize the different phosphorylation state of the CTD, or by SDS-PAGE in which they resolve at 200 and 240 kDa, respectively. Although intermediately migrating forms can be generated *in vitro*, these forms appear to contribute little, if any, to the RNA polymerase II detected *in vivo*.

During HSV-1 infection, however, the II_a and II_o forms are depleted. In their place, a novel phosphorylated form of RNAPII, II_i is present (Rice, Long et al. 1994; Rice, Long et al. 1995). This form migrates between 215 and 230kDa. It is first detected by 3hpi and becomes the predominant form at 5hpi. RNAPII_i is not cell-type dependent or species specific. It is observed in both monkey (Vero) and human (HeLa) cells. It was proposed that the novel phosphorylated form RNAPII_i preferentially transcribes the viral genome over the cellular genome (Rice, Long et al. 1994).

RNAPII_i was shown to be dependent on the IE protein ICP22 and the viral protein kinase U_L13 (Long, Leong et al. 1999). However, HSV-1 mutants in which the ICP22 or U_L13 genes have been deleted show restricted growth in only certain cell lines (Rice, Long et al. 1995; Long, Leong et al. 1999). For example, ICP22 and U_L13 mutant viruses show cell type dependent growth restrictions such that they are able to grow relatively efficiently on Vero, but not on BHK or HEL

cells (Rice, Long et al. 1995; Long, Leong et al. 1999). These defects are the result of delayed expression of E proteins and decreased level of L proteins, but not of mislocalization of RNAPII to viral replication compartments (Rice, Long et al. 1994; Spencer, Dahmus et al. 1997; Long, Leong et al. 1999). Therefore, RNAPII_i is not absolutely required for HSV-1 transcription or its proper localization to HSV-1 replication sites.

1.3.8. Cyclin-dependent kinases (CDKs)

The most critical phosphorylations of RNAPII are performed by CDKs. CDKs are a family of highly conserved serine/threonine protein kinases involved in the regulation of the cell cycle (CDK1, CDK2, CDK3, CDK4, CDK6, CDK7), transcription (CDK7, CDK8, CDK9), or neuronal functions (CDK5). CDKs are heterodimeric complexes composed of a catalytic subunit, the CDK, and a regulatory subunit, the cyclin. CDKs are inactive in the absence of their cyclin partners.

The cyclin partners of the CDKs involved in transcription, CDK7, 8, and 9, are constitutively expressed. In the context of transcription, CDKs are therefore mostly regulated through their association with different multi-protein complexes involved in the different stages of transcription (described in section 1.3.4.2.1).

In contrast, the CDKs involved in cell cycle progression are tightly regulated by the transient expression of their cyclin subunits, phosphorylation (by the CDK7-containing CDK activation kinase (CAK), interaction with protein

inhibitors (Cip and INK4 family members), and subcellular localization. CDKs involved in cell cycle regulation can be further classified as interphase (CDK2, 3, 4, and 6) or mitotic (CDK1) CDKs.

Interphase CDKs are responsible for driving the cells through G1, S, and G2 phases of the cell cycle. During early G1, CDK4 and CDK6 form complexes with the D-type cyclins (D1, D2, and D3) and execute critical regulatory events for G1. CDK2/cyclin E complexes promote S-phase entry by triggering the G1/S transition. CDK2/cyclin A complexes further promote S-phase progression. Following DNA replication, the mitotic CDK, CDK1 is activated by cyclins A and B to promote progress through the G2/M transition. Finally, exit from mitosis occurs following the degradation of cyclin B and subsequent inactivation of CDK1. CDK3 has been proposed to promote exit from G0 back into the cell cycle through its association with cyclin C, which is expressed to high levels during G0 (Ren and Rollins 2004).

The classic model of cell cycle regulation has recently been challenged by genetic evidence. Mice lacking CDK2 (Berthet, Aleem et al. 2003; Ortega, Prieto et al. 2003), CDK3 (Ye, Zhu et al. 2001), CDK4 (Rane, Dubus et al. 1999; Tsutsui, Hesabi et al. 1999), or CDK6 (Malumbres, Sotillo et al. 2004) survive (recently reviewed in Santamaria and Ortega 2006). In fact, in mice, it appears that CDK1 is able to drive the cell cycle alone, in the absence of all interphase CDKs (CDK2, 3, 4, and 6) (Santamaria, Barriere et al. 2007). Santamaria *et al.* recently showed that mouse embryos lacking CDK2, 4, and 6 still undergo organogenesis and develop to midgestation (Santamaria, Barriere et al. 2007). In

contrast, CDK1^{-/-} embryos failed to develop beyond the two cell stage. CDK1 was likely able to compensate for the loss of the other CDKs through its ability to bind D and E type cyclins and phosphorylate pRb (Santamaria, Barriere et al. 2007). However, this functional redundancy is not simply a characteristic of all CDKs. Genetic substitution of CDK1 by CDK2 was not able to compensate for the loss of CDK1 (Satyanarayana, Berthet et al. 2008).

One of the best characterized functions of CDKs is the phosphorylation of retinoblastoma (pRb) tumor suppressor and the pRb-related pocket proteins p130 and 107 (reviewed in Sidle, Palaty et al. 1996). In their hypophosphorylated state, these proteins bind and repress the activity of different members of the E2F transcription factor family. Pocket protein-E2F complexes function as active repressor complexes. They occupy E2F binding sites on DNA and recruit chromatin modifying proteins such as HDACs (Brehm, Miska et al. 1998; Luo, Postigo et al. 1998; Magnaghi-Jaulin, Groisman et al. 1998). As the cells cycle progresses, pocket proteins are phosphorylated, first by CDK4/6 and then by CDK2, disrupting the repressor complex. This results in the release of E2F and subsequent activation of target genes, most of which are involved in regulating further progression through the cell cycle.

Much like the idea that individual CDKs are required at specific stages of the cell cycle, it was also thought that E2F function was indispensable for controlling cell proliferation. However, similar to the redundancy observed with CDKs, mice deficient for individual or combinations of E2F genes were not

generally defective in cell proliferation (recently reviewed in Chen, Tsai et al. 2009).

Regardless of their functional redundancy, CDKs, pocket proteins and E2F transcription factors are involved in regulating cell proliferation. Not surprisingly, many viruses that depend on host cell DNA replication proteins have evolved mechanisms to promote host cell proliferation. One such mechanism is the targeting and subsequent inactivation of pRb which results in E2F-directed transcriptional activation. In fact, E2F was originally discovered as a cellular factor that bound to the adenovirus E2 promoters (Kovesdi, Reichel et al. 1986; Yee, Reichel et al. 1987). It was later shown that the viral protein E1A sequesters pRb thus relieving E2F repression. This mechanism is also shared by the large T antigen of SV40 and E7 protein of human papilloma viruses (Whyte, Buchkovich et al. 1988; Dyson, Howley et al. 1989; Hu, Dyson et al. 1990). Consistent with the ability to promote cell proliferation, E1A, large T antigen, and E7 are all classified as oncoproteins. As a result, adeno-, polya-, and papilloma- viruses are all referred to as DNA tumor viruses.

1.3.8.1. Cell cycle regulation during HSV-1 infection

In contrast to the DNA tumor viruses, HSV-1 encodes its own DNA replication proteins and consequently wild type HSV-1 replicates equally well in cells in all stages of the cell cycle (Cohen, Vaughan et al. 1971). However, the role of cell cycle during HSV-1 infection has been largely contested. HSV-1 and HSV-2

have been shown to induce events that correlate with progression as well as inhibition of the cell cycle.

Early work showed that HSV-1 infection of cells in G₁ prevents progression into S-phase, in that the infected cells do not undergo high levels of DNA synthesis (de Bruyn Kops and Knipe 1988). However, cells infected after entry into S-phase completed DNA replication (de Bruyn Kops and Knipe 1988). Cellular factors present during the G₁/S stage of the cell cycle are able to compensate for mutations in HSV-1 transcriptional transactivators, ICP0 (Cai and Schaffer 1991) or VP16 (Daksis and Preston 1992) which display growth defects when infecting cells in G₀ or G₂, respectively.

Induction of an “S-phase-like” nuclear environment has been reported by two groups. Hilton *et al.*, reported an induction of the release of E2F and the formation of the S-phase form of the p107/E2F complex that contains cyclin A during HSV-1 infection (Hilton, Mounghane et al. 1995). Consistently, Hossain *et al.* showed that there is an increase in hyperphosphorylated pRb as well as CDK2 activation during HSV-2 infection (Hossain, Holt et al. 1997). Our lab has also observed that cyclin A levels remain constant for up to 7hpi (Provencher, VMI, MSc Thesis). Interestingly, although these events are characteristic of cell cycle progression, the infected cells do not activate CDK4/6 or CDK1 and do not progress through the cell cycle (Hossain, Holt et al. 1997). The inactivation of CDK4/6 likely results from the destabilization of D-type cyclins (Ehmann, McLean et al. 2000; Song, Liu et al. 2000; Everett 2004).

Conversely, pRb has also been reported to be hypophosphorylated during HSV-1 infection (Ehmann, McLean et al. 2000; Song, Liu et al. 2000). In any event, pRb likely does not play a significant role in the replication cycle of HSV-1. Normal levels of HSV-1 viral protein accumulation, viral DNA replication and progeny virus yield were reported in pRb^{-/-} mouse embryonic fibroblasts (Ehmann, Burnett et al. 2001).

CDK2 activity has been reported to be activated (Hossain, Holt et al. 1997), unaffected (Song, Liu et al. 2000), or downregulated (Ehmann, McLean et al. 2000; Ehmann, Burnett et al. 2001) during HSV-1 or HSV-2 infection. However, the group who reported the decrease in CDK2 activity showed that cyclin A expression was completely inhibited at 8hpi in the presence of serum. Curiously, mock infected cells also failed to express cyclin A after 8h in the presence of serum (Ehmann, McLean et al. 2000).

Therefore, in contrast to other DNA viruses which do not encode their own replication proteins and thereby must promote host cell proliferation, HSV-1 infection does not require host cell cycle progression. However, the induction of an S-phase-like nuclear environment strongly suggests the importance of cellular proteins induced during cell cycle progression, for HSV-1 replication. Perhaps the most convincing evidence for the importance of cellular proteins in HSV-1 replication is that collected using pharmacological CDK inhibitors (PCI). These studies have clearly shown the importance of CDKs during HSV-1 infection (discussed below in section 1.3.9.1).

1.3.9. Pharmacological cyclin-dependent kinase inhibitors (PCIs)

PCIs are a heterogeneous group of small molecules that share the ability to preferentially inhibit CDKs. Most PCIs are small (≤ 600 Da), flat, heterocycles that compete with ATP for the binding to the ATP-binding pocket of the target CDKs. PCIs form hydrogen bonds with the target CDKs, mostly with main-chain groups or with conserved residues in the ATP binding pocket. However, most of the specificity of PCIs is conferred by their fitting into secondary pockets in the ATP-binding domain of the target CDKs (De Azevedo, Leclerc et al. 1997). These pockets are not occupied by the ATP co-substrate and consequently are not so widely conserved among protein kinases.

Based on their specificities, PCIs can be classified as non-specific, pan-specific, oligo-specific, or mono-specific (Appendix 1 and reviewed in Schang, St Vincent et al. 2006). Non-specific PCIs, such as staurosporine, inhibit CDKs and a variety of unrelated protein kinases. Pan-specific PCIs, such as flavopiridol (Flavo) and 5,6-dichloro-1-beta-D-ribofuranosylbenzimidazole (DRB) inhibit most or all CDKs indiscriminately. Oligo-specific PCIs, such as roscovitine (Rosco) and purvalanol (Purv) have preference for only a subset of CDKs. These PCIs can be further classified accordingly to whether they preferentially inhibit CDKs involved in transcription (CDK7, CDK8, and CDK9) (described in section 1.3.7.1), or CDKs involved in the regulation of the cell-cycle (CDK1, CDK2, CDK4, CDK6, and CDK7) (described in section 1.3.8) (Schang, St Vincent et al. 2006). Finally, mono-specific PCIs, such as P1446A-05 and PD-0332991 are reported to specifically target CDK4/6 cyclin D. However, there are no published

reports characterizing this putatively selective inhibition in any detail. P1446A-05 and PD-0332991 are currently in Phase I clinical trials against advanced refractory malignancies and non-Hodgkins lymphoma, respectively. However, considering that knockout experiments have clearly shown the CDKs (with the exception of CDK1) are functionally redundant, it is unlikely that mono-specific PCIs will provide better therapy than oligo-specific ones.

1.3.9.1. The specificity of Rosco

Rosco, 2-(R)-(1-ethyl-2-hydroxyethylamino)-6-benzylamino-9-isopropylpurine, is a tri-substituted purine that potently and selectively inhibits of a subset of CDKs (Appendix 1) (Meijer, Borgne et al. 1997). Over the years, the specificity of Rosco has been evaluated by many different groups (see references in Appendix 1). Rosco specificity has been evaluated by *in vitro* kinase assays and also by techniques more amenable to large scale screening such as phage display (Fabian, Biggs et al. 2005; Karaman, Herrgard et al. 2008). The phage display screens involve a competition binding assay that measures the interaction between a “test” compound (in this case Rosco) and the kinase domain of tagged kinases (for example, Fabian *et al.* 2005 screened a panel 119 protein kinases). Briefly, the kinase domain is expressed as a fusion with the T7 bacteriophage major capsid protein, referred to as “tagged kinases”. “Bait” ligands, which are small molecules that bind the ATP-binding binding pocket of the tagged kinases ($K_d < 1\mu\text{M}$) are attached to biotin and immobilized on streptavidin-coated beads. The phages expressing the tagged kinases are then bound to the immobilized probes

and competition assays are performed with “test” compounds. If the free test compound binds with higher affinity to the ATP-binding pocket of the tagged kinase, fewer phages remain bound to the bait. The amount of phage still bound to the solid support after the competition is then evaluated by either phage plaque assays or quantitative PCR (qPCR) of phage DNA. Both quantitation methods enable near single-molecule protein detection, allowing accurate detection of as few as 10–100 binding events.

Rosco has been tested against 57% (295 or 518) of the kinases encoded by the human genome (Appendix 1). Rosco is thus arguably one of the most extensively characterized protein kinase inhibitors. Rosco selectively inhibits CDK1, 2, 3, 5, 7, and 9 with $IC_{50} < 0.7 \mu M$. At higher concentrations, it also inhibits DYRK1A ($IC_{50} 3.1 \mu M$), PAK4 ($IC_{50} 6.9 \mu M$), GSK3B ($IC_{50} 32 \mu M$), Erk1 ($IC_{50} 34 \mu M$), Erk2 ($IC_{50} 14 \mu M$), CK1 δ ($IC_{50} 17 \mu M$), CaMK2 α ($IC_{50} 32 \mu M$). Rosco also binds to, and inhibits, one non-protein kinase, pyridoxal kinase. However, Rosco did not inhibit the kinase activity of pyridoxal kinase at lower than physiological concentrations of ATP (Bach, Knockaert et al. 2005). Therefore, Rosco is not likely to inhibit pyridoxal kinase *in vivo*. Rosco does not inhibit, or bind with high affinity to, 282 other protein kinases, 4 other kinases, and 2 viral protein kinases (Appendix 1).

1.3.9.2. Effects of Rosco on HSV-1 replication

Initial studies revealed that Rosco inhibited the accumulation of HSV-1 IE and E transcripts, as well as HSV-1 DNA replication (Schang, Phillips et al. 1998;

Schang, Rosenberg et al. 1999; Schang, Rosenberg et al. 2000). Although Rosco inhibited the VP16-dependent activation of IE gene expression, it did not change the affinity of the VP16/Oct-1/HCF complex for TAATGARAT-containing DNA *in vitro* (Jordan, Schang et al. 1999). As a caveat of these experiments, Oct-1 was expressed in bacteria and then added to the binding reactions. Any potential effects of Rosco on Oct-1 would not have been detected by these assays. Rosco also inhibits the posttranslational modifications of the transcriptional activators ICP0 and ICP4 (Advani, Hagglund et al. 2001; Davido, Leib et al. 2002). Consistent with targeting cellular proteins required for multiple HSV-1 functions, Rosco inhibited the replication of both wild-type strains as well as strains of HSV-1 that were resistant to conventional antivirals. Furthermore, Rosco-resistant HSV-1 mutants could not be isolated even after 11 passages in selective media. PAA, in contrast, which inhibits the HSV-1 DNA polymerase, quickly selected for drug-resistant mutants. Titres had already reached 50% of wild-type after 11 passages (Schang, Phillips et al. 1998).

1.3.9.3. Effects of Rosco on other human pathogenic viruses

The effects of PCIs have since been found to inhibit replication of a variety of other human pathogenic viruses, including HCMV, VZV, EBV, HIV-1, KSHV, human T-lymphotropic virus (HTLV), adenovirus, and several animal retroviruses (reviewed in Schang, St Vincent et al. 2006).

For example, Rosco inhibited HCMV IE and E functions such as the expression of viral transcriptional regulators and viral DNA synthesis (Sanchez,

McElroy et al. 2004). Rosco also inhibited HCMV DNA replication when added at both early (Bresnahan, Boldogh et al. 1997) and late (Sanchez, McElroy et al. 2004) times post infection. Furthermore, the effects of Rosco on late viral functions and replication occurred even in the presence of viral regulators of transcription (Sanchez, McElroy et al. 2004). Interestingly, Rosco had differential effects on expression of different HCMV genes. For example, Rosco inhibited the expression of IE1-72 while activating that of IE2-86, an alternatively spiced transcript from the same transcriptional unit. Similar differential effects were observed on another transcriptional unit encoding the alternatively spiced proteins UL31x1 (inhibited) and UL37 (induced). Therefore, Rosco appears to differentially inhibit expression of alternatively spiced HCMV gene products (Sanchez, McElroy et al. 2004).

VZV replication was also inhibited in the presence of Rosco, likely by inhibition of expression and subcellular localization of several VZV IE proteins such as IE62 (Taylor, Kinchington et al. 2004; Habran, Bontems et al. 2005).

Similarly, Kudoh *et al.* showed that Rosco inhibited EBV replication. Rosco inhibited accumulation of the IE and E EBV proteins, even in the presence of the required transactivators of gene expression (Kudoh, Daikoku et al. 2004).

The effects of Rosco were shown to extend beyond the herpesviruses. Rosco was shown to inhibit HIV replication in primary or immortalized human cells, and HIV reactivation from latency in cultured cells (Nelson, Gelman et al. 2001; Wang, de la Fuente et al. 2001; Schang, Bantly et al. 2002; Agbottah, de La Fuente et al. 2005). Rosco inhibited transcription from a HIV LTR promoter in

the presence or absence of Tat. It also inhibited transcription of HIV mutants that are not known to require CDK9 (Wang, de la Fuente et al. 2001). Consistent with targeting cellular proteins required for viral functions, Rosco inhibited equally well the replication of multidrug-resistant and wild-type HIV strains (Schang, Bantly et al. 2002).

As expected, viruses that are not known to require CDKs such as vaccinia or lymphocytic choriomeningitis virus were not inhibited by Rosco (Schang, Bantly et al. 2002).

Therefore, Rosco inhibits the replication and transcription of many unrelated viruses. Furthermore, Rosco often inhibits multiple functions within the replicative lifecycle of individual viruses. One of the potential mechanisms whereby PCIs such as Rosco may inhibit multiple functions of many otherwise unrelated nuclear DNA viruses is through epigenetic modulation of chromatin structure.

1.4. Chromatin

1.4.1. Histone octamer and the nucleosome core particle

Nuclear DNA is typically packaged in a nucleoprotein complex called chromatin. The basic repeating unit of chromatin is the nucleosome core particle or nucleosome, which consists of 146bp of DNA making 1.75 superhelical turns around an octamer containing the four core histones, H2A, H2B, H3, and H4 (Kornberg 1974). Histones are highly basic proteins that bind to DNA and neutralize the negative charge of the phosphate backbone. This extensive charge

neutralization allows for the packaging of DNA into the nucleus. The level of compaction can reach up to 10,000-fold during the condensation of mitotic chromosomes.

The histone octamer is composed of stable H3-H4 tetramers flanked by two H2A-H2B dimers. Each of the core histones consist of a structured C-terminal histone fold domain (HFD) and an N-terminal tail domain (Arents, Burlingame et al. 1991). The HFD is comprised of three α -helices (α_1 , α_2 , and α_3) separated by two loops (L1 and L2) (Arents and Moudrianakis 1995). H2A also contains a C-terminal tail domain.

In vitro, nucleosomes can be assembled using purified histones and DNA (Luger, Rechsteiner et al. 1999). H2A/H2B and H3/H4 heterodimers initially form through interactions between their respective HFDs. The H3/H4 tetramers then form through a four helix bundle between neighboring H3 molecules resulting in the dimerization of the H3/H4 dimers. Histone octamers are formed when H2A/H2B dimers associate on opposite sides of the H3/H4 tetramer through four helix bundles that form between H2B and H4 (Luger, Mader et al. 1997). The nucleosome contains two-fold symmetry along the dyad axis which passes through the two neighboring H3 molecules and the entry and exit points of DNA (Luger, Mader et al. 1997). The intranucleosomal interactions within the canonical histone octamer are very stable. These interactions are established in the absence of DNA. Addition of DNA does not result in any significant alteration of these interactions (Luger, Mader et al. 1997).

In vivo, the situation is certainly more complex. H2A/H2B dimers and H3/H4 tetramers do not exist free in the nucleus but are instead assembled into nucleosomes through their interactions with chaperone proteins (see recent reviews Eitoku, Sato et al. 2008; Park and Luger 2008).

The crystal structures of canonical and variant histone-containing nucleosomes have provided a wealth of information about the structural role of chromatin and nucleosome stability (Chakravarthy, Bao et al. 2004; Zlatanova, Bishop et al. 2009). However, they provide only static pictures. Furthermore, they provide only details on the protein interior of the nucleosome core, whereas the core histone tails are not observed in the crystal structures (Arents, Burlingame et al. 1991; Luger, Mader et al. 1997; Suto, Clarkson et al. 2000).

Chromatin is a highly dynamic macromolecular complex, even at the level of the individual nucleosome. For example, nucleosomal DNA is thought to consistently undergo partial unfolding presumably from short-lived dissociations of histone-DNA interactions (reviewed in Zlatanova, Seebart et al. 2008). Depending on the distances in which histone-DNA interactions are transiently disrupted, this is referred to as either “breathing” (typically 10-30bp from the DNA ends) or “opening” (70-80bp) (Marky and Manning 1995; Tomschik, Zheng et al. 2005). In both cases, nucleosomal DNA would become more accessible to cleavage by nucleases.

1.4.2. Micrococcal nuclease as a tool to study chromatin

Nucleases have been instrumental in the characterization of chromatin structure (Noll 1974). Restriction enzymes and endonucleases such as DNases and micrococcal nuclease (MCN) have all been used to study and describe characteristics of chromatin such as DNA accessibility, nucleosome positioning and remodeling, as well as linker histone incorporation, among many other aspects.

MCN was used to demonstrate the regular repeating structure of chromatin through its preferential cleavage of exposed linker DNA between nucleosomes (Axel, Melchior et al. 1974; Greil, Igo-Kemenes et al. 1976). MCN has since been used extensively to study and characterize unique forms of chromatin, including chromatin found at the centromeres, telomeres, or packaged into sperm. Since DNA digestion obviously requires access to the DNA template, MCN also provides important information about the accessibility of the nucleosome DNA.

MCN randomly cleaves protein-free DNA. In the context of chromatin, however, MCN digestions first cleave linker DNA sparsely, releasing polynucleosome chains. Longer digestions eventually cleave the polynucleosomes to mononucleosomes. As a result of the partial unfolding of the DNA ends of the nucleosome, either by “breathing” or “opening”, prolonged exposure to stringent MCN digestion conditions eventually results in the degradation of DNA in mononucleosomes.

Standard MCN digestions of regularly chromatinized DNA therefore result in protection of poly- and mono- nucleosome-sized DNA fragments.

Purification and subsequent resolution of the resulting DNA fragments by gel electrophoresis result in the appearance of a nucleosome “ladder”. Each “rung” corresponds to a multiple of nucleosome-sized DNA, with the mononucleosome sized fragments migrating as the fastest band. Furthermore, the width of each band or “rung” represents both the relative stability of the nucleosome occupying that DNA and the position in which the nucleosome is found. The latter is referred to as nucleosome “phasing”. “Phased” nucleosomes are positioned within a small range of a genomic locus and thus result in the protection of homogeneously sized fragments of DNA following MCN digestion. These resolve as a thin defined band, or “rung”, on the nucleosome ladder. In contrast, nucleosomes with a continuous distribution throughout an array result in the protection of heterogeneously size DNA which resolve as wider undefined bands.

Nucleosome arrays assembled on DNA containing nucleosome positioning sequences result in “phased” nucleosomes. This occurs, for example, when nucleosome arrays are assembled on templates containing tandem repeats of sequences such as 5S ribosomal DNA (Simpson and Stafford 1983; Hayes, Tullius et al. 1990) or the artificial “pentamer-TG” (Shrader and Crothers 1989; Shrader and Crothers 1990) sequences. These sequences contain “positioning power”, such that nucleosomes assembled on tandem arrays of these sequences occupy preferred positions. Therefore, MCN cleaves at relatively the same site within each repeat resulting in a nucleosome ladder with well defined bands (Young and Carroll 1983). This was further demonstrated by Widom *et al.*, who isolated a DNA representing the strongest nucleosome positioning sequence

identified to date using SELEX (systematic evolution of ligands by exponential enrichment) (Lowary and Widom 1998). MCN digestion of nucleosome arrays assembled on DNA containing 12 tandem copies of this sequence resulted in the release of nucleosome ladders containing 12, thin, easily identifiable “rungs”. These results are consistent with nucleosomes stably occupying essentially the exact same position on each repeat. Dorigo *et al.* have since used base-pair resolution mapping with site-directed hydroxyl radicals to show that histone octamers assembled on these arrays occupy a single nucleosome position (Dorigo, Schalch et al. 2003).

In addition to providing information about ordered nucleosomes, MCN has also been used to characterize specialized chromatin structures and intrinsically unstable nucleosomes. Centromeres, for example, are specialized chromatin structures that are responsible for equal segregation of chromosomes at mitosis. They contain specialized nucleosomes with the centromere-specific histone H3 variant, CENP-A (called CenH3 in *Drosophila*). Dalal *et al.* have shown that in *Drosophila*, CenH3-containing centromeric nucleosomes protect only 120bp of DNA from MCN digestion (Dalal, Wang et al. 2007). Such atypical protection was shown to be the result of forming of unique nucleosome structures called “hemisomes” (Dalal, Furuyama et al. 2007; Dalal, Wang et al. 2007). Hemisomes contain only one copy of CenH3, H2A, H2B, and H4 assembled in a tetrameric structure. Dalal *et al.* further showed that these hemisomes show a typical “beads-on-a-string” appearance by electron microscopy. However, they resist condensation under physiological conditions.

Hemisomes are only half the height of canonical octameric nucleosomes, as determined by atomic force microscopy. This particular structure provides a potential explanation for the protection of only 120bp (Dalal, Wang et al. 2007).

In addition to specialized chromatin structures, MCN has also been used in the characterization of particularly unstable cellular nucleosomes (Jin and Felsenfeld 2007; Jin, Zang et al. 2009). Jin *et al.* have recently reported hybrid nucleosomes containing the histone variants H2A.Z and H3.3 that have the properties of highly unstable nucleosomes (Jin and Felsenfeld 2007).

Nucleosomes prepared from MCN digested nuclei readily detected (by chromatin immunoprecipitation assays-ChIP) hybrid nucleosomes containing either H2A.Z or H3.3 along with the remaining canonical core histones (H2B, H3, and H4 or H2A, H2B, H4, respectively). However, nucleosomes containing both H2A.Z and H3.3 were not detected under standard conditions (Jin and Felsenfeld 2007). In fact, H2A.Z/H3.3-containing hybrid nucleosomes could only be detected when cells were crosslinked with formaldehyde prior to MCN digestion (Jin, Zang et al. 2009). More recently, Jin *et al.* have shown that these H3.3/H2A.Z-containing hybrid nucleosomes mark “nucleosome-free regions” of active promoters and other regulatory regions (Jin, Zang et al. 2009).

1.4.3. Linker histone (H1)

The accessibility of chromatin to nuclease is also modulated by the binding of linker histones. Although linker histones are generically referred to as H1, they represent a large group of variants that include seven somatic variants (H1.0-

H1.5, and H1.X), three testes-specific variants (H1t, H1T2, and H1LS1), and an oocyte-specific variant (H1oo) (recently reviewed in Godde and Ura 2008).

Linker histones consist of a globular “winged helix” central domain flanked by basic N- and C- terminal tail domains (Ramakrishnan, Finch et al. 1993). The globular domain of H1 typically binds at the entry and exit point of nucleosomes thereby minimizing the “breathing” or “opening”. H1 binding closes off two full turns of DNA protecting an extra 20bp of DNA from MCN digestion. The resulting particle therefore contains 168bp of DNA, the histone octamer, and one molecule of linker histone and is called the chromatosome. Early evaluations of electron micrographs of H1-containing chromatin found that DNA enters and exits the nucleosome on the same side, whereas in H1-depleted chromatin, the entrance and exit points are far more random and more or less on opposite side of the nucleosome (Thoma, Koller et al. 1979). Studies using a series of crosslinking experiments with photoactive dNTPs later showed that linker histones simultaneously bind the central portion of the nucleosomal DNA (near the entry and exit point) and one of either the outgoing or incoming strands. Therefore histone H1 associates asymmetrically to one side of the nucleosome core particle (Pruss, Bartholomew et al. 1996).

The C-terminal tail of H1 interacts with linker DNA regions between nucleosomes, thereby promoting higher order chromatin folding (Finch and Klug 1976; Thoma and Koller 1977; Thoma, Koller et al. 1979; Hamiche, Schultz et al. 1996; Hendzel, Lever et al. 2004; Lu and Hansen 2004; Lu, Hamkalo et al. 2009).

In contrast to the relatively stable association of the core histones, linker histones bind to chromatin in a far more dynamic manner (Lever, Th'ng et al. 2000; Misteli, Gunjan et al. 2000). Based on their highly dynamic interaction with chromatin, linker histones have been proposed to control access to nucleosomal DNA, thereby acting as “gates” (reviewed in Zlatanova, Seebart et al. 2008; Happel and Doenecke 2009). Therefore, presence of linker proteins at the entry and exits points of the nucleus would regulate “breathing” and thus access to nucleosomal DNA. By extension, H1 would therefore regulate processes such as transcription and DNA repair (Zlatanova, Seebart et al. 2008). For example, linker histone H5 is a chicken erythrocyte-specific H1 variant that contains several lysine to arginine substitutions. These differences result in tighter binding to chromatin than canonical H1. In the context of the “gating” model proposed by Zlatanova *et al.*, therefore, H5 would “lock” the gate through its high affinity binding leading to the repression of transcription and replication observed in chicken erythrocytes. Zlatanova *et al.* also propose that the concept of “gating” may be extended to proteins that do not directly bind DNA, like heterochromatin protein 1 (HP1). Such protein may cooperate with linker histones to form “double locks” (Zlatanova, Seebart et al. 2008).

The importance of H1 *in vivo* was demonstrated by Fan *et al.*, who showed that mice lacking three of the seven somatic variants died by mid-gestation (Fan, Nikitina et al. 2003). The cells from these mice, however, were still viable. Although development may require a certain threshold of H1, therefore, an appreciable loss of H1 is tolerated by individual cells. More

recently, Hashimoto *et al.*, created a chicken cell line in which all 12 alleles of the six H1 variant were knocked out (Hashimoto, Takami et al. 2010). These cells were also viable and did not display any morphological changes in chromatin spreads. They also showed no defects in mitotic chromosome condensation and segregation. Surprisingly, the only visible effect on chromatin structure in either study was a slight decrease in nucleosome spacing (Fan, Nikitina et al. 2003; Hashimoto, Takami et al. 2010). Taken together, these results suggest that cells have evolved redundant mechanisms to compact chromatin within the nucleus. Alternatively, the level of chromatin compaction within the nucleus is not critical.

1.4.4. Higher order chromatin folding

Chromatin fibers are composed of stretches of DNA bound to multiple core histones octamers at ~160-210bp intervals, often referred to as nucleosome arrays. Such arrays were classically described as the 10nm fiber, which has the appearance of “beads on string” under the electron microscope (Olins and Olins 1974). However, it is now clear that this structure most likely does not exist *in vivo*. Instead, internucleosomal interactions and linker histones promote further compaction of chromatin into higher order structures (Hendzel, Lever et al. 2004; Lu and Hansen 2004; Lu, Hamkalo et al. 2009).

In *vivo*, chromatin is more likely compacted into a 30nm fiber. However, the exact arrangement of nucleosomes within this structure is still under debate. The two debated models are the one-start solenoid helix and the two-start zig-zag ribbon. In the one-start solenoid helical model, a linear array of nucleosomes

forms a coiled fiber (Finch and Klug 1976). In contrast, the two-start zig-zag model, nucleosomes are assembled in a zig-zag ribbon that twists or supercoils (Woodcock, Frado et al. 1984; Williams, Athey et al. 1986). Recently, the crystal structure of a tetranucleosome has been solved by Schalch *et al.* and supports earlier studies using disulfide crosslinking (Dorigo, Schalch et al. 2004) of a two-start zig-zag model (Schalch, Duda et al. 2005). It should be noted, however, that H1 was not present in these studies.

Recent work by Eltsov *et al.* revealed no evidence for the 30nm fiber. Human metaphase chromosomes were examined *in vivo* using cryo-electron microscopy of vitreous sections, a technique proposed to enable direct high-resolution examination of cell structures in a close to native state. Instead of the 30nm fiber, a compact uniform chromatin mass was observed (Eltsov, Maclellan et al. 2008). The authors propose a “melt” model of chromatin folding to explain the absence of any underlying structure. This model predicts that nucleosomes of adjacent fibers interdigitate and intermix at increased chromatin concentrations, resulting in the “melting” of the 30nm fiber into a uniform mass. This model requires intrafiber and interfiber nucleosome affinities to be identical. The authors do point out, however, that there may be situations in which the 30nm fiber is required. For example, the condensation of genomic DNA in starfish spermatozooids requires the 30nm fiber (Woodcock 1994). Moreover, the transition of the homogeneous melt into 30nm fibers would likely be mediated by an increase in intrafiber nucleosome affinities, potentially by histone modifications or by binding of specific proteins.

Intra- and inter- chromatin fiber interactions and their roles in higher-order chromatin structure and dynamics have been an active area of research for the past 40 years (recently reviewed in Woodcock and Ghosh 2010). Because of the heterogeneity of chromatin within the cells, much of what we know about chromatin folding has been learned through the use of nucleosomes arrays assembled *in vitro*. These arrays contain strong nucleosome positioning sequences (see section 1.4.1) and thus have allowed for the study of homogeneous chromatin fibers under conditions in which individual parameters can be evaluated. The role of, for example, ionic concentration, linker histone binding, core histone tails, and post translational modifications on chromatin folding were all first characterized using these systems.

Early work established that chromatin folding is highly dependent on ionic concentration. The presence of monovalent cations led to a moderate induction of chromatin folding at relatively high concentrations. In contrast, divalent cations (most notably Mg^{2+}) were far more effective at inducing chromatin folding and could be used at much lower concentrations (~100-fold). The effects of divalent cations were presumably the result of direct binding and neutralization of the residual charge of the phosphate backbone. Such neutralization would promote intranucleosomal interactions within the nucleosome array. The effect was still observed when arrays were assembled using histones in which the tails had been proteolytically removed, indicating that intranucleosomal interactions occurs independently of the presence of the histone tails (Ausio, Dong et al. 1989; Hayes, Clark et al. 1991; Polach, Lowary et al. 2000). Interestingly, oligomerization of

nucleosome array could not be compensated for by divalent cations and was dependent on the presence of the histone tails (Garcia-Ramirez, Dong et al. 1992; Fletcher and Hansen 1995; Tse and Hansen 1997). Taken together, these findings revealed that although charge neutralization likely plays a role, higher order chromatin folding is most likely mediated by internucleosomal interactions involving histone tails (Fletcher and Hansen 1995; Zheng and Hayes 2003).

1.4.5. Histone post-translational modifications (PTMs)

Histone tails (as well as globular domains) of both linker and core histone are subject to a vast array of post-translational modifications (PTMs) (recently reviewed in Kouzarides 2007; Campos and Reinberg 2009). These modifications include methylation of arginine (R) residues; methylation, acetylation, ubiquitination, ADP-ribosylation, and sumoylation of lysine (K) residues; and phosphorylation of serine (S) and threonine (T) residues. Histone PTMs affect higher order chromatin folding and regulate processes such as DNA repair (recently reviewed in Venkitaraman 2010) and transcription (recently reviewed in Li, Carey et al. 2007). In the context of transcription, histone PTMs regulate the balance between transcriptionally active euchromatin and transcriptionally repressed heterochromatin. Euchromatic marks are modifications typically associated with active transcription, such as the acetylation (ac) of lysine residues in H3 (K4, 9, 14, 18, 23, 27, or 56) or H4 (K5, 8, 12, or 16), as well as di- and tri-methylation (me) of H3 (K4, 36, or 79). In contrast, heterochromatin marks are

modifications that typically localize to inactive genes or silenced regions, such as tri-methylation of H3 (K9 and K27) and H4K20.

1.4.5.1. Histone acetylation

Histone acetylation is a reversible modification catalyzed by K-acetyltransferases (KATs; formerly HATs) and histone deacetylases (HDACs). KATs transfer the acetyl group from acetyl-coenzyme A to lysine residues within the N-terminal tails or core domain of histones, whereas HDACs catalyze the removal of the acetyl group from the lysine residues.

Acetylation is primarily associated with active transcription. This association is thought to occur at least in part by decreasing the net charge of the nucleosome thereby loosening intranucleosomal and internucleosomal interactions (Garcia-Ramirez, Rocchini et al. 1995). The model is supported by the observation that acetylated histones are easier to displace from DNA both *in vivo* (Reinke and Horz 2003; Zhao, Herrera-Diaz et al. 2005) and *in vitro* (Ito, Ikehara et al. 2000; Chandy, Gutierrez et al. 2006; Hassan, Awad et al. 2006). However, acetylated lysine residues also serve as binding sites for effector complexes (reviewed in Seet, Dikic et al. 2006). For example, bromo-domain containing proteins specifically recognize acetylated residues. In addition, modifications such as the acetylation of lysine 16 of histone H4 directly influence higher order chromatin structure. Shogren-Knaak *et al.* recently demonstrated that acetylation of lysine 16 of the N-terminal tail of H4 (H4K16ac) alone could

disrupt internucleosomal interactions thus preventing formation of 30nm-like fibers (Shogren-Knaak, Ishii et al. 2006).

1.4.5.2. Methylation

Histone methylation is a reversible modification catalyzed by K-methyltransferases (KMTs, formerly histone methyltransferases) and K-Demethylases (KDMs, formerly lysine demethylases). Histone methylation is associated with both active and repressed chromatin. Rather than affecting the overall charge of the histone tail, methylation serves to recruit various effector proteins to the DNA template. These recruited proteins carry out a variety of cellular processes, such as, transcriptional activation and gene silencing. The combinatorial regulation mediated by multiple/sequential modifications as well as the interdependence of other modifications is thought to act as an epigenetic code, called the “histone code” (Strahl and Allis 2000; Jenuwein and Allis 2001).

1.4.6. Histone variants

In addition to PTMs and their wide variety of biological outcomes, incorporation of histone variants is also used to modulate chromatin structure and function. Histone variants are often encoded by single copy genes that are spliced, polyadenylated, and expressed outside of S-phase. In contrast, the genes encoding canonical core histones are typically clustered in repeat arrays and their transcription is tightly coupled to DNA replication. The genes for canonical

histones are also not spliced or polyadenylated, and are expressed only during S-phase.

Histones variants have been identified for H1, H2A, H2B and H3. The H1 family of linker histone is the most divergent class of class of histone proteins and encodes, somatic, oocyte-, and testes- specific variants (see section 1.4.3) (recently reviewed in Happel and Doenecke 2009). There are five H3 variants, H3.1, H3.2, H3.3, CENP-A, and the testis specific H3T. H3.1 and H3.2 are canonical H3 assembled into chromatin in a replication-coupled manner (behind the replication fork during DNA replication). H3.3, CENP-A, and H3T are specialized H3 variants involved in marking active transcription, in centromere maintenance, or in spermatogenesis, respectively (recently reviewed in Elsaesser, Goldberg et al. 2010). Only one H2B variant has been identified, hTSH2B. It is a testes-specific form that may have non-chromatin roles. Only 20% of hTSH2B localizes to the nucleus in mature sperm (Zalensky, Siino et al. 2002). Finally, there are four H2A variants, H2A.Z, H2A.X, H2A Barr body-deficient (Bbd), and macro H2A (mH2A). The H2A variants are involved primarily in transcription regulation, ranging from activation (H2ABbd) to silencing (mH2A). H2A.Z is also involved in transcription regulation and has been implicated in both gene activation as well as heterochromatin silencing. In contrast, H2A.X is involved in DNA damage responses. Following double stranded DNA breaks, H2A.X becomes phosphorylated. Phosphorylated H2A.X is referred to as γ H2A.X. It acts to recruit or retain DNA repair proteins, histone modifying complexes, and chromatin remodeling complexes at the sites of DNA damage.

1.5. Viruses and chromatin

1.5.1. Chromatinization of polyoma and papilloma viruses

The genomes of many nuclear replicating DNA viruses persist in the nucleus of the host cells for considerable periods. Normally, nuclear DNA is chromatinized. Therefore, it is not surprising that the genomes of most nuclear replicating DNA viruses are also chromatinized.

The genomes of the small DNA-tumor viruses of the polyoma and papilloma virus families are assembled into nucleosomal minichromosomes during their DNA replication. These viruses depend on the host cell DNA replication enzymes. They therefore activate cellular DNA synthesis (Dulbecco, Hartwell et al. 1965; Weil, Michel et al. 1965; Hancock and Weil 1969). It is therefore not surprising that the assembly of nucleosomes on these viral minichromosomes occurs via the same mechanisms as for the host cell (reviewed in Waga and Stillman 1998). The association between histones and the viral DNA is maintained throughout the replicative cycle, even in the encapsidated virions (Griffith 1975; Meinke, Hall et al. 1975; Christiansen, Landers et al. 1977). As a result, MCN digestions of polyoma or papilloma virus DNA from infected cells or disrupted capsids releases viral DNA fragments characteristic of nucleosome DNA (Cremisi, Pignatti et al. 1975; Germond, Hirt et al. 1975; Griffith 1975; Bellard, Oudet et al. 1976; Favre, Breitburd et al. 1977). As a notable exception, the SV40 origin of replication, which is bound by the large T antigen, is free of nucleosomes (Jakobovits, Bratosin et al. 1980).

1.5.2. Chromatinization of adenovirus

In the nuclei of infected cells, the genomes of adenoviruses are chromatinized at early times during infection (Sergeant, Tigges et al. 1979; Tate and Philipson 1979; Daniell, Groff et al. 1981; Dery, Toth et al. 1985). Unlike polyoma- and papilloma- viruses, however, adenoviruses are packaged in chromatin-like structures with viral core proteins, not histones. These viral proteins include an histone H3-related protein VII (Brown, Westphal et al. 1975; Corden, Engelking et al. 1976; Mirza and Weber 1981; Mirza and Weber 1982)

1.5.3. Chromatinization of herpesviruses

The role of chromatinization in the lifecycle of HSV-1 is far more complex and not yet fully understood. As such, chromatinization of HSV-1 DNA is an area of active research (recently reviewed in Lieberman 2008; Placek, Huang et al. 2009; Bloom, Giordani et al. 2010; Kristie, Liang et al. 2010; Paulus, Nitzsche et al. 2010; Sinclair 2010).

1.5.3.1. Encapsidated HSV-1 DNA

The genomes of polyoma-, papilloma-, and adeno- viruses are organized in chromatin, or chromatin-like structures, by cellular histones or virally encoded histone-like proteins, respectively. In contrast, none of the many groups that have evaluated the proteins in the virions of various herpesviruses (including HSV-1, HSV-2, HCMV, EBV, KSHV, RRV, and MHV68) have found all core histones

(Gibson and Roizman 1971; Cohen, Ponce de Leon et al. 1980; Pignatti and Cassai 1980; Hall, Aghili et al. 1982; Baldick and Shenk 1996; Bortz, Whitelegge et al. 2003; Johannsen, Luftig et al. 2004; Kattenhorn, Mills et al. 2004; Varnum, Streblow et al. 2004; Bechtel, Winant et al. 2005; Zhu, Chong et al. 2005; O'Connor and Kedes 2006; Loret, Guay et al. 2008; Oh and Fraser 2008). As the single exception, mass spectrometry performed on MCMV virions identified H2A. However, not one of the other core histones was detected in these experiments (Kattenhorn, Mills et al. 2004)

Consistent with HSV-1 DNA being free of nucleosome-like structures within the capsid, disruption of HSV-1 nucleocapsids by treatment with alkaline buffer (pH 9.3), pyridine, Sarkosyl, or NaCl/urea and subsequent MCN digestion revealed no indication of nucleosome sized fragments (Leinbach and Summers 1980).

1.5.3.2. HSV-1 DNA during latency

In humans, HSV-1 typically infects, and replicates in, the basal epithelial cells of the vermillion border of the lip. Following lytic replication in these cells, HSV-1 infects the sensory neurons that innervate the site of the primary infection. The virus enters the neuron by fusion at the axonal termini. Nucleocapsids then travel via retrograde axonal transport to the cell bodies of the neurons, located within the trigeminal ganglia (TG) (Lycke, Kristensson et al. 1984; Penfold, Armati et al. 1994). Once inside the nuclei, the viral genomes persist as chromatinized circular

episomes (Rock and Fraser 1983; Rock and Fraser 1985; Mellerick and Fraser 1987; Deshmane and Fraser 1989).

In the TG, a period of acute infection typically precedes the establishment of latency. In the mouse model, this acute period lasts approximately 7 days. During this time, all HSV-1 genes are expressed and viral DNA replication occurs (Spivack and Fraser 1988; Valyi-Nagy, Deshmane et al. 1991; Kramer, Chen et al. 1998). Following the acute phase, the HSV-1 genomes become transcriptionally silent, with the exception of the loci encoding the latency associated transcript (LAT). Characteristics of the latent state include the absence of viral replication, the absence of detectable viral proteins, and the presence of LAT. Other studies have indicated that limited amounts of ICP4 and thymidine kinase (TK) transcripts can be detected during latency by sensitive, quantitative polymerase chain reaction (PCR) (Kramer and Coen 1995; Feldman, Ellison et al. 2002).

Following the establishment of latency, the HSV-1 genomes are maintained as transcriptionally silent episomes, with the exception of the LAT locus. Latency is proposed to be, at least in part, maintained through the assembly of transcriptionally silent heterochromatin on latent HSV-1 genomes (Kubat, Amelio et al. 2004; Kubat, Tran et al. 2004; Neumann, Bhattacharjee et al. 2007; Cliffe, Garber et al. 2009; Kwiatkowski, Thompson et al. 2009).

Periodically, the latent genome is induced to reenter the lytic replication cycle, in an event referred to as reactivation. Reactivation occurs following a variety of poorly defined stimuli such as physical or emotional stress, fever, UV

irradiation, heat shock, tissue damage, neuronal explant and hormonal alterations. These stimuli trigger HSV-1 to re-enter into the lytic replication cycle. Reactivation is characterized by HSV-1 lytic gene transcription, expression of viral proteins, DNA replication, packaging of the viral DNA, and anterograde axonal transport of the new virus to the sites of primary infection. The molecular mechanism of HSV-1 reactivation from latency, however, remains one of the least understood, yet most clinically relevant, aspects of HSV-1 infection.

Much of what we understand about latency and reactivation comes from animals models. In the mouse, infection of the footpad, flank, ear, or eye leads to lytic replication at the site of infection, followed by the establishment of latency at the innervating sensory ganglia. Mice, however, do not experience spontaneous true clinical reactivation. Infectious virus cannot be spontaneously isolated from the site of infection once the primary infection has been cleared. However, reactivation can be induced through the exposure of latently infected mice to hyperthermia (Sawtell and Thompson 1992). Furthermore, mouse ganglia undergo explant-induced reactivation following excision. Therefore, reactivation studies in mice are performed mostly *ex vivo* and techniques such as *in situ* hybridization (ISH) or RT-PCR to detect viral transcripts or DNA.

Infection of the eyes in rabbits and the vagina in guinea pigs, serve as *in vivo* models to study HSV-1 and HSV-2 infections, respectively. The rabbit eye model is particularly advantageous. Reactivation can be efficiently induced by the iontophoresis of epinephrine into the eye. Reactivation is not reliably induced in the guinea pig model. However, HSV-2 reactivates more frequently in the

guinea pig model than HSV-1, similar to the situation observed in humans.

Therefore, guinea pigs serve as attractive systems in comparative analysis of the factors responsible for the differences in the reactivation frequency of HSV-1 and HSV-2.

Although no one model truly recapitulates all aspects of human infection, mice, rabbits, and guinea pigs have all greatly contributed to our current understanding of latency and reactivation. Unfortunately, however, no encompassing model has yet been derived by analyzing the data from the different animal models.

One attractive model for the regulation of reactivation involves HCF-1. HCF-1 is sequestered out of the nucleus in TG neurons (Kolb and Kristie 2008). HCF-1 is possibly localized in unstimulated sensory neurons at the Golgi. However, the potential mechanisms for Golgi retention are unclear. Regardless of the specific cellular localization, extranuclear HCF-1 would not be able to interact with its proposed partners and therefore unable to activate HSV-1 IE transcription.

Following a reactivation stimulus, HCF-1 relocalizes to the nucleus. Once in the nucleus, HCF-1 presumably interacts with some yet unidentified cellular proteins to bind HSV-1 IE promoters. Then, IE transcription is activated through an LSD-1-dependent mechanism. This proposed role for HCF-1 and recruitment of the KDM LSD-1 supports a model in which reactivation from latency is regulated, at least in part, by epigenetic modulation of the chromatin structure assembled on latent HSV-1 genomes (Liang, Vogel et al. 2009).

1.5.3.3. HSV-1 DNA during lytic infection

In contrast to latent HSV-1 DNA, HSV-1 DNA was classically considered to be mostly nucleosome-free during lytic infections (Mouttet, Guetard et al. 1979; Leinbach and Summers 1980; Sinden, Pettijohn et al. 1982; Muggeridge and Fraser 1986; Deshmane and Fraser 1989). Such conclusions were reached following a series of reports, dating back over 30 years, in which MCN digestion was used to probe the intranuclear structure of HSV-1 DNA.

In the first report, Mouttet *et al.* examined newly synthesized, progeny, HSV-1 DNA. HSV-1 infected cells were labeled with ^3H -thymidine from 6 to 7hpi and nuclei were isolated and digested with MCN. As expected for DNA in regularly spaced nucleosomes, cellular chromatin was protected to nucleosome-sized fragments. In contrast, HSV-1 DNA was cleaved to heterogeneous sized fragments. No repeating nucleosome-sized fragments were observed. It was therefore concluded that during lytic infection, the intranuclear state of HSV-1 DNA is different than that of the DNA in cellular chromatin (Mouttet, Guetard et al. 1979).

Concomitantly, another report compared the structure of parental and progeny HSV-1 DNA also using MCN (Leinbach and Summers 1980). Using dual labeling, these authors first evaluated the accessibility of infecting (parental) HSV-1 DNA and DNA in cellular chromatin in the same nucleus. Briefly, HSV-1 virus stocks were grown in the presence of ^{32}P -orthophosphate, such that the genomes of the isolated virus were labeled with ^{32}P . Meanwhile, the cells to be

infected were labeled with ^3H -thymidine prior to infection, such that cellular DNA was labeled with ^3H . Parental HSV-1 DNA was much more resistant to MCN digestion than DNA in cellular chromatin. For example, only 10% of the parental HSV-1 DNA was released as soluble chromatin after 20 minutes of MCN digestion, compared to 60% of cellular DNA. As expected, cellular DNA was protected to tri-, di, mono- nucleosome-size fragments the course of digestion. In contrast, HSV-1 DNA was present as two populations. The first and most prominent population was poorly accessible to MCN and migrated as large DNA fragments ($>14,850\text{bp}$) at the top of the gels (Leinbach and Summers 1980). The authors concluded that this HSV-1 DNA most likely represented intact genomes, and attributed the presence of these intact genomes to HSV-1 DNA that had entered the nucleus but was not yet uncoated. However, the resolution of even 0.7% agarose gels is insufficient to resolve fragments larger than 20,000bp (significantly shorter than the 152,000bp of an intact HSV-1 genome). Furthermore, the high molecular weight HSV-1 DNA was degraded over the course of digestion, albeit with much slower kinetics than cellular DNA.

The second and relatively minor population of HSV-1 DNA was a heterogeneously sized population ranging from <75 to $\sim 300\text{bp}$, which was mostly degraded over the course of digestion. Further examination of these low molecular weight fragments revealed that they were both nucleosome- and sub-nucleosome sized (Leinbach and Summers 1980). Taken together, Leinbach *et al.* concluded that only a minor percentage of parental HSV-1 DNA in the nucleus was uncoated and used as templates for transcription and replication.

In contrast to parental HSV-1 DNA, Leinbach *et al.* showed that progeny HSV-1 DNA (from nuclei labeled between 16 and 17hpi as well as 12 and 13hpi) was far more accessible to MCN than DNA in cellular chromatin. Digestion for 40min resulted in the release of 85% of the progeny HSV-1 DNA as soluble chromatin, compared to only 55% cellular DNA (Leinbach and Summers 1980). The digestion kinetics of the progeny HSV-1 DNA resembled more closely those of protein-free HSV-1 DNA than those of chromatinized cellular DNA. The examination of low molecular weight DNA fragments revealed that cellular DNA was protected to tri-, di-, and mono- nucleosome-size fragments, as expected, whereas the majority of HSV-1 DNA was digested to heterogeneous sized fragments (Leinbach and Summers 1980). Leinbach *et al.* did, however, also observe a minor percentage of HSV-1 DNA protected to nucleosome sized fragments (Leinbach and Summers 1980). These results suggested that the majority of progeny HSV-1 DNA was not in the same structures as DNA in cellular chromatin. However, in contrast to Mouttet *et al.*, Leinbach *et al.* also detected a small percentage of HSV-1 DNA protected to nucleosome size, a difference that was attributed to labeling at 12 to 13hpi (Leinbach and Summers 1980) rather than 6 to 7hpi (Mouttet, Guetard *et al.* 1979).

The intranuclear state of HSV-1 DNA was also probed using the DNA photoaffinity probe 4, 5', 8-trimethylpsoralen (Me₃psoralen) (Sinden, Pettijohn *et al.* 1982). The rate of binding of Me₃psoralen to DNA is dependent on both the accessibility of the DNA and the amount of torsional tension in the helical winding of the DNA (Sinden, Carlson *et al.* 1980). The authors proposed that,

rather than being complexed with nucleosomes, HSV-1 DNA may contain unrestrained superhelical turns (such as negative supercoils) much like DNA in bacterial chromosomes. As a result, HSV-1 DNA would be maintained in a state of torsional strain and thus bind more Me₃psoralen. The authors found that prior to HSV-1 DNA replication, HSV-1 DNA was ~1.3-fold less accessible than DNA in cellular chromatin. Following HSV-1 DNA replication, HSV-1 DNA accessibility increase by 5-fold, such that it became ~2-fold more accessible than DNA in cellular chromatin. In addition, the introduction of single-stranded DNA breaks using γ -irradiation showed that HSV-1 DNA does not contain unrestrained torsional tension, either in the capsid or during the replicative cycle. However, it is now known that both replicating HSV-1 DNA and HSV-1 DNA packaged into capsids have a large number of single-stranded breaks without any inducing agent. These results suggest that intranuclear HSV-1 DNA has different properties than regular nucleosomal DNA.

The *in vivo* structure of HSV-1 DNA was also evaluated in trigeminal ganglia of acutely infected mice (Muggeridge and Fraser 1986). Nuclei were purified from brainstems of mice infected with HSV-1 for 7 days. As expected, MCN digestion of the β -globin locus within the cellular genome resulted in the typical nucleosome ladder with regularly spaced nucleosomes, characteristic of chromatinized DNA. In contrast, HSV-1 DNA from the brain acutely infected with HSV-1 was digested to heterogeneous sized fragments, along with a minor percentage of nucleosome-sized ones. There was also a percentage of HSV-1 DNA that was poorly accessible to MCN, such that it was mostly resistant to even

the harshest MCN conditions used. In contrast to DNA in cellular chromatin, the population of HSV-1 DNA protected to nucleosome size represented only a minority of the total HSV-1 DNA. Similar digestion patterns were observed for HSV-1 DNA in an infected neuroblastoma cell line. The authors provided the following suggestions to explain their results, i) a small number of the HSV-1 genomes may be chromatinized, ii) parts of each of the HSV-1 genomes may be chromatinized, or iii) HSV-1 DNA may be complexed with non-histone proteins that are not as tightly associated with DNA as canonical histones are, and thus provide less protection than typical nucleosomes (Muggeridge and Fraser 1986).

Muller *et al.* provided evidence for the coexistence of a mixture of HSV-1 DNA in different structures within the nuclei of infected cells (Muller, Schroder et al. 1980). Nuclear spreads prepared at late stages during infection were examined by electron microscopy. The authors noted four forms of chromatin in the nuclei of HSV-1 cells. In addition to the typical 10nm “beads on string” nucleosomal arrangement, three forms were unique to infected cells. The first was thin filaments, indistinguishable from protein-free plasmid DNA. Another contained protein-free stretches but was sparsely and irregularly associated with 10-22nm granules different from nucleosomes. The last form was a densely stained uniformly thick (~17nm) strand. All forms were clearly identified on HSV-1 DNA, as determined by their association with newly assembled capsid structures. Furthermore, all the forms identified could be observed on the same DNA strand (Muller, Schroder et al. 1980). Taken together, their results

suggested that nucleosomal and non-nucleosomal stretches of DNA can exist on the same HSV-1 DNA molecule.

The co-existence of nucleosome and nucleosome-free stretches of DNA on the same molecule of DNA had previously been reported for SV-40. For this virus, ~350bp surrounding the origin of replication/large T antigen binding site was nucleosome-free, whereas the rest of the genome contained regularly spaced nucleosomes (Jakobovits, Bratosin et al. 1980). In contrast, there is no nuclease evidence to support regular spacing of nucleosomes on HSV-1 DNA.

The lack of a role for chromatin during HSV-1 lytic infection was further supported by several reports showing that infecting HSV-1 genomes localized to nuclear domains adjacent to ND10s, domains which are devoid of cellular chromatin or histones (Ascoli and Maul 1991; Ishov and Maul 1996; Maul, Ishov et al. 1996). Moreover, HSV-1 replication compartments at late times post infection are also partially depleted of histones (K.L. Conn PhD Thesis, Monier, Armas et al. 2000; Simpson-Holley, Colgrove et al. 2005).

For the 25 years following its initial characterization, HSV-1 DNA was therefore widely accepted to be nucleosome-free during lytic infections. More recently, however, ChIP assays have demonstrated that histones associate with HSV-1 DNA during lytic infections (Herrera and Triezenberg 2004; Kent, Zeng et al. 2004; Huang, Kent et al. 2006; Narayanan, Ruyechan et al. 2007; Knipe and Cliffe 2008; Oh and Fraser 2008; Ferenczy and Deluca 2009; Kutluay, DeVos et al. 2009; Kutluay and Triezenberg 2009; Liang, Vogel et al. 2009; Placek, Huang

et al. 2009). These results have thus prompted a re-evaluation of the classic model.

In one of the initial ChIP studies, Herrera *et al.* found that the VP16 activation domain (AD) was required for recruiting TBP and the large subunit of RNAPII, but not Oct-1, to IE promoters. Furthermore, the AD was also involved in the recruitment of the KAT3A (formerly CBP) and KAT3B (formerly p300) to IE promoters. The role of the AD in the recruitment of the ATP-dependent chromatin remodelers Brg-1 and Brm to IE promoters was more complex. Whereas the AD was required for the recruitment of both Brg-1 and Brm to the ICP0 promoter, it was required for the recruitment of either Brm or Brg-1 on ICP4 or ICP27 promoters, respectively (Herrera and Triezenberg 2004).

Herrera *et al.* also evaluated the presence of H3 and H3 acetylated on residues 9 or 14 (AcH3) at various loci throughout the HSV-1 genome. They showed that H3 and AcH3 were depleted from IE promoters at 2hpi in the presence of a functional AD. In contrast, both H3 and AcH3 were present on the ICP27 coding sequence, or on selected E (TK) and late (gC and VP16) promoters. H3 was found on all HSV-1 loci tested in the absence of the VP16 AD, whereas AcH3 was absent (Herrera and Triezenberg 2004).

From these results, these authors proposed that the VP16 AD is required either to exclude histones from IE promoters or to remove them, perhaps through the recruitment of KATs or other chromatin remodelers.

However, subsequent studies from the same group have shown that neither the recruitment of KATs or chromatin remodelers to, nor the removal of histones

from, HSV-1 DNA is required for HSV-1 gene expression (Kutluay, DeVos et al. 2009; Kutluay and Triezenberg 2009).

Using small interfering RNAs targeting KAT2A (formerly GCN5), KAT2B (formerly PCAF), KAT3A, KAT3B, or ATP-dependent chromatin remodelers (Brg-1 and BRM), or cell lines which lack functional KAT3B, Brg-1, or Brm, the authors showed that neither recruitment of the KATs nor the chromatin remodelers were required for IE gene expression (Kutluay, DeVos et al. 2009).

The authors then evaluated whether histone occupancy played a role in regulating HSV-1 transcription. Consistent with a model in which histone occupancy inhibits HSV-1 transcription, both the removal of the VP16 AD or the inhibition of RNAPII transcription resulted in an increase in the occupancy of all core histones (H2A, H2B, H3 and H4) on HSV-1 loci (Kutluay and Triezenberg 2009). However, activation of IE transcription by providing HSV-2 VP16 in *trans* did not result in the removal of these histones. Thus, eviction of histones from HSV-1 DNA appears not to be required for HSV-1 gene expression (Kutluay and Triezenberg 2009).

Together, the results from the Triezenberg group show that although the proper activation of IE gene transcription requires the VP16 AD, it does not require the recruitment of HATs or chromatin remodelers to, or the eviction of histones from, HSV-1 DNA.

In the second of the two initial ChIP studies, Kent *et al.* first showed that HSV-1 infection does not alter global H3 levels, as evaluated by Western

blot. Histones bearing the modifications normally associated with transcription activation, H3K9ac and H3K14ac were globally increased in the nuclei of cells lytically infected with HSV-1. The levels of the histone modification H3K9me2, which is normally associated with transcriptional repression, were globally decreased in the same nuclei (Kent, Zeng et al. 2004).

In a later report, the same group showed that the protein methylation inhibitor 5'-deoxy-5'-methylthioadenosine (MTA) reduced the level of H3K4me3 associated with IE, E, and L promoters. MTA also inhibited transcription driven by these promoters, and consequently HSV-1 DNA replication (Huang, Kent et al. 2006). These results suggest a role for H3K4 methylation in the regulation of HSV-1 transcription. However, subsequent knock down of Set-1 (the KMT responsible for H3K4 methylation) resulted in only a modest effect on HSV-1 transcription or HSV-1 DNA replication (Huang, Kent et al. 2006). These results suggest that Set-1 is not solely responsible for the methylation events required for optimal activation of HSV-1 IE transcription.

1.6. Rationale and hypothesis

Infecting HSV-1 genomes localize to nuclear domains which are devoid of cellular chromatin and histones, and micrococcal nuclease (MCN) digestions of lytically infected cells release HSV-1 DNA primarily in heterogeneously sized fragments. It was therefore classically concluded that most HSV-1 DNA was not associated with histones during lytic infections. More recent ChIP assays, in contrast, indicate that histones do interact with HSV-1 DNA during lytic

infections. Although only a minority of HSV-1 DNA co-immunoprecipitates with histones in the vast majority of these studies, histone modifications were proposed to regulate HSV-1 transcription. However, it remained unclear how the association of histones with a minority of HSV-1 DNA could regulate viral transcription globally. Moreover, the biophysical properties of intranuclear HSV-1 DNA nucleoprotein complexes during lytic infection were unclear.

The goal of my PhD studies was therefore to investigate the biophysical properties of the intranuclear HSV-1 DNA complexes during lytic infections. Differing from all previous work, however, I used classical chromatin purification techniques. This approach led to data supporting the association of HSV-1 DNA in unstable nucleosomes, a most unexpected finding.

1.7. References

- Advani, S. J., R. Hagglund, et al. (2001). "Posttranslational processing of infected cell proteins 0 and 4 of herpes simplex virus 1 is sequential and reflects the subcellular compartment in which the proteins localize." J Virol **75**(17): 7904-12.
- Agbottah, E., C. de La Fuente, et al. (2005). "Antiviral activity of CYC202 in HIV-1-infected cells." J Biol Chem **280**(4): 3029-42.
- Akoulitchev, S., T. P. Makela, et al. (1995). "Requirement for TFIIH kinase activity in transcription by RNA polymerase II." Nature **377**(6549): 557-60.
- Allison, L. A., M. Moyle, et al. (1985). "Extensive homology among the largest subunits of eukaryotic and prokaryotic RNA polymerases." Cell **42**(2): 599-610.
- Ammosova, T., R. Berro, et al. (2006). "Phosphorylation of HIV-1 Tat by CDK2 in HIV-1 transcription." Retrovirology **3**: 78.
- Arents, G., R. W. Burlingame, et al. (1991). "The nucleosomal core histone octamer at 3.1 Å resolution: a tripartite protein assembly and a left-handed superhelix." Proc Natl Acad Sci U S A **88**(22): 10148-52.
- Arents, G. and E. N. Moudrianakis (1995). "The histone fold: a ubiquitous architectural motif utilized in DNA compaction and protein dimerization." Proc Natl Acad Sci U S A **92**(24): 11170-4.
- Ascoli, C. A. and G. G. Maul (1991). "Identification of a novel nuclear domain." J Cell Biol **112**(5): 785-95.
- Ausio, J., F. Dong, et al. (1989). "Use of selectively trypsinized nucleosome core particles to analyze the role of the histone "tails" in the stabilization of the nucleosome." J Mol Biol **206**(3): 451-63.
- Axel, R., W. Melchior, Jr., et al. (1974). "Specific sites of interaction between histones and DNA in chromatin." Proc Natl Acad Sci U S A **71**(10): 4101-5.
- Bach, S., M. Knockaert, et al. (2005). "Roscovitine targets, protein kinases and pyridoxal kinase." J Biol Chem **280**(35): 31208-19.
- Baldick, C. J., Jr. and T. Shenk (1996). "Proteins associated with purified human cytomegalovirus particles." J Virol **70**(9): 6097-105.
- Batterson, W., D. Furlong, et al. (1983). "Molecular genetics of herpes simplex virus. VIII. further characterization of a temperature-sensitive mutant defective in release of viral DNA and in other stages of the viral reproductive cycle." J Virol **45**(1): 397-407.
- Bechtel, J. T., R. C. Winant, et al. (2005). "Host and viral proteins in the virion of Kaposi's sarcoma-associated herpesvirus." J Virol **79**(8): 4952-64.
- Bellard, M., P. Oudet, et al. (1976). "Subunit structure of simian-virus-40 minichromosome." Eur J Biochem **70**(2): 543-53.
- Berthet, C., E. Aleem, et al. (2003). "Cdk2 knockout mice are viable." Curr Biol **13**(20): 1775-85.

- Bloom, D. C., N. V. Giordani, et al. (2010). "Epigenetic regulation of latent HSV-1 gene expression." *Biochim Biophys Acta* **1799**(3-4): 246-56.
- Booy, F. P., W. W. Newcomb, et al. (1991). "Liquid-crystalline, phage-like packing of encapsidated DNA in herpes simplex virus." *Cell* **64**(5): 1007-15.
- Bortz, E., J. P. Whitelegge, et al. (2003). "Identification of proteins associated with murine gammaherpesvirus 68 virions." *J Virol* **77**(24): 13425-32.
- Brehm, A., E. A. Miska, et al. (1998). "Retinoblastoma protein recruits histone deacetylase to repress transcription." *Nature* **391**(6667): 597-601.
- Bresnahan, W. A., I. Boldogh, et al. (1997). "Inhibition of cellular Cdk2 activity blocks human cytomegalovirus replication." *Virology* **231**(2): 239-47.
- Brown, D. T., M. Westphal, et al. (1975). "Structure and composition of the adenovirus type 2 core." *J Virol* **16**(2): 366-87.
- Buratowski, S. (2009). "Progression through the RNA polymerase II CTD cycle." *Mol Cell* **36**(4): 541-6.
- Cai, W. and P. A. Schaffer (1991). "A cellular function can enhance gene expression and plating efficiency of a mutant defective in the gene for ICP0, a transactivating protein of herpes simplex virus type 1." *J Virol* **65**(8): 4078-90.
- Campadelli-Fiume, G. (2007). The egress of alphaherpesviruses from the cell. *Human Herpesviruses Biology, Therapy, and Immunoprophylaxis*. G. C.-F. Ann Arvin, Edward Mocarski, Patrick S. Moore, Bernard Roizman, Richard Whitley, and Koichi Yamanishi. New York, Cambridge University Press: 151-162.
- Campadelli-Fiume, G., M. Amasio, et al. (2007). "The multipartite system that mediates entry of herpes simplex virus into the cell." *Rev Med Virol* **17**(5): 313-26.
- Campos, E. I. and D. Reinberg (2009). "Histones: annotating chromatin." *Annu Rev Genet* **43**: 559-99.
- Chakravarthy, S., Y. Bao, et al. (2004). "Structural characterization of histone H2A variants." *Cold Spring Harb Symp Quant Biol* **69**: 227-34.
- Chandy, M., J. L. Gutierrez, et al. (2006). "SWI/SNF displaces SAGA-acetylated nucleosomes." *Eukaryot Cell* **5**(10): 1738-47.
- Chen, H. Z., S. Y. Tsai, et al. (2009). "Emerging roles of E2Fs in cancer: an exit from cell cycle control." *Nat Rev Cancer* **9**(11): 785-97.
- Christiansen, G., T. Landers, et al. (1977). "Characterization of components released by alkali disruption of simian virus 40." *J Virol* **21**(3): 1079-84.
- Cliffe, A. R., D. A. Garber, et al. (2009). "Transcription of the Herpes Simplex Virus Latency-Associated Transcript Promotes the Formation of Facultative Heterochromatin on Lytic Promoters." *J Virol*.
- Cohen, G. H., M. Ponce de Leon, et al. (1980). "Structural analysis of the capsid polypeptides of herpes simplex virus types 1 and 2." *J Virol* **34**(2): 521-31.
- Cohen, G. H., R. K. Vaughan, et al. (1971). "Deoxyribonucleic acid synthesis in synchronized mammalian KB cells infected with herpes simplex virus." *J Virol* **7**(6): 783-91.

- Corden, J., H. M. Engelking, et al. (1976). "Chromatin-like organization of the adenovirus chromosome." Proc Natl Acad Sci U S A **73**(2): 401-4.
- Corden, J. L., D. L. Cadena, et al. (1985). "A unique structure at the carboxyl terminus of the largest subunit of eukaryotic RNA polymerase II." Proc Natl Acad Sci U S A **82**(23): 7934-8.
- Cremisi, C., P. F. Pignatti, et al. (1975). "Chromatin-like structures in polyoma virus and simian virus 10 lytic cycle." J Virol **17**(1): 204-11.
- Daksis, J. I. and C. M. Preston (1992). "Herpes simplex virus immediate early gene expression in the absence of transduction by Vmw65 varies during the cell cycle." Virology **189**(1): 196-202.
- Dalal, Y., T. Furuyama, et al. (2007). "Structure, dynamics, and evolution of centromeric nucleosomes." Proc Natl Acad Sci U S A **104**(41): 15974-81.
- Dalal, Y., H. Wang, et al. (2007). "Tetrameric structure of centromeric nucleosomes in interphase *Drosophila* cells." PLoS Biol **5**(8): e218.
- Daniell, E., D. E. Groff, et al. (1981). "Adenovirus chromatin structure at different stages of infection." Mol Cell Biol **1**(12): 1094-105.
- Davido, D. J., D. A. Leib, et al. (2002). "The cyclin-dependent kinase inhibitor roscovitine inhibits the transactivating activity and alters the posttranslational modification of herpes simplex virus type 1 ICP0." J Virol **76**(3): 1077-88.
- Davison, A. J. and N. M. Wilkie (1981). "Nucleotide sequences of the joint between the L and S segments of herpes simplex virus types 1 and 2." J Gen Virol **55**(Pt 2): 315-31.
- De Azevedo, W. F., S. Leclerc, et al. (1997). "Inhibition of cyclin-dependent kinases by purine analogues: crystal structure of human cdk2 complexed with roscovitine." Eur J Biochem **243**(1-2): 518-26.
- de Bruyn Kops, A. and D. M. Knipe (1988). "Formation of DNA replication structures in herpes virus-infected cells requires a viral DNA binding protein." Cell **55**(5): 857-68.
- Deng, L., T. Ammosova, et al. (2002). "HIV-1 Tat interaction with RNA polymerase II C-terminal domain (CTD) and a dynamic association with CDK2 induce CTD phosphorylation and transcription from HIV-1 promoter." J Biol Chem **277**(37): 33922-9.
- Dery, C. V., M. Toth, et al. (1985). "The structure of adenovirus chromatin in infected cells." J Gen Virol **66** (Pt 12): 2671-84.
- Deshmane, S. L. and N. W. Fraser (1989). "During latency, herpes simplex virus type 1 DNA is associated with nucleosomes in a chromatin structure." J Virol **63**(2): 943-7.
- Dietrich, M. A., J. P. Prenger, et al. (1990). "Analysis of the genes encoding the largest subunit of RNA polymerase II in *Arabidopsis* and soybean." Plant Mol Biol **15**(2): 207-23.
- Dorigo, B., T. Schalch, et al. (2003). "Chromatin fiber folding: requirement for the histone H4 N-terminal tail." J Mol Biol **327**(1): 85-96.
- Dorigo, B., T. Schalch, et al. (2004). "Nucleosome arrays reveal the two-start organization of the chromatin fiber." Science **306**(5701): 1571-3.

- Dulbecco, R., L. H. Hartwell, et al. (1965). "Induction of Cellular DNA Synthesis by Polyoma Virus." Proc Natl Acad Sci U S A **53**: 403-10.
- Dyson, N., P. M. Howley, et al. (1989). "The human papilloma virus-16 E7 oncoprotein is able to bind to the retinoblastoma gene product." Science **243**(4893): 934-7.
- Egloff, S. and S. Murphy (2008). "Cracking the RNA polymerase II CTD code." Trends Genet **24**(6): 280-8.
- Ehmann, G. L., H. A. Burnett, et al. (2001). "Pocket protein p130/Rb2 is required for efficient herpes simplex virus type 1 gene expression and viral replication." J Virol **75**(15): 7149-60.
- Ehmann, G. L., T. I. McLean, et al. (2000). "Herpes simplex virus type 1 infection imposes a G(1)/S block in asynchronously growing cells and prevents G(1) entry in quiescent cells." Virology **267**(2): 335-49.
- Eitoku, M., L. Sato, et al. (2008). "Histone chaperones: 30 years from isolation to elucidation of the mechanisms of nucleosome assembly and disassembly." Cell Mol Life Sci **65**(3): 414-44.
- Elgadi, M. M., C. E. Hayes, et al. (1999). "The herpes simplex virus vhs protein induces endoribonucleolytic cleavage of target RNAs in cell extracts." J Virol **73**(9): 7153-64.
- Elliott, G., G. Mouzakis, et al. (1995). "VP16 interacts via its activation domain with VP22, a tegument protein of herpes simplex virus, and is relocated to a novel macromolecular assembly in coexpressing cells." J Virol **69**(12): 7932-41.
- Elliott, G. and P. O'Hare (1998). "Herpes simplex virus type 1 tegument protein VP22 induces the stabilization and hyperacetylation of microtubules." J Virol **72**(8): 6448-55.
- Elsaesser, S. J., A. D. Goldberg, et al. (2010). "New functions for an old variant: no substitute for histone H3.3." Curr Opin Genet Dev **20**(2): 110-7.
- Eltsov, M., K. M. Maclellan, et al. (2008). "Analysis of cryo-electron microscopy images does not support the existence of 30-nm chromatin fibers in mitotic chromosomes in situ." Proc Natl Acad Sci U S A **105**(50): 19732-7.
- Everett, R. D. (2004). "Herpes simplex virus type 1 regulatory protein ICP0 does not protect cyclins D1 and D3 from degradation during infection." J Virol **78**(18): 9599-604.
- Everett, R. D. and J. Murray (2005). "ND10 components relocate to sites associated with herpes simplex virus type 1 nucleoprotein complexes during virus infection." J Virol **79**(8): 5078-89.
- Everly, D. N., Jr., P. Feng, et al. (2002). "mRNA degradation by the virion host shutoff (Vhs) protein of herpes simplex virus: genetic and biochemical evidence that Vhs is a nuclease." J Virol **76**(17): 8560-71.
- Everly, D. N., Jr. and G. S. Read (1999). "Site-directed mutagenesis of the virion host shutoff gene (UL41) of herpes simplex virus (HSV): analysis of functional differences between HSV type 1 (HSV-1) and HSV-2 alleles." J Virol **73**(11): 9117-29.

- Fabian, M. A., W. H. Biggs, 3rd, et al. (2005). "A small molecule-kinase interaction map for clinical kinase inhibitors." Nat Biotechnol **23**(3): 329-36.
- Fan, Y., T. Nikitina, et al. (2003). "H1 linker histones are essential for mouse development and affect nucleosome spacing in vivo." Mol Cell Biol **23**(13): 4559-72.
- Favre, M., F. Breitburd, et al. (1977). "Chromatin-like structures obtained after alkaline disruption of bovine and human papillomaviruses." J Virol **21**(3): 1205-9.
- Feldman, L. T., A. R. Ellison, et al. (2002). "Spontaneous molecular reactivation of herpes simplex virus type 1 latency in mice." Proc Natl Acad Sci U S A **99**(2): 978-83.
- Fenwick, M. L. and M. M. McMenamin (1984). "Early virion-associated suppression of cellular protein synthesis by herpes simplex virus is accompanied by inactivation of mRNA." J Gen Virol **65 (Pt 7)**: 1225-8.
- Ferenczy, M. W. and N. A. Deluca (2009). "Epigenetic Modulation of Gene Expression from Quiescent Hsv Genomes." J Virol.
- Fields, B. N., D. M. Knipe, and P. M. Howley. (2007). Fields' virology, 5th ed. Philadelphia, Wolters Kluwer Health/Lippincott Williams & Wilkins.
- Finch, J. T. and A. Klug (1976). "Solenoidal model for superstructure in chromatin." Proc Natl Acad Sci U S A **73**(6): 1897-901.
- Fletcher, T. M. and J. C. Hansen (1995). "Core histone tail domains mediate oligonucleosome folding and nucleosomal DNA organization through distinct molecular mechanisms." J Biol Chem **270**(43): 25359-62.
- Flores, O., H. Lu, et al. (1992). "Factors involved in specific transcription by mammalian RNA polymerase II. Identification and characterization of factor IIIH." J Biol Chem **267**(4): 2786-93.
- Flores, O., E. Maldonado, et al. (1989). "Factors involved in specific transcription by mammalian RNA polymerase II. Factors IIE and IIF independently interact with RNA polymerase II." J Biol Chem **264**(15): 8913-21.
- Garber, D. A., S. M. Beverley, et al. (1993). "Demonstration of circularization of herpes simplex virus DNA following infection using pulsed field gel electrophoresis." Virology **197**(1): 459-62.
- Garcia-Ramirez, M., F. Dong, et al. (1992). "Role of the histone "tails" in the folding of oligonucleosomes depleted of histone H1." J Biol Chem **267**(27): 19587-95.
- Garcia-Ramirez, M., C. Rocchini, et al. (1995). "Modulation of chromatin folding by histone acetylation." J Biol Chem **270**(30): 17923-8.
- Ge, H., E. Martinez, et al. (1996). "Activator-dependent transcription by mammalian RNA polymerase II: in vitro reconstitution with general transcription factors and cofactors." Methods Enzymol **274**: 57-71.
- Germond, J. E., B. Hirt, et al. (1975). "Folding of the DNA double helix in chromatin-like structures from simian virus 40." Proc Natl Acad Sci U S A **72**(5): 1843-7.

- Gianni, T., M. Amasio, et al. (2009). "Herpes simplex virus gD forms distinct complexes with fusion executors gB and gH/gL in part through the C-terminal profusion domain." J Biol Chem **284**(26): 17370-82.
- Gibson, W. (1996). "Structure and assembly of the virion." Intervirology **39**(5-6): 389-400.
- Gibson, W. and B. Roizman (1971). "Compartmentalization of spermine and spermidine in the herpes simplex virion." Proc Natl Acad Sci U S A **68**(11): 2818-21.
- Godde, J. S. and K. Ura (2008). "Cracking the enigmatic linker histone code." J Biochem **143**(3): 287-93.
- Godowski, P. J. and D. M. Knipe (1986). "Transcriptional control of herpesvirus gene expression: gene functions required for positive and negative regulation." Proc Natl Acad Sci U S A **83**(2): 256-60.
- Gold, M. O., J. P. Tassan, et al. (1996). "Viral transactivators E1A and VP16 interact with a large complex that is associated with CTD kinase activity and contains CDK8." Nucleic Acids Res **24**(19): 3771-7.
- Gold, M. O., X. Yang, et al. (1998). "PITALRE, the catalytic subunit of TAK, is required for human immunodeficiency virus Tat transactivation in vivo." J Virol **72**(5): 4448-53.
- Goodrich, J. A., T. Hoey, et al. (1993). "Drosophila TAFII40 interacts with both a VP16 activation domain and the basal transcription factor TFIIB." Cell **75**(3): 519-30.
- Greil, W., T. Igo-Kemenes, et al. (1976). "Nuclease digestion in between and within nucleosomes." Nucleic Acids Res **3**(10): 2633-44.
- Griffith, J. D. (1975). "Chromatin Structure: Deduced from a Minichromosome." Science **187**(4182): 1202-1203.
- Habran, L., S. Bontems, et al. (2005). "Varicella-zoster virus IE63 protein phosphorylation by roscovitine-sensitive cyclin-dependent kinases modulates its cellular localization and activity." J Biol Chem **280**(32): 29135-43.
- Hall, D. B. and K. Struhl (2002). "The VP16 activation domain interacts with multiple transcriptional components as determined by protein-protein cross-linking in vivo." J Biol Chem **277**(48): 46043-50.
- Hall, M. R., N. Aghili, et al. (1982). "Chromosomal organization of the herpes simplex virus type 2 genome." Virology **123**(2): 344-56.
- Hamiche, A., P. Schultz, et al. (1996). "Linker histone-dependent DNA structure in linear mononucleosomes." J Mol Biol **257**(1): 30-42.
- Hancock, R. and R. Weil (1969). "Biochemical evidence for induction by polyoma virus of replication of the chromosomes of mouse kidney cells." Proc Natl Acad Sci U S A **63**(4): 1144-50.
- Happel, N. and D. Doenecke (2009). "Histone H1 and its isoforms: contribution to chromatin structure and function." Gene **431**(1-2): 1-12.
- Hardy, W. R. and R. M. Sandri-Goldin (1994). "Herpes simplex virus inhibits host cell splicing, and regulatory protein ICP27 is required for this effect." J Virol **68**(12): 7790-9.

- Harris-Hamilton, E. and S. L. Bachenheimer (1985). "Accumulation of herpes simplex virus type 1 RNAs of different kinetic classes in the cytoplasm of infected cells." J Virol **53**(1): 144-51.
- Hashimoto, H., Y. Takami, et al. (2010). "Histone H1 null vertebrate cells exhibit altered nucleosome architecture." Nucleic Acids Res.
- Hassan, A. H., S. Awad, et al. (2006). "The Swi2/Snf2 bromodomain is required for the displacement of SAGA and the octamer transfer of SAGA-acetylated nucleosomes." J Biol Chem **281**(26): 18126-34.
- Hayes, J. J., D. J. Clark, et al. (1991). "Histone contributions to the structure of DNA in the nucleosome." Proc Natl Acad Sci U S A **88**(15): 6829-33.
- Hayes, J. J., T. D. Tullius, et al. (1990). "The structure of DNA in a nucleosome." Proc Natl Acad Sci U S A **87**(19): 7405-9.
- Heldwein, E. E. and C. Krummenacher (2008). "Entry of herpesviruses into mammalian cells." Cell Mol Life Sci **65**(11): 1653-68.
- Heldwein, E. E., H. Lou, et al. (2006). "Crystal structure of glycoprotein B from herpes simplex virus 1." Science **313**(5784): 217-20.
- Henzel, M. J., M. A. Lever, et al. (2004). "The C-terminal domain is the primary determinant of histone H1 binding to chromatin in vivo." J Biol Chem **279**(19): 20028-34.
- Hengartner, C. J., V. E. Myer, et al. (1998). "Temporal regulation of RNA polymerase II by Srb10 and Kin28 cyclin-dependent kinases." Mol Cell **2**(1): 43-53.
- Herrera, F. J. and S. J. Triezenberg (2004). "VP16-dependent association of chromatin-modifying coactivators and underrepresentation of histones at immediate-early gene promoters during herpes simplex virus infection." J Virol **78**(18): 9689-96.
- Herrmann, C. H., M. O. Gold, et al. (1996). "Viral transactivators specifically target distinct cellular protein kinases that phosphorylate the RNA polymerase II C-terminal domain." Nucleic Acids Res **24**(3): 501-8.
- Hilton, M. J., D. Mounghane, et al. (1995). "Induction by herpes simplex virus of free and heteromeric forms of E2F transcription factor." Virology **213**(2): 624-38.
- Hirose, Y. and Y. Ohkuma (2007). "Phosphorylation of the C-terminal domain of RNA polymerase II plays central roles in the integrated events of eucaryotic gene expression." J Biochem **141**(5): 601-8.
- Honess, R. W. (1984). "Herpes simplex and 'the herpes complex': diverse observations and a unifying hypothesis. The eighth Fleming lecture." J Gen Virol **65** (Pt 12): 2077-107.
- Honess, R. W. and B. Roizman (1973). "Proteins specified by herpes simplex virus. XI. Identification and relative molar rates of synthesis of structural and nonstructural herpes virus polypeptides in the infected cell." J Virol **12**(6): 1347-65.
- Honess, R. W. and B. Roizman (1974). "Regulation of herpesvirus macromolecular synthesis. I. Cascade regulation of the synthesis of three groups of viral proteins." J Virol **14**(1): 8-19.

- Hossain, A., T. Holt, et al. (1997). "Analysis of cyclin-dependent kinase activity after herpes simplex virus type 2 infection." J Gen Virol **78** (Pt 12): 3341-8.
- Hu, Q. J., N. Dyson, et al. (1990). "The regions of the retinoblastoma protein needed for binding to adenovirus E1A or SV40 large T antigen are common sites for mutations." Embo J **9**(4): 1147-55.
- Huang, J., J. R. Kent, et al. (2006). "Trimethylation of histone H3 lysine 4 by Set1 in the lytic infection of human herpes simplex virus 1." J Virol **80**(12): 5740-6.
- Ikeda, K., T. Stuehler, et al. (2002). "The H1 and H2 regions of the activation domain of herpes simplex virion protein 16 stimulate transcription through distinct molecular mechanisms." Genes Cells **7**(1): 49-58.
- Ingles, C. J., M. Shales, et al. (1991). "Reduced binding of TFIID to transcriptionally compromised mutants of VP16." Nature **351**(6327): 588-90.
- Ishov, A. M. and G. G. Maul (1996). "The periphery of nuclear domain 10 (ND10) as site of DNA virus deposition." J Cell Biol **134**(4): 815-26.
- Ito, T., T. Ikehara, et al. (2000). "p300-mediated acetylation facilitates the transfer of histone H2A-H2B dimers from nucleosomes to a histone chaperone." Genes Dev **14**(15): 1899-907.
- Jakobovits, E. B., S. Bratosin, et al. (1980). "A nucleosome-free region in SV40 minichromosomes." Nature **285**(5762): 263-5.
- Jenuwein, T. and C. D. Allis (2001). "Translating the histone code." Science **293**(5532): 1074-80.
- Jin, C. and G. Felsenfeld (2007). "Nucleosome stability mediated by histone variants H3.3 and H2A.Z." Genes Dev **21**(12): 1519-29.
- Jin, C., C. Zang, et al. (2009). "H3.3/H2A.Z double variant-containing nucleosomes mark 'nucleosome-free regions' of active promoters and other regulatory regions." Nat Genet **41**(8): 941-5.
- Johannsen, E., M. Luftig, et al. (2004). "Proteins of purified Epstein-Barr virus." Proc Natl Acad Sci U S A **101**(46): 16286-91.
- Johnson, D. C. and P. G. Spear (1984). "Evidence for translational regulation of herpes simplex virus type 1 gD expression." J Virol **51**(2): 389-94.
- Jones, F. E., C. A. Smibert, et al. (1995). "Mutational analysis of the herpes simplex virus virion host shutoff protein: evidence that vhs functions in the absence of other viral proteins." J Virol **69**(8): 4863-71.
- Jones, K. A. and R. Tjian (1985). "Sp1 binds to promoter sequences and activates herpes simplex virus 'immediate-early' gene transcription in vitro." Nature **317**(6033): 179-82.
- Jordan, R., L. Schang, et al. (1999). "Transactivation of herpes simplex virus type 1 immediate-early gene expression by virion-associated factors is blocked by an inhibitor of cyclin-dependent protein kinases." J Virol **73**(10): 8843-7.
- Karaman, M. W., S. Herrgard, et al. (2008). "A quantitative analysis of kinase inhibitor selectivity." Nat Biotechnol **26**(1): 127-32.

- Kattenhorn, L. M., R. Mills, et al. (2004). "Identification of proteins associated with murine cytomegalovirus virions." J Virol **78**(20): 11187-97.
- Kent, J. R., P. Y. Zeng, et al. (2004). "During lytic infection herpes simplex virus type 1 is associated with histones bearing modifications that correlate with active transcription." J Virol **78**(18): 10178-86.
- Kim, J. B. and P. A. Sharp (2001). "Positive transcription elongation factor B phosphorylates hSPT5 and RNA polymerase II carboxyl-terminal domain independently of cyclin-dependent kinase-activating kinase." J Biol Chem **276**(15): 12317-23.
- Klemm, R. D., J. A. Goodrich, et al. (1995). "Molecular cloning and expression of the 32-kDa subunit of human TFIID reveals interactions with VP16 and TFIIB that mediate transcriptional activation." Proc Natl Acad Sci U S A **92**(13): 5788-92.
- Knipe, D. M., W. Batterson, et al. (1981). "Molecular genetics of herpes simplex virus. VI. Characterization of a temperature-sensitive mutant defective in the expression of all early viral gene products." J Virol **38**(2): 539-47.
- Knipe, D. M. and A. Cliffe (2008). "Chromatin control of herpes simplex virus lytic and latent infection." Nat Rev Microbiol **6**(3): 211-21.
- Kobayashi, N., T. G. Boyer, et al. (1995). "A class of activation domains interacts directly with TFIIA and stimulates TFIIA-TFIID-promoter complex assembly." Mol Cell Biol **15**(11): 6465-73.
- Kolb, G. and T. M. Kristie (2008). "Association of the cellular coactivator HCF-1 with the Golgi apparatus in sensory neurons." J Virol **82**(19): 9555-63.
- Koleske, A. J. and R. A. Young (1995). "The RNA polymerase II holoenzyme and its implications for gene regulation." Trends in Biochemical Sciences **20**(3): 113-116.
- Kornberg, R. D. (1974). "Chromatin structure: a repeating unit of histones and DNA." Science **184**(139): 868-71.
- Kotsakis, A., L. E. Pomeranz, et al. (2001). "Microtubule reorganization during herpes simplex virus type 1 infection facilitates the nuclear localization of VP22, a major virion tegument protein." J Virol **75**(18): 8697-711.
- Kouzarides, T. (2007). "Chromatin modifications and their function." Cell **128**(4): 693-705.
- Kovesdi, I., R. Reichel, et al. (1986). "Identification of a cellular transcription factor involved in E1A trans-activation." Cell **45**(2): 219-28.
- Kramer, M. F., S. H. Chen, et al. (1998). "Accumulation of viral transcripts and DNA during establishment of latency by herpes simplex virus." J Virol **72**(2): 1177-85.
- Kramer, M. F. and D. M. Coen (1995). "Quantification of transcripts from the ICP4 and thymidine kinase genes in mouse ganglia latently infected with herpes simplex virus." J Virol **69**(3): 1389-99.
- Kristie, T. M. (2007). Early events pre-initiation of alphaherpes viral gene expression. Human Herpesviruses Biology, Therapy, and Immunoprophylaxis. G. C.-F. Ann Arvin, Edward Mocarski, Patrick S. Moore, Bernard Roizman, Richard Whitley, and Koichi Yamanishi. New York, Cambridge University Press: 112-127.

- Kristie, T. M., Y. Liang, et al. (2010). "Control of alpha-herpesvirus IE gene expression by HCF-1 coupled chromatin modification activities." Biochim Biophys Acta **1799**(3-4): 257-65.
- Kristie, T. M. and P. A. Sharp (1990). "Interactions of the Oct-1 POU subdomains with specific DNA sequences and with the HSV alpha-trans-activator protein." Genes Dev **4**(12B): 2383-96.
- Kristie, T. M. and P. A. Sharp (1993). "Purification of the cellular C1 factor required for the stable recognition of the Oct-1 homeodomain by the herpes simplex virus alpha-trans-induction factor (VP16)." J Biol Chem **268**(9): 6525-34.
- Kubat, N. J., A. L. Amelio, et al. (2004). "The herpes simplex virus type 1 latency-associated transcript (LAT) enhancer/rcr is hyperacetylated during latency independently of LAT transcription." J Virol **78**(22): 12508-18.
- Kubat, N. J., R. K. Tran, et al. (2004). "Specific histone tail modification and not DNA methylation is a determinant of herpes simplex virus type 1 latent gene expression." J Virol **78**(3): 1139-49.
- Kudoh, A., T. Daikoku, et al. (2004). "Inhibition of S-phase cyclin-dependent kinase activity blocks expression of Epstein-Barr virus immediate-early and early genes, preventing viral lytic replication." J Virol **78**(1): 104-15.
- Kutluay, S. B., S. L. DeVos, et al. (2009). "Transcriptional coactivators are not required for herpes simplex virus type 1 immediate-early gene expression in vitro." J Virol **83**(8): 3436-49.
- Kutluay, S. B. and S. J. Triezenberg (2009). "Regulation of histone deposition on the herpes simplex virus type 1 genome during lytic infection." J Virol **83**(11): 5835-45.
- Kwiatkowski, D. L., H. W. Thompson, et al. (2009). "Polycomb group protein Bmi1 binds to the HSV-1 latent genome and maintains repressive histone marks during latency." J Virol.
- La Boissiere, S., T. Hughes, et al. (1999). "HCF-dependent nuclear import of VP16." Embo J **18**(2): 480-9.
- LaMarco, K. L. and S. L. McKnight (1989). "Purification of a set of cellular polypeptides that bind to the purine-rich cis-regulatory element of herpes simplex virus immediate early genes." Genes Dev **3**(9): 1372-83.
- Leinbach, S. S. and W. C. Summers (1980). "The structure of herpes simplex virus type 1 DNA as probed by micrococcal nuclease digestion." J Gen Virol **51**(Pt 1): 45-59.
- Lever, M. A., J. P. Th'ng, et al. (2000). "Rapid exchange of histone H1.1 on chromatin in living human cells." Nature **408**(6814): 873-6.
- Li, B., M. Carey, et al. (2007). "The role of chromatin during transcription." Cell **128**(4): 707-19.
- Liang, Y., J. L. Vogel, et al. (2009). "Inhibition of the histone demethylase LSD1 blocks alpha-herpesvirus lytic replication and reactivation from latency." Nat Med **15**(11): 1312-7.
- Lieberman, P. M. (2008). "Chromatin organization and virus gene expression." J Cell Physiol **216**(2): 295-302.

- Lin, Y. S. and M. R. Green (1991). "Mechanism of action of an acidic transcriptional activator in vitro." *Cell* **64**(5): 971-81.
- Lin, Y. S., I. Ha, et al. (1991). "Binding of general transcription factor TFIIB to an acidic activating region." *Nature* **353**(6344): 569-71.
- Long, M. C., V. Leong, et al. (1999). "ICP22 and the UL13 protein kinase are both required for herpes simplex virus-induced modification of the large subunit of RNA polymerase II." *J Virol* **73**(7): 5593-604.
- Loret, S., G. Guay, et al. (2008). "Comprehensive characterization of extracellular herpes simplex virus type 1 virions." *J Virol* **82**(17): 8605-18.
- Lowary, P. T. and J. Widom (1998). "New DNA sequence rules for high affinity binding to histone octamer and sequence-directed nucleosome positioning." *J Mol Biol* **276**(1): 19-42.
- Lu, H., L. Zawel, et al. (1992). "Human general transcription factor IIIH phosphorylates the C-terminal domain of RNA polymerase II." *Nature* **358**(6388): 641-5.
- Lu, X., B. Hamkalo, et al. (2009). "Chromatin condensing functions of the linker histone C-terminal domain are mediated by specific amino acid composition and intrinsic protein disorder." *Biochemistry* **48**(1): 164-72.
- Lu, X. and J. C. Hansen (2004). "Identification of specific functional subdomains within the linker histone H10 C-terminal domain." *J Biol Chem* **279**(10): 8701-7.
- Luger, K., A. W. Mader, et al. (1997). "Crystal structure of the nucleosome core particle at 2.8 Å resolution." *Nature* **389**(6648): 251-60.
- Luger, K., T. J. Rechsteiner, et al. (1999). "Preparation of nucleosome core particle from recombinant histones." *Methods Enzymol* **304**: 3-19.
- Luo, R. X., A. A. Postigo, et al. (1998). "Rb interacts with histone deacetylase to repress transcription." *Cell* **92**(4): 463-73.
- Lycke, E., K. Kristensson, et al. (1984). "Uptake and transport of herpes simplex virus in neurites of rat dorsal root ganglia cells in culture." *J Gen Virol* **65** (Pt 1): 55-64.
- Mackem, S. and B. Roizman (1982). "Structural features of the herpes simplex virus alpha gene 4, 0, and 27 promoter-regulatory sequences which confer alpha regulation on chimeric thymidine kinase genes." *J Virol* **44**(3): 939-49.
- Magnaghi-Jaulin, L., R. Groisman, et al. (1998). "Retinoblastoma protein represses transcription by recruiting a histone deacetylase." *Nature* **391**(6667): 601-5.
- Malumbres, M., R. Sotillo, et al. (2004). "Mammalian cells cycle without the D-type cyclin-dependent kinases Cdk4 and Cdk6." *Cell* **118**(4): 493-504.
- Mandal, S. S., C. Chu, et al. (2004). "Functional interactions of RNA-capping enzyme with factors that positively and negatively regulate promoter escape by RNA polymerase II." *Proc Natl Acad Sci U S A* **101**(20): 7572-7.
- Marky, N. L. and G. S. Manning (1995). "A theory of DNA dissociation from the nucleosome." *J Mol Biol* **254**(1): 50-61.

- Marshall, N. F. and D. H. Price (1995). "Purification of P-TEFb, a transcription factor required for the transition into productive elongation." J Biol Chem **270**(21): 12335-8.
- Maul, G. G., A. M. Ishov, et al. (1996). "Nuclear domain 10 as preexisting potential replication start sites of herpes simplex virus type-1." Virology **217**(1): 67-75.
- Meijer, L., A. Borgne, et al. (1997). "Biochemical and cellular effects of roscovitine, a potent and selective inhibitor of the cyclin-dependent kinases cdc2, cdk2 and cdk5." Eur J Biochem **243**(1-2): 527-36.
- Meinke, W., M. R. Hall, et al. (1975). "Proteins in intracellular simian virus 40 nucleoprotein complexes: comparison with simian virus 40 core proteins." J Virol **15**(3): 439-48.
- Mellerick, D. M. and N. W. Fraser (1987). "Physical state of the latent herpes simplex virus genome in a mouse model system: evidence suggesting an episomal state." Virology **158**(2): 265-75.
- Memedula, S. and A. S. Belmont (2003). "Sequential recruitment of HAT and SWI/SNF components to condensed chromatin by VP16." Curr Biol **13**(3): 241-6.
- Mirza, M. A. and J. Weber (1982). "Structure of adenovirus chromatin." Biochim Biophys Acta **696**(1): 76-86.
- Mirza, M. A. and J. M. Weber (1981). "Structure of adenovirus chromatin as probed with restriction endonucleases." Virology **108**(2): 351-60.
- Misteli, T., A. Gunjan, et al. (2000). "Dynamic binding of histone H1 to chromatin in living cells." Nature **408**(6814): 877-81.
- Mittler, G., E. Kremmer, et al. (2001). "Novel critical role of a human Mediator complex for basal RNA polymerase II transcription." EMBO Rep **2**(9): 808-13.
- Miyamoto, K. and C. Morgan (1971). "Structure and development of viruses as observed in the electron microscope. XI. Entry and uncoating of herpes simplex virus." J Virol **8**(6): 910-8.
- Mocarski, E. S. and B. Roizman (1982). "Structure and role of the herpes simplex virus DNA termini in inversion, circularization and generation of virion DNA." Cell **31**(1): 89-97.
- Monier, K., J. C. Armas, et al. (2000). "Annexation of the interchromosomal space during viral infection." Nat Cell Biol **2**(9): 661-5.
- Mouttet, M. E., D. Guetard, et al. (1979). "Random cleavage of intranuclear herpes simplex virus DNA by micrococcal nuclease." FEBS Lett **100**(1): 107-9.
- Muggeridge, M. I. and N. W. Fraser (1986). "Chromosomal organization of the herpes simplex virus genome during acute infection of the mouse central nervous system." J Virol **59**(3): 764-7.
- Muller, U., C. H. Schroder, et al. (1980). "Coexistence of nucleosomal and various non-nucleosomal chromatin configurations in cells infected with herpes simplex virus." Eur J Cell Biol **23**(1): 197-203.
- Narayanan, A., M. L. Nogueira, et al. (2005). "Combinatorial transcription of herpes simplex virus and varicella zoster virus immediate early genes is

- strictly determined by the cellular coactivator HCF-1." J Biol Chem **280**(2): 1369-75.
- Narayanan, A., W. T. Ruyechan, et al. (2007). "The coactivator host cell factor-1 mediates Set1 and MLL1 H3K4 trimethylation at herpesvirus immediate early promoters for initiation of infection." Proc Natl Acad Sci U S A **104**(26): 10835-40.
- Neely, K. E., A. H. Hassan, et al. (1999). "Activation domain-mediated targeting of the SWI/SNF complex to promoters stimulates transcription from nucleosome arrays." Mol Cell **4**(4): 649-55.
- Nekhai, S., M. Zhou, et al. (2002). "HIV-1 Tat-associated RNA polymerase C-terminal domain kinase, CDK2, phosphorylates CDK7 and stimulates Tat-mediated transcription." Biochem J **364**(Pt 3): 649-57.
- Nelson, P. J., I. H. Gelman, et al. (2001). "Suppression of HIV-1 expression by inhibitors of cyclin-dependent kinases promotes differentiation of infected podocytes." J Am Soc Nephrol **12**(12): 2827-31.
- Neumann, D. M., P. S. Bhattacharjee, et al. (2007). "In vivo changes in the patterns of chromatin structure associated with the latent herpes simplex virus type 1 genome in mouse trigeminal ganglia can be detected at early times after butyrate treatment." J Virol **81**(23): 13248-53.
- Nishikawa, J., T. Kokubo, et al. (1997). "Drosophila TAF(II)230 and the transcriptional activator VP16 bind competitively to the TATA box-binding domain of the TATA box-binding protein." Proc Natl Acad Sci U S A **94**(1): 85-90.
- Noll, M. (1974). "Subunit structure of chromatin." Nature **251**(5472): 249-51.
- O'Connor, C. M. and D. H. Kedes (2006). "Mass spectrometric analyses of purified rhesus monkey rhadinovirus reveal 33 virion-associated proteins." J Virol **80**(3): 1574-83.
- Oh, J. and N. W. Fraser (2008). "Temporal association of the herpes simplex virus genome with histone proteins during a lytic infection." J Virol **82**(7): 3530-7.
- Olins, A. L. and D. E. Olins (1974). "Spheroid chromatin units (v bodies)." Science **183**(122): 330-2.
- Ortega, S., I. Prieto, et al. (2003). "Cyclin-dependent kinase 2 is essential for meiosis but not for mitotic cell division in mice." Nat Genet **35**(1): 25-31.
- Ossipow, V., J. P. Tassan, et al. (1995). "A mammalian RNA polymerase II holoenzyme containing all components required for promoter-specific transcription initiation." Cell **83**(1): 137-46.
- Park, Y. J. and K. Luger (2008). "Histone chaperones in nucleosome eviction and histone exchange." Curr Opin Struct Biol **18**(3): 282-9.
- Paulus, C., A. Nitzsche, et al. (2010). "Chromatinisation of herpesvirus genomes." Rev Med Virol **20**(1): 34-50.
- Penfold, M. E., P. Armati, et al. (1994). "Axonal transport of herpes simplex virions to epidermal cells: evidence for a specialized mode of virus transport and assembly." Proc Natl Acad Sci U S A **91**(14): 6529-33.
- Peng, J., Y. Zhu, et al. (1998). "Identification of multiple cyclin subunits of human P-TEFb." Genes Dev **12**(5): 755-62.

- Petroski, M. D. and E. K. Wagner (1998). "Purification and characterization of a cellular protein that binds to the downstream activation sequence of the strict late UL38 promoter of herpes simplex virus type 1." J Virol **72**(10): 8181-90.
- Pignatti, P. F. and E. Cassai (1980). "Analysis of herpes simplex virus nucleoprotein complexes extracted from infected cells." J Virol **36**(3): 816-28.
- Placek, B. J., J. Huang, et al. (2009). "The histone variant H3.3 regulates gene expression during lytic infection with herpes simplex virus type 1." J Virol **83**(3): 1416-21.
- Poffenberger, K. L. and B. Roizman (1985). "A noninverting genome of a viable herpes simplex virus 1: presence of head-to-tail linkages in packaged genomes and requirements for circularization after infection." J Virol **53**(2): 587-95.
- Polach, K. J., P. T. Lowary, et al. (2000). "Effects of core histone tail domains on the equilibrium constants for dynamic DNA site accessibility in nucleosomes." J Mol Biol **298**(2): 211-23.
- Pruss, D., B. Bartholomew, et al. (1996). "An asymmetric model for the nucleosome: a binding site for linker histones inside the DNA gyres." Science **274**(5287): 614-7.
- Ramakrishnan, V., J. T. Finch, et al. (1993). "Crystal structure of globular domain of histone H5 and its implications for nucleosome binding." Nature **362**(6417): 219-23.
- Rane, S. G., P. Dubus, et al. (1999). "Loss of Cdk4 expression causes insulin-deficient diabetes and Cdk4 activation results in beta-islet cell hyperplasia." Nat Genet **22**(1): 44-52.
- Read, G. S. and N. Frenkel (1983). "Herpes simplex virus mutants defective in the virion-associated shutoff of host polypeptide synthesis and exhibiting abnormal synthesis of alpha (immediate early) viral polypeptides." J Virol **46**(2): 498-512.
- Reinberg, D. and R. G. Roeder (1987). "Factors involved in specific transcription by mammalian RNA polymerase II. Purification and functional analysis of initiation factors IIB and IIE." J Biol Chem **262**(7): 3310-21.
- Reinke, H. and W. Horz (2003). "Histones are first hyperacetylated and then lose contact with the activated PHO5 promoter." Mol Cell **11**(6): 1599-607.
- Ren, S. and B. J. Rollins (2004). "Cyclin C/cdk3 promotes Rb-dependent G0 exit." Cell **117**(2): 239-51.
- Rice, S. A., M. C. Long, et al. (1995). "Herpes simplex virus immediate-early protein ICP22 is required for viral modification of host RNA polymerase II and establishment of the normal viral transcription program." J Virol **69**(9): 5550-9.
- Rice, S. A., M. C. Long, et al. (1994). "RNA polymerase II is aberrantly phosphorylated and localized to viral replication compartments following herpes simplex virus infection." J Virol **68**(2): 988-1001.

- Rice, S. A., M. C. Long, et al. (1994). "RNA polymerase II is aberrantly phosphorylated and localized to viral replication compartments following herpes simplex virus infection." *Journal of Virology* **68**(2): 988-1001.
- Rickert, P., W. Seghezzi, et al. (1996). "Cyclin C/CDK8 is a novel CTD kinase associated with RNA polymerase II." *Oncogene* **12**(12): 2631-40.
- Roche, S., S. Bressanelli, et al. (2006). "Crystal structure of the low-pH form of the vesicular stomatitis virus glycoprotein G." *Science* **313**(5784): 187-91.
- Rock, D. L. and N. W. Fraser (1983). "Detection of HSV-1 genome in central nervous system of latently infected mice." *Nature* **302**(5908): 523-5.
- Rock, D. L. and N. W. Fraser (1985). "Latent herpes simplex virus type 1 DNA contains two copies of the virion DNA joint region." *J Virol* **55**(3): 849-52.
- Roy, R., J. P. Adamczewski, et al. (1994). "The MO15 cell cycle kinase is associated with the TFIIH transcription-DNA repair factor." *Cell* **79**(6): 1093-101.
- Sanchez, V., A. K. McElroy, et al. (2004). "Cyclin-dependent kinase activity is required at early times for accurate processing and accumulation of the human cytomegalovirus UL122-123 and UL37 immediate-early transcripts and at later times for virus production." *J Virol* **78**(20): 11219-32.
- Santamaria, D., C. Barriere, et al. (2007). "Cdk1 is sufficient to drive the mammalian cell cycle." *Nature* **448**(7155): 811-5.
- Santamaria, D. and S. Ortega (2006). "Cyclins and CDKS in development and cancer: lessons from genetically modified mice." *Front Biosci* **11**: 1164-88.
- Satyanarayana, A., C. Berthet, et al. (2008). "Genetic substitution of Cdk1 by Cdk2 leads to embryonic lethality and loss of meiotic function of Cdk2." *Development* **135**(20): 3389-400.
- Sawadogo, M. and R. G. Roeder (1985). "Factors involved in specific transcription by human RNA polymerase II: analysis by a rapid and quantitative in vitro assay." *Proc Natl Acad Sci U S A* **82**(13): 4394-8.
- Sawtell, N. M. and R. L. Thompson (1992). "Rapid in vivo reactivation of herpes simplex virus in latently infected murine ganglionic neurons after transient hyperthermia." *J Virol* **66**(4): 2150-6.
- Schalch, T., S. Duda, et al. (2005). "X-ray structure of a tetranucleosome and its implications for the chromatin fibre." *Nature* **436**(7047): 138-41.
- Schang, L. M., A. Bantly, et al. (2002). "Pharmacological cyclin-dependent kinase inhibitors inhibit replication of wild-type and drug-resistant strains of herpes simplex virus and human immunodeficiency virus type 1 by targeting cellular, not viral, proteins." *J Virol* **76**(15): 7874-82.
- Schang, L. M., J. Phillips, et al. (1998). "Requirement for cellular cyclin-dependent kinases in herpes simplex virus replication and transcription." *J Virol* **72**(7): 5626-37.
- Schang, L. M., A. Rosenberg, et al. (1999). "Transcription of herpes simplex virus immediate-early and early genes is inhibited by roscovitine, an inhibitor specific for cellular cyclin-dependent kinases." *J Virol* **73**(3): 2161-72.

- Schang, L. M., A. Rosenberg, et al. (2000). "Roscovitine, a specific inhibitor of cellular cyclin-dependent kinases, inhibits herpes simplex virus DNA synthesis in the presence of viral early proteins." *J Virol* **74**(5): 2107-20.
- Schang, L. M., M. R. St Vincent, et al. (2006). "Five years of progress on cyclin-dependent kinases and other cellular proteins as potential targets for antiviral drugs." *Antivir Chem Chemother* **17**(6): 293-320.
- Schek, N. and S. L. Bachenheimer (1985). "Degradation of cellular mRNAs induced by a virion-associated factor during herpes simplex virus infection of Vero cells." *J Virol* **55**(3): 601-10.
- Seet, B. T., I. Dikic, et al. (2006). "Reading protein modifications with interaction domains." *Nat Rev Mol Cell Biol* **7**(7): 473-83.
- Sergeant, A., M. A. Tigges, et al. (1979). "Nucleosome-like structural subunits of intranuclear parental adenovirus type 2 DNA." *J Virol* **29**(3): 888-98.
- Serizawa, H., T. P. Makela, et al. (1995). "Association of Cdk-activating kinase subunits with transcription factor TFIID." *Nature* **374**(6519): 280-2.
- Shiekhattar, R., F. Mermelstein, et al. (1995). "Cdk-activating kinase complex is a component of human transcription factor TFIID." *Nature* **374**(6519): 283-7.
- Shogren-Knaak, M., H. Ishii, et al. (2006). "Histone H4-K16 acetylation controls chromatin structure and protein interactions." *Science* **311**(5762): 844-7.
- Shrader, T. E. and D. M. Crothers (1989). "Artificial nucleosome positioning sequences." *Proc Natl Acad Sci U S A* **86**(19): 7418-22.
- Shrader, T. E. and D. M. Crothers (1990). "Effects of DNA sequence and histone-histone interactions on nucleosome placement." *J Mol Biol* **216**(1): 69-84.
- Sidle, A., C. Palaty, et al. (1996). "Activity of the retinoblastoma family proteins, pRB, p107, and p130, during cellular proliferation and differentiation." *Crit Rev Biochem Mol Biol* **31**(3): 237-71.
- Simpson-Holley, M., R. C. Colgrove, et al. (2005). "Identification and functional evaluation of cellular and viral factors involved in the alteration of nuclear architecture during herpes simplex virus 1 infection." *J Virol* **79**(20): 12840-51.
- Simpson, R. T. and D. W. Stafford (1983). "Structural features of a phased nucleosome core particle." *Proc Natl Acad Sci U S A* **80**(1): 51-5.
- Sinclair, J. (2010). "Chromatin structure regulates human cytomegalovirus gene expression during latency, reactivation and lytic infection." *Biochim Biophys Acta* **1799**(3-4): 286-95.
- Sinden, R. R., J. O. Carlson, et al. (1980). "Torsional tension in the DNA double helix measured with trimethylpsoralen in living E. coli cells: analogous measurements in insect and human cells." *Cell* **21**(3): 773-83.
- Sinden, R. R., D. E. Pettijohn, et al. (1982). "Organization of herpes simplex virus type 1 deoxyribonucleic acid during replication probed in living cells with 4,5',8-trimethylpsoralen." *Biochemistry* **21**(18): 4484-90.
- Sodeik, B., M. W. Ebersold, et al. (1997). "Microtubule-mediated transport of incoming herpes simplex virus 1 capsids to the nucleus." *J Cell Biol* **136**(5): 1007-21.

- Song, B., J. J. Liu, et al. (2000). "Herpes simplex virus infection blocks events in the G1 phase of the cell cycle." *Virology* **267**(2): 326-34.
- Spencer, C. A., M. E. Dahmus, et al. (1997). "Repression of host RNA polymerase II transcription by herpes simplex virus type 1." *J Virol* **71**(3): 2031-40.
- Spivack, J. G. and N. W. Fraser (1988). "Expression of herpes simplex virus type 1 latency-associated transcripts in the trigeminal ganglia of mice during acute infection and reactivation of latent infection." *J Virol* **62**(5): 1479-85.
- Stern, S. and W. Herr (1991). "The herpes simplex virus trans-activator VP16 recognizes the Oct-1 homeo domain: evidence for a homeo domain recognition subdomain." *Genes Dev* **5**(12B): 2555-66.
- Stern, S., M. Tanaka, et al. (1989). "The Oct-1 homoeodomain directs formation of a multiprotein-DNA complex with the HSV transactivator VP16." *Nature* **341**(6243): 624-30.
- Strahl, B. D. and C. D. Allis (2000). "The language of covalent histone modifications." *Nature* **403**(6765): 41-5.
- Strang, B. L. and N. D. Stow (2005). "Circularization of the herpes simplex virus type 1 genome upon lytic infection." *J Virol* **79**(19): 12487-94.
- Strang, B. L. and N. D. Stow (2007). "Blocks to herpes simplex virus type 1 replication in a cell line, tsBN2, encoding a temperature-sensitive RCC1 protein." *J Gen Virol* **88**(Pt 2): 376-83.
- Stringer, K. F., C. J. Ingles, et al. (1990). "Direct and selective binding of an acidic transcriptional activation domain to the TATA-box factor TFIID." *Nature* **345**(6278): 783-6.
- Strom, T. and N. Frenkel (1987). "Effects of herpes simplex virus on mRNA stability." *J Virol* **61**(7): 2198-207.
- Sturm, R. A. and W. Herr (1988). "The POU domain is a bipartite DNA-binding structure." *Nature* **336**(6199): 601-4.
- Subramanian, R. P. and R. J. Geraghty (2007). "Herpes simplex virus type 1 mediates fusion through a hemifusion intermediate by sequential activity of glycoproteins D, H, L, and B." *Proc Natl Acad Sci U S A* **104**(8): 2903-8.
- Suto, R. K., M. J. Clarkson, et al. (2000). "Crystal structure of a nucleosome core particle containing the variant histone H2A.Z." *Nat Struct Biol* **7**(12): 1121-4.
- Taddeo, B., W. Zhang, et al. (2006). "The U(L)41 protein of herpes simplex virus 1 degrades RNA by endonucleolytic cleavage in absence of other cellular or viral proteins." *Proc Natl Acad Sci U S A* **103**(8): 2827-32.
- Tate, V. E. and L. Philipson (1979). "Parental adenovirus DNA accumulates in nucleosome-like structures in infected cells." *Nucleic Acids Res* **6**(8): 2769-85.
- Taylor, S. L., P. R. Kinchington, et al. (2004). "Roscovitine, a cyclin-dependent kinase inhibitor, prevents replication of varicella-zoster virus." *J Virol* **78**(6): 2853-62.

- Thoma, F. and T. Koller (1977). "Influence of histone H1 on chromatin structure." Cell **12**(1): 101-7.
- Thoma, F., T. Koller, et al. (1979). "Involvement of histone H1 in the organization of the nucleosome and of the salt-dependent superstructures of chromatin." J Cell Biol **83**(2 Pt 1): 403-27.
- Thomas, M. C. and C. M. Chiang (2006). "The general transcription machinery and general cofactors." Crit Rev Biochem Mol Biol **41**(3): 105-78.
- Tomschik, M., H. Zheng, et al. (2005). "Fast, long-range, reversible conformational fluctuations in nucleosomes revealed by single-pair fluorescence resonance energy transfer." Proc Natl Acad Sci U S A **102**(9): 3278-83.
- Triezenberg, S. J., K. L. LaMarco, et al. (1988). "Evidence of DNA: protein interactions that mediate HSV-1 immediate early gene activation by VP16." Genes Dev **2**(6): 730-42.
- Tse, C. and J. C. Hansen (1997). "Hybrid trypsinized nucleosomal arrays: identification of multiple functional roles of the H2A/H2B and H3/H4 N-termini in chromatin fiber compaction." Biochemistry **36**(38): 11381-8.
- Tsutsui, T., B. Hesabi, et al. (1999). "Targeted disruption of CDK4 delays cell cycle entry with enhanced p27(Kip1) activity." Mol Cell Biol **19**(10): 7011-9.
- Tumbar, T., G. Sudlow, et al. (1999). "Large-scale chromatin unfolding and remodeling induced by VP16 acidic activation domain." J Cell Biol **145**(7): 1341-54.
- Umene, K. and T. Nishimoto (1996). "Replication of herpes simplex virus type 1 DNA is inhibited in a temperature-sensitive mutant of BHK-21 cells lacking RCC1 (regulator of chromosome condensation) and virus DNA remains linear." J Gen Virol **77** (Pt 9): 2261-70.
- Utley, R. T., K. Ikeda, et al. (1998). "Transcriptional activators direct histone acetyltransferase complexes to nucleosomes." Nature **394**(6692): 498-502.
- Valyi-Nagy, T., S. Deshmane, et al. (1991). "Induction of cellular transcription factors in trigeminal ganglia of mice by corneal scarification, herpes simplex virus type 1 infection, and explantation of trigeminal ganglia." J Virol **65**(8): 4142-52.
- van Leeuwen, H., M. Okuwaki, et al. (2003). "Herpes simplex virus type 1 tegument protein VP22 interacts with TAF-I proteins and inhibits nucleosome assembly but not regulation of histone acetylation by INHAT." J Gen Virol **84**(Pt 9): 2501-10.
- Varnum, S. M., D. N. Strelow, et al. (2004). "Identification of proteins in human cytomegalovirus (HCMV) particles: the HCMV proteome." J Virol **78**(20): 10960-6.
- Venkitaraman, A. R. (2010). "Modifying chromatin architecture during the response to DNA breakage." Crit Rev Biochem Mol Biol **45**(1): 2-13.
- Vignali, M., D. J. Steger, et al. (2000). "Distribution of acetylated histones resulting from Gal4-VP16 recruitment of SAGA and NuA4 complexes." Embo J **19**(11): 2629-40.

- Wada, T., T. Takagi, et al. (1998). "DSIF, a novel transcription elongation factor that regulates RNA polymerase II processivity, is composed of human Spt4 and Spt5 homologs." Genes Dev **12**(3): 343-56.
- Wada, T., T. Takagi, et al. (1998). "Evidence that P-TEFb alleviates the negative effect of DSIF on RNA polymerase II-dependent transcription in vitro." Embo J **17**(24): 7395-403.
- Waga, S. and B. Stillman (1998). "The DNA replication fork in eukaryotic cells." Annu Rev Biochem **67**: 721-51.
- Walker, S., S. Hayes, et al. (1994). "Site-specific conformational alteration of the Oct-1 POU domain-DNA complex as the basis for differential recognition by Vmw65 (VP16)." Cell **79**(5): 841-52.
- Wang, D., C. de la Fuente, et al. (2001). "Inhibition of human immunodeficiency virus type 1 transcription by chemical cyclin-dependent kinase inhibitors." J Virol **75**(16): 7266-79.
- Weil, R., M. R. Michel, et al. (1965). "Induction of cellular DNA synthesis by polyoma virus." Proc Natl Acad Sci U S A **53**(6): 1468-75.
- Weinheimer, S. P. and S. L. McKnight (1987). "Transcriptional and post-transcriptional controls establish the cascade of herpes simplex virus protein synthesis." J Mol Biol **195**(4): 819-33.
- Whitton, J. L. and J. B. Clements (1984). "Replication origins and a sequence involved in coordinate induction of the immediate-early gene family are conserved in an intergenic region of herpes simplex virus." Nucleic Acids Res **12**(4): 2061-79.
- Whitton, J. L., F. J. Rixon, et al. (1983). "Immediate-early mRNA-2 of herpes simplex viruses types 1 and 2 is unspliced: conserved sequences around the 5' and 3' termini correspond to transcription regulatory signals." Nucleic Acids Res **11**(18): 6271-87.
- Whyte, P., K. J. Buchkovich, et al. (1988). "Association between an oncogene and an anti-oncogene: the adenovirus E1A proteins bind to the retinoblastoma gene product." Nature **334**(6178): 124-9.
- Williams, S. P., B. D. Athey, et al. (1986). "Chromatin fibers are left-handed double helices with diameter and mass per unit length that depend on linker length." Biophys J **49**(1): 233-48.
- Woodcock, C. L. (1994). "Chromatin fibers observed in situ in frozen hydrated sections. Native fiber diameter is not correlated with nucleosome repeat length." J Cell Biol **125**(1): 11-9.
- Woodcock, C. L., L. L. Frado, et al. (1984). "The higher-order structure of chromatin: evidence for a helical ribbon arrangement." J Cell Biol **99**(1 Pt 1): 42-52.
- Woodcock, C. L. and R. P. Ghosh (2010). "Chromatin higher-order structure and dynamics." Cold Spring Harb Perspect Biol **2**(5): a000596.
- Wysocka, J., M. P. Myers, et al. (2003). "Human Sin3 deacetylase and trithorax-related Set1/Ash2 histone H3-K4 methyltransferase are tethered together selectively by the cell-proliferation factor HCF-1." Genes Dev **17**(7): 896-911.

- Xiao, H., A. Pearson, et al. (1994). "Binding of basal transcription factor TFIIH to the acidic activation domains of VP16 and p53." Mol Cell Biol **14**(10): 7013-24.
- Yamaguchi, Y., T. Takagi, et al. (1999). "NELF, a multisubunit complex containing RD, cooperates with DSIF to repress RNA polymerase II elongation." Cell **97**(1): 41-51.
- Yang, X., M. O. Gold, et al. (1997). "TAK, an HIV Tat-associated kinase, is a member of the cyclin-dependent family of protein kinases and is induced by activation of peripheral blood lymphocytes and differentiation of promonocytic cell lines." Proc Natl Acad Sci U S A **94**(23): 12331-6.
- Yang, X., C. H. Herrmann, et al. (1996). "The human immunodeficiency virus Tat proteins specifically associate with TAK in vivo and require the carboxyl-terminal domain of RNA polymerase II for function." J Virol **70**(7): 4576-84.
- Yao, X. D. and P. Elias (2001). "Recombination during early herpes simplex virus type 1 infection is mediated by cellular proteins." J Biol Chem **276**(4): 2905-13.
- Yao, X. D., M. Matecic, et al. (1997). "Direct repeats of the herpes simplex virus a sequence promote nonconservative homologous recombination that is not dependent on XPF/ERCC4." J Virol **71**(9): 6842-9.
- Ye, X., C. Zhu, et al. (2001). "A premature-termination mutation in the Mus musculus cyclin-dependent kinase 3 gene." Proc Natl Acad Sci U S A **98**(4): 1682-6.
- Yee, A. S., R. Reichel, et al. (1987). "Promoter interaction of the E1A-inducible factor E2F and its potential role in the formation of a multi-component complex." Embo J **6**(7): 2061-8.
- Young, D. and D. Carroll (1983). "Regular arrangement of nucleosomes on 5S rRNA genes in *Xenopus laevis*." Mol Cell Biol **3**(4): 720-30.
- Zalensky, A. O., J. S. Siino, et al. (2002). "Human testis/sperm-specific histone H2B (hTSH2B). Molecular cloning and characterization." J Biol Chem **277**(45): 43474-80.
- Zelus, B. D., R. S. Stewart, et al. (1996). "The virion host shutoff protein of herpes simplex virus type 1: messenger ribonucleolytic activity in vitro." J Virol **70**(4): 2411-9.
- Zhao, J., J. Herrera-Diaz, et al. (2005). "Domain-wide displacement of histones by activated heat shock factor occurs independently of Swi/Snf and is not correlated with RNA polymerase II density." Mol Cell Biol **25**(20): 8985-99.
- Zheng, C. and J. J. Hayes (2003). "Intra- and inter-nucleosomal protein-DNA interactions of the core histone tail domains in a model system." J Biol Chem **278**(26): 24217-24.
- Zhou, M., M. A. Halanski, et al. (2000). "Tat modifies the activity of CDK9 to phosphorylate serine 5 of the RNA polymerase II carboxyl-terminal domain during human immunodeficiency virus type 1 transcription." Mol Cell Biol **20**(14): 5077-86.

- Zhou, Z. H., D. H. Chen, et al. (1999). "Visualization of tegument-capsid interactions and DNA in intact herpes simplex virus type 1 virions." J Virol **73**(4): 3210-8.
- Zhu, F. X., J. M. Chong, et al. (2005). "Virion proteins of Kaposi's sarcoma-associated herpesvirus." J Virol **79**(2): 800-11.
- Zlatanova, J., T. C. Bishop, et al. (2009). "The nucleosome family: dynamic and growing." Structure **17**(2): 160-71.
- Zlatanova, J., C. Seebart, et al. (2008). "The linker-protein network: control of nucleosomal DNA accessibility." Trends Biochem Sci **33**(6): 247-53.

CHAPTER 2: MATERIALS AND METHODS

2.1. Centrifugation

Three centrifuges were used throughout these studies:

1. Eppendorf 5810 R
 - a. Rotors:
 - i. Swinging bucket rotor (SBR); A-4-62
 - ii. Fixed angle rotor (FAR); F34-6-38
 - iii. Eppendorf rotor (ER); FA45-30-11
2. Beckman Avanti J-E
 - a. Rotor:
 - i. JA-14
3. Beckman XL-90 ultracentrifuge
 - a. Rotor:
 - i. SW40 Ti

For simplicity, all centrifugations are described in parentheses in the following order; speed, time, temp, rotor. For centrifugations using the Eppendorf 5810 R centrifuge, the rotor is named using the abbreviations SBR, FAR or ER (described above).

2.2. Cells and viruses

Vero CCL-81 cells (African green monkey kidney fibroblasts), and human foreskin fibroblasts (HFF) were maintained in complete media, Dulbecco's modified Minimum Eagle's Medium (DMEM) supplemented with 5% fetal bovine serum

(FBS), 50mU/ml penicillin, and 50ng/ml streptomycin. A low passage (p10) HSV-1 strain KOS (Smith, 1964) was used throughout this study (gift from the late Dr. P.A. Schaffer, UPenn, PA, USA).

2.3. Drugs

Cyclohexamide (CHX) stock (5mg/ml) was prepared in serum free media (SFM) and diluted to a concentration of 50 μ g/ml in SFM, phosphate buffered saline (PBS - 1mM KH₂PO₄, 154mM NaCl, 3 mM Na₂HPO₄, pH 7.4), or complete media immediately before use. Cells were pre-treated with complete media supplemented with 50 μ g/ml CHX for 1 h prior to infection and maintained in CHX throughout the infection procedure (i.e. inoculum, PBS washes, and complete media after rinses).

Phosphonoacetic acid (PAA) stock (100mM) was prepared in serum free DMEM and brought to pH 7.0 using 10N NaOH. Aliquots were stored at -20°C and thawed prior to use. The stock was diluted to a concentration of 400 μ M in complete media and added to cells after adsorption.

Actinomycin D (ActD) stock (1mg/ml) was prepared in ethanol and used at a concentration of 10 μ g/ml.

Roscovitine (Rosco) stock (100mM) was prepared in dimethyl sulfoxide (DMSO). Aliquots were stored at -20°C and thawed prior to use. The stock was diluted to a concentration of 100 μ M in complete media pre-warmed to 37°C and typically added to cells after adsorption. Rosco was used in the concentration range of 25-100 μ M.

Purvalanol (Purv) and Flavopiridol (Flavo) were prepared in DMSO as 10mM stocks, and used in the concentration ranges of 5-30 μ M (Purv) or 31.25-500nM (Flavo).

α -Amanitin (α -Ama) stock (1mg/ml) was prepared in distilled water and used at a concentration of 50 μ g/ml in complete medium or 2 μ g/ml in run-on transcription buffer (described in section 2.13).

2.4. Viral stock preparation

Viral stocks of HSV-1, strain KOS, were prepared by infecting T-150 flasks seeded 12h before with approximately 5×10^6 Vero cells (50-60% confluency).

Immediately prior to infection, one flask was trypsinized and the cells were counted. Cells were infected with a multiplicity of infection (MOI) of 0.01 plaque forming units (PFU) per cell in a final volume of 3ml SFM per flask. Adsorption was typically performed for 1h at 37°C. To prevent drying of cells, flasks were rocked and rotated every 10min. After adsorption, viral inoculum was removed and cells were washed twice with 10ml of 4°C PBS followed by addition of 10ml complete medium pre-warmed to 33°C. Flasks were then transferred to a 33°C incubator and virus was harvested when HSV-1-specific cytopathic effect (CPE) was evident in 100% of cells, approximately 4-5 days post infection. Briefly, infected cells were scraped from T-150 flasks. Cells and media were pooled in 50ml conicals, and pelleted by centrifugation (3200xg, 30min, 4°C, SBR). The virus in the supernatants was pelleted by high speed centrifugation (10,000xg, 90min, 4°C, JA-14). Meanwhile, the cell pellet was resuspended in a minimal

volume of SFM (0.5ml per 6 flasks) and transferred to 14ml screw-cap conical tubes. Then, it was subjected to three freeze-thaw cycles (cycling between ethanol/dry ice and 37°C water baths), and sonicated using a 550W Sonicator Ultrasonic Processor XL (Heat System, Ultrasonics, Inc.; New York, NY, USA) in an ice-water bath for 3 cycles of 30s at 20% (110W), at 15s intervals.

Subsequently, the cellular debris from the sonicated sample was pelleted (3200xg, 30min, 4°C, SBR). Supernatants were used to resuspend the viral pellet from the higher speed centrifugation, to prepare the final viral stock. Viral stocks were titrated by standard plaque assays (see section 2.6).

2.5. HSV-1 infection

Cells were infected with MOI from 5 to 50 PFU (as described for each experiment). Infections were typically performed in 100mm diameter tissue culture dishes seeded 12h prior to infection with approximately 1×10^7 cells. Dishes were infected with 1ml of viral inocula in SFM. Adsorption was typically performed for 1h at 37°C. To prevent drying of cells, dishes were rocked and rotated every 10min. After adsorption, the viral inoculum was removed and the cells were washed twice with 4°C PBS. Complete medium pre-warmed to 37°C was then added and the cells were incubated at 37°C. Complete medium was supplemented as required with Rosco, Purv, Flavo, CHX, ActD or α -Ama. Infected cells were harvested by trypsinization at the times indicated in each experiment.

2.6. Standard Plaque Assay

Approximately 2×10^5 Vero cells were seeded in 6-well plates (50-60% confluency) 12h prior to infection. Final volumes of 500 μ l containing serial 10-fold dilutions in SFM (10^{-1} to 10^{-8}) of viral stocks or samples were prepared in 14ml snap cap tubes. Typically, dilutions 10^{-3} through 10^{-8} were titrated. Briefly, 200 μ l of the corresponding dilutions were used to infect seeded cells (see section 2.5). Following the PBS rinses, cells were overlaid with 2ml of methyl cellulose (2% w/v in complete medium) pre-warmed to 37°C and incubated at 33°C in 5% CO₂ until plaques were well defined (3-4 days). Cells were then fixed and stained with 2ml of crystal violet in methanol (1% crystal violet, 17% methanol in H₂O). Twenty four hours later, plates were washed and dried, and individual plaques were counted.

2.7. UV inactivation of HSV-1

HSV-1 stocks to be irradiated were pelleted by centrifugation (10,000xg, 90min, 4°C, JA14). The HSV-1 pellet was resuspended in 4°C PBS and kept on ice. One hundred microliter aliquots were placed in uncovered 35mm diameter tissue culture dishes and subjected to UV irradiation at 3000 mJoules (UV Stratalinker 2400, Stratagene; La Jolla, CA, USA) for 30s to 5min. The original and the UV-inactivated virus suspensions were then titrated by standard plaque assays. Viral stocks inactivated by four orders of magnitude were used in all experiments.

2.8. Phages

Recombinant bacteriophage M13 harboring the 5' end of selected HSV-1 genes were a generous gift from Dr. C. Spencer (University of Alberta, Edmonton, AB, Canada). These phages contain single-stranded DNA sense or anti-sense to HSV-1 transcripts ICP4 (IE), ICP27 (IE), ICP8 (E), UL36 (E), gC (L), and VP16 (L). Single-stranded phage DNA was isolated and transferred to positively charged membranes (Gene Screen Plus, NEN Life Science; Boston, MA, USA) by vacuum slot blotting.

2.8.1. High M13 phage stock preparation titer

Stab cultures of F' plasmid-containing bacteria (SURE cells, Stratagene; La Jolla, CA, USA) were grown overnight (~16h) at 37°C with shaking (220rpm) in an orbital shaking incubator (Weiss Gallenkamp; Loughborough, UK) in 3ml of LB supplemented with tetracycline (12µg/ml). Four hundred microliters of the overnight culture was then diluted 10-fold in LB supplemented with tetracycline and grown at 37°C until the optical density at 600nm (OD₆₀₀) of the cell suspension reached 0.6 (~1.5-2h). This culture was used to either make high titre M13 stocks or for large scale preparations of single stranded phage DNA

In a 14ml snap cap tube, 20µl of the SURE cells were infected with 100µl of bacteriophage suspension from a single M13 plug (see Section 2.8.2). Bacteria were incubated at room temperature for 5min. Then, 2ml of 37°C LB media was added. The infected culture was grown at 37°C with shaking (220rpm) for 5-6 hrs. Bacteria from the cultures were pelleted by centrifugation (3200xg, 10min, 4°C,

SBR) and the supernatant containing high titer M13 stock ($\sim 10^{12}$ PFU/ml) was aliquoted and stored at -20°C .

2.8.2. *Plating bacteriophage M13*

SURE cells were streaked on LB agar plates (15g/L) supplemented with $12\mu\text{g/ml}$ tetracycline. Following incubation at 37°C for 24-36 hrs, a single, well isolated, colony was picked with a sterile loop. Five milliliters of LB were inoculated with this culture and grown at 37°C with shaking (220rpm) for 6-8 hrs, to prepare plating bacteria. Meanwhile, 6-well plates containing 3ml LB agar (15g/L) supplemented with 5mM MgCl_2 and $12\mu\text{g/ml}$ tetracycline were warmed to 37°C , and 350 μl of melted LB top agar (7g/L) supplemented with 5mM MgCl_2 was added to sterile 1.5ml eppendorf tubes and equilibrated at 47°C . Serial 10-fold dilutions (10^{-1} to 10^{-8}) of high titer phage stocks were prepared in sterile 96-well plates in final volumes of 100 μl . Typically, dilutions 10^{-3} through 10^{-8} were titrated. Briefly, 12 μl of the corresponding phage dilutions was added to the eppendorf tubes containing the LB top agar at 47°C and vortexed gently. Twenty four microliters of plating bacteria was then added to the mixture, vortexed gently, and poured onto the corresponding well in the pre-warmed 6-well plates. Plates were stored at room temperature for 5min to allow the soft agar to harden and then transferred to 37°C incubator. Eight to twelve hours later, using a P200 pipette tip bacteriophage plugs were collected from dilutions containing well-isolated plaques. Multiple plaques were isolated for each phage. Each individual M13 plug was expelled into 1ml of LB and incubated at room temperature for 1-2 hrs, allowing

the bacteriophage to diffuse away from the agar (each plaque contains $\sim 10^6$ - 10^8 PFU). Both the residual agar plug and bacteriophage suspension were then stored at -20°C .

2.8.3. Large scale preparation of single-stranded phage DNA

One milliliter of a SURE cell culture grown to OD_{600} of 0.6 was infected with 1ml of high titre M13 stock and incubated at room temperature for 5 min. The mixture was subsequently added to 100ml of room temperature LB in a 500ml Erlenmeyer flask. The infected culture was grown at 37°C with shaking (220rpm) for 5-6 hrs. The 100ml of infected culture was then divided into 2-50ml conicals and centrifuged (2600xg, 20min, 4°C , FAR). The supernatant from each tube was transferred to fresh 50ml conicals containing 1.5g of NaCl and 2.0g of polyethylene glycol 8000 (PEG 8000). Conicals were agitated on a horizontal rocker for 1h at room temperature and centrifuged (8200xg, 20min, 4°C , FAR). The pellet from both 50ml conicals was resuspended in 2.5ml of tris EDTA buffer (TE - 10 mM Tris pH 7.5, 1mM EDTA), and the DNA was isolated by phenol extraction.

2.9. Isolation of HSV-1 and Cellular DNA for probes

HSV-1 and Vero cell DNA was isolated from purified HSV-1 virions or uninfected Vero cells, respectively, by proteinase K digestion and phenol extraction (described in section 2.10). Viral (5 μg) or cellular (10 μg) DNA were digested separately with Hind III (1U/ μg of DNA) overnight at 37°C . Fragments were resolved by agarose gel electrophoresis and transferred to positively-charged membranes (Gene Screen

Plus, NEN Life Science; Boston, MA, USA) for subsequent Southern blot hybridizations.

2.10. DNA Isolation by Proteinase K and phenol extraction

Samples were digested for 3 to 12h at 65°C with 100µg/ml proteinase K in the presence of 0.5% sodium dodecyl sulphate (SDS). One volume of phenol:chloroform:isoamyl alcohol (25:24:1) was then added and mixed by vortexing. The resulting emulsion was centrifuged (3200xg, 10min, 4°C, SBR). The aqueous phase (top) was removed to a new conical and the organic phase (bottom) was back extracted with an equal volume of TE. Following centrifugation, the aqueous phase of the back extraction was pooled with the aqueous phase from the original extraction. Samples were then extracted with one volume of chloroform:isoamyl alcohol. The aqueous phase of this extraction was precipitated with either 3 volumes of 95% ethanol, or 1 volume of 100% isopropanol, by incubation at -20°C for a minimum of 1h. DNA was then pelleted by centrifugation (12,000xg or 21,000xg, 20min, 4°C, FAR or ER, respectively). DNA pellet was rinsed briefly with 70% ethanol. Ethanol was removed from the tube and the DNA pellet was typically resuspended in TE. Concentration of DNA was determined by reading absorbance at 260nm (A_{260}). $1A_{260}$ was considered to correspond to 38µg/ml for ssDNA or 50µg/ml for dsDNA. Alternatively, DNA concentration was determined by ethidium bromide stained agarose gel electrophoresis.

2.11. DNA transfer to membranes by vacuum slot blot

Slot blots were prepared using a BIO-DOT SF apparatus (Bio-Rad, Hercules, CA, USA). Briefly, 4 μ g of DNA per well in a final volume 100 μ l was denatured by adding 1 volume (100 μ l) of denaturation solution (0.5N NaOH, 0.5M NaCl) and incubating for 10min at 65°C. Tubes were then chilled in an ice-water bath for 5-10min. Samples were then diluted with 800 μ l of neutralization buffer (0.125N NaOH, 0.1X SSC) and chilled on ice until the slot blot apparatus was assembled. The slot blot apparatus was assembled using 4 pieces of filter paper and one positively-charged nylon membrane cut to size and presoaked in 0.4M Tris pH 7.5. Each well was washed twice under vacuum with 1ml of neutralization solution. At the end of the second wash, the vacuum was stopped and the DNA samples (1ml) were loaded into the corresponding wells. Vacuum was resumed and wells were rinsed twice with 1ml of neutralization solution. Following the final rinse, the slot blot apparatus was disassembled (with vacuum still on to prevent back flow) and the membrane was labeled, soaked briefly in 0.5M Tris pH 7.5, 0.5M NaCl, and air dried.

2.12. Isolation of nuclei

Cells were rinsed with PBS at 4°C, trypsinized, and resuspended in 20 ml of complete media. Resuspended cells were then pelleted by centrifugation (3200xg, 10min, 4°C, SBR), and resuspended in 20ml of hypotonic cell swelling buffer (CSB - 10 mM Tris pH 7.5, 10 mM NaCl, 5 mM MgCl₂). Cells were pelleted again (3200xg, 10min, 4°C, SBR) and resuspended and lysed in CSB buffer with

0.5% (v/v) Nonidet P-40 at 4°C. Lysis was verified by periodically removing a sample of the nuclei suspension and checking for intact cells by light microscopy. When lysis was deemed complete (<5% intact cells), typically 8min, nuclei were isolated by differential centrifugation (1800xg, 10min, 4°C, SBR).

2.13. Run-on analyses

For each treatment, two 100 mm diameter dishes (each containing approximately 6×10^6 Vero cells) were mock infected or infected at an MOI of 20 PFU/cell.

Infected cells were treated with complete media supplemented or not with 100 μ M Rosco for 5h (starting at 1hpi), and harvested at 6 hpi.

Run-on assays were performed as described by Spencer, Rice *et al.* (Rice, Long et al. 1995; Spencer, Dahmus et al. 1997), with several modifications. Briefly, isolated nuclei were resuspended in 150 μ l nuclear freezing buffer (NFB - 50 mM Tris pH 8.0, 5 mM MgCl₂, 40% glycerol, 0.5 mM DTT), and immediately snap-frozen in liquid nitrogen and stored at -80°C. Afterwards, 150 μ l of thawed nuclei suspension was mixed with 150 μ l of transcription run-on buffer (20 mM Tris pH 8.0, 20 mM MgCl₂, 3 mM DTT, 0.5mM of each ATP, CTP and UTP, and 10 μ Ci of [α -³²P] GTP). Final buffer concentrations were, 30 mM Tris pH 8.0, 1 mM DTT, 7.5 mM MgCl₂, 20% glycerol, 140 mM KCl. Transcription reactions proceeded at 30°C for 30 minutes, and were then stopped by incubation with 50 μ g (434 Worthington U) of DNase I (Invitrogen, Carlsbad, CA, USA) for 15 minutes at 30°C. Proteins were digested in proteinase K buffer (PKB - 100 mM Tris pH 7.5, 50 mM EDTA, 10% SDS) containing 100 μ g/ml of proteinase K, for 1h at

37°C. RNA was extracted with one volume of acid phenol:chloroform:isoamyl alcohol (25:24:1), precipitated with 1 volume of isopropanol and stored at -20°C. RNA was pelleted by centrifugation (21,000xg, 30min, 4°C, ER) and resuspended in 200 µl of TE buffer.

The RNA was denatured at 100°C for 5 min and diluted in 5ml of Rapid Hybrid Buffer (Amersham Biosciences, Piscataway, NJ, USA) pre-warmed to 60 or 37°C (for analyses of HSV-1 or cellular transcription, respectively).

Meanwhile, hybridization bottles with membranes containing phage or genomic DNA were pre-hybridized in 10 ml Rapid Hybrid Buffer at 60 or 37°C (for analyses of HSV-1 or cellular transcription, respectively). Hybridizations were started by discarding pre-hybridization buffer and adding the denatured RNA in Rapid Hybrid Buffer. Hybridizations were performed at 60 or 37°C for 48 or 72 h, for analyses of HSV-1 or cellular transcription, respectively. Membranes were washed twice in wash 1 buffer (2 X SSC, 0.1% SDS) for 20 minutes at room temperature. For analyses of HSV-1 transcription, membranes were further washed in wash 2 buffer (0.5 X SSC, 0.5% SDS) for 15 minutes at 50°C. Membranes were exposed to Kodak PhosphorImager screens. The membranes were imaged and the signal hybridized to HSV-1 or Vero genomic fragments was quantitated using Bio-Rad molecular imager FX (Bio-Rad, Hercules, CA, USA). Counts hybridized to the genomic fragments under each treatment were normalized to counts hybridized to the respective genomic fragments in the absence of any drug (control), and are presented as percentage.

Nucleic acids were precipitated after the proteinase K digestion in 10%

trichloroacetic acid (TCA) at 4°C. Precipitates were then washed three times by resuspension in 10% TCA at 4°C and centrifugation (14,000xg, 20min, 4°C, ER). Nucleic acid pellets were finally resuspended in 0.5% SDS. Radioactivity incorporated into TCA-precipitable material was expressed as percentage of the radioactivity used as substrate in the run-on reactions (as [α -³²P] GTP). RNAPII-specific incorporation was then calculated by subtracting the percentage radioactivity incorporated into TCA-precipitable material in the presence of 10µg/ml ActD (background), and is presented as percentage of control (no drug present in the run-on transcription reactions).

2.14. Random-primed DNA labeling

DNA was radiolabeled with [α -³²P] dCTP using the Rediprime II Random Prime Labelling System from Amersham Biosciences according to the manufacturer's instructions (Amersham Biosciences, Piscataway, NJ, USA). Briefly, 50ng of probe was denatured for 10 min at 100°C and immediately transferred to ice for 5 min. The denatured DNA and 5 µl (50µCi) of [α -³²P] dCTP were added to the random-prime reaction tubes, thoroughly mixed, and incubated for 1h at 37°C. After 1h, the contents of the labeling reaction were denatured for 10min at 100°C and immediately cooled in ice for 5 minutes before adding to Rapid Hybrid Buffer prewarmed to the hybridization temperature.

2.15. Nuclease digestion

Nuclei were digested with either BamHI or micrococcal nuclease (MCN). For

BamHI digestions, nuclei were rinsed twice with React 3 buffer (50mM Tris pH7.5, 10mM MgCl₂, 100mM NaCl), the first time with 10ml and the second with 1ml. Nuclei were pelleted by centrifugation after each rinse (1,800xg, 20min, 4°C, SBR; or 5000xg, 15min, 4°C, ER, respectively). Nuclei were then resuspended to a final volume of 100µl in React 3 buffer containing 10U of BamHI per 1x10⁶ nuclei. Digestions were carried out at 37°C for 4h.

For standard MCN digestions, nuclei were resuspended in MCN buffer (1x10⁷ nuclei per 100µl) containing 0.005, 0.05, 0.5, or 5U of MCN per 1x10⁷ nuclei, as indicated. Digestions were performed at 39°C and stopped at the indicated times with the addition of 5µl of 0.5M ethylene glycol tetra-acetic acid (EGTA). Samples were digested with proteinase K and DNA was isolated by phenol extraction.

2.16. Chromatin Fractionation

MCN-digested nuclei were lysed by adding one volume of chromatin extraction buffer (CEB - 2mM Tris pH 8.0, 3mM MgCl₂, 1mM EGTA, 2% Triton X-100) and incubated with rotation for 10min at 4°C. Then, so-called “soluble” and “insoluble” chromatin fractions were separated by differential centrifugation (8,000xg, 20min, 4°C, ER).

2.17. Isolation of unstable nucleosomes by serial MCN digestion

Undigested nuclei were lysed by adding one volume of CEB and incubating for 10min at 4°C with rotation. The undigested chromatin was then pelleted by

centrifugation (8,000xg, 20min, 4°C, ER). Resuspension of the pelleted chromatin for subsequent washes and digestion was facilitated by mechanical disruption, by sliding the tube along the eppendorf rack and pipetting up and down. Pelleted chromatin was washed once by resuspension in 80µl of MCN buffer (10mM Tris pH 8.0, 1mM CaCl₂), without MCN. The washed chromatin pellet was then subjected to serial MCN digestion (Lacasse et al 2010). Briefly, the chromatin pellet was resuspended in 80µl of MCN buffer (containing 0.625U MCN/ml) and digested for 5min during differential centrifugation (8,000xg, 5min, 23°C, ER). Following the centrifugation, the supernatant (soluble chromatin) was removed and quenched with 5µl of 0.5M EGTA to prevent further degradation of unstable nucleosomes. Meanwhile, the pellet (insoluble chromatin) was resuspended with fresh MCN digestion buffer (containing 0.625U MCN/ml) and the entire procedure was repeated 6 or 9 times. For a cartoon representation of the serial digestion protocol, see Fig 3.7.

Soluble chromatin fractions from the serial MCN digestions were either pooled and resolved together in sucrose gradients or individually analyzed by Southern blot hybridization. For sucrose gradient analysis, 40µl of each soluble chromatin fraction was pooled resulting in either 240 or 360µl (6 or 9 serial digestion repeats, respectively) to be resolved on sucrose gradients. For analysis of the DNA in the individual soluble chromatin fractions, 40µl of the soluble chromatin fraction was taken to a final volume of 200µl with STE and digested overnight with proteinase K. DNA was then isolated by phenol-chloroform extraction.

2.18. Sucrose gradient ultracentrifugation

Continuous 0 to 10% sucrose gradients were prepared using a Gradient Master (Biocomp, Fredericton NB, Canada), with sucrose gradient buffer (SGB - 10mM Tris pH8.0, 1.5mM MgCl₂, 0.5M EGTA) containing 0, 80, 225, or 450mM NaCl. Soluble chromatin was loaded on top of pre-formed gradients and centrifuged (284,000xg, 180min, 4°C, SW-40 Ti). Twelve 1ml fractions were collected from the bottom of the tube. After the removal of the final fraction, the pellet was recovered in 1ml of STE (as fraction 13). Fractions were digested with proteinase K overnight and DNA was isolated by phenol-chloroform extraction.

2.19. Size exclusion chromatography

Size exclusion chromatography (SEC) was performed in Econo-Pac Disposable Chromatography Columns (Biorad, Hercules, CA, USA) packed with Sephadex G-100 (GE Healthcare, Piscataway, NJ, USA). Prior to chromatography, columns were prepared using a Sephadex G-100 slurry that was packed by gravity to a final packed column volume of 10ml and rinsed three times with 20ml gel filtration buffer (GFB - 10mM Tris pH8.0, 150mM NaCl, 1.5mM MgCl₂, 0.5mM EGTA). Fractions 11 and 12 (2ml final volume) from the sucrose gradients were pooled and loaded onto 2 identical columns. Multiple columns were used for each sample to maximize resolution by minimizing sample volume (1ml). Columns were washed with GFB, twice with one volume (1ml) and once with five volumes (5ml). Fractions (1ml) were collected from duplicate columns and

pooled. DNA was either isolated from the individual column fractions or pooled and subsequently crosslinked with formaldehyde for MCN redigestion experiments

2.20. Formaldehyde crosslinking of purified nucleosomes and MCN redigestion

SEC fractions 4-6 from duplicate columns were pooled (8ml total) and split into two 4ml aliquots. Samples were then crosslinked or not with 0.1% formaldehyde (by adding 10.4µl of 37% buffered formalin) for 1h at 4°C with inversion. Crosslinking was quenched by the addition of 480µl of 1M glycine to a final concentration of 125mM glycine, incubating the samples for 10min at 4°C with inversion. Crosslinked samples were then subjected to MCN redigestion. Briefly, MCN (0.05U/ml) was added to the crosslinked samples. One milliliter aliquots were removed at 0, 5, 15, 30, 60min and quenched with 0.5M EGTA. Samples were then digested with proteinase K, and DNA was isolated by phenol-chloroform extraction.

2.21. Southern Blot Hybridization

2.21.1. Upward capillary transfer

DNA fragments were resolved by agarose gel electrophoresis. Gels were then rocked in 0.2M HCl for 45 min, to depurinate larger DNA fragments and facilitate their transfer out of the gel and onto the membrane. Following depurination, the double stranded DNA (dsDNA) in the gels was denatured by rocking the gels in

alkaline transfer buffer (ATB - 0.4N NaOH, 1M NaCl) twice for 15min. The gel was then rocked in neutralization buffer (NB - 0.5M Tris pH 7.5, 1.5M NaCl) twice for 15min. Meanwhile, the paper towels, filter paper, and membrane (Gene Screen Plus, NEN Life Science; Boston, MA, USA) were cut to size. Cut membranes were presoaked in 10X SSC (1X SSC - 150 mM NaCl, 15 mM sodium citrate) for at least 15min. Meanwhile, the capillary transfer apparatus was assembled. Gels were blotted for 24-48 hrs, ensuring constant excess 10X SSC buffer. After blotting, membranes were labeled and soaked briefly (1 min) in 0.4N NaOH and then 0.2M Tris pH7.5, 2X SSC. Membranes were then air dried.

2.21.2 Hybridization

Membranes were pre-hybridized with 10ml rapid hybrid buffer (Amersham Biosciences, Piscataway, NJ, USA) at 75°C or 60°C for HSV-1 or cellular DNA, respectively, for a minimum of 1h. The probes were selected fragments from the HSV-1 EcoRI library (JK for the probe enriched in immediate early (IE) loci, G and L for the probe enriched in late (L) loci) or Vero cell DNA. Plasmid DNA from the HSV-1 EcoRI library (a generous gift from the late Dr. P.A. Schaffer, UPenn, PA, USA) was isolated using GeneElute HP Plasmid Maxiprep Kit (Sigma, St. Louis, MO, USA). Vero cell DNA was isolated from uninfected Vero cells by proteinase K digestion and phenol-chloroform extraction. Probes were labeled following random-primer labeling. Hybridizations were performed for 3h at 75°C or 60°C for HSV-1 or cellular DNA, respectively. Membranes were washed twice for 15min at room temperature with wash 1 buffer. If needed,

membranes were further washed for 10min at 60°C or 50°C, for HSV-1 or cellular DNA, respectively, with wash 2 buffer. Membranes were exposed to Kodak PhosphorImager screens and quantitated using Bio-Rad molecular imager FX (Bio-Rad).

2.22. The following procedures were performed by Dr. Prerna Diwan

2.22.1 Construction of the ICP0-RFP plasmid

Plasmid vector pA1-pICP0-LacZ (11051bp) containing the HSV-1 IE promoter ICP0 driving the expression of LacZ was a generous gift of Dr. A. Epstein (Université Claude Bernard Lyon, France). Using this plasmid as the starting vector, an expression vector with the ICP0 promoter driving expression of red fluorescent protein (RFP) was constructed. The RFP gene was derived from pDsRed1-N1 vector (Clontech, Palo Alto, CA, USA), and the ICP0 promoter from pA1-pICP0-LacZ. The 720 bp *Sal* I –*Not* I RFP fragment was excised from pDsRed1-N1 vector and subcloned following removal of 3489 bp *Sal* I–*Not* I fragment containing the LacZ cassette. The resulting 8282 bp construct was named pICP0-RFP5, and was used for transient transfection of Vero cells and for the creation of stably-transfected cell lines.

2.22.2 Stable transfection of Clone 57 cell line

Vero cells were transfected using lipofectamine (Gibco BRL, Rockville, MD, USA) according to the manufacturer's instructions. Briefly, Vero cells were seeded at 60-70% confluence in six-well plates. The following day, cells were transfected

with 4 µg pICP0-RFP5 and 0.6 µg pcDNA plasmids. The latter contains the gene for G-418 resistance. Cells were incubated with DNA-lipofectamine at 37°C for 4 h followed by addition of 1 volume of DMEM supplemented with 10% FBS. After 24 h of incubation, media was replaced with fresh complete media. For transient transfection experiments, transfected cells were then trypsinized and seeded in replicate wells. For the construction of the stably transfected Vero cell lines, confluent cells were passed 1:2 in media supplemented with 800 µg/ml of G418. After 10-15 days, when only the G418 resistant transfected cells survived, cells were expanded and the concentration of G418 was lowered to 400µg/ml for maintenance of transfected cells. Transfected cells were cloned by limiting dilution in 96 well plates. Individual clones were screened for expression of RFP.

2.22.3 Northern blot analyses

Approximately 2×10^6 Vero cells in 100 mm diameter tissue culture dishes were pre-treated with 50µg/ml CHX for 1 h before infection with HSV-1 KOS at a MOI of 5 PFU/cell. Cells were washed with PBS containing 50µg/ml CHX. Then, complete media supplemented with CHX and different concentrations of Rosco, Purv or Flavo was added. Total cellular RNA was extracted from mock and HSV-1 infected cells at 3, 6 and 9 hpi using the guanidinium isothiocyanate method. RNA concentrations were estimated spectrophotometrically at 260 nm. RNA samples were stored in isopropanol at -70°C. The RNA samples were centrifuged, resuspended, size fractionated on agarose-formaldehyde denaturing gels (30 µg

RNA/sample) and transferred to GeneScreen Plus nylon membranes for Northern blot hybridizations.

Hybridizations were performed in Rapid Hybrid Buffer for 4 h using RFP or ICP0 probes. Briefly, the RFP probe was prepared by digesting the pDsRed1-N1 plasmid with *Sal1* and *Not1* and purifying the 720 bp fragment. ICP0 probe was prepared by digesting the pRP0 plasmid with *XhoI* and *HindIII* and purifying the 888bp fragment. Probes were labeled by random-priming.

Hybridization with RFP was performed at 65°C, and for ICP0 at 80°C. Hybridized membranes were washed twice with wash buffer 1 at room temperature for 15 minutes and with wash buffer 2 at 65°C for 10 minutes. Membranes were exposed to Kodak PhosphorImager screens, and imaged using Bio-Rad molecular imager FX. For hybridization with subsequent probes, specific signal was first removed by washing the membranes with stripping solution for 2 hours and then wash buffer 2 for 10 minutes at 68°C. Stripped membranes were exposed and then used for re-hybridization with a different probe.

2.23. REFERENCES

- Rice, S. A., M. C. Long, et al. (1995). "Herpes simplex virus immediate-early protein ICP22 is required for viral modification of host RNA polymerase II and establishment of the normal viral transcription program." J Virol **69**(9): 5550-9.
- Spencer, C. A., M. E. Dahmus, et al. (1997). "Repression of host RNA polymerase II transcription by herpes simplex virus type 1." J Virol **71**(3): 2031-40.

CHAPTER 3: DURING LYTIC INFECTIONS, HERPES SIMPLEX VIRUS TYPE 1 DNA IS IN COMPLEXES WITH THE PROPERTIES OF UNSTABLE NUCLEOSOMES

*A version of this chapter has been published. Lacasse, JJ. and L.M. Schang.
Journal of Virology 2010; 84(4):1920-33*

3.1. Introduction

At the time when these experiments were performed, the existence or structure of any intranuclear HSV-1 DNA nucleoprotein complexes during lytic infection was unclear. Primarily, the results obtained from classical studies (MCN digestions, trimethylsporolen photocrosslinking, and electron micrography), and those obtained from more recent ChIP assays, were most difficult to reconcile.

Whereas classical evidence suggested HSV-1 DNA was primarily nucleosome-free (Mouttet, Guetard et al. 1979; Leinbach and Summers 1980; Sinden, Pettijohn et al. 1982; Muggeridge and Fraser 1986; Deshmane and Fraser 1989), ChIP assays reported association of HSV-1 DNA with histones, and proposed that chromatin regulates HSV-1 transcription (Herrera and Triezenberg 2004; Kent, Zeng et al. 2004; Huang, Kent et al. 2006; Narayanan, Ruyechan et al. 2007; Knipe and Cliffe 2008; Oh and Fraser 2008; Ferenczy and Deluca 2009; Kutluay, DeVos et al. 2009; Kutluay and Triezenberg 2009; Liang, Vogel et al. 2009; Placek, Huang et al. 2009).

Considering this association of histones and chromatin modifying proteins with HSV-1 DNA, most current models therefore propose that chromatin regulates HSV-1 transcription in lytically infected cells. However, only a small percentage of HSV-1 DNA was found to consistently co-immunoprecipitate with histones in all (Herrera and Triezenberg 2004; Kent, Zeng et al. 2004; Huang, Kent et al. 2006; Kutluay, Doroghazi et al. 2008; Kutluay, DeVos et al. 2009; Kutluay and Triezenberg 2009; Placek, Huang et al. 2009) except one (Cliffe and Knipe 2008) published papers, or to be protected from MCN in sizes corresponding to nucleosomal DNA (Leinbach and Summers 1980; Muggeridge and Fraser 1986; Deshmane and Fraser 1989). It therefore remained unclear how histone association of only a small percentage of HSV-1 DNA could regulate HSV-1 transcription globally. Furthermore, the biophysical properties of the complexes containing histones and HSV-1 DNA also remained unclear. Therefore, using classical chromatin purification techniques, I systematically analyzed the biophysical properties of the complexes formed with HSV-1 DNA at 5 hours during lytic infections.

3.2. Results

3.2.1. At 5h after infection, HSV-1 DNA is in complexes that do not fractionate as protein-free DNA.

As a first step in characterizing the biophysical properties of nuclear HSV-1 DNA in lytically infected cells, I used standard biochemical fractionation techniques to test whether nuclear HSV-1 DNA had the biophysical properties of protein-free

DNA. Briefly, nuclei from HSV- or mock- infected cells were harvested at 5hpi and protein-free DNA was resolved from DNA in larger complexes by differential centrifugation. However, replicating HSV-1 genomes form long branched concatemers (Severini, Scraba et al. 1996). Nuclei were therefore first digested with BamHI, to cleave these long branched concatemers into subgenomic linear fragments (ranging from 50 to 5,000 bps), and thus minimize mechanical trapping during fractionation. Nuclei were then lysed and DNA-protein complexes were resolved by differential centrifugation into so-called “soluble” and “insoluble” fractions. The “soluble” fraction contains soluble proteins, protein-free DNA and small complexes, including mono-, di-, and some short poly-nucleosomes. The “insoluble” fraction contains larger complexes including large poly-nucleosome chains and nuclear matrix. As a control, protein-free HSV-1 DNA was added to nuclei of mock-infected cells before BamHI digestion.

As expected, 83% of the detected protein-free HSV-1 DNA added to mock-infected nuclei fractionated to the “soluble” fraction (Fig 3.1A, HSV Protein-free; Table 3.1). In contrast, and also as expected, only 19% of the detected chromatinized cellular DNA fractionated to the “soluble” fraction (Fig 3.1A, Cellular Nuclear; Table 3.1). Likewise, only 27% of the detected HSV-1 DNA from the nuclei of infected cells fractionated to the “soluble” fraction, whereas 73% fractionated to the insoluble fraction (Fig 3.1A, HSV Nuclear; Table 3.1). The majority of nuclear HSV-1 DNA and chromatinized cellular DNA therefore fractionated to the insoluble fraction during the first differential centrifugation (73% and 81%, respectively - Table 3.1). This HSV-1 DNA,

however, was still digested to heterogeneously sized fragments and is therefore accessible to BamHI (Fig 3.1A, HSV Nuclear-Insoluble).

The DNA and DNA-protein complexes that fractionated in the “soluble” fraction were then further resolved by sucrose gradient fractionation. As expected, the detected protein-free HSV-1 DNA fractionated to the lowest density fractions (Fig 3.1A and B, HSV Protein-free, fractions 9-12). In contrast, the detected HSV-1 DNA from nuclei of infected cells fractionated to heavier fractions (Fig 3.1A and B, HSV Nuclear, fractions 6-10). These were mostly the same fractions to which the detectable “soluble” cellular DNA in mono-, di-, and short poly-nucleosomes resolved (Fig 3.1A, Cellular Nuclear).

In summary, the majority of the nuclear HSV-1 DNA detected at 5 hpi in lytically infected cells does not fractionate as protein-free DNA. Instead, it resolves to the same fractions as chromatinized cellular DNA (Fig 3.1B).

3.2.2. MCN digestion releases HSV-1 DNA in complexes that fractionate as cellular nucleosomes.

HSV-1 DNA released as “soluble” complexes fractionated as chromatinized cellular DNA. We then tested whether this nuclear HSV-1 DNA was in complexes with properties similar to those of nucleosomes.

Nuclei from infected cells were harvested at 5hpi and digested with MCN. Digested nuclei were then lysed and resolved into “soluble” and “insoluble” fractions. The soluble fraction is often referred to as “soluble chromatin” and contains mono-, di- and relatively short poly-nucleosomes complexes. Complexes

released as soluble chromatin were then further resolved by sucrose gradient centrifugation (Fig 3.2A). Poly-nucleosomes resolve to heavier fractions, mono- and di- nucleosomes to lighter fractions, and protein-free DNA to the lightest ones. As expected, the cellular DNA released as soluble chromatin resolved as various sizes of poly-nucleosomes in fractions 2 to 9, and as mono-, di-, and tri-nucleosomes in fractions 10 and 11 (Fig 3.2A, Cellular). In contrast, all the HSV-1 DNA released under these conditions as soluble chromatin was in complexes that resolved to the same fractions as cellular mono- to tri-nucleosomes, and most of it was in the fractions containing mostly mono- to di-nucleosomes (Fig 3.2A and B, HSV fractions 10, 11). No HSV-1 DNA released with the soluble chromatin fractionated as poly-nucleosomes or to the lightest fraction.

The complexes in fractions 10 and 11 were then subjected to size exclusion chromatography. Fractions were collected and analyzed by Southern blot (Fig 3.2C). For this experiment, I performed slightly more stringent MCN digestions, such that fractions 10 and 11 were more enriched for mono- and di- over tri- nucleosomes. The HSV-1 DNA-containing complexes continued to fractionate as cellular mono- and di- nucleosomes after chromatography (Fig 3.2C, Fraction 4). Therefore, MCN digestion releases HSV-1 DNA in small complexes that fractionate as cellular mono- to di- nucleosomes following differential centrifugation followed by sucrose gradient centrifugation and size exclusion chromatography. Unlike the DNA in cellular nucleosomes, which is protected to homogenous sizes corresponding to mono- and di- nucleosomes (146 and 292bps, respectively), however, the HSV-1 DNA in such complexes was

protected to a range of heterogeneous fragments from mono- to di- nucleosome size (146 to 292bps - Fig 3.2A, compare Fraction 11, HSV and Cellular).

3.2.3. Nuclear HSV-1 DNA is more accessible to MCN than DNA in most cellular chromatin.

Mostly all HSV-1 DNA released as soluble chromatin by 150s MCN digestion (Fig 3.2) was in small fragments in complexes that fractionated as mono- to di-nucleosomes, whereas the DNA in cellular chromatin was primarily in large fragments in poly-nucleosome complexes. I next tested whether these differences reflected differences in MCN accessibility.

Nuclei of infected cells were harvested at 5hpi and digested with different concentrations of MCN for increasing times, to reach from very little to almost total DNA digestion. Nuclear DNA was purified, resolved by agarose gel electrophoresis and analyzed by ethidium bromide staining and Southern blot. Cellular and HSV-1 hybridizations are shown in standard exposures to compare total DNA levels, and also in over exposures, to analyze the similarities and differences between the smaller cellular and HSV-1 DNA fragments (Fig 3.3A, standard and over exposure).

As expected for chromatinized cellular DNA, low MCN concentrations digested cellular DNA to a typical nucleosome ladder of sizes corresponding to multiples of 160 bp (Fig 3.3A, 0.005U, lanes 4-6). In contrast, and as previously reported (Leinbach and Summers 1980; Muggeridge and Fraser 1986; Lentine and Bachenheimer 1990; Kent, Zeng et al. 2004), HSV-1 DNA was digested primarily

to a smear presumably reflecting heterogeneously sized fragments (Fig 3.3A, most apparent at 0.005U, lane 5). Also consistent with previous reports (Leinbach and Summers 1980; Muggeridge and Fraser 1986; Lentine and Bachenheimer 1990; Kent, Zeng et al. 2004), a minor population of HSV-1 DNA was protected to sizes consistent with mono- or di- nucleosomes (most apparent at 0.05U, lanes 4 and 5 - over exposure).

As the concentration of MCN increased, eventually most (98%) cellular DNA was completely degraded (Fig 3.3B, compare 0.005 and 5U). Also consistent with previous reports (Leinbach and Summers 1980; Muggeridge and Fraser 1986; Lentine and Bachenheimer 1990; Kent, Zeng et al. 2004), a minor percentage (approximately 10%) of HSV-1 DNA was poorly accessible to even high MCN concentrations (Fig 3.3C, 0.5U). However, even this poorly accessible population was almost completely digested (up to 98%) when the concentration of MCN was increased by 100-fold (Fig 3.3C, HSV 5U).

In addition to differences in the size distribution of DNA fragments released, the kinetics of MCN digestion were also different between HSV-1 DNA and DNA in cellular chromatin. HSV-1 DNA was digested approximately 3-fold more rapidly than DNA in cellular chromatin (Table 3.2). For example, 50% of HSV-1 or cellular DNA (T_{50}) was digested by 0.05U MCN in 6.74 or 19.5min, respectively (Fig 3.3, B, C; Table 3.2). Most HSV-1 DNA is therefore more accessible to MCN than most DNA in cellular chromatin. However, the 10% of HSV-1 DNA that was poorly accessible was 5.3-fold more resistant to MCN digestion than DNA in cellular chromatin (Table 3.2, 0.5U). For example, 0.5U

MCN digested 90% of HSV-1 or cellular DNA (T_{90}) in 27.4 or 5.2min, respectively (Fig 3.3, B, C; Table 3.2).

In summary, most HSV-1 DNA was far more accessible to MCN at 5 hpi than DNA in cellular chromatin. However, a small percentage of HSV-1 DNA was far less accessible to MCN than DNA in cellular chromatin. Further contrasting with DNA in most cellular chromatin, most HSV-1 DNA was cleaved primarily to heterogeneous sizes, whereas the least accessible fraction was protected from digestion as long fragments.

3.2.4. HSV-1 DNA released as soluble chromatin is mostly in complexes that fractionate as mono- to di- nucleosomes.

HSV-1 DNA is far more accessible to MCN than DNA in cellular chromatin, and is digested in 150s primarily to heterogeneously sized fragments (Fig 3.3).

Nevertheless, only a small percentage of this digested HSV-1 DNA is released as soluble chromatin in complexes that fractionate as cellular mono- to di-nucleosomes in sucrose gradients (Fig 3.2). Instead, the vast majority is in heterogeneously sized complexes that fractionate as insoluble chromatin.

Different MCN digestion times release cellular chromatin as progressively shorter poly-nucleosome complexes. I therefore tested whether different times of MCN digestion could also release HSV-1 DNA in differently sized nucleosome-like complexes. I selected conditions that result in digestions ranging from either most HSV-1 DNA not digested (equivalent to Fig 3.3, HSV-0.005, lanes 2 and 3), to

most HSV-1 DNA digested to heterogeneous sizes (equivalent to Fig 3.3, HSV-0.05, lanes 2 and 3).

Briefly, nuclei of infected cells were harvested at 5hpi and digested with MCN for 15, 30, 150, or 300s, before being lysed and resolved into “soluble” and “insoluble” chromatin. Soluble chromatin was further resolved by sucrose gradient centrifugation and analyzed by Southern blot. As expected, brief digestions (15 or 30s) released only large poly-nucleosomes from cellular chromatin (Fig 3.4, Cellular-fractions 1-8). Cellular mono- and di- nucleosomes fractionating to fractions 10 and 11 were released only after 150s. At 300s, mono- and di- nucleosomes accounted for 55% of the cellular DNA released as soluble chromatin (Fig 3.4, Cellular). In contrast, HSV-1 DNA was released already at 15s only in complexes that resolved to fractions 10 and 11 (Fig 3.4, HSV-15s). In fact, mostly all HSV-1 DNA released into the soluble fraction at any MCN digestion time was in complexes that fractionate as mono- to di- nucleosomes (Fig 3.4, HSV), even at the mildest MCN digestions (which release >97% of cellular DNA in large poly-nucleosomes - Fig 3.4, compare HSV and Cellular - 15s, fractions 10 and 11). Consistent with the results presented in Fig 3.2, the HSV-1 DNA in the released complexes was protected to heterogeneous sizes ranging from mono- to di- nucleosome-sized DNA.

3.2.5. Complexes containing HSV-1 or cellular DNA resolve to different fractions at low salt concentrations

HSV-1 DNA is in complexes that fractionate as cellular mono- to di- nucleosomes even after extensive fractionation. However, the HSV-1 DNA within these complexes is more accessible to MCN than the DNA in cellular nucleosomes (Fig 3.2). The increased accessibility may result from instability of the HSV-1 DNA-protein interactions. Alternatively, HSV-1 DNA may non-specifically interact with cellular nucleosomes, thereby leading to co-fractionation and partial protection from MCN. I therefore evaluated the stability of the interactions. If HSV-1 DNA interacts with cellular chromatin non-specifically, then it should co-fractionate better in the absence of salt, whereas disruption of such interactions with salt should result in less co-fractionation. Neither inter- nor intra-nucleosome interactions are disrupted at NaCl concentrations below 225mM NaCl (Christiansen and Griffith 1977; Ausio, Dong et al. 1989), whereas 450mM NaCl disrupts inter- but not intra-nucleosome interactions (Christiansen and Griffith 1977; Ausio, Dong et al. 1989).

Nuclei from infected cells were harvested at 5hpi and digested with MCN for 150s. The soluble chromatin was resolved on sucrose gradients containing various NaCl concentrations. The fractions were collected and analyzed by Southern blot. Consistent with the experiments presented in Fig 3.4, cellular DNA was released primarily as large poly-nucleosomes. The pattern of fractionation of cellular DNA did not change much as the concentration of NaCl was increased from 0 to 225mM, as expected (Christiansen and Griffith 1977; Ausio, Dong et al.

1989). Only ~15% of the DNA in soluble cellular chromatin was released as mono- or di- nucleosomes (Fig 3.5, Cellular-0, 80mM, fractions 10-11; 225mM, fractions 11-12). When the concentration of salt was increased to 450mM, however, the cellular DNA that fractionated as mono- and di- nucleosomes increased from 15% to 24% (Fig 3.5, Cellular-450, fractions 11-12), as expected from disruption of internucleosome interactions. Without such disruption, some mono-nucleosomes fractionate in the pellet by interacting with larger polynucleosomes. Therefore, ~9% of the cellular DNA released by 150s MCN digestion was in mono- or di- nucleosomes tightly bound to larger polynucleosomes. In contrast, the HSV-1 DNA released as soluble chromatin was primarily in complexes that fractionated as mono- to di- nucleosomes even in the absence of NaCl (Fig 3.5, HSV, 0mM, fractions 9-11), when most cellular DNA fractionated as polynucleosomes (Fig 3.5, Cellular, 0mM, fractions-9).

Although all the HSV-1 DNA that was released into the soluble chromatin at any NaCl concentration always migrated as mono- to di-nucleosomes, the absolute amounts released into the soluble chromatin as mono-to-di nucleosomes increased as the salt concentration increased. Therefore, a percentage of the HSV-1 DNA released as mono- to di-nucleosomes still fractionated to the pellet, with the largest cellular and viral poly-nucleosomes, at salt concentrations that do not disrupt inter-nucleosome interactions, but was released into the soluble chromatin at concentrations that disrupt them. These results suggest that HSV-1 DNA is in nucleosome-like complexes that interact with nucleosome-like affinities with the longer cellular (or viral) poly-nucleosomes.

At 5 hpi, therefore, HSV-1 DNA does not co-fractionate with cellular nucleosomes through non-specific interactions. Instead, it is in complexes with similar biophysical properties to cellular nucleosomes.

3.2.6. Nuclear HSV-1 DNA is in unstable nucleoprotein complexes

Different MCN digestions released as little as 2% (15s) or as much as 23% (150s) of detectable HSV-1 DNA as soluble chromatin. Curiously, all this HSV-1 DNA was in complexes that fractionate as cellular mono- to di- nucleosomes (Fig 3.4). Therefore, only a small percentage of nuclear HSV-1 DNA may be in nucleosome-like complexes, whereas most may not be associated with proteins, and therefore quickly degraded by MCN (Fig 3.6A or B). Alternatively, HSV-1 DNA may be in unstable nucleosome-like complexes, which because of their instability still allow MCN access to their DNA. Unstable HSV-1 DNA-containing complexes are expected to be rapidly released by MCN but then also rapidly degraded, resulting in only a small percentage of nucleosome-like complexes detected at any given digestion time (Fig 3.6C). To differentiate between these possibilities, I modified the MCN digestions to “trap” the potential digestion intermediates, preventing their degradation (Fig 3.7).

Briefly, cells were infected and nuclei were harvested at 5hpi. So-called soluble and insoluble chromatin were fractionated without MCN digestion. The insoluble chromatin was then digested with MCN and the released soluble chromatin was periodically removed. To do so, insoluble chromatin was resuspended in MCN digestion buffer (0.05U MCN/ml) and digested during the

differential centrifugation. The insoluble chromatin is thus pelleted whereas the soluble chromatin released by MCN digestion remains in the supernatant. The supernatant was removed after 5min and the MCN in it was immediately quenched to prevent further digestion of the released soluble chromatin. The insoluble chromatin pellet was resuspended with fresh MCN digestion buffer and the entire procedure was repeated nine times. The soluble fractions were pooled, resolved together by sucrose gradients and analyzed by Southern blot (Fig 3.8).

Under these conditions, the cellular DNA released as soluble chromatin fractionated as mono-, di- (Fig 3.8, fractions 10 and 11), and larger poly-nucleosomes complexes (Fig 3.8, fractions 5-9), as expected from regularly chromatinized DNA. Unlike the standard continuous MCN digestion, however, the HSV-1 DNA released by our modified digestion was also in complexes that resolved to the same fractions as cellular poly-nucleosomes (Fig 3.8, HSV-fractions 5-9), as well as in complexes fractionating as mono- to di- nucleosomes (Fig 3.8, HSV-fractions 10 and 11). Moreover, the HSV-1 DNA was protected to more discrete sizes under these conditions than under continuous MCN digestions (Fig 3.2A and Fig 3.8, compare fractions 10, 11). Therefore, HSV-1 DNA fractionates as cellular poly-nucleosomes when MCN digestion of the soluble fraction is restricted (Fig 3.8). Standardized by the recovery of cellular DNA, 78% of the total nuclear HSV-1 DNA fractionated as soluble chromatin, leaving only 22% in the insoluble chromatin pellet (Table 3.3), very much like the DNA in cellular chromatin (Table 3.3). These results indicate that the majority of

nuclear HSV-1 DNA is in unstable complexes that fractionate as cellular nucleosomes and protect their DNA to similar sizes as cellular nucleosomes do.

In summary, HSV-1 DNA can be isolated in complexes that fractionate as cellular poly-nucleosomes, as long as MCN activity is rapidly quenched after the release of the complexes containing HSV-1 DNA into the soluble chromatin.

These results suggest that the majority of nuclear HSV-1 DNA is in complexes that are highly unstable and as such are rapidly degraded by standard MCN digestions.

3.2.7. HSV-1 nucleosome-like complexes are stabilized by crosslinking.

Particularly unstable cellular nucleosomes are digested by MCN unless stabilized by crosslinking (Jin and Felsenfeld 2007; Jin, Zang et al. 2009). I therefore evaluated the stability of the HSV-1 DNA containing complexes by subjecting them to MCN redigestion.

I first evaluated the stability of the complexes released by moderate (150s) MCN digestions. These digestions release mostly mono-nucleosomes with a small percentage of di-nucleosomes (Fig 3.9A, Total). Crosslinking resulted in essentially complete protection from MCN redigestion (T_{50} ; >60min) (Table 3.4 and Fig 3.9A, C - Crosslink). Consistent with the stability of most cellular nucleosomes, moreover, even the non-crosslinked cellular nucleosomes were still resistant to MCN redigestion. More than 50% of cellular DNA in non-crosslinked nucleosomes was still protected from 60min MCN redigestion (T_{50} ; >60min) (Table 3.4, Fig 3.9A, C - No Crosslink). Crosslinking also stabilized the HSV-1

nucleosome-like complexes, resulting in a 6-fold increase in the time required to digest 50% of the HSV-1 DNA (T_{50} , 9 and 54min, respectively) (Table 3.4 and Fig 3.9A, C compare HSV-Crosslink and No Crosslink). Consistent with the proposed instability of the HSV-1 nucleosome-like complexes, however, HSV-1 DNA in the non-crosslinked samples was digested >6-fold more rapidly than cellular DNA (T_{50} , 9 and >60min, respectively; T_{90} , 54min and non determinable, respectively - Table 3.4 and Fig 3.9A, C). As in the experiments presented in Fig 3.3, 3.4, and 3.8, therefore, HSV-1 DNA in non-crosslinked (or crosslinked) nucleosome-like complexes is far more accessible to MCN than DNA in cellular nucleosomes.

I next evaluated the stability of the complexes released by very mild (15s) MCN digestions (Fig 3.9B and D), which by definition release only the most accessible complexes. Under the proposed model, these complexes should be the most unstable. As expected, very little DNA was released as mononucleosomes by such mild digestions, as observed by ethidium bromide staining (Fig 3.9B, Total DNA). Nonetheless, both cellular and HSV-1 DNA were detected by Southern blot.

Consistent with the release of the most unstable nucleosomes, the cellular nucleosomes in this soluble chromatin were >15-fold more sensitive to MCN digestion than those released by the moderate (150s) MCN digestions (T_{50} , 3.8 and >60, respectively) (Table 3.4 and Fig 3.9A, C). The nucleosomes released by 15s digestions were in fact so unstable that crosslinking only modestly (1.7-fold) stabilized them (T_{50} ; 3.8 and 6.5min for non-crosslinked and crosslinked ones,

respectively) (Table 3.4 and Fig 3.9B, D). Approximately 75% of the DNA in the highly accessible cellular nucleosomes was in these unstable nucleosomes and therefore digested during the first 15min (Fig 3.9D). In addition to these unstable nucleosomes, however, there was also a population of more stable ones. The DNA in these nucleosomes was much less accessible to MCN and it was thus digested at a much slower rate. Only approximately 10% of the DNA in these latter complexes was digested between 15 and 60min (Fig 3.9B, D).

The HSV-1 DNA in the unstable nucleosomes released by the very brief MCN digestion was also rapidly degraded by MCN redigestion, resulting in a very similar T_{50} to the DNA in the most unstable cellular nucleosomes (3 and 3.8min, respectively, Table 3.4 and Fig 3.9). Also like the most unstable cellular nucleosomes, crosslinking resulted in only a slight (1.5-fold) protection from redigestion (T_{50} , 3.4 and 3min, respectively) (Table 3.4 and Fig 3.9). Crosslinking also resulted in a modest increase (3-fold) in the time required to digest 90% of DNA (T_{90}) (Table 3.4 and Fig 3.9). In contrast to the DNA in the most accessible cellular nucleosomes, however, there was no significant population of HSV-1 DNA resistant to MCN re-digestion, even after crosslinking (Table 3.4 and Fig 3.9). These results indicate that most of the complexes released by brief MCN digestion from cellular and HSV-1 genomes are similarly unstable. However, whereas the unstable cellular nucleosomes are only a minority, essentially all the HSV-1 DNA-containing complexes are unstable. In summary, HSV-1 DNA is in unstable complexes that are as accessible as the most unstable cellular nucleosomes.

3.3. References

- Ausio, J., F. Dong, et al. (1989). "Use of selectively trypsinized nucleosome core particles to analyze the role of the histone "tails" in the stabilization of the nucleosome." *J Mol Biol* **206**(3): 451-63.
- Christiansen, G. and J. Griffith (1977). "Salt and divalent cations affect the flexible nature of the natural beaded chromatin structure." *Nucleic Acids Res* **4**(6): 1837-51.
- Cliffe, A. R. and D. M. Knipe (2008). "Herpes simplex virus ICP0 promotes both histone removal and acetylation on viral DNA during lytic infection." *J Virol* **82**(24): 12030-8.
- Deshmane, S. L. and N. W. Fraser (1989). "During latency, herpes simplex virus type 1 DNA is associated with nucleosomes in a chromatin structure." *J Virol* **63**(2): 943-7.
- Ferenczy, M. W. and N. A. Deluca (2009). "Epigenetic Modulation of Gene Expression from Quiescent Hsv Genomes." *J Virol*.
- Herrera, F. J. and S. J. Triezenberg (2004). "VP16-dependent association of chromatin-modifying coactivators and underrepresentation of histones at immediate-early gene promoters during herpes simplex virus infection." *J Virol* **78**(18): 9689-96.
- Huang, J., J. R. Kent, et al. (2006). "Trimethylation of histone H3 lysine 4 by Set1 in the lytic infection of human herpes simplex virus 1." *J Virol* **80**(12): 5740-6.
- Jin, C. and G. Felsenfeld (2007). "Nucleosome stability mediated by histone variants H3.3 and H2A.Z." *Genes Dev* **21**(12): 1519-29.
- Jin, C., C. Zang, et al. (2009). "H3.3/H2A.Z double variant-containing nucleosomes mark 'nucleosome-free regions' of active promoters and other regulatory regions." *Nat Genet* **41**(8): 941-5.
- Kent, J. R., P. Y. Zeng, et al. (2004). "During lytic infection herpes simplex virus type 1 is associated with histones bearing modifications that correlate with active transcription." *J Virol* **78**(18): 10178-86.
- Knipe, D. M. and A. Cliffe (2008). "Chromatin control of herpes simplex virus lytic and latent infection." *Nat Rev Microbiol* **6**(3): 211-21.
- Kutluay, S. B., S. L. DeVos, et al. (2009). "Transcriptional coactivators are not required for herpes simplex virus type 1 immediate-early gene expression in vitro." *J Virol* **83**(8): 3436-49.
- Kutluay, S. B., J. Doroghazi, et al. (2008). "Curcumin inhibits herpes simplex virus immediate-early gene expression by a mechanism independent of p300/CBP histone acetyltransferase activity." *Virology* **373**(2): 239-47.
- Kutluay, S. B. and S. J. Triezenberg (2009). "Regulation of histone deposition on the herpes simplex virus type 1 genome during lytic infection." *J Virol* **83**(11): 5835-45.

- Leinbach, S. S. and W. C. Summers (1980). "The structure of herpes simplex virus type 1 DNA as probed by micrococcal nuclease digestion." J Gen Virol **51**(Pt 1): 45-59.
- Lentine, A. F. and S. L. Bachenheimer (1990). "Intracellular organization of herpes simplex virus type 1 DNA assayed by staphylococcal nuclease sensitivity." Virus Res **16**(3): 275-92.
- Liang, Y., J. L. Vogel, et al. (2009). "Inhibition of the histone demethylase LSD1 blocks alpha-herpesvirus lytic replication and reactivation from latency." Nat Med **15**(11): 1312-7.
- Mouttet, M. E., D. Guetard, et al. (1979). "Random cleavage of intranuclear herpes simplex virus DNA by micrococcal nuclease." FEBS Lett **100**(1): 107-9.
- Muggeridge, M. I. and N. W. Fraser (1986). "Chromosomal organization of the herpes simplex virus genome during acute infection of the mouse central nervous system." J Virol **59**(3): 764-7.
- Narayanan, A., W. T. Ruyechan, et al. (2007). "The coactivator host cell factor-1 mediates Set1 and MLL1 H3K4 trimethylation at herpesvirus immediate early promoters for initiation of infection." Proc Natl Acad Sci U S A **104**(26): 10835-40.
- Oh, J. and N. W. Fraser (2008). "Temporal association of the herpes simplex virus genome with histone proteins during a lytic infection." J Virol **82**(7): 3530-7.
- Placek, B. J., J. Huang, et al. (2009). "The histone variant H3.3 regulates gene expression during lytic infection with herpes simplex virus type 1." J Virol **83**(3): 1416-21.
- Severini, A., D. G. Scraba, et al. (1996). "Branched structures in the intracellular DNA of herpes simplex virus type 1." J Virol **70**(5): 3169-75.
- Sinden, R. R., D. E. Pettijohn, et al. (1982). "Organization of herpes simplex virus type 1 deoxyribonucleic acid during replication probed in living cells with 4,5',8-trimethylpsoralen." Biochemistry **21**(18): 4484-90.

| DNA | Insoluble | Soluble |
|-------------------------|-----------|---------|
| HSV Protein-Free | 17% | 83% |
| HSV Nuclear | 73% | 27% |
| Cellular Nuclear | 81% | 19% |

Table 3.1. HSV-1 DNA in nuclei of lytically infected cells does not fractionate as protein-free DNA. Percentages of DNA from nuclei digested with BamHI that fractionate to the **soluble** or **insoluble** fractions.

| [MCN] | T ₅₀ | | T ₉₀ | |
|--------------|-----------------|---------|-----------------|---------|
| | Cellular | HSV | Cellular | HSV |
| 0.005 | >60min | 51.1min | >60min | >60min |
| 0.05 | 19.5min | 6.7min | >60min | 32.6min |
| 0.5 | 0.7min | 0.4min | 5.2min | 27.4min |
| 5 | 0.3min | 0.3min | 2.5min | 0.2min |

Table 3.2. Nuclear HSV-1 DNA is more accessible to MCN than DNA in most cellular chromatin. Digestion times required to degrade 50% (T₅₀) or 90% (T₉₀) of HSV-1 or Cellular DNA, graphically calculated from the average digestion curves (n=3).

| DNA | Insoluble | Soluble |
|-----------------|-----------|---------|
| Cellular | 26% | 74% |
| HSV | 22% | 78% |

Table 3.3. HSV-1 DNA is quantitatively recovered as poly-nucleosomes after the modified MCN digestion. Percentage of HSV-1 or cellular DNA fractionating in the **soluble** and **insoluble** fractions after being digested as per the modified MCN digestion protocol, standardized by recovery of cellular DNA.

Nucleosomes in Moderately Accessible Chromatin

| | Cell | | HSV | |
|-----------------------|--------------|-----------|--------------|-----------|
| | No crosslink | Crosslink | No crosslink | Crosslink |
| T₅₀ | >60min | >60min | 9min | 54min |
| T₉₀ | >60min | >60min | >60min | >60min |

Nucleosomes in Most Accessible Chromatin

| | Cell | | HSV | |
|-----------------------|--------------|-----------|--------------|-----------|
| | No crosslink | Crosslink | No crosslink | Crosslink |
| T₅₀ | 3.8min | 6.5min | 3min | 4.4min |
| T₉₀ | >60min | >60min | 10min | 30min |

Table 3.4. Unstable HSV-1 nucleosomes are partially stabilized by crosslinking. Digestion times required to degrade 50% (**T₅₀**) and 90% (**T₉₀**) of total DNA from nucleosome fractions previously crosslinked with formaldehyde.

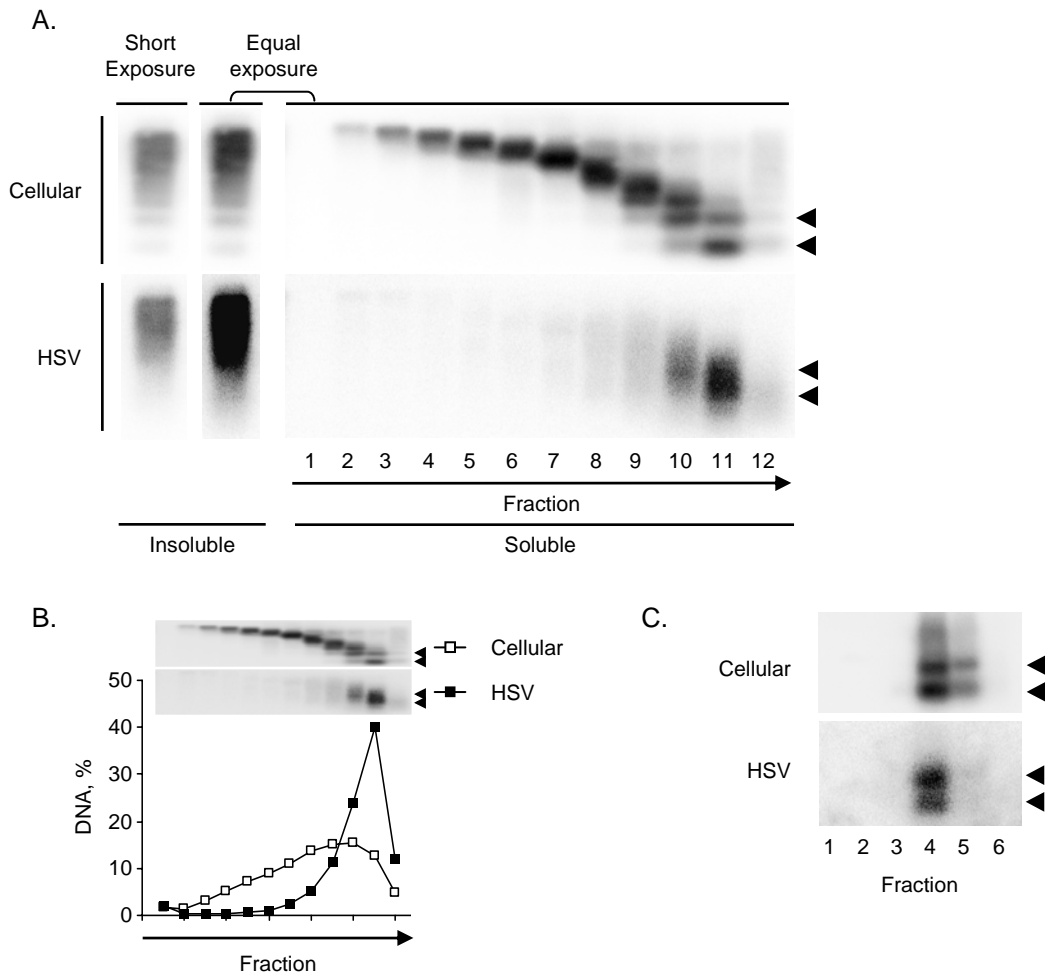


Figure 3.2. MCN digestion releases HSV-1 DNA in complexes that fractionate as cellular mono- to di-nucleosomes. Nuclei of infected cells were digested for 150s with 0.05U of MCN per 1×10^7 nuclei and the soluble DNA-protein complexes were resolved on sucrose gradients (**A**, **B**). Following a similar experiment, fractions 10 and 11 from the gradients were further fractionated by size exclusion chromatography (**C**). DNA from each fraction was analyzed by Southern blot with HSV-1 or cellular probes. **A.** Images of the membrane hybridized with cellular (**Cellular**) HSV-1 (**HSV**) probes. Bottom fractions to the left. **B.** Line graphs presenting HSV-1 and cellular DNA in each fraction as percent of DNA in the gradient. The panels on the top are the same shown in **A**, shown as reference for the graph below and resized to fit in the figure. **C.** Images of the membranes hybridized with cellular (**Cellular**) or HSV-1 (**HSV**) specific probes. Arrowheads indicate migration of mono- or di-nucleosomes.

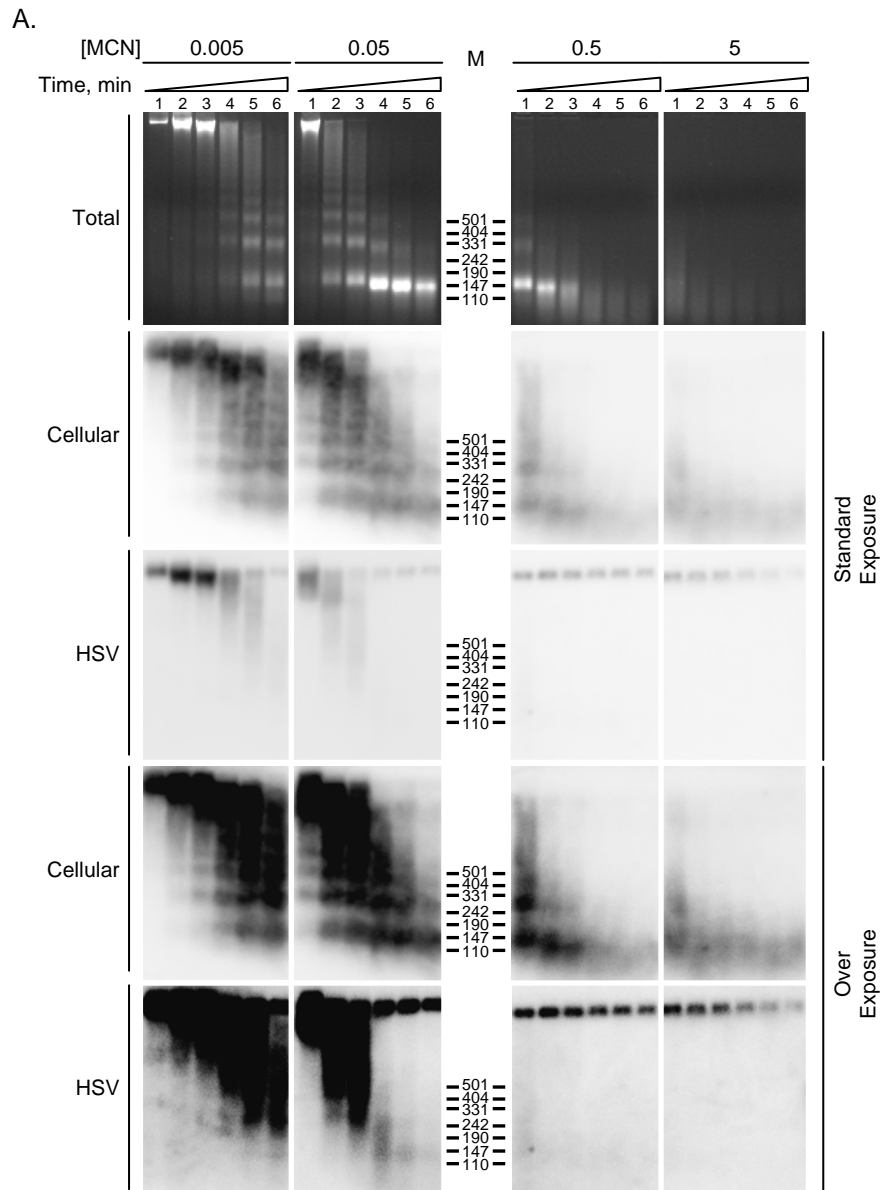

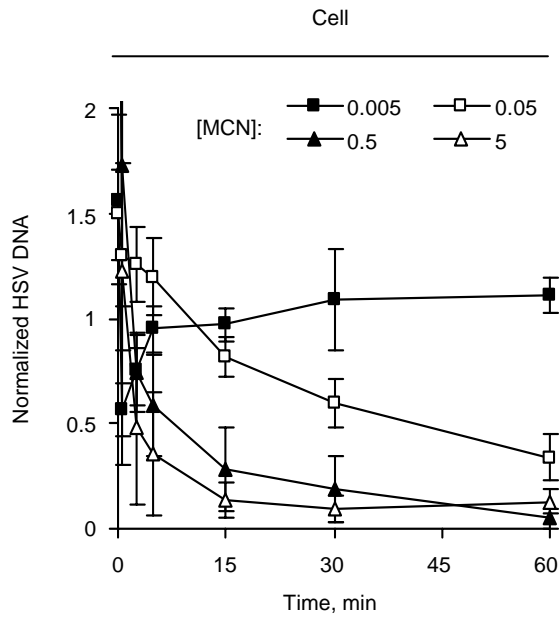


Figure 3.3. Nuclear HSV-1 DNA is more accessible to MCN than DNA in most cellular chromatin. Purified nuclei of infected cells were digested for 0.5, 2.5, 5, 15, 30, and 60min () with 0.005, 0.05, 0.5, or 5U MCN per 1×10^7 nuclei and the DNA was analyzed by Southern blot with HSV-1 or cellular probes. **A.** Images of the ethidium bromide stained gels (**Total**) and membranes hybridized with cellular (**Cellular**) or HSV-1 (**HSV**) specific probes. **M**, molecular weight marker. Normal and overexposures (bottom panels), in which the nucleosome-sized and MCN-resistant HSV-1 DNA are more clearly visible, are shown. To achieve comparable signal intensities, only 50% of sample was loaded for 0.5min, 0.005 to 5U.

B.



C.

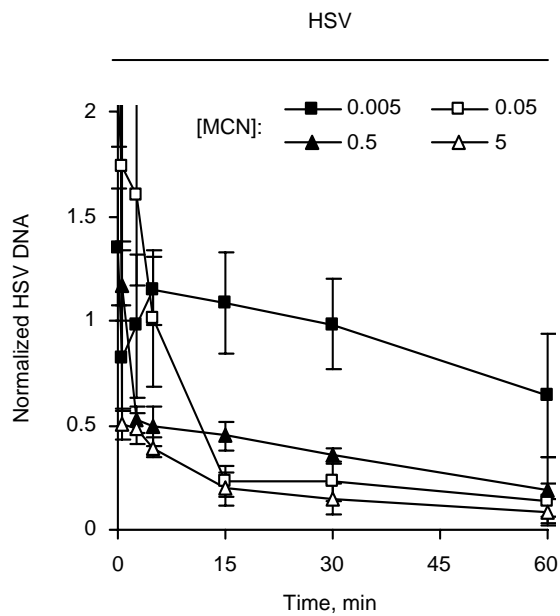


Figure 3.3. (continued) Nuclear HSV-1 DNA is more accessible to MCN than DNA in most cellular chromatin.

B and C, Line graphs of the quantitated Southern blots from **Figure 3.3 A** presenting normalized levels of cellular (**B**) and HSV-1 (**C**) DNA against digestion time (averages \pm SD, $n=3$).

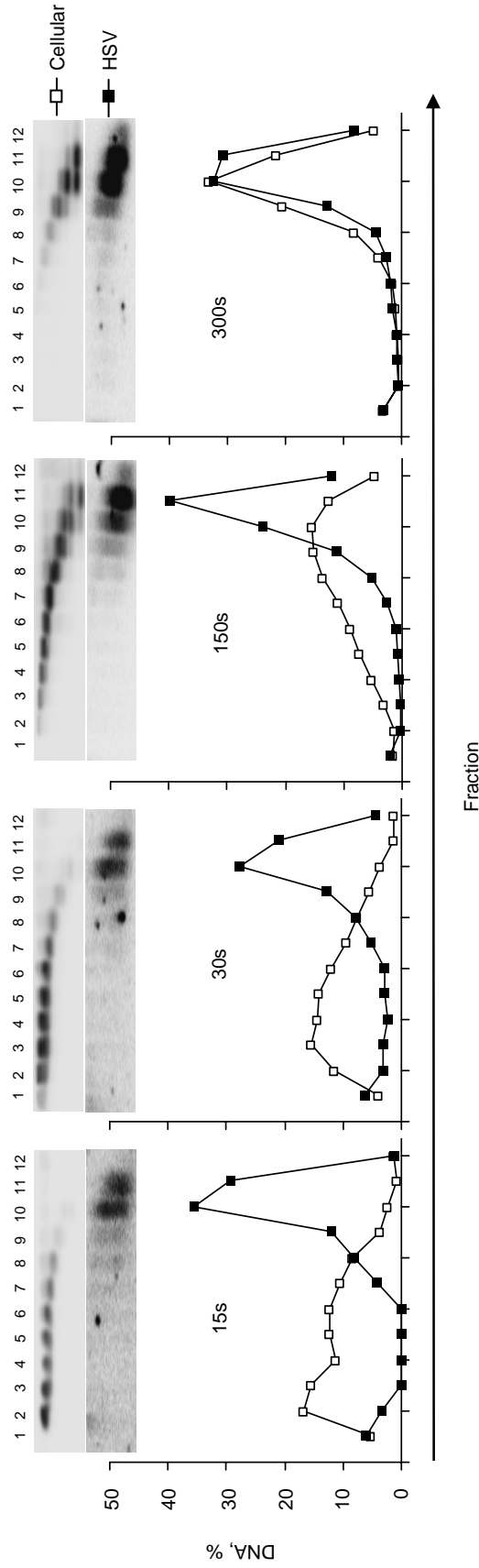


Figure 3.4. Most HSV-1 DNA released by MCN as soluble chromatin is in complexes that fractionate as mono- to di- nucleosomes. Nuclei of infected cells were digested for 15, 30, 150, or 300s with 0.05U of MCN per 1×10^7 nuclei. The soluble DNA-protein complexes were resolved on sucrose gradients. DNA from each fraction was analyzed by Southern blot with HSV-1 or cellular specific probes. Line graphs presenting cellular and HSV-1 DNA in each fraction as percent of DNA in the gradient. Inserts on top, images of the membranes hybridized with cellular (**Cellular**) or HSV-1 (**HSV**) probes, resized to fit the graph. Bottom fractions loaded to the left.

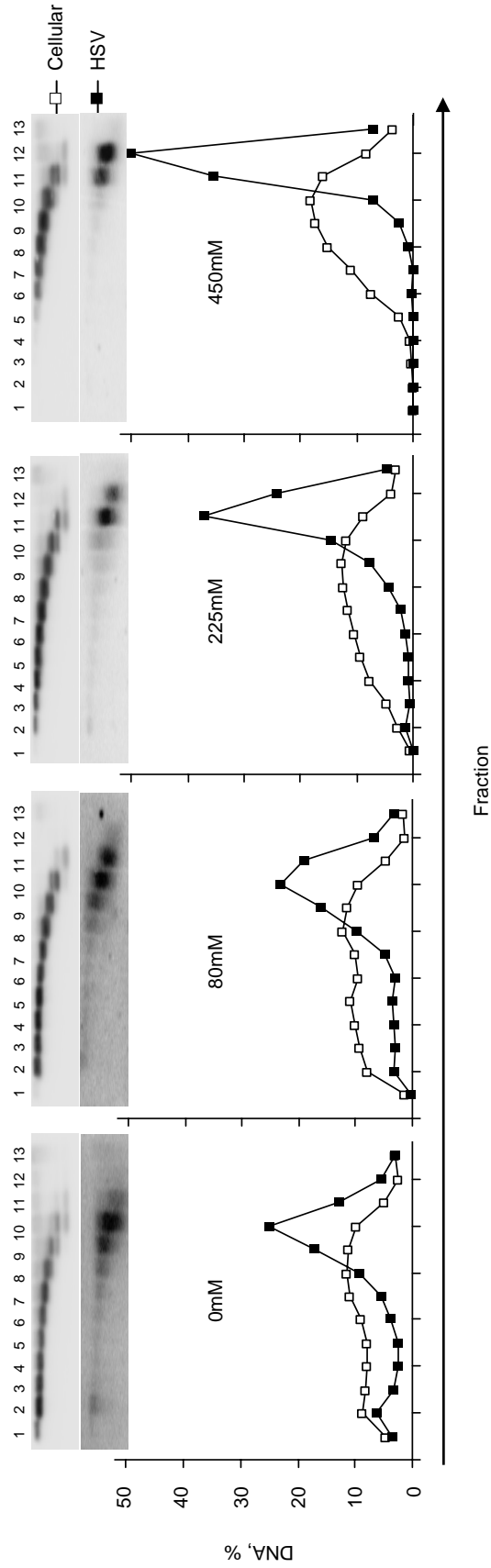


Figure 3.5. HSV-1 or cellular DNA-containing complexes resolve to different fractions at low salt concentrations. Nuclei of infected cells were digested for 150s with 0.05U MCN per 1×10^7 nuclei and then lysed. The soluble DNA-protein complexes were resolved on sucrose gradients containing 0, 80, 225, or 450mM NaCl. DNA from each fraction was analyzed by Southern blot with HSV-1 or cellular specific probes. Line graphs presenting cellular and HSV-1 DNA in each fraction as percent of DNA in the gradient. Inserts on top, images of the membrane hybridized with cellular (**Cellular**) or HSV-1 (**HSV**) probes, resized to fit the graphs. Bottom fractions loaded to the left.

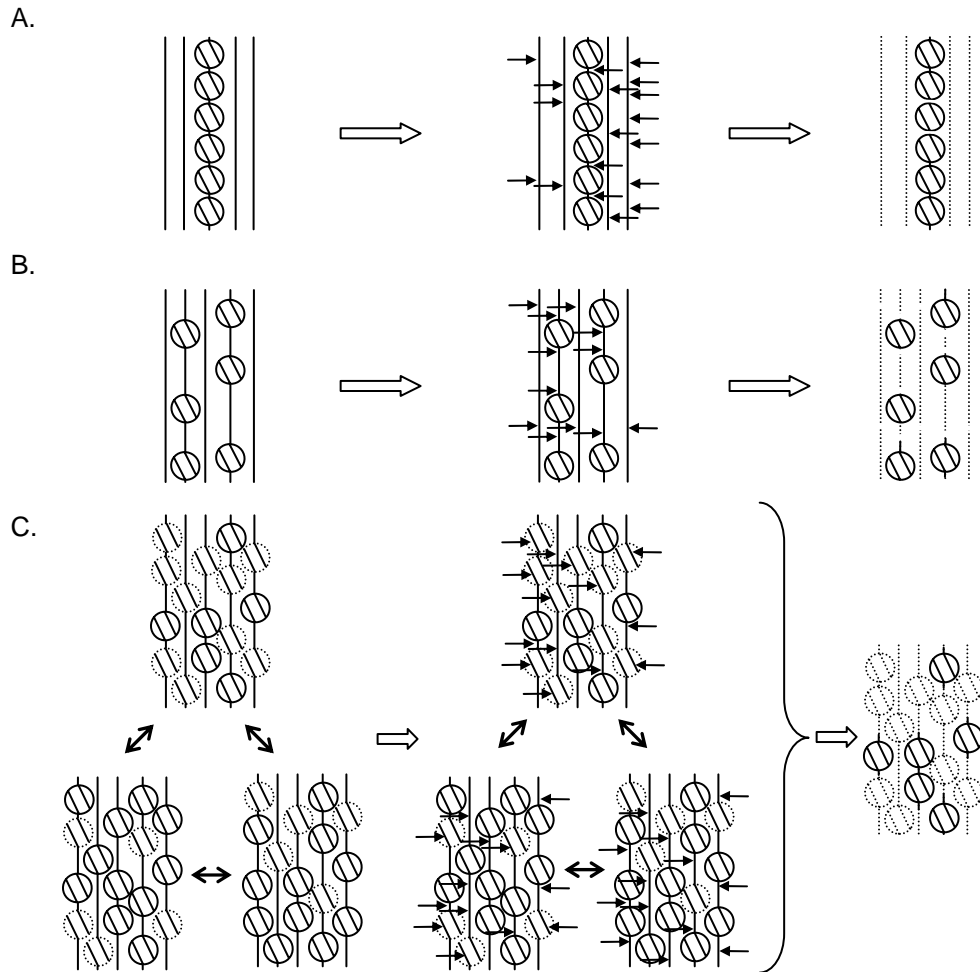


Figure 3.6. Potential types of HSV-1 nucleoprotein complexes. Cartoons representing three potential models of HSV-1 DNA nucleoprotein complexes in lytically infected cells. **A, B,** A small percentage of HSV-1 genomes are either regularly chromatinized (**A**) or irregularly chromatinized with randomly positioned nucleosomes (**B**). Protein-free genomes are represented as straight lines without histones. Sites of MCN digestion are indicated by arrows. MCN first cleaves randomly the protein-free genomes and the linker region between nucleosomes. Protein-free genomes are completely digested by longer digestions, whereas chromatinized genomes are protected to mononucleosome sizes. As a result, only a small percentage of HSV-1 DNA is protected to nucleosome size fragments, or co-immunoprecipitates with histones. **C.** Most HSV-1 DNA is in unstable nucleosome-like complexes. Unstable nucleosomes are represented with dotted lines. MCN first cleaves the DNA within the unstable nucleosomes and the linker DNA. DNA within the unstable nucleosomes is then promptly degraded. As a result, only a minor fraction of HSV-1 is protected to nucleosome-sized fragments at any given time, or co-immunoprecipitates with histones.

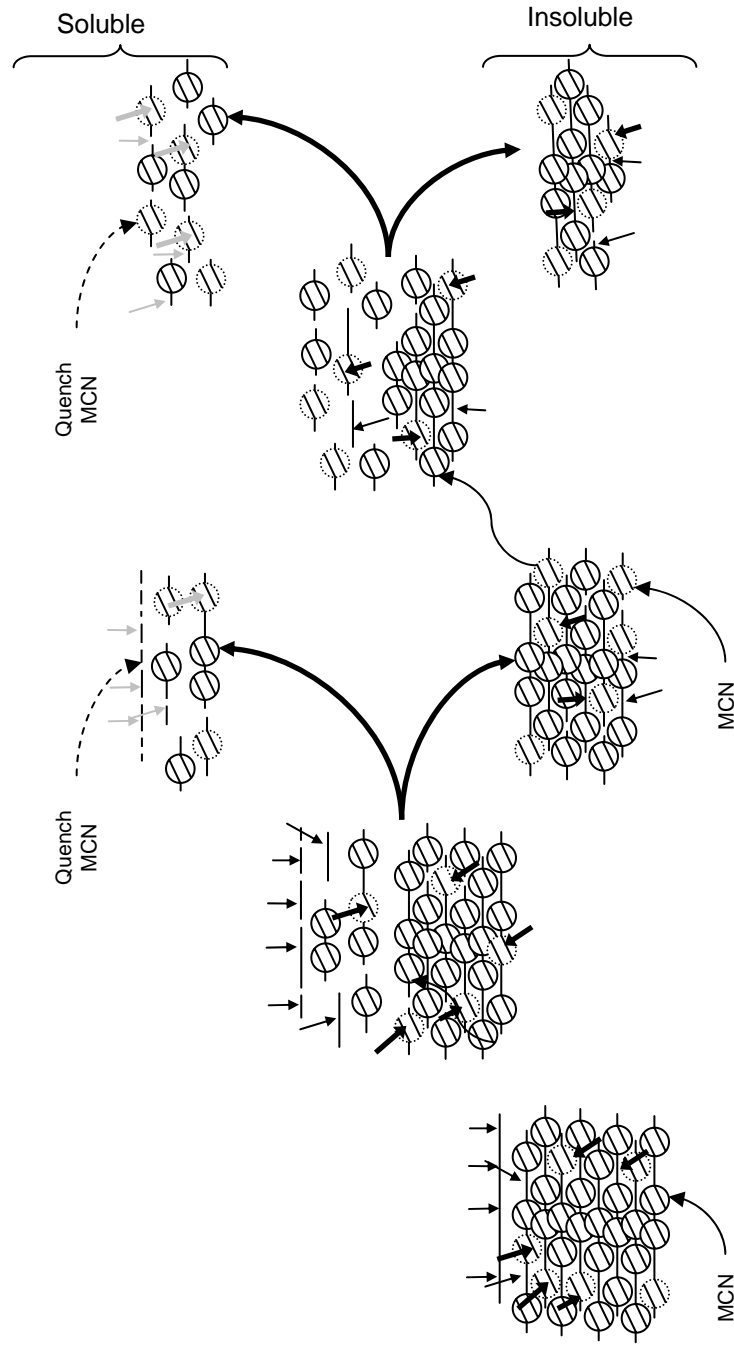


Figure 3.7. Modified MCN digestion protocol. Cartoon representing the modified MCN digestion protocol designed to “trap” potential intermediate unstable HSV-1 nucleosome-like complexes. MCN digestion cleaves randomly the protein-free genomes and linker DNA, as well as the DNA within the unstable nucleosomes. “Soluble chromatin” remains in the supernatant whereas the “insoluble chromatin” pellets. Soluble chromatin is removed and MCN is quenched. Insoluble chromatin is resuspended with fresh MCN digestion buffer. The process was repeated nine times.

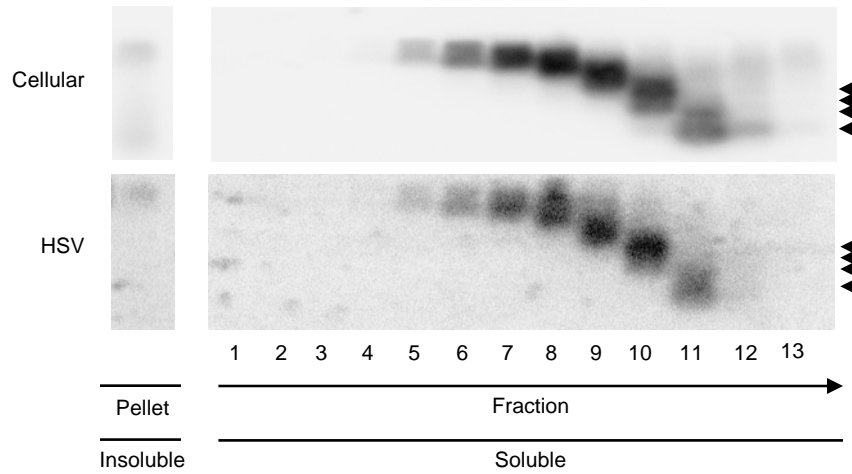


Figure 3.8. HSV-1 DNA fractionates as poly-nucleosomes after the modified MCN digestion. Nuclei of infected cells were lysed and soluble and insoluble chromatin were fractionated. Insoluble chromatin was resuspended in MCN digestion buffer (0.05U MCN/ml), and subjected to modified MCN digestions. Supernatants were periodically removed and quenched, and the insoluble pellets were resuspended with fresh MCN. Soluble DNA-protein complexes were pooled and further resolved on sucrose gradients. DNA from each fraction was analyzed by Southern blot with HSV-1 or cellular specific probes. Images of the membranes hybridized with cellular (**Cellular**) or HSV-1 (**HSV**) specific probes. Arrowheads indicate migration of mono-, di-, tri-, or tetra- nucleosomes.

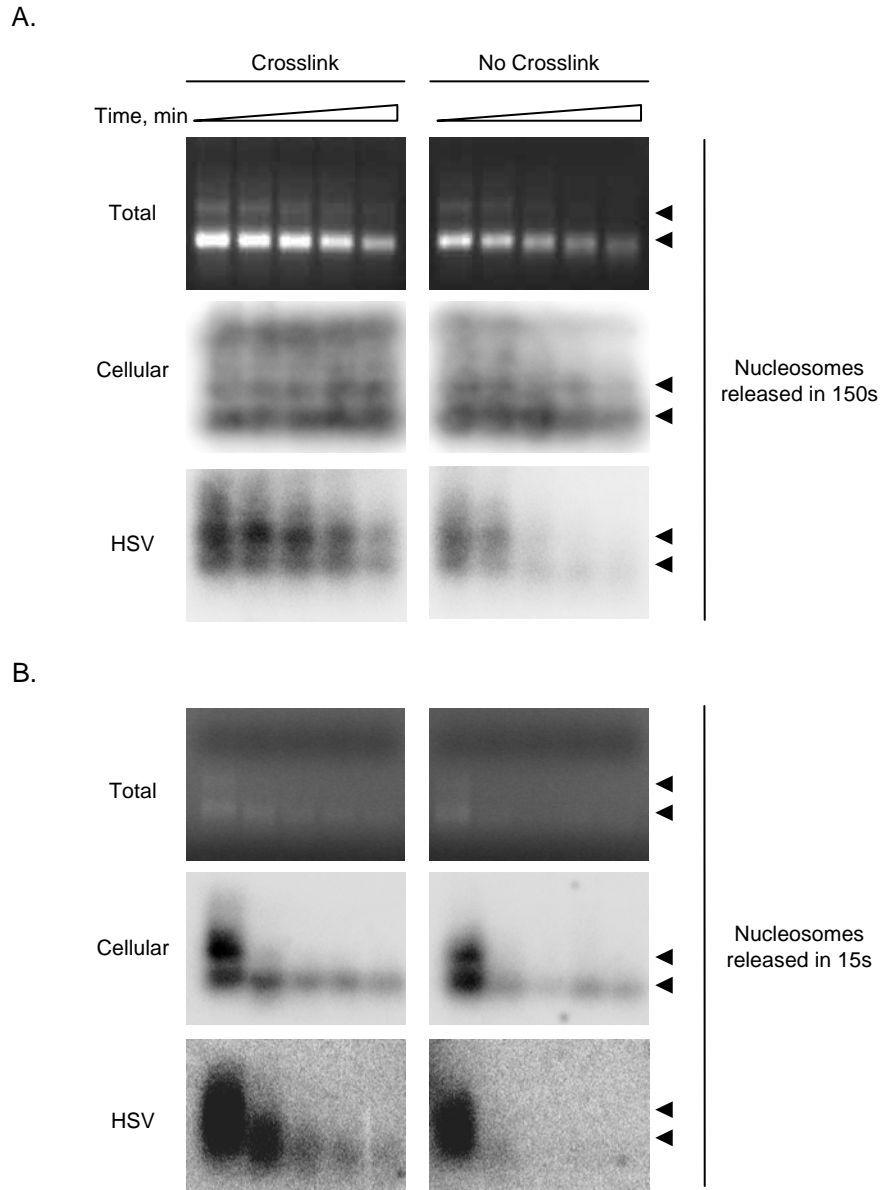


Figure 3.9. Unstable HSV-1 nucleosome-like complexes are partially stabilized by crosslinking. Nuclei of infected cells were digested with 0.05U MCN per 1×10^7 nuclei for **150s** or **15s** and lysed. Soluble DNA-protein complexes were resolved on sucrose gradients, and the relevant fractions from the sucrose gradients were then further fractionated by size exclusion chromatography. Relevant fractions from the size exclusion columns were either crosslinked (**Crosslink**) or not (**No Crosslink**) for 1h at 4°C, quenched with 125mM glycine for 10min and redigested with 0.05U/ml MCN for 0, 5, 15, 30, 60min (). DNA was analyzed by Southern blot with HSV-1 or cellular probes. **A, B.** Images of the ethidium bromide stained gels (**Total**) and membranes hybridized with cellular (**Cellular**) or HSV-1 (**HSV**) specific probes. Different exposures are shown for each hybridization. Arrowheads indicate migration of mono- or di- nucleosomes.

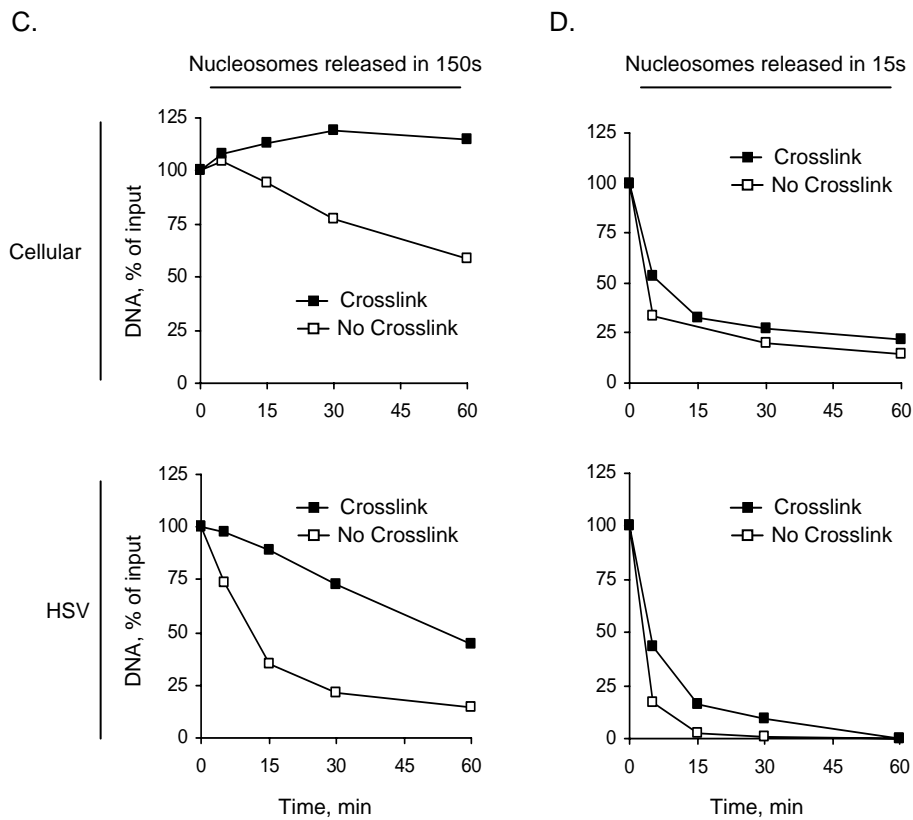


Figure 3.9. (continued) Unstable HSV-1 nucleosome-like complexes are partially stabilized by crosslinking.

C, D. Line graphs of the quantitated Southern blots from **Figure 4.9 A and B** presenting cellular and HSV-1 DNA against digestion time, expressed as percent of DNA prior to digestion.

CHAPTER 4: THE ACCESSIBILITY OF LYTIC HSV-1 GENOMES DEPENDS ON THE TRANSCRIPTIONAL ACTIVATION STATE

This chapter contains unpublished data

4.1. Introduction

Using classical chromatin characterization techniques, I have shown that most HSV-1 DNA is at 5hpi in unstable nucleoprotein complexes and, consequently, more accessible to MCN than most DNA in cellular chromatin (Chapter 3, and Lacasse and Schang 2010). HSV-1 DNA was protected from MCN redigestion only after crosslinking, like the most unstable cellular nucleosomes. Moreover, the HSV-1 DNA was quantitatively recovered in complexes with the biophysical properties of mono- to poly-nucleosomes following a modified “serial” MCN digestion protocol that I developed to “trap” unstable digestion intermediates. I proposed that HSV-1 DNA exists mainly in unstable nucleosome-like complexes during lytic infections. However, the previous study had only analyzed a single time post infection, 5 hours. It therefore remained unknown whether HSV-1 DNA was in unstable nucleosomes at other times. Herein, I tested whether such unstable nucleosomes are present at other times during lytic infection.

4.2 Results

4.2.1. The accessibility of HSV-1 DNA changes throughout the lytic infection cycle

Standard MCN digestion of HSV-1 DNA during lytic infection releases HSV-1 DNA in unique patterns of fragments, different from those patterns released from cellular chromatin. The unique pattern results from HSV-1 DNA being in unstable nucleoprotein complexes, like most unstable cellular nucleosomes (Lacasse and Schang 2010).

Our initial characterization of the HSV-1 nucleoprotein complexes was performed at 5hpi. At this time, all classes of HSV-1 genes are transcribed, HSV-1 DNA is replicated, and histones interact with HSV-1 DNA (Herrera and Triezenberg 2004; Kent, Zeng et al. 2004; Cliffe and Knipe 2008; Kutluay, DeVos et al. 2009; Kutluay and Triezenberg 2009; Placek, Huang et al. 2009). However, it still remained unclear whether HSV-1 DNA was in unstable nucleosomes at other times during infection. As a first step in evaluating the biophysical properties of the potential HSV-1 nucleoprotein complexes present throughout the lytic infection cycle, I performed a time course evaluation of the accessibility of HSV-1 DNA to MCN.

Vero cells were infected with 5 PFU of HSV-1 per cell. Nuclei of infected cells were isolated at 2, 5, 7, and 9 hpi and digested with MCN (0.05U/1x10⁷ cells) for 0.5, 2.5, 5, 15, 30 and 60 minutes. DNA was purified, resolved by agarose gel electrophoresis, and analyzed by ethidium bromide staining and Southern blot hybridization. Hybridizations with cellular probes are shown in

standard exposures. Hybridizations with HSV-1 probes are also shown overexposed, to highlight the changes in the accessibility of HSV-1 DNA during lytic infection (Fig. 4.1A).

As expected for chromatinized cellular DNA, and consistent with our previous report (Lacasse and Schang 2010), standard MCN digestion resulted in the digestion of cellular DNA to sizes of typical nucleosome ladders (corresponding to multiples of 160bp-Fig. 4.1A, Cellular). As evaluated by the time required to digest 50% of cellular DNA (T_{50}), the accessibility of cellular chromatin remained relatively constant throughout the course of infection (Fig 4.1B). T_{50} varied by only less than 1.4-fold, ranging from >60, 50.1, to 41.1min for 2, 5, and 9hpi, respectively (Fig 4.1B and Table 4.1). Consistently, the T_{50} for MCN digestion was 60.8min in a separate experiment in which nuclei were harvested at 7hpi (Fig 4.1B and Table 4.1).

Whereas cellular DNA levels remained constant throughout the time course, the levels of HSV-1 DNA increased. At 2hpi, only unreplicated infecting HSV-1 DNA was detected. At 5hpi, HSV-1 DNA replication had begun and the amount of HSV-1 DNA had increased and continued to do so until 9hpi, the last time point evaluated (Fig 4.1A, HSV - standard exposure).

In contrast to cellular DNA, the accessibility of HSV-1 DNA containing IE or L loci changed as the infection progressed. At 2hpi, most HSV-1 IE or L DNA was poorly accessible to MCN (Fig 4.1A, 2hpi – HSV IE and L). These results are consistent with a previous report, which found the infecting HSV-1 DNA to be more resistant to MCN digestion than the replicated HSV-1 DNA

(Leinbach and Summers 1980). At 5hpi, the percentage of HSV-1 IE or L loci DNA that was poorly accessible to MCN had decreased to 14.5%, whereas the remaining 85.5% of HSV-1 DNA was digested mostly to heterogeneously sized fragments with a minor population of nucleosome-sized fragments (Fig 4.1A-5hpi and 4.1D). These results are also consistent with previous results (Chapter 3 and Lacasse and Schang 2010). MCN digestions of nuclei harvested at 5, 7 (from a different experiment), or 9 hpi gave almost identical digestion patterns of HSV-1 DNA digestion (Fig 4.1A compare 5hpi to 7 and 9hpi). However, the percentage of poorly accessible DNA, DNA not digested by the harshest digestion conditions used, increased from 14.5% at 5hpi to 25.4% at 9hpi (Fig 4.1D and E). Consistently, 28.4% of HSV-1 DNA was found to be poorly accessible in a separate experiment evaluating the accessibility of HSV-1 DNA at 7hpi (Fig 4.1E).

With the exception of the minor percentage of poorly accessible HSV-1 DNA, the majority of HSV-1 DNA had increased accessibility over the course of infection. This was reflected in a 3.6 and 3.2-fold decrease in T_{50} at 5 and 9hpi, respectively, in comparison to 2hpi (Table 4.1). Consistently, a 2.8-fold decrease in accessibility was observed at 7hpi (in comparison to 2hpi) in a separate experiment (Table 4.1). At any time after infection, however, HSV-1 DNA was digested more rapidly than DNA in most cellular chromatin (Table 4.1). Consistent with our previous report, HSV-1 DNA was more accessible to MCN than DNA in most cellular chromatin (Table 4.1). Even at 2hpi, when HSV-1 DNA was poorly accessible to MCN, HSV-1 DNA was still 1.5 fold more

accessible than most DNA in cellular chromatin. This difference increased to 3.5-fold at 5hpi, consistent with the previously reported 3-fold increased accessibility of HSV-1 DNA over DNA in cellular chromatin (Lacasse and Schang 2010).

Preliminary analyses at 5hpi had shown no major differences between probes enriched in IE or L loci. As expected from these preliminary experiments, the probe enriched in L loci detected very similar patterns of HSV-1 DNA fragments as the IE loci-enriched probe (Fig 4.1A and Table 4.1, T₅₀; 11.4 and 11.6min, IE and L probe, respectively). Likewise, no major differences were observed when membranes containing the DNA of nuclei digested at 2, 5, 7 (from a different experiment), or 9hpi were hybridized using probes enriched in HSV-1 IE or L loci (Fig 4.1A, C-F). Taken together, these results indicate that HSV-1 DNA becomes more accessible to MCN digestion at later times during infection.

4.2.2. HSV-1 IE and L DNA is in nucleosome-like complexes throughout the lytic infection cycle

Standard MCN digestions revealed differences in the accessibility of HSV-1 DNA throughout the course of infection. However, it remained unclear whether HSV-1 DNA was also in unstable nucleosomes at all times. We therefore subjected nuclei isolated at 2, 5, or 9hpi to our modified “serial” MCN digestion designed to “trap” unstable nucleosome-like complexes. The soluble chromatin fractions were pooled and resolved together by sucrose gradients and analyzed by Southern blot hybridization. In the previous experiments (Chapter 3 and Lacasse and Schang 2010), the serial digestion was repeated nine times. However, the vast

majority of cellular and HSV-1 DNA is released during the first three cycles. We therefore reduced the number of cycles from 9 to 6 for the ensuing experiments.

The cellular DNA released as soluble chromatin by the serial MCN digestions fractionated as mono-, di- (fractions 10 to 12), and poly- (fractions 4 to 9) nucleosomes complexes, as expected for regularly chromatinized DNA (Fig 4.2A). HSV-1 infection did not affect to any obvious extent the cellular DNA complexes released as soluble chromatin (Fig 4.2A, C). However, the percentage of cellular DNA released as soluble chromatin increased from 79.7 to 90.1% between 2 and 9hpi (Fig 4.2B). There was an apparent linear relationship between the progression of HSV-1 infection and the percentage of cellular DNA released as soluble chromatin. Least squares analysis was performed, indicating an R^2 value of 0.88. Progression of HSV-1 infection therefore correlates with an increase in the accessibility of bulk cellular chromatin to MCN.

Similarly to cellular DNA, the HSV-1 IE DNA released as soluble chromatin was also in complexes that fractionate as mono-, di-, and poly-nucleosomes throughout the course of infection. The DNA in the soluble chromatin fraction accounted for 85.6, 96.3, and 93.4% of nuclear HSV-1 IE DNA at 2, 5 and 9hpi, respectively, indicating that the majority of HSV-1 DNA is in nucleosome-like complexes throughout the course of infection. Therefore, serial MCN digestion recovers HSV-1 IE DNA in nucleosome-like complexes, which were presumably rapidly degraded during the standard continuous MCN digestion.

As observed following standard MCN digestions, however, HSV-1 IE DNA was less accessible to MCN at 2hpi compared to 5 or 9hpi. For example, 96.3 and 93.4% of HSV-1 IE DNA was released as soluble chromatin at 5 and 9hpi, respectively, compared to 85.6% at 2hpi (Fig 4.2D and Table 4.3). At 2hpi, moreover, the HSV-1 IE DNA released as soluble chromatin was in larger, heavier, polynucleosomes-like complexes that resolved to fractions 9 to 12, whereas those released at 5 and 9hpi resolved primarily to fractions 11 to 13 (Fig 4.2A, E). These results indicate that HSV-1 IE DNA is less accessible to MCN at early times post infection (2hpi).

We next hybridized the same membranes with the probe enriched in L loci. Interestingly, no L loci DNA was detected in the HSV-1 DNA released into the soluble fraction at 2 hpi. In contrast, L loci DNA was easily detected in the soluble chromatin at 5 and 9hpi (Fig 4.2A and F). These results indicate that HSV-1 IE and L loci are differentially accessible at 2hpi.

Taken together, these results show that most HSV-1 DNA is in nucleosome-like complexes throughout the course of HSV-1 infection. These results also show the accessibility of HSV-1 DNA to MCN to change over the course of infection. At early times (2hpi), HSV-1 DNA is poorly accessible to MCN, but it becomes more accessible later (5 and 9hpi). Moreover, the accessibility of specific HSV-1 loci also appears to change throughout the course of infection. IE, but not L, loci are released as soluble chromatin at 2hpi. However, this difference in accessibility between IE and L loci is minimized as the infection progresses (5, 7, and 9hpi) (Fig 4.1C, D and Table 4.1), and IE and L

loci become detected to similar levels in the complexes released as soluble chromatin (Fig 4.2).

4.2.3. Inhibition of HSV-1 replication at different stages changes the accessibility of HSV-1 DNA to MCN digestion

The change in the accessibility of HSV-1 DNA between 2 and 5hpi coincides with the transition from transcription of IE, E, but not L genes (2hpi), to transcription of IE, E, and L genes and ongoing DNA replication (5hpi). Both transcription and DNA replication affect accessibility of DNA to MCN (Palen and Cech 1983). We therefore evaluated the effects, if any, that inhibition of different stages of the HSV-1 replication cycle had on the accessibility of HSV-1 DNA to MCN. To this end, we used small-molecule inhibitors. PAA inhibits the HSV-1 DNA polymerase and, consequently, inhibits DNA replication and L gene transcription, without affecting IE or E gene transcription. CHX inhibits protein synthesis and thereby inhibits E and L gene transcription without affecting IE transcription. Rosco inhibits the accumulation of IE, E and L transcripts.

Cells were infected with 10 PFU of HSV-1 per cell and treated with no drug, PAA, CHX, or Rosco. The nuclei were isolated at 7hpi, when HSV-1 IE, E, and L transcription, as well as DNA replication is ongoing, and subjected to standard MCN digestions. Nuclear DNA was purified, resolved by agarose gel electrophoresis, and analyzed by ethidium bromide staining and Southern blot hybridization. Hybridizations with cellular probes are shown in standard exposures. Hybridizations with HSV-1 probes are shown in overexposures, to

highlight the differences between HSV-1 and cellular DNA, and the changes in the accessibility of HSV-1 DNA in the presences of inhibitors (Fig. 4.3A).

As previously shown, standard MCN digestion resulted in the digestion of cellular DNA to a typical nucleosome ladder corresponding to multiples of 160bp (Fig. 4.3A). None of the drugs had any major effects on the accessibility of DNA in cellular chromatin, as evaluated by the DNA fragments released (Fig 4.3A) or digestion kinetics (Fig 4.3B). Only Rosco mildly increased the accessibility of DNA in cellular chromatin (Fig 4.3B, Rosco-30 and 60min).

In contrast, all inhibitors decreased the accessibility of HSV-1 IE DNA. MCN digestion of nuclei from untreated cells yielded the previously observed patterns (Fig 4.1A, 7hpi and Lacasse and Schang 2010). In contrast, neither the nucleosome nor the heterogeneously sized HSV-1 IE DNA fragments were detected in the nuclei of cells treated with PAA, CHX, or Rosco (Fig 4.3A). The pattern of digestion of HSV-1 IE DNA in nuclei of cells treated with any of the drugs was in fact very similar to that of HSV-1 IE DNA at 2hpi in the absence of any drug (Fig 4.1A). As expected, the decrease in accessibility in the presence of drugs was reflected in increases in T_{50} . Treatment with PAA increased the T_{50} of HSV-1 IE loci DNA by 2.8-fold (14.3 to 40.0min, from ND to PAA), whereas CHX and Rosco increased the T_{50} by more than 4-fold (to >60min - Table 4.2).

To evaluate whether the drugs differentially affected the accessibility of different HSV-1 loci, we next hybridized the membranes with the probe enriched in L loci. As previously observed (Fig 4.1), HSV-1 IE and L loci are equally accessible at 7hpi in the absence of any drug (Fig 4.3A and C). Similarly, no

major differences were observed in the pattern or kinetics of digestion between IE and L loci in nuclei from cells treated with CHX or Rosco (Fig 4.3A, E, and F). In the presence of PAA, however, L loci DNA was 1.5-fold less accessible than IE loci DNA (T_{50} ; 60 and 40min, respectively) (Table 4.2 and Fig 4.3D). These results suggest that HSV-1 IE or L loci are differentially accessible in the presence of PAA. All the drugs decreased the accessibility of MCN to HSV-1 IE or L DNA, thereby increasing the T_{50} (Table 4.2). Therefore, inhibiting HSV-1 replication at different stages decreases the accessibility of HSV-1 DNA to MCN. Furthermore, HSV-1 IE or L loci DNA may become differentially accessible to MCN if the block on HSV-1 replication is such that the transcription of one gene class, but not the other, is inhibited.

4.2.4. HSV-1 DNA is in nucleosome-like complexes when the HSV-1 replication cycle is inhibited at different stages

Accessibility of HSV-1 DNA increases during lytic infection (Fig 4.1 and 4.2). Furthermore, the accessibility of HSV-1 DNA also changes with transcription. For example, at 2hpi, when transcription is limited to IE and E genes, HSV-1 IE but not L loci are released as soluble chromatin.

Therefore, we next evaluate whether drugs that inhibit various stages of the HSV-1 replicative cycle also differentially affect the accessibility of HSV-1 IE or L DNA. To this end, we performed serial MCN digestions on nuclei from cells infected and treated with no drug, PAA, CHX, or Rosco. Nuclei were harvested at 7hpi and serial MCN digestions were performed. The soluble

chromatin fractions were pooled and resolved together by sucrose gradients and analyzed by Southern blot hybridization with probes enriched in IE or L HSV-1 loci.

Consistent with previous experiments, the soluble chromatin released by serial digestion of nuclei from untreated cells released cellular DNA in complexes that fractionated as mono-, di- (fractions 10 to 12), and poly- (fractions 1 to 9) nucleosomes complexes (Fig 4.4A). Interestingly, there was an apparent increase in the percentage of cellular DNA released as soluble chromatin from 80.5% in the absence of drug to 92.8, 88.4 and 88.0% in the presence of PAA, CHX, and Rosco, respectively (Fig 4.4B). However, the least squares regression calculated from the data presented in Fig 4.1 predicts that 88% of the cellular DNA should have been released as soluble chromatin at 7hpi in the absence of any drug. Further repeats would have to be performed to evaluate whether the drugs indeed increase the accessibility of bulk cellular chromatin to MCN. In any event, none of the drugs decreased the accessibility of bulk cellular chromatin to MCN.

In contrast to cellular DNA, PAA, CHX and Rosco decreased the accessibility of HSV-1 DNA. As previously observed (Fig 4.2), serial MCN digestion of nuclei from untreated cells released HSV-1 IE loci in nucleoprotein complexes that fractionated as cellular polynucleosomes (fractions 2 to 9) and mono- to dinucleosomes (fractions 10 to 12) (Fig. 4.4A-No Drug, and 4.4C). Similarly, digestion of nuclei from cells treated with PAA, CHX, and Rosco also released HSV-1 IE loci in nucleoprotein complexes that fractionate as cellular polynucleosomes (fractions 6 to 9) and mono- to dinucleosomes (fractions 10 to

11) (Fig. 4.4A-PAA, CHX, and Rosco, and 4.4E and G). Consistent with the results of the standard MCN digestion, PAA, CHX, and Rosco all decreased the percentage of HSV-1 DNA released as soluble chromatin, albeit to varying degrees. The percentage of HSV-1 DNA released into the soluble chromatin decreased from 86.9% in the absence of any drug (Fig 4.4B and Table 4.2) to 74.5, 44.8, and 29.5% in the presence of PAA, CHX, and Rosco, respectively (Fig 4.4D and Table 4.2). Therefore, the inhibitors decrease the percentage of HSV-1 IE DNA that that is accessible to MCN and thus released as soluble chromatin.

Serial MCN digestion of nuclei from cells infected for 2 hours in the absence of any drug revealed differences in the accessibility of HSV-1 IE and L loci. Considering the similarities in the transcription status of the HSV-1 DNA from those nuclei or those from cells treated with PAA, CHX, or Rosco, we next hybridized the membranes with the L loci enriched probe. As expected, for 7hpi no differences were observed when membranes with DNA from untreated nuclei were hybridized with the probe enriched in L loci. In both cases, HSV-1 DNA was in nucleoprotein complexes that fractionated as cellular polynucleosomes and mono- to di- nucleosomes (Fig 4.4A). The percentage of DNA released in soluble chromatin was also the same, 86.9 and 87.0% for IE and L loci, respectively (Table 4.4). These results are consistent with IE and L loci being equally accessible at 7hpi in the absence of any drug (Fig 4.2). In contrast, PAA, CHX, or Rosco, all decreased the percentage of DNA containing HSV-1 L loci released in soluble chromatin, from 87% in untreated cells to 56.1, 32.3, and 14.0% in PAA, CHX, and Rosco treated cells, respectively (Fig 4.4F).

Next, I evaluated whether the drugs differentially affected the accessibility of HSV-1 IE and L loci DNA. To this end, I calculated the ratio of the percentages of IE and L HSV-1 DNA released in soluble chromatin. This analysis revealed that treatment with PAA, CHX, or Rosco resulted in a 1.3, 1.4, or 2.1-fold, respectively, decrease in the accessibility of HSV-1 DNA L loci DNA in comparison to IE loci DNA. Taken together, these results indicate that the accessibility of HSV-1 DNA to MCN is decreased when HSV-1 transcription is inhibited.

4.3 References

- Cliffe, A. R. and D. M. Knipe (2008). "Herpes simplex virus ICP0 promotes both histone removal and acetylation on viral DNA during lytic infection." J Virol **82**(24): 12030-8.
- Herrera, F. J. and S. J. Triezenberg (2004). "VP16-dependent association of chromatin-modifying coactivators and underrepresentation of histones at immediate-early gene promoters during herpes simplex virus infection." J Virol **78**(18): 9689-96.
- Kent, J. R., P. Y. Zeng, et al. (2004). "During lytic infection herpes simplex virus type 1 is associated with histones bearing modifications that correlate with active transcription." J Virol **78**(18): 10178-86.
- Kutluay, S. B., S. L. DeVos, et al. (2009). "Transcriptional coactivators are not required for herpes simplex virus type 1 immediate-early gene expression in vitro." J Virol **83**(8): 3436-49.
- Kutluay, S. B. and S. J. Triezenberg (2009). "Regulation of histone deposition on the herpes simplex virus type 1 genome during lytic infection." J Virol **83**(11): 5835-45.
- Lacasse, J. J. and L. M. Schang (2010). "During lytic infections, herpes simplex virus type 1 DNA is in complexes with the properties of unstable nucleosomes." J Virol **84**(4): 1920-33.
- Leinbach, S. S. and W. C. Summers (1980). "The structure of herpes simplex virus type 1 DNA as probed by micrococcal nuclease digestion." J Gen Virol **51**(Pt 1): 45-59.
- Palen, T. E. and T. R. Cech (1983). "Transcribed and non-transcribed regions of Tetrahymena ribosomal gene chromatin have different accessibilities to micrococcal nuclease." Nucleic Acids Res **11**(7): 2077-91.
- Placek, B. J., J. Huang, et al. (2009). "The histone variant H3.3 regulates gene expression during lytic infection with herpes simplex virus type 1." J Virol **83**(3): 1416-21.

| Time post infection (h) | T ₅₀ (min) | | |
|----------------------------|-----------------------|--------|--------|
| | Cellular | HSV | |
| | | IE | L |
| 2 | >60 | 40.6 | 59.5 |
| 5 | 50.1 | 11.4 | 11.6 |
| 7 * | 60.8 * | 14.3 * | 12.4 * |
| 9 | 41.1 | 12.7 | 11.9 |

Table 4.1. The accessibility of HSV-1 DNA changes during lytic infection.

Digestion times required to degrade 50% (T₅₀) of HSV-1 or Cellular DNA, graphically calculated from the digestion curves.

* Data for 7hpi is from a separate experiment (see Fig 4.3A)

| Treatment | T ₅₀ (min) | | |
|------------|-----------------------|------|------|
| | Cellular | HSV | |
| | | IE | L |
| ND | >60 | 14.3 | 12.4 |
| PAA | >60 | 40.0 | >60 |
| CHX | >60 | >60 | >60 |
| R | 35.7 | >60 | >60 |

Table 4.2. Inhibition of HSV-1 transcription changes the accessibility of HSV-1 IE or L DNA to MCN digestion. Digestion times required to degrade 50% (T₅₀) of HSV-1 or Cellular DNA in nuclei isolated at 7hpi, graphically calculated from the digestion curves.

| | Time post infection (h) | DNA, % | |
|-----------------|----------------------------|-----------|---------|
| | | Insoluble | Soluble |
| Cellular | 2 | 20.3 | 79.7 |
| | 5 | 12.5 | 87.5 |
| | 9 | 9.9 | 90.1 |
| IE | 2 | 14.4 | 85.6 |
| | 5 | 3.7 | 96.3 |
| | 9 | 6.6 | 93.4 |
| L | 2 | 99.5 | 0.5 |
| | 5 | 3.5 | 96.5 |
| | 9 | 5.7 | 94.3 |

Table 4.3. HSV-1 IE and L DNA is in nucleosome-like complexes throughout the lytic infection cycle. Percentages of **cellular**, HSV-1 **IE**, of HSV-1 **L** DNA fractionating as **Insoluble** or **Soluble** chromatin following serial MCN digestions of HSV-1 infected nuclei harvested at **2**, **5**, or **9**hpi.

| | Treatment | DNA, % | |
|-----------------|-----------|-----------|---------|
| | | Insoluble | Soluble |
| Cellular | No Drug | 19.5 | 80.5 |
| | PAA | 7.2 | 92.8 |
| | CHX | 11.6 | 88.4 |
| | Rosco | 12.0 | 88.0 |
| IE | No Drug | 13.1 | 86.9 |
| | PAA | 25.5 | 74.5 |
| | CHX | 55.2 | 44.8 |
| | Rosco | 70.5 | 29.5 |
| L | No Drug | 13.0 | 87.0 |
| | PAA | 43.9 | 56.1 |
| | CHX | 67.7 | 32.3 |
| | Rosco | 86.0 | 14.0 |

Table 4.4. HSV-1 DNA fractionates as nucleosome-like complexes when HSV-1 replication is inhibited. Percentages of **cellular**, HSV-1 **IE**, of HSV-1 **L** DNA fractionating in **Insoluble** or **Soluble** chromatin following serial MCN digestions of nuclei infected with HSV-1 for 7h in the presence of **No Drug**, **PAA**, **CHX**, or **Rosco**.

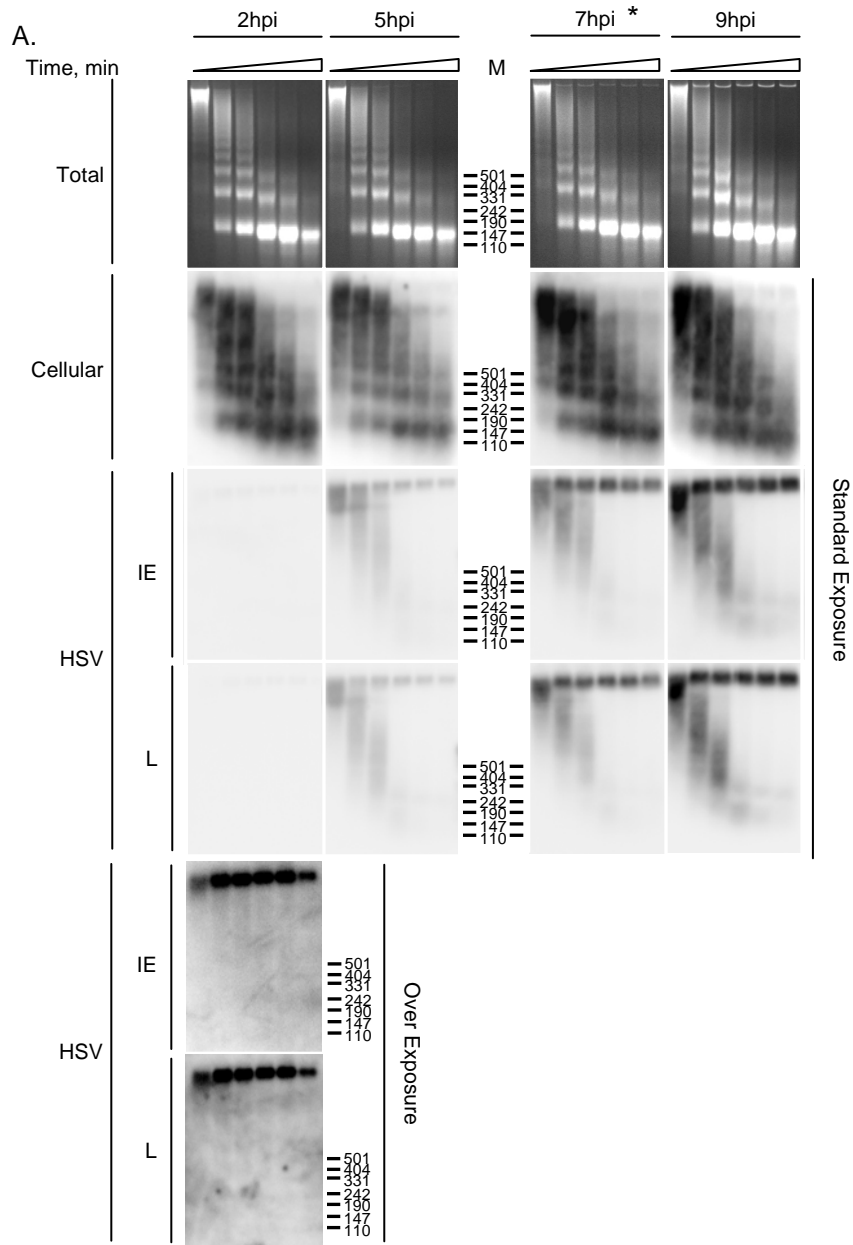



Figure 4.1. The accessibility of HSV-1 DNA changes during lytic infection. Nuclei of infected cells isolated at 2, 5, 7, and 9 hours post infection were digested for 0.5, 2.5, 5, 15, 30, and 60min () with 0.05U MCN per 1×10^7 nuclei. The DNA was analyzed by Southern blot with HSV-1 or cellular probes. **A.** Images of the ethidium bromide stained gels (**Total**) or membranes hybridized with cellular (**Cellular**) or HSV-1 (**HSV**) specific probes. The HSV-1 probes were specific for either immediate-early (**IE**) or late (**L**) genes. **M**, molecular weight marker. Normal and overexposures (bottom panels), in which the MCN-resistant and absence of nucleosome-sized HSV-1 DNA is more clearly visible, are shown. To achieve comparable signal intensities, only 67% of sample was loaded for 0.5min. * Data for 7hpi is from a separate experiment (see Fig 4.3A).

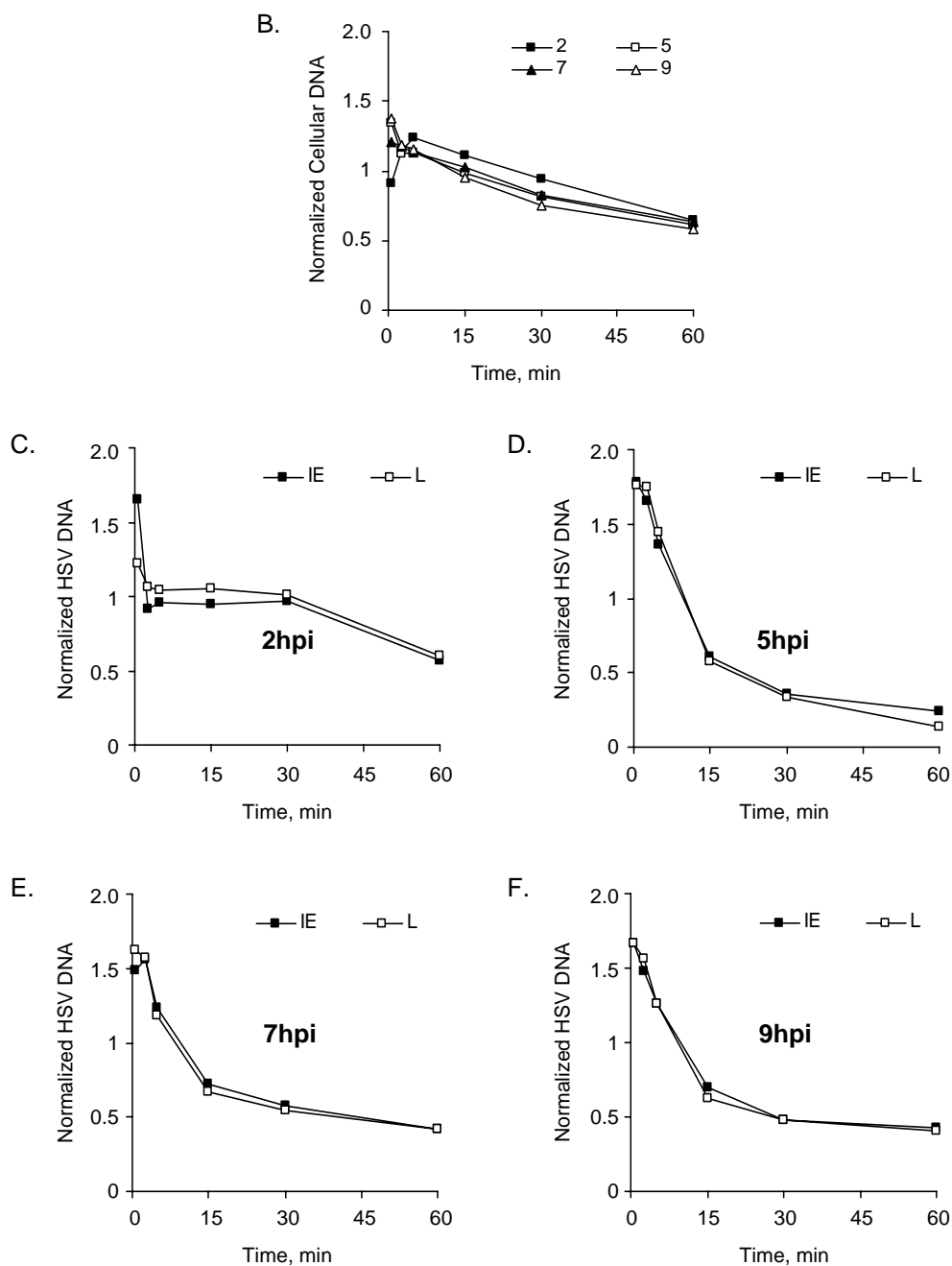


Figure 4.1. (continued) The accessibility of HSV-1 DNA changes during lytic infection.

B-F, Line graphs of the quantitated Southern blots from **Figure 4.1 A** presenting normalized levels of cellular (**B**), HSV-1 IE and L DNA at 2 (**C**), 5 (**D**), 7 (**E**), and 9 (**F**) hpi against digestion time.

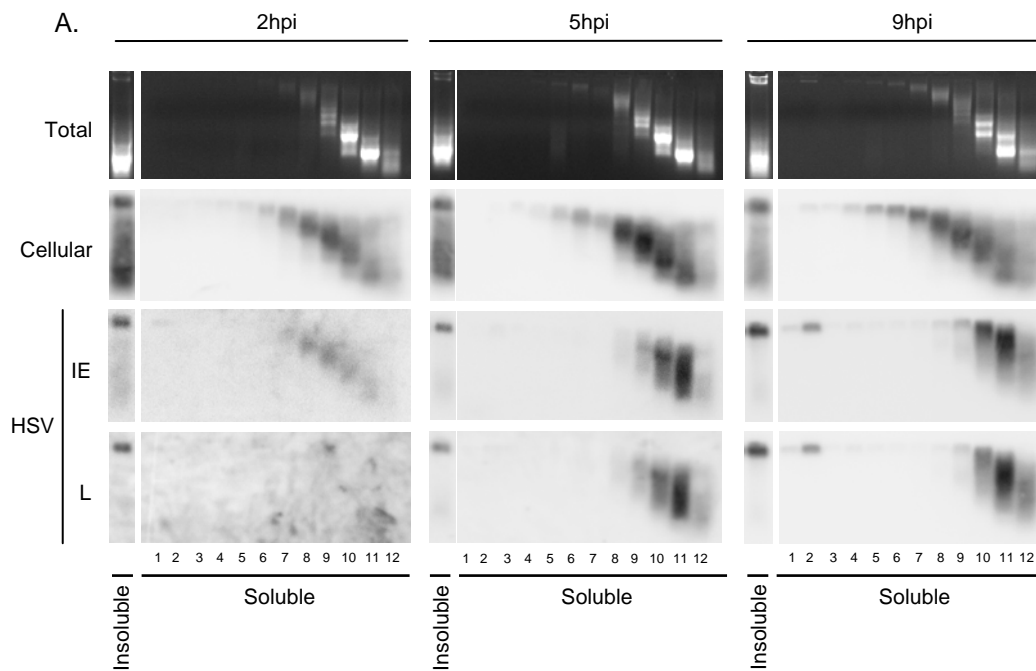


Figure 4.2. HSV-1 IE and L DNA is in nucleosome-like complexes throughout the lytic infection cycle. At 2, 5, and 9hpi, nuclei of infected cells were lysed and soluble and insoluble chromatin were fractionated. Insoluble chromatin was resuspended in MCN digestion buffer (0.05U MCN/ml), and subjected to serial MCN digestions. Supernatants were periodically removed and quenched, and the insoluble pellets were resuspended with fresh MCN. Soluble DNA-protein complexes were pooled and further resolved on sucrose gradients. DNA from each fraction was analyzed by Southern blot with HSV-1 or cellular specific probes. Images of the membranes hybridized with cellular (**Cellular**) or HSV-1 (**HSV**) specific probes. The HSV-1 probes were specific for either immediate-early (**IE**) or late (**L**) genes. **A.** Images of the ethidium bromide stained gels (**Total**) and membranes hybridized with cellular (**Cellular**) or HSV-1 (**HSV**) specific probes. HSV-1 probes were specific for either immediate-early (**IE**) or late (**L**) genes. To achieve comparable signal intensities, only 50% of the soluble fractions were loaded.

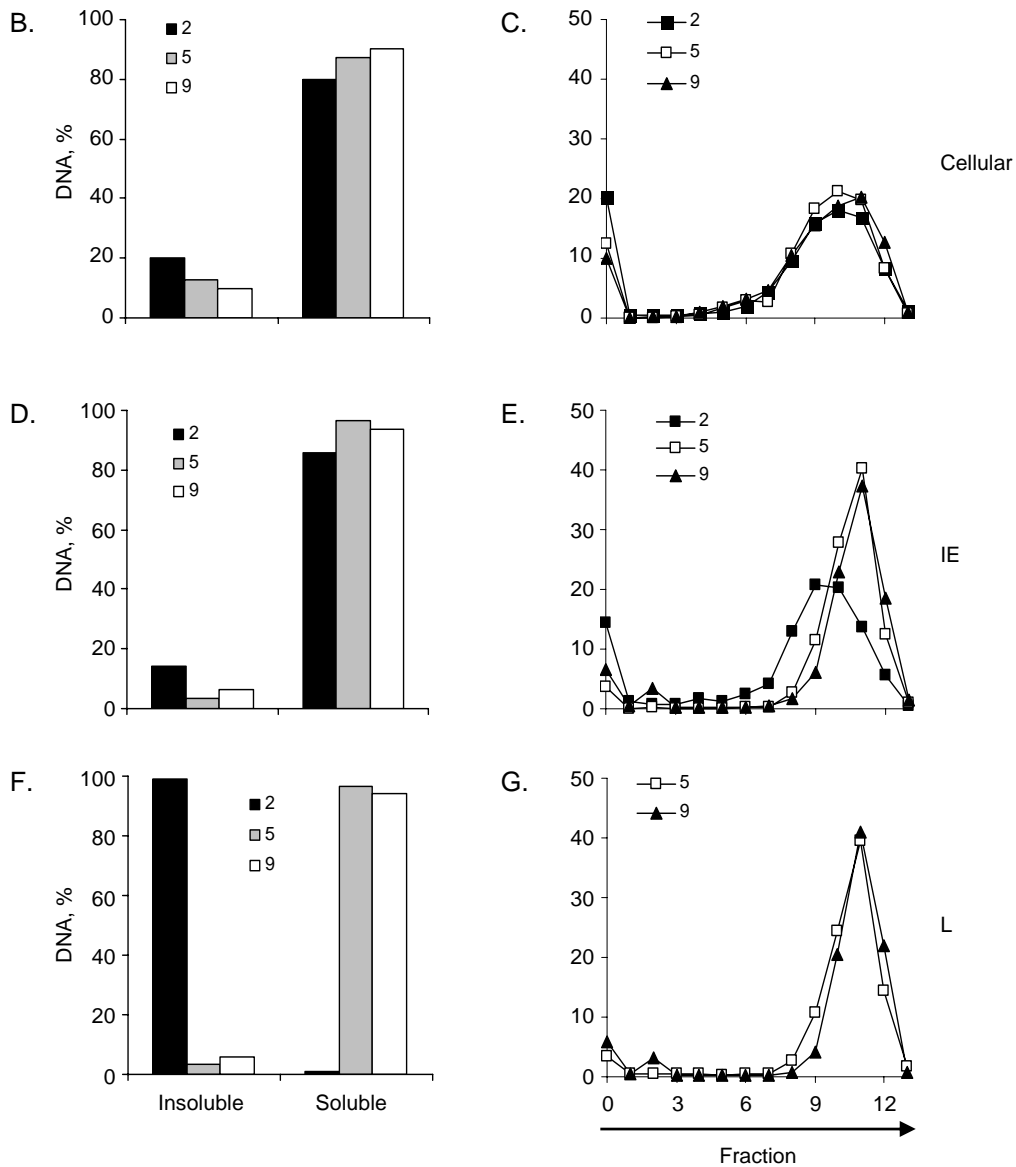


Figure 4.2. (continued) HSV-1 IE and L DNA is in nucleosome-like complexes throughout the lytic infection cycle.

B, D, and F. Bar graphs of the quantification of the Southern blots presenting the percentage of cellular (**B**), HSV-1 IE (**D**), or HSV-1 L (**F**) DNA fractionating in the pellet (**Insoluble**) or supernatant (**Soluble**) following serial MCN digestions. **C, E, and G.** Line graphs presenting cellular (**C**), HSV-1 IE (**E**), and L (**G**) DNA in each fraction as percent of DNA in the gradient. There was no detectable signal when probing the 2hpi gradient with the L gene specific HSV-1 probe.

A.

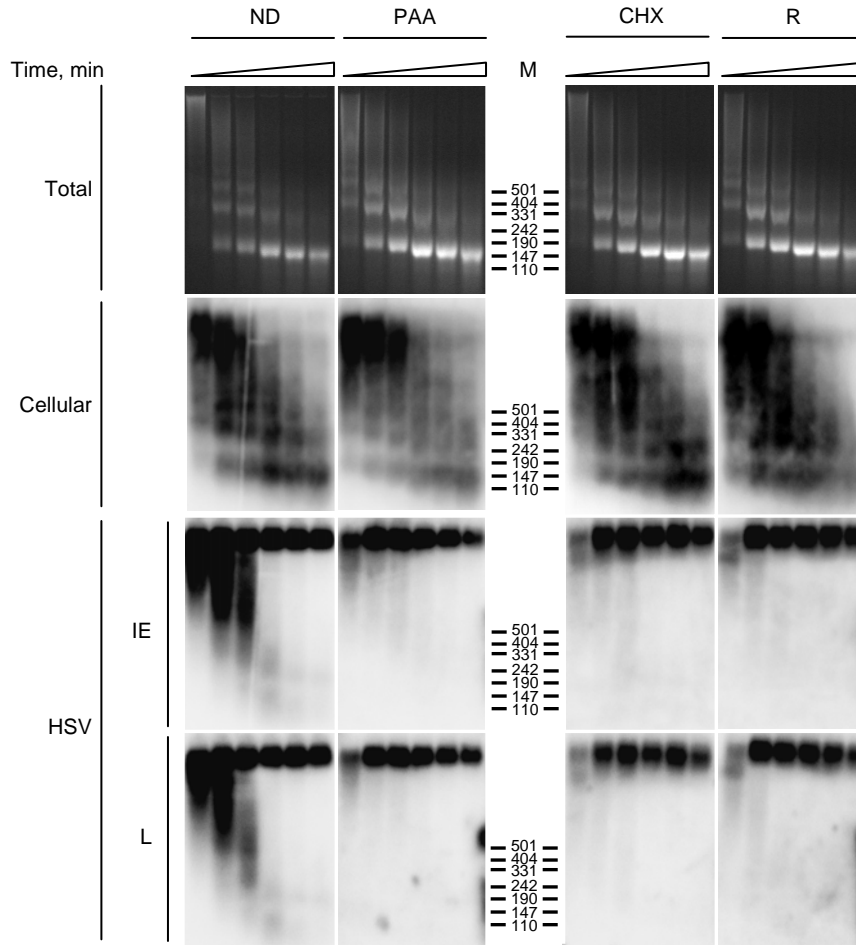



Figure 4.3. Inhibition of HSV-1 replication at different stages changes the accessibility of HSV-1 DNA to MCN digestion. Purified nuclei of infected cells treated with no drug (ND), PAA, CHX, or Rosco (R) were digested for 0.5, 2.5, 5, 15, 30, and 60min () with 0.05 U MCN per 1×10^7 nuclei. DNA was analyzed by Southern blot with HSV-1 or cellular probes. **A.** Images of the ethidium bromide stained gels (**Total**) and membranes hybridized with cellular (**Cellular**) or HSV-1 (**HSV**) specific probes. HSV-1 probes were specific for either immediate-early (**IE**) or late (**L**) genes. **M**, molecular weight marker. Exposures in which the nucleosome-sized and MCN-resistant HSV-1 DNA are most clearly visible, are shown. To achieve comparable signal intensities, only 67% of sample was loaded for 0.5min.

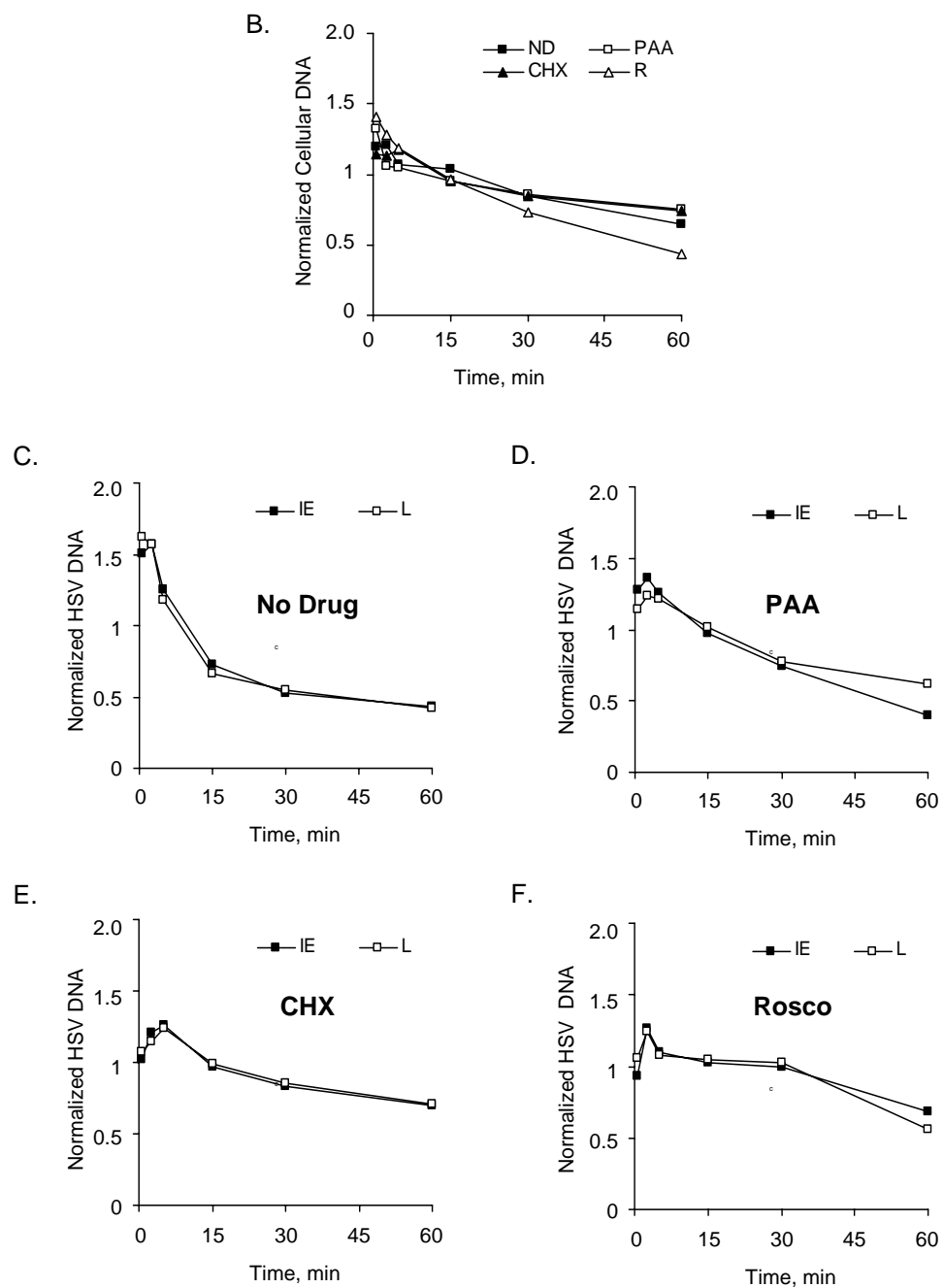


Figure 4.3. (continued) Inhibition of HSV-1 replication at different stages changes the accessibility of HSV-1 DNA to MCN digestion.
B-F, Line graphs of the quantitated Southern blots from **Figure 4.3 A** presenting normalized levels of cellular (**B**), HSV-1 IE and L DNA in the presence of no drug (**C**), PAA (**D**), CHX (**E**), and Rosco (**F**) against digestion time.

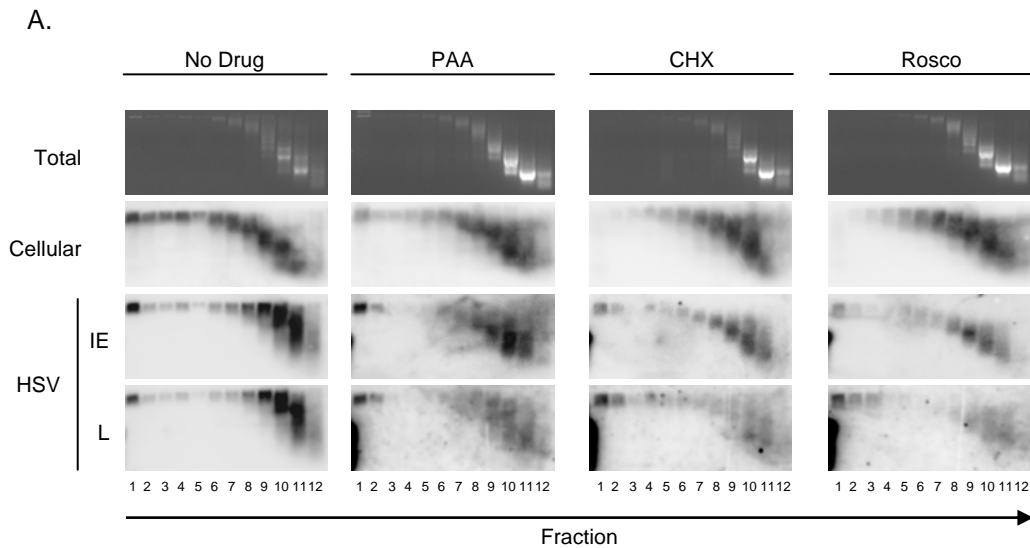


Figure 4.4. HSV-1 DNA is in nucleosome-like complexes when HSV-1 replication is inhibited at different stages. Infected cells were treated with no drug (ND), PAA, CHX or Rosco (R) and nuclei were harvested at 7hpi. Nuclei were then lysed and soluble and insoluble chromatin were fractionated. Insoluble chromatin was resuspended in MCN digestion buffer (0.05U MCN/ml), and subjected to serial MCN digestions. Supernatants were periodically removed and quenched, and the insoluble pellets were resuspended with fresh MCN. Soluble DNA-protein complexes were pooled and further resolved on sucrose gradients. DNA from each fraction was analyzed by Southern blot with HSV-1 or cellular specific probes. Images of the membranes hybridized with cellular (**Cellular**) or HSV-1 (**HSV**) specific probes. **A.** Images of the ethidium bromide stained gels (**Total**) and membranes hybridized with cellular (**Cellular**) or HSV-1 (**HSV**) specific probes. HSV-1 probes were specific for either immediate-early (**IE**) or late (**L**) genes. To achieve comparable signal intensities, only 50% of the soluble fractions were loaded.

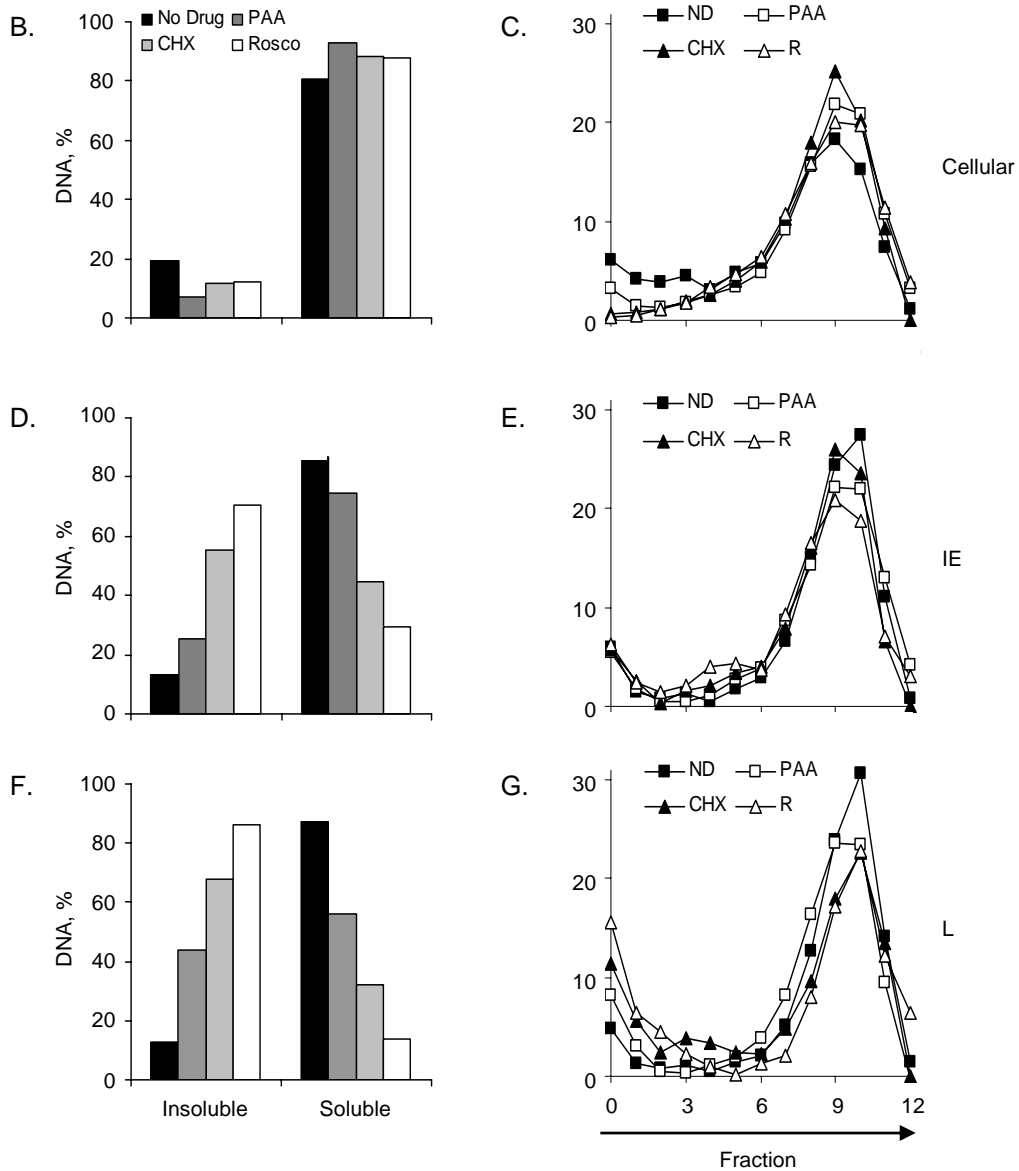


Figure 4.4. (continued) HSV-1 DNA is in nucleosome-like complexes when HSV-1 replication is inhibited at different stages.

B, D, and F. Bar graphs of the quantitated Southern blots presenting the percentage of cellular (**B**), HSV-1 IE (**D**), and HSV-1 L (**F**) DNA fractionating as the pellet (**Insoluble**) or supernatant (**Soluble**) following serial MCN digestions. **C, E, and G.** Line graphs presenting cellular (**C**), HSV-1 IE (**E**), and L (**G**) DNA in each fraction as percent of DNA in the gradient.

CHAPTER 5: ROSCOVITINE INHIBITS ACTIVATION OF PROMOTERS IN HERPES SIMPLEX VIRUS TYPE 1 GENOMES INDEPENDENTLY OF PROMOTER-SPECIFIC FACTORS

*This chapter contains unpublished results and published work. Diwan P. *, JJ. Lacasse*, and LM. Schang *Both of these authors contributed equally to the published work.*

Journal of Virology 2004; 78(17): 9352-65

5.1. Introduction

In the previous chapter, I showed that most HSV-1 DNA is in nucleosome-like complexes throughout the HSV-1 replication cycle. However, the accessibility of HSV-1 DNA to MCN digestion changed over the course of infection, increasing by 3.6-fold between 2 and 5hpi. Interestingly, this period coincides with the transition from transcription of IE and E (2hpi), to the start of DNA replication and L gene expression (5hpi).

Three small-molecule inhibitors that blocked different stages of HSV-1 transcription also decreased the accessibility of HSV-1 DNA to MCN to varying degrees. Furthermore, the extent to which they inhibited accessibility of HSV-1 DNA to MCN appeared to correlate with the extent to which the drugs inhibited HSV-1 transcription. For example, HSV-1 IE DNA was 2.5- and 1.5-fold less accessible in the presence of Rosco than in the presence of CHX or PAA, respectively. When evaluating HSV-1 L DNA, the decrease in accessibility

increased to 4- and 2.5-fold, respectively. Consistently, Rosco also has the greatest effect of the three drugs on HSV-1 transcription. It inhibits the accumulation of HSV-1 IE, E, and L transcripts, as well as DNA replication (Schang, Rosenberg et al. 1999; Schang, Rosenberg et al. 2000). Taken together, these results suggest that accessibility of HSV-1 DNA may regulate transcription. Alternatively, changes in HSV-1 DNA accessibility may be a consequence of transcription (Weisbrod 1982; Reeves 1984).

I propose that HSV-1 DNA becomes less accessible in the presence of Rosco, thus preventing access of MCN and transcription proteins to HSV-1 DNA. Rosco should therefore inhibit initiation, but not affect ongoing HSV-1 transcription. I also propose that these effects should be specific to HSV-1 DNA, since Rosco does not affect global cellular RNAPII transcription (Lam, Pickeral et al. 2001), or the accessibility of bulk cellular chromatin to MCN digestion (Fig 4.3, 4.4, 5.2, and 5.5). To test these hypotheses I performed “run-on” transcription assays on nuclei isolated from both mock and HSV-1 infected cells in the absence or presence of Rosco.

5.2. Results

5.2.1. Rosco prevents initiation, but does not inhibit ongoing, HSV-1 transcription.

Run-on transcription assays were performed as a first step in evaluating the relationship between the accessibility of HSV-1 DNA and HSV-1 transcription.

In order to maximize the detection of low levels of transcription, the MOI was increased from 5 to 20 PFU per cell.

Briefly, Vero cells were infected with 20 PFU of HSV-1 per cell and treated or not with Rosco at one hour after infection. Cells were harvested 5 h later and their nuclei were isolated. Run-on transcription assays were performed as described by Spencer, Rice *et al.* (Rice, Long *et al.* 1995; Spencer, Dahmus *et al.* 1997), with several modifications (Diwan, Lacasse *et al.* 2004). The effects of Rosco were tested on promoter specific (i.e., sense) and “non-promoter-specific” (i.e., antisense) HSV-1 transcription, by probing the run-on RNAs with single-stranded DNA sense or antisense to selected viral genes. The phages containing the probes were a generous gift of Dr. C. Spencer (Cross Cancer Institute, Edmonton, Alberta, Canada).

Run-on transcription assays performed with nuclei of mock infected cells (negative controls) resulted in only low background levels of hybridization to viral genes, as expected. Run-on transcription assays performed with nuclei of HSV-1 infected cells (positive controls) resulted in abundant viral transcription, also as expected (Fig. 5.1A). Transcription occurred from both sense (“promoter-specific”) and antisense (“non-promoter-specific”) strands, which is characteristic of HSV-1 (Rice, Long *et al.* 1995; Spencer, Dahmus *et al.* 1997). Run-on assays performed with nuclei of cells infected in the presence of Rosco resulted in inhibition of transcription of all viral genes analyzed (Fig. 5.1A) - even though no Rosco was present during the transcription reactions. Under these conditions, Rosco prevented transcription from both sense (i.e., “promoter-specific”) and

anti-sense (i.e., “non-promoter-specific”) DNA strands. In contrast, run-on transcription assays performed in the presence of Rosco, but using nuclei of cells infected in the absence of the drug, resulted in no inhibition of either sense or anti-sense transcription (Fig. 5.1A).

Transcription of HSV-1 E and L genes depends on previous expression of IE proteins, which is inhibited by Rosco (Fig 5.1A and Schang, Rosenberg et al. 1999). Therefore, the experiments presented in Fig. 5.1A tested the direct effects of Rosco on transcription of IE genes but not on transcription of E or L genes. Moreover, IE proteins were present during transcription only when Rosco was added to the transcription reactions, but not when Rosco was added to the infected cells (because Rosco prevents transcription of IE genes – Fig 5.1A and Schang, Rosenberg et al. 2000). To test the effects of Rosco on HSV-1 transcription in the presence of IE proteins, I followed a cyclohexamide (CHX) release experimental design. Briefly, cells were infected with HSV-1 in the presence of CHX for 5h. At this time, CHX was removed and control or Rosco-containing media was added. Following this procedure, high levels of all HSV-1 IE proteins are synthesized after removal of CHX, translated from the IE transcripts over-accumulated during the 5h in the presence of CHX (Schang, Rosenberg et al. 1999).

Rosco prevented initiation of transcription of IE, E, and L genes after a CHX release (Fig. 5.1B), which is consistent with its inhibitory effects on accumulation of IE, E, and L transcripts in the presence of IE proteins (Schang, Rosenberg et al. 1999). Rosco also prevented initiation of both sense and anti-sense transcription in the presence of IE proteins, as it did in their absence.

Moreover, Rosco had no effect on ongoing transcription (Fig. 5.1B), as it had no effect on ongoing transcription in the absence of IE proteins (Fig. 5.1A). These results reveal that Rosco inhibits the activation of HSV-1 promoters independent of specific activators. Therefore, the functions targeted by Rosco participate in activation of IE gene transcription by cellular proteins and HSV-1 structural proteins, as well as in regulation of E gene transcription by HSV-1 IE proteins.

5.2.2. Rosco prevents initiation of HSV-1, but not cellular, transcription

Rosco prevents initiation of HSV-1 transcription but does not inhibit ongoing transcription. These effects could be specific for HSV-1 transcription, or general to HSV-1 and cellular transcription. Therefore, I next analyzed the effects of Rosco on global viral and cellular transcription. HSV- or mock- infected cells were treated with Rosco or control medium for 5h, nuclei were then isolated and run-on transcriptions were performed. The RNAs purified from the transcription reactions were hybridized to membranes containing the entire genome of HSV-1 or Vero cells, and the hybridized signal was quantitated to assess the effects of Rosco on global HSV-1 or cellular transcription, respectively. Mock infected cells were selected to analyze the effects of Rosco on cellular transcription because several HSV-1 proteins inhibit cellular transcription. Therefore, the inhibitory effects of Rosco on HSV-1 transcription in infected cells would complicate the analyses of its potential effects on cellular transcription.

When cells were infected in the presence of Rosco, global HSV-1 transcription was inhibited, even though no drug was present in the transcription

reactions (Fig. 5.2A, B). When mock infected cells were treated with Rosco, however, no major effects on global cellular transcription were detected (Fig. 5.2C). Furthermore, and consistent with the results shown in Fig. 5.1A, Rosco added to the run-on transcription had no effect on global HSV-1 or cellular transcription (Fig. 5.2), indicating again that Rosco does not inhibit ongoing transcription. These experiments further suggested that Rosco prevents initiation of transcription of all HSV-1 genes, since no significant levels of transcription of any HSV-1 genome fragment could be detected in nuclei of cells infected in the presence of Rosco (Fig. 5.2B).

5.2.3. Cellular transcription in the presence of Rosco is performed by RNA Pol II

The reaction conditions used in our experiments are designed to favor transcription by RNA Pol II over RNA Pol I or III. However, either of these last two polymerases could have synthesized the cellular transcripts observed in the experiments presented in Fig. 5.2C (only RNA Pol II synthesizes HSV-1 transcripts). Therefore, I tested next whether cellular transcription in the presence of Rosco was indeed performed by RNA Pol II.

Briefly, nuclei were purified from mock infected cells treated or not with Rosco. Run-on reactions were then performed in the presence of no drug, α -amanitin, or Rosco, and RNA was precipitated with trichloroacetic acid (TCA). Global cellular transcription was then calculated using the percentage of radioactivity incorporated into RNA.

Run-on transcription in nuclei of cells treated or not with Rosco *in vivo* was equally inhibited by α -amanitin (by 60 and 58% relative to control, respectively) (Fig. 5.3). In contrast, Rosco added to the run-on transcription reactions failed to significantly inhibit transcription in nuclei of even cells treated with Rosco *in vivo* (Fig. 5.3). The highest level of inhibition by Rosco added *in vitro* (to nuclei of cells treated with Rosco *in vivo*) was that observed in the experiment presented in Fig. 5.3 (25% inhibition). Since α -amanitin inhibited cellular transcription by approximately 60% and most cellular transcription is performed by RNA Pol I or Pol III, these experiments also prove that, as expected, the run-on conditions used in our assays strongly favor transcription by RNA Pol II over Pol I or Pol III.

5.2.4. Inhibition of transcription by Rosco is specific for the HSV-1 genome

The experiments presented in the previous sections show that Rosco prevents initiation of transcription of HSV-1 genes but not of cellular genes. Preventing initiation of transcription of IE genes was especially surprising because Rosco does not inhibit formation of the Oct1/HCF/VP16 transactivating complex, or the affinity of this complex for its cognate TAATGARAT sequences *in vitro* (Jordan, Schang et al. 1999), at least with bacterially expressed Oct-1. Preventing initiation of all classes of HSV-1 genes was therefore consistent with Rosco having genome-, rather than promoter-, specific effects. Beyond specific promoters, however, the HSV-1 genome itself may play a major role in transcription regulation. I have shown that the majority of nuclear HSV-1 DNA is in unstable nucleosome-like complexes that have different biophysical properties than the majority of DNA in

cellular chromatin (Chapter 3 and Lacasse and Schang 2010). Also, a variety of non-HSV-1 promoters recombined into the HSV-1 genome are regulated as HSV-1 E promoters (Smiley, Smibert et al. 1987; Panning and Smiley 1989; Smibert and Smiley 1990). Furthermore, transcription driven by the HSV-1 ICP0 promoter is inhibited by α -interferon (α -IFN) when the promoter is in the HSV-1 genome, but not when it is recombined into the cellular genome (Nicholl and Preston 1996). In addition, I have shown that Rosco inhibits the accessibility of HSV-1 DNA, but not bulk cellular chromatin, to MCN (Fig 4.3). These results are consistent with the HSV-1 specific effects of Rosco on transcription. Therefore, I next evaluated the effects of Rosco on the transcription of a RFP reporter gene driven by an HSV-1 ICP0 promoter recombined into the cellular genome.

To this end, Dr. Diwan created a recombinant plasmid in which the promoter of ICP0, including all its known regulatory elements, drives the expression of a reporter red fluorescent protein (RFP) (Fig 5.4A). In transient transfection, Rosco inhibited the activation of this ICP0 promoter by UV-inactivated HSV-1 (Fig 5.4B). This was consistent with a previous report in which Rosco inhibited the activation of another ICP0 reporter construct under similar circumstances (Jordan, Schang et al. 1999).

The ICP0 reporter construct was transfected into Vero cells, and stably transfected cells were selected and cloned. The stably-transfected ICP0 promoter did not direct expression of RFP in non-infected cells, but it was activated by HSV-1 in 13 of 110 clones tested. Two of these clones were selected for further analyses, clones 57 and 32. The ICP0 reporter construct was integrated into the

cellular genome in each of these two clones as multiple copies per cell (Diwan, Lacasse et al. 2004), and was activated by virion proteins (Fig. 5.4C).

The inhibitory concentration of Rosco is cell-type dependent. We therefore tested the potency of Rosco toward HSV-1 replication in Vero clones 57 and 32. Replication of HSV-1 in both clones, and parental Vero cells, was more sensitive to Rosco than in other Vero cells used in previous publications. Seventy-five micromolar Rosco inhibited HSV replication by four orders of magnitude in the two clones and the parental cells (Fig. 5.4D). Vero cells clone 57 and 32 displayed similar phenotypes throughout the experiments; results from clone 57 are presented herein.

We next evaluated the effects of Rosco on the activation of ICP0 promoters recombined in the cellular genome. Clone 57 cells were infected in the presence of CHX and 0, 25, 50, 75, or 100 μ M Rosco. In the presence of CHX, the ICP0 promoter is activated only by cellular proteins and structural HSV-1 proteins such as VP16. Infected cells were harvested at 3, 6 and 9hpi, and RNA was analyzed by Northern blot hybridization.

Consistent with its effects on HSV-1 transcription (Fig 5.1, 5.2, and Schang, Phillips et al. 1998; Schang, Rosenberg et al. 1999; Schang, Rosenberg et al. 2000), Rosco inhibited transcription regulated by the ICP0 promoters in the viral genome (Fig. 5.5A, ICP0). Surprisingly, however, Rosco did not efficiently inhibit transcription regulated by the ICP0 promoters recombined in the cellular genome (Fig. 5.5A, RFP). This differential sensitivity to Rosco could be because RNA polymerase I or III, rather than RNAPII (which transcribes all HSV-1 genes),

transcribed RFP from the cellular genome. However, α -amanitin inhibited transcription of ICP0 and RFP as efficiently as actinomycin D (ActD; Fig. 5.5B). Therefore, both ICP0 and RFP were transcribed by RNA Pol II. Taken together, these results indicate that Rosco inhibits transcription driven by a promoter when in the context of the extrachromosomal HSV-1 genome, but not the same promoter in the context of the cellular genome. Such effects are consistent with a model in which Rosco specifically decreases the accessibility of HSV-1 genomes thereby preventing their transcription. Therefore, the effects of Rosco appear to be promoter-independent and genome-dependent.

5.2.5. Inhibition of transcription by Rosco depends on genome but not on promoter specific factors.

In the experiments presented in Fig. 5.1, Rosco inhibited initiation of transcription of IE genes under conditions in which their promoters were regulated by cellular and virion proteins acting alone (Fig 5.1A), or acting in combination with IE proteins (Fig 5.1B). In the experiments presented in Fig. 5.5A, we evaluated the effects of Rosco on transcription from IE promoters recombined in the cellular genome only under conditions in which no IE proteins were present. At least two IE proteins regulate the activities of IE promoters in the viral genome, ICP0 and ICP4. Therefore, we next evaluated the effects of Rosco on the expression of RFP driven by the ICP0 promoter in the context of the cellular genome (Fig 5.6A) or an extrachromosomal plasmid (Fig 5.6B), in the presence of IE proteins. To this end, we use the CHX release experimental design used in the experiments

presented in Fig. 5.1B. Parental Vero cells were transiently transfected with the ICP0-RFP construct (Fig 5.6B). Twenty-four hours later, transiently transfected Vero cells (Fig 5.6B) and Vero clone 57 cells (Fig 5.6A) were independently seeded into individual wells. Seeded cells were infected in the presence of CHX for five hours, when CHX-containing medium was removed and replaced with medium containing 0, 25, 50, 75, or 100 μ M Rosco. Sixteen hours later, the expression of RFP was examined by fluorescent microscopy, because the efficiency of transfection of Vero cells is too low to permit examination of RNA levels by Northern blotting.

As in all other experiments, Rosco did not inhibit HSV-induced expression of RFP driven by the ICP0 promoter in the context of the cellular genome (Fig. 5.6A and C). The percentage of cells expressing RFP decreased only marginally when Rosco was increased from 0 to 100 μ M (from 95% of cells expressing RFP to 75% - Fig. 5.6A), this decrease is consistent with the effects of Rosco on the activity of the same reporter gene when it is regulated by structural and cellular proteins acting alone (Fig 5.4A). In contrast, Rosco efficiently inhibited HSV-induced expression of RFP when driven by the ICP0 promoter in the context of an extrachromosomal plasmid (from 100% of transfected cells expressing RFP to less than 15 % - Fig 5.6B and D). This was consistent with the effects of Rosco on the same reporter gene when it is regulated by HSV-1 structural and cellular proteins alone (Fig 5.4B). Rosco, however, did not inhibit the basal activity of ICP0 promoters from extrachromosomal plasmids (Fig 5.4B

and 5.6D, bottom panels), consistent with a previous report using a similar construct (Jordan, Schang et al. 1999).

5.2.6. The effects of Rosco on MCN accessibility have the same genome and promoter dependence as its effects on transcription

Rosco prevents initiation, but does not inhibit ongoing HSV-1 transcription. This effect is specific to HSV-1 genomes. Rosco does not inhibit global cellular transcription, nor does it inhibit the HSV-induced expression of RFP driven by the ICP0 promoter in the context of the cellular genome. Therefore, the effects of Rosco are specific to the extrachromosomal HSV-1 genome and not the ICP0 promoter. These results are consistent with a model in which Rosco decreases access of transcription proteins to HSV-1 genomes, thereby preventing activation of HSV-1 transcription. This specificity would thus explain why Rosco prevents the activation of transcription from otherwise unrelated IE and E promoters in the same extrachromosomal HSV-1 genomes. Therefore, I next evaluated whether the effects of Rosco on accessibility were also genome-specific. To this end, I tested effects of Rosco on the accessibility of the genes driven by the ICP0 promoter in the context of the extrachromosomal HSV-1 genome, or the RFP gene in the context of the cellular genome (the ICP0 or RFP genes, respectively).

Clone 57 cells were infected with 10 PFU of HSV-1 per cell and treated or not with 100 μ M Rosco at one hour after infection. Nuclei were isolated at 5hpi and then digested with MCN (0.05U/1x10⁷) for 0.5, 2.5, 5, 15, 30, 60 minutes. DNA was purified, resolved by agarose gel electrophoresis, and analyzed by ethidium

bromide staining and Southern blot hybridization. The probes used were specific for the gene driven by the ICP0 promoter recombined into the cellular genome (RFP) or in extrachromosomal HSV-1 genome (ICP0). RFP and ICP0 hybridizations are shown in standard exposures to compare total DNA levels, and overexposures of ICP0 are also shown to analyze the differences in accessibility in the presence of Rosco (Figure 5.7A).

I have previously shown that Rosco does not largely affect the MCN accessibility of DNA in most cellular chromatin (Fig 4.3, 4.4, 5.2, and 5.5). Consistently, RFP was digested in untreated or Rosco-treated nuclei with similar kinetics and to similar patterns of digestion products (Fig 5.7A, B). Therefore, Rosco does not inhibit the accessibility of a reporter gene driven by the ICP0 promoter in the context of the cellular genome (or its transcription). However, the pattern of RFP hybridization was distinct from the pattern typically observed for bulk cellular DNA probes (compare Fig 5.7A-RFP to Fig 4.3A-Cellular). Most notably, neither the typical nucleosome ladder nor the typical mononucleosomal DNA were observed. The latter was highly unexpected. The ongoing transcription of the ICP0-driven RFP gene (which is activated by HSV-1 structural and cellular proteins but not inhibited by Rosco under these conditions) may destabilize the nucleosomes. RFP DNA would then become highly accessible to MCN and thus rapidly degraded. Consistent with this hypothesis, the majority of RFP DNA was detected in polynucleosome-like complexes following serial MCN digestion (91.2 and 84.4% in absence and presence of Rosco, respectively) (Fig 5.8). Alternatively, the ICP0 promoter sequence itself (or the recruitment of HSV-1

structural and cellular proteins) may destabilize the surrounding chromatin environment, such that the DNA in the nearby nucleosomes becomes highly accessible to MCN.

The same membranes were then re-hybridized with a probe specific for the ICP0 gene driven by the ICP0 promoter in the HSV-1 genome (ICP0 itself). MCN digestion of the nuclei of the infected but otherwise untreated cells resulted in the typical HSV-1 DNA hybridization pattern. Mainly, the majority of ICP0 DNA was in fragments protected to heterogeneous or nucleosome sizes (compare ND in Fig 5.7 and Fig.4.3). In contrast, all detectable ICP0 DNA in nuclei from Rosco treated cells was poorly accessible to MCN (Fig 5.7A), consistent with the results presented in Fig 4.3. Standard MCN digestion of nuclei from cells treated with Rosco had resulted in such a pattern of fragments when hybridized with probes enriched with HSV-1 IE loci (Fig 4.3). Therefore, Rosco selectively decreases the accessibility (and transcription) of genes driven by the ICP0 promoter in the context of the extrachromosomal HSV-1 genome. Rosco exhibits the same selectivity towards inhibition of transcription driven by the ICP0 promoter in the two different contexts. The MCN accessibility of a gene driven by the same promoter in the context of the cellular genome, in which transcription is not affected by Rosco, was unaffected. Taken together, these results indicate that Rosco has similar genome-dependent and promoter-independent effects on transcription and DNA accessibility.

5.2.7. The effects of Rosco on accessibility are specific for the HSV-1 genome

Standard MCN digestions showed that Rosco decreases the accessibility of an ICP0 promoter-driven gene in the context of the extrachromosomal HSV-1 DNA, but not in the context of the cellular genome. I have previously shown that serial MCN digestions have higher resolution and provide additional information about the nucleoprotein complexes released by MCN. Therefore, I next evaluated whether the DNA released as soluble chromatin following serial MCN digestion also supported a model requiring differences in accessibility.

Briefly, clone 57 cells were infected and their nuclei were harvested at 5hpi, to be subjected to serial MCN digestion. The soluble fractions were pooled and resolved together by sucrose gradients and analyzed by Southern blot hybridization.

The DNA released as soluble chromatin from the locus driven by the ICP0 promoter in the context of the cellular genome in cells infected with HSV-1 and left untreated or treated with Rosco was in mono-, di- (fractions 10 and 11), and poly- (fractions 5 to 9) nucleosomes complexes (Fig 5.8A and B). The complexes containing RFP DNA released as soluble chromatin from cells infected and treated with Rosco was in slightly heavier complexes fractionating primarily as cellular polynucleosomes (fractions 6 to 10) (Fig 5.8B). As evaluated by standard MCN digestions in Fig 5.7, however, Rosco did not have any major effects on RFP DNA in the context of the cellular genome. Therefore, Rosco may or may not affect the polynucleosome-like complexes released as soluble chromatin by

serial MCN digestion. The percentage of RFP DNA released as soluble chromatin apparently decreased from 91.2 to 84.4% in untreated or Rosco treated cells, respectively (Fig 5.8C). Consistent with the lack of effects of Rosco on transcription of genes driven by HSV-1 promoters in the context of the cellular genome, Rosco does not have any major effects either on the accessibility of such genes.

The effects of Rosco on the accessibility of ICP0 loci in the context of the extrachromosomal HSV-1 genome, in contrast, were more obvious. In untreated cells, 91.5% of the DNA of the gene driven by the ICP0 promoter in the context of the viral genome (ICP0 itself) was released as soluble chromatin, and fractionated as short polynucleosomes (fraction 9), or mono- to di- nucleosomes (fractions 10 and 11) (Fig 5.8A, B, and D). In contrast, less than 1% of the DNA of the gene driven by the ICP0 promoter in the context of the viral genome (ICP0 itself) was released as soluble chromatin in the nuclei of cells treated with Rosco (Fig 5.8A, D). Instead, more than 99% of the DNA of the gene driven by the ICP0 promoter in the context of the viral genome (ICP0 itself) resolved to the insoluble chromatin fraction (Fig 5.8A, R; ICP0-Insoluble). In fact, even following a gross overexposure, no DNA of the gene driven by the ICP0 promoter in the context of the viral genome (ICP0 itself) could be detected fractionating as soluble chromatin (Fig 5.8A, R-overexposure). Therefore, the effects of Rosco on the accessibility of HSV-1 DNA are genome-dependent but promoter-independent, very much like its effects on transcription. Taken together, these

results are consistent with a model in which Rosco prevents activation of HSV-1 transcription by decreasing the accessibility of genomic HSV-1 DNA.

5.3 References

- Diwan, P., J. J. Lacasse, et al. (2004). "Roscovitine inhibits activation of promoters in herpes simplex virus type 1 genomes independently of promoter-specific factors." *J Virol* **78**(17): 9352-65.
- Jordan, R., L. Schang, et al. (1999). "Transactivation of herpes simplex virus type 1 immediate-early gene expression by virion-associated factors is blocked by an inhibitor of cyclin-dependent protein kinases." *J Virology* **73**(10): 8843-8847.
- Jordan, R., L. Schang, et al. (1999). "Transactivation of herpes simplex virus type 1 immediate-early gene expression by virion-associated factors is blocked by an inhibitor of cyclin-dependent protein kinases." *J Virol* **73**(10): 8843-7.
- Lacasse, J. J. and L. M. Schang (2010). "During lytic infections, herpes simplex virus type 1 DNA is in complexes with the properties of unstable nucleosomes." *J Virol* **84**(4): 1920-33.
- Lam, L. T., O. K. Pickeral, et al. (2001). "Genomic-scale measurement of mRNA turnover and the mechanisms of action of the anti-cancer drug flavopiridol." *Genome Biol* **2**(10): RESEARCH0041.
- Nicholl, M. J. and C. M. Preston (1996). "Inhibition of herpes simplex virus type 1 immediate-early gene expression by alpha interferon is not VP16 specific." *Journal of Virology* **70**(9): 6336-6339.
- Panning, B. and J. R. Smiley (1989). "Regulation of cellular genes transduced by herpes simplex virus." *Journal of Virology* **63**(5): 1929-1937.
- Reeves, R. (1984). "Transcriptionally active chromatin." *Biochim Biophys Acta* **782**(4): 343-93.
- Rice, S. A., M. C. Long, et al. (1995). "Herpes simplex virus immediate-early protein ICP22 is required for viral modification of host RNA polymerase II and establishment of the normal viral transcription program." *Journal of Virology* **69**(9): 5550-5559.
- Schang, L. M., J. Phillips, et al. (1998). "Requirement for cellular cyclin-dependent kinases in herpes simplex virus replication and transcription." *J Virology* **72**(7): 5626-5637.
- Schang, L. M., A. Rosenberg, et al. (1999). "Transcription of herpes simplex virus immediate-early and early genes is inhibited by roscovitine, an inhibitor specific for cellular cyclin-dependent kinases." *J Virol* **73**(3): 2161-72.
- Schang, L. M., A. Rosenberg, et al. (1999). "Transcription of herpes simplex virus immediate-early and early genes is inhibited by roscovitine, an inhibitor specific for cellular cyclin-dependent kinases." *Journal of Virology* **73**(3): 2161-2172.
- Schang, L. M., A. Rosenberg, et al. (2000). "Roscovitine, a specific inhibitor of cellular cyclin-dependent kinases, inhibits herpes simplex-virus DNA synthesis in the presence of viral early proteins." *J Virology* **74**(5): 2107-2120.

- Schang, L. M., A. Rosenberg, et al. (2000). "Roscovitine, a specific inhibitor of cellular cyclin-dependent kinases, inhibits herpes simplex virus DNA synthesis in the presence of viral early proteins." J Virol **74**(5): 2107-20.
- Smibert, C. A. and J. R. Smiley (1990). "Differential regulation of endogenous and transduced beta-globin genes during infection of erythroid cells with a herpes simplex virus type 1 recombinant." Journal of Virology **64**(8): 3882-3894.
- Smiley, J. R., C. Smibert, et al. (1987). "Expression of a cellular gene cloned in herpes simplex virus: rabbit beta-globin is regulated as an early viral gene in infected fibroblasts." Journal of Virology **61**(8): 2368-2377.
- Spencer, C. A., M. E. Dahmus, et al. (1997). "Repression of host RNA polymerase II transcription by herpes simplex virus type 1." Journal of Virology **71**(3): 2031-2040.
- Weisbrod, S. (1982). "Active chromatin." Nature **297**(5864): 289-95.

| | Treatment | DNA, % | |
|-------------|-----------|-----------|---------|
| | | Insoluble | Soluble |
| RFP | No Drug | 8.8 | 91.2 |
| | Rosco | 15.6 | 84.4 |
| ICP0 | No Drug | 8.5 | 91.5 |
| | Rosco | 99.5 | 0.5 |

Table 5.5. Rosco specifically inhibits the accessibility of HSV-1 loci in the viral genome, but HSV-1 loci recombined into the cellular genome.

Percentages of DNA containing **RFP** and **ICP0** loci fractionating in **Insoluble** or **Soluble** chromatin following serial MCN digestions of clone 57 nuclei infected with HSV-1 for 5h in the presence of **No Drug** or **Rosco**.

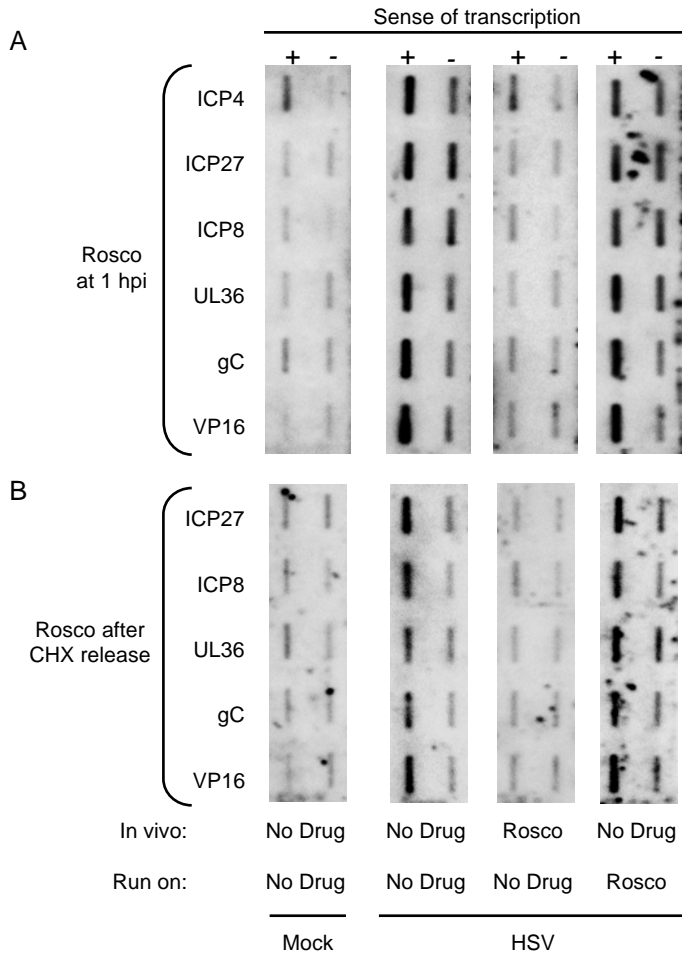


Figure 5.1. Rosco prevents initiation, but does not inhibit ongoing, HSV-1 transcription. Four membranes slot-blotted with single-stranded DNA complementary to (+), or same sense as (-), two IE (ICP4, ICP27), two E (ICP8, UL36) and two L (gC, VP16) HSV-1 genes and probed with RNA isolated from “run-on” transcription reactions.

A. Cells were mock infected (**Mock**), or infected with HSV-1 (**HSV**) in the presence of (**In vivo**) vehicle (**No Drug**) or Rosco (**Rosco**). Nuclei were isolated at 6 hpi, and run-on transcription reactions were performed in the presence of (**Run on**) vehicle (**No Drug**) or 100 μ M Rosco (**Rosco**). The higher background in the ICP4 sense probe is consistently observed, and most likely due to cross-hybridization with cellular RNAs.

B. Cells were mock infected (**Mock**), or infected with HSV-1 (**HSV**) in the presence of CHX. Six hours later, CHX-containing medium was removed and replaced with medium containing (**In vivo**) vehicle (**No Drug**), or Rosco (**Rosco**). Nuclei were isolated at 3 hours after changing the media, and run-on transcription reactions were performed in the presence of (**Run on**) vehicle (**No Drug**) or 100 μ M Rosco (**Rosco**). Transcription of ICP4 could not be evaluated in these experiments because the cross-hybridizing cellular RNAs are too strongly induced by CHX.

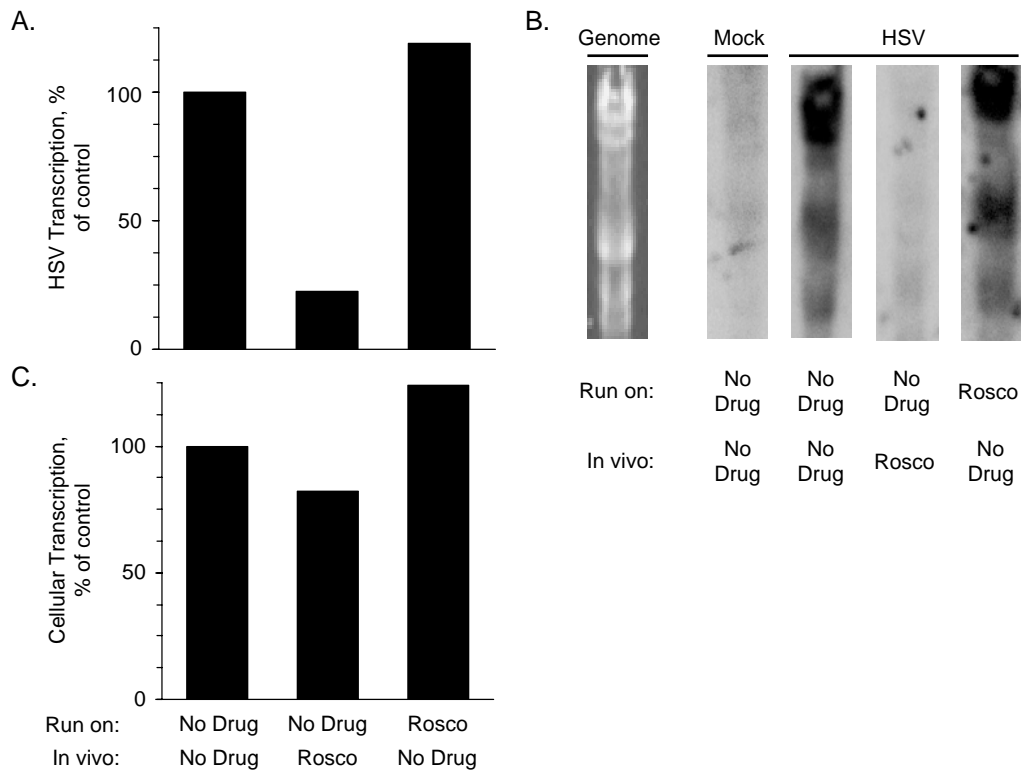


Figure 5.2. Rosco prevents initiation of HSV-1, but not cellular, transcription.

A. Bar graph showing the percentage of HSV-1 run-on transcription in the presence or absence of Rosco. Cells were infected with HSV-1 in the presence of (**In vivo**) vehicle (**No Drug**) or 100 μ M Rosco (**Rosco**). Nuclei were isolated at 6 hpi, and run-on transcription reactions were performed in the presence of (**Run on**) vehicle (**No Drug**) or 100 μ M Rosco (**Rosco**). RNA was purified and probed with membranes containing the entire HSV-1 genome as Hind III fragments. Radioactivity hybridized to the HSV-1 genome fragments was quantitated using a Bio-Rad molecular imager and FX software package, and expressed as percentage of transcription in the absence of Rosco in vivo or in vitro (first bar).

B. Four membranes Southern-blotted with Hind III HSV-1 DNA fragments and probed with RNA isolated from “run-on” transcription reactions. A picture of a gel stained with ethidium bromide is presented on the left to show the positions of the HSV-1 genome fragments (**Genome**). Cells were mock infected (**Mock**) or infected with HSV-1 (**HSV-1**) in the presence of (**In vivo**) vehicle (**No Drug**) or Rosco (**Rosco**). Nuclei were isolated at 6 hpi, and run-on transcription reactions were performed in the presence of (**Run on**) vehicle (**No Drug**) or 100 μ M Rosco (**Rosco**). RNA was purified and probed with membranes containing the entire HSV-1 genome as Hind III fragments.

C. Bar graph showing the percentage of global cellular run-on transcription in the presence or absence of Rosco. Cells were mock infected in the presence of (**In vivo**) vehicle (**No Drug**) or 100 μ M Rosco (**Rosco**). Nuclei were isolated 6 hours later, and run-on transcription reactions were performed in the presence of (**Run on**) vehicle (**No Drug**) or 100 μ M Rosco (**Rosco**). RNA was purified and probed with membranes containing the entire Vero cell genome as Hind III fragments. Radioactivity hybridized to the Vero cell genomic fragments was quantitated using a Bio-Rad molecular imager and FX software package, and expressed as percentage of transcription in the absence of Rosco in vivo or in vitro (first bar).

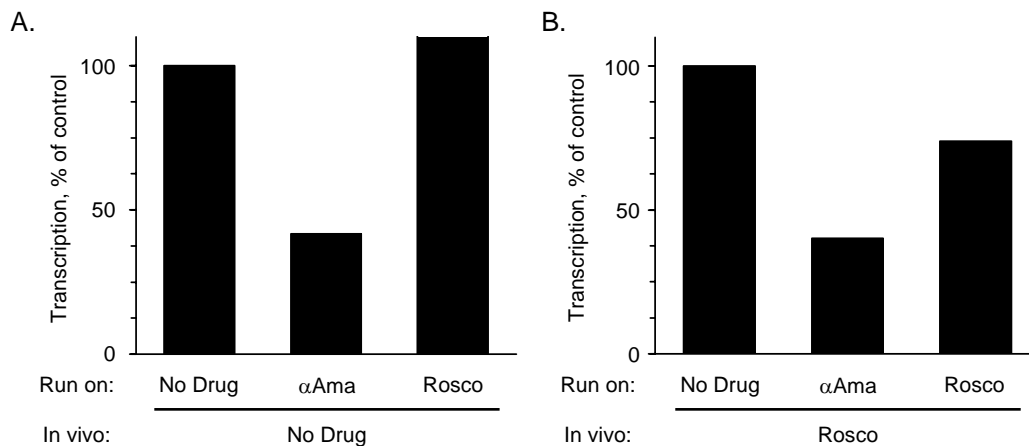


Figure 5.3. Cellular transcription in the presence of Rosco is performed by RNA Pol II.

A. Bar graph showing the percentage of global cellular run-on transcription in the presence or absence of Rosco. Cells were mock infected in the presence of (**In vivo**) vehicle (**No Drug**). Nuclei were isolated 6 h later, and run-on transcription reactions were performed in the presence of (**Run on**) vehicle (**No Drug**), α -amanitin (**αAma**), or 100 μ M Rosco (**Rosco**). RNA was then precipitated with TCA and the percentage of radioactivity incorporated into RNA was calculated. Background incorporation was subtracted, and transcription is presented as the percentage of radioactivity incorporated into RNA in run on reactions performed in the absence of any drug.

B. Bar graph showing the percentage of global cellular run-on transcription in the presence or absence of Rosco. Cells were mock infected in the presence of (**In vivo**) 100 μ M Rosco (**Rosco**). Nuclei were isolated 6 h later, and run-on transcription reactions were performed in the presence of (**Run on**) vehicle (**No Drug**), α -amanitin (**αAma**), or 100 μ M Rosco (**Rosco**). RNA was then precipitated with TCA and the percentage of radioactivity incorporated into RNA was calculated. Background incorporation was subtracted, and transcription is presented as the percentage of radioactivity incorporated into RNA in run on reactions performed in the absence of any drug. The actual levels of transcription for all run on conditions (no drug, α -Ama, Rosco) were approximately 30% higher in nuclei of cells treated with Rosco in vivo than in nuclei of control cells, consistent with the data shown in Fig. 5.2 C.

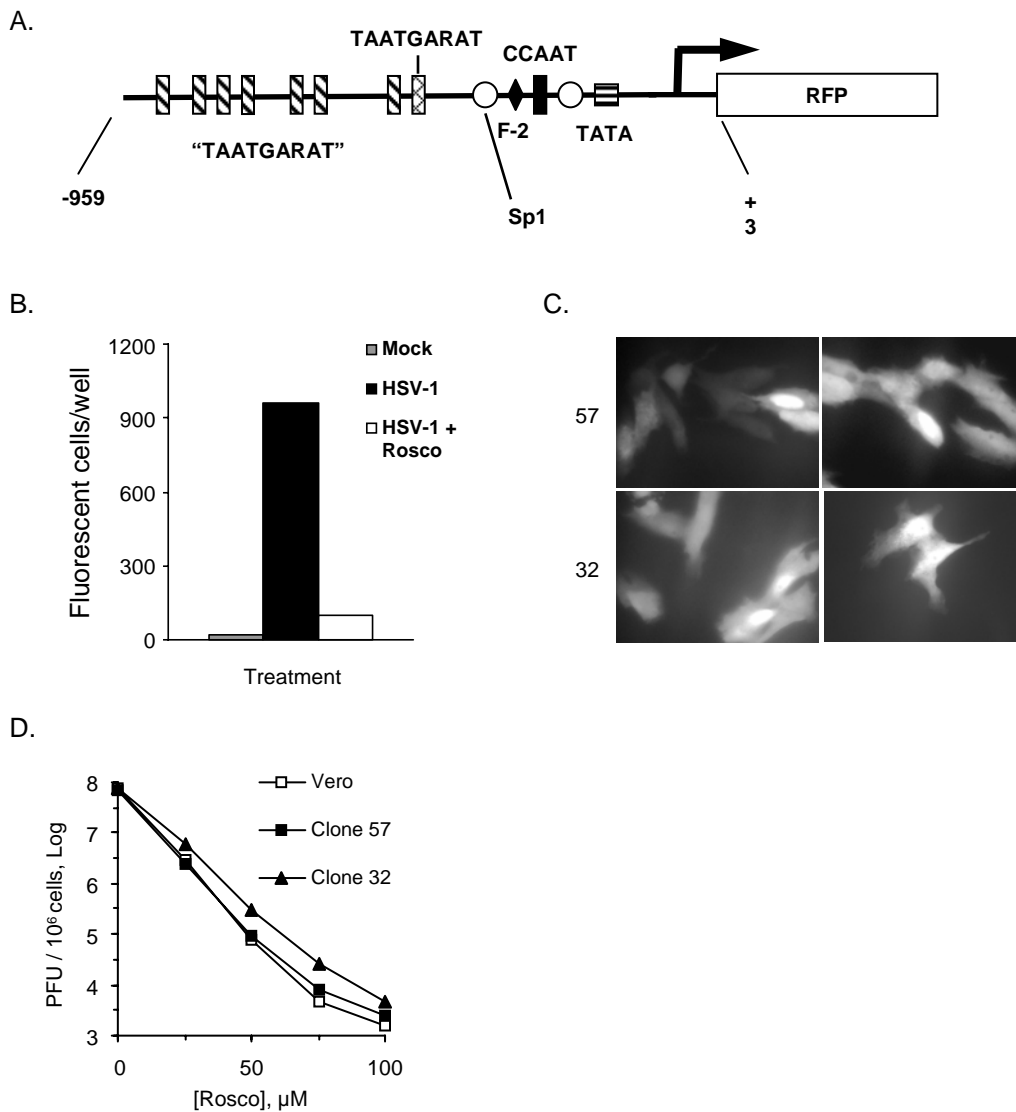


Figure 5.4. Characterization of Vero clones stably transfected with ICP0-driven RFP (pICP0-RFP).

A. A diagram of the ICP0-RFP construct that was stably transfected into Vero cells. The major regulatory elements in the promoter are indicated. “TAATGARAT”, TAATGARAT sequences (one or two nucleotides deviate from the consensus TAATGARAT motif)

B and C. Two stably transfected clones, named clone 57 and 32 were infected with the equivalent of 0.5 PFU/cell of UV-inactivated HSV-1 KOS. Twenty-four hours later, cells were evaluated by optic and fluorescence microscopy. No plaques were visible, but a large fraction of Vero clone 57 or 32 cells expressed RFP. Representative UV micrographs are presented (original magnification, 400 A).

D. Dose-response analysis of the sensitivity of HSV replication to Rosco in parental Vero and clones 57 and 32 cells. Cells were infected with 2.5 PFU/cell of HSV-1 KOS and treated with 0, 25, 50, 75, or 100 μM Rosco. Twenty-four hours later, cells were harvested, virus was isolated and titrated by standard plaque assays. Log of PFU/ million cells are plotted against drug concentration. This experiment was performed by Dr. Diwan

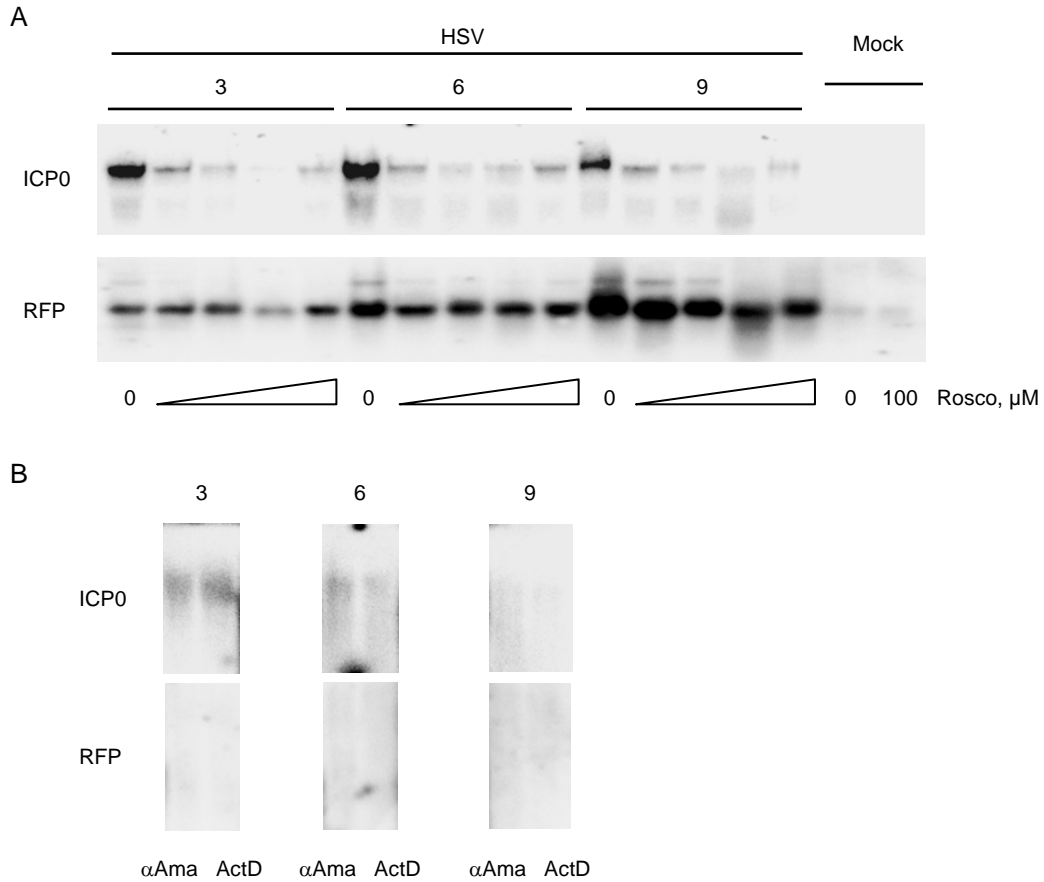


Figure 5.5. Inhibition of transcription by Rosco is specific for the HSV-1 genome.

A. Northern blot analyses of expression of ICP0 (ICP0 - top panels) and RFP (RFP - bottom panels) in Vero clone 57 cells infected with HSV-1 in the presence of CHX. Cells were infected with 5 PFU/cell (**HSV**) and treated with CHX and 0, 25, 50, 75, or 100 μ M (0,) Rosco. Mock infected cells (**Mock**), treated with CHX and 0 or 100 μ M Rosco were included as negative control. Cells were harvested at 3, 6, and 9 hpi (3, 6, 9), RNA was extracted, resolved by gel electrophoresis, and blotted to Nylon membranes. Membranes were then hybridized with RFP probe, stripped, and re-hybridized with ICP0 probe. The decrease in signal in both RFP and ICP0 in the 75 μ M Rosco 3 hpi line is an artifact due to experimental error and is not reproducible.

B. Northern blot analyses of expression of ICP0 (**ICP0** - top panels) and RFP (**RFP** - bottom panels) in Vero clone 57 cells infected with HSV-1 in the presence of CHX. Cells were infected with 5 PFU/cell and treated with CHX and 50 μ g/ml α -amanitin (**αAma**) or 10 μ g/ml actinomycin D (**ActD**). Cells were harvested at 3, 6, and 9 hpi (**3, 6, 9**), RNA was extracted, resolved by gel electrophoresis, and blotted to Nylon membranes. Membranes were then hybridized with RFP probe, stripped, and re-hybridized with ICP0 probe. This experiment was performed by Dr. Diwan.

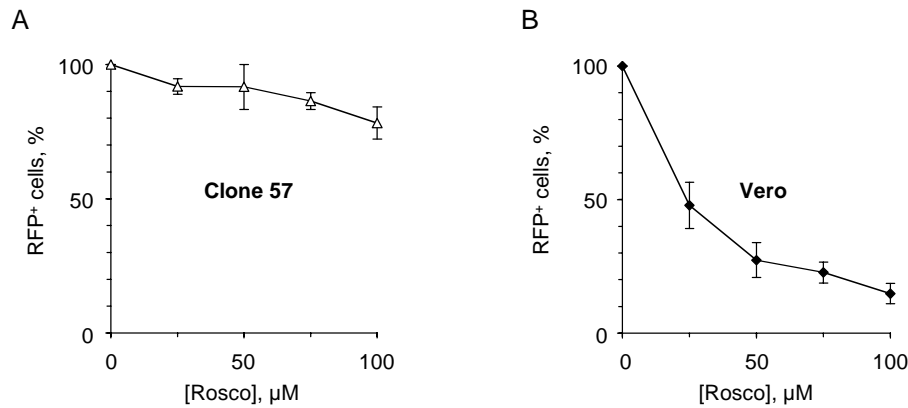


Figure 5.6. Inhibition of transcription by Rosco depends on genome but not promoter specific factors.

A. Vero cells clone 57 (stably transfected with pICP0-RFP) were seeded in individual wells and mock infected or infected with 2.5 PFU/cell of HSV-1 KOS in the presence of CHX. Six hours later, CHX containing medium was replaced by fresh medium containing 0, 25, 50, 75, or 100 μM Rosco. Twenty-four hours after infection, cells were fixed and number of RFP+ cells was evaluated under UV microscopy. Percentage of RFP+ cells is presented as averages of two independent experiments (plus minus range) plotted against Rosco concentration.

B. Vero cells were transiently transfected with pICP0-RFP. Transfected cells were seeded in 5 individual wells and mock infected or infected with 2.5 PFU/cell of HSV-1 KOS in the presence of CHX. Six hours later, CHX containing medium was replaced by fresh medium containing 0, 25, 50, 75, or 100 μM Rosco. Twenty-four hours after infection, cells were fixed and number of RFP+ cells was evaluated under UV microscopy. Percentage of RFP+ cells in the presence of the different concentrations of Rosco (where the number of RFP+ cells in the absence of Rosco is set at 100%), and corrected by efficiency of transfection, is presented as averages of two independent experiments (plus minus range) and plotted against Rosco concentration. This experiment was performed by Dr. Diwan.

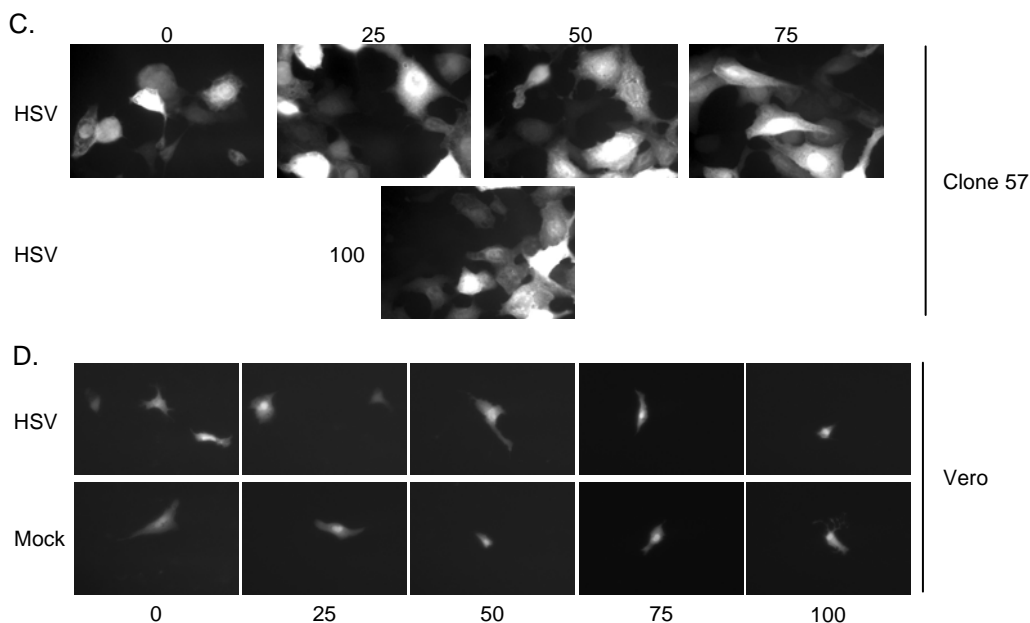


Figure 5.6. (continued) Inhibition of transcription by Rosco depends on genome but not promoter specific factors.

C. Vero cells clone 57 (stably transfected with pICP0-RFP5) were seeded in individual wells and infected with 2.5 PFU/cell of HSV-1 KOS in the presence of CHX (**HSV**). Six hours later, CHX containing medium was replaced by fresh medium containing 0, 25, 50, 75, or 100 μM Rosco (**0, 25, 50, 75**). Twenty-four hours after infection, cells were fixed and RFP+ cells were photographed under UV microscopy. Representative micrographs are presented. Original magnification, 200 A.

D. Vero cells were transiently transfected with pICP0-RFP5. Transfected cells were seeded in individual wells and mock infected (**Mock**) or infected with 2.5 PFU/cell of HSV-1 KOS in the presence of CHX (**HSV**). Six hours later, CHX containing medium was replaced by fresh medium containing 0, 25, 50, 75, or 100 μM Rosco (**0, 25, 50, 75, 100**). Twenty-four hours after infection, cells were fixed and RFP+ cells were photographed under UV microscopy. Representative micrographs are presented. Original magnification, 100 A. This experiment was performed by Dr. Diwan

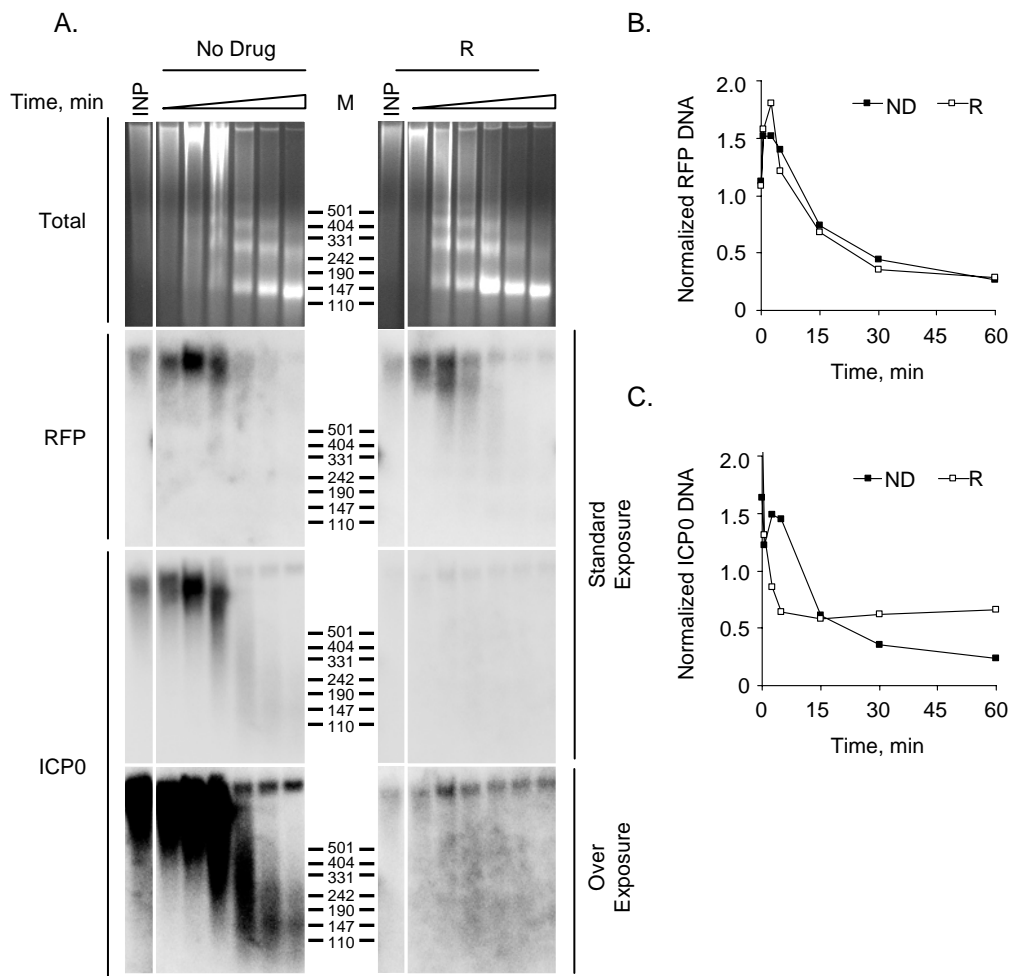


Figure 5.7. The effects of Rosco on MCN accessibility correlate with its effects on transcription. Infected cells were treated with no drug (ND) or Rosco (R). Nuclei of infected cells were isolated at 5 hours post infection and were digested for 0 (INP), 0.5, 2.5, 5, 15, 30, and 60min () with 0.05U MCN per 1×10^7 nuclei. The DNA was analyzed by Southern blot with probes specific for genes driven by the ICP0 promoter recombined into the cellular genome (RFP) or in the native viral genome (ICP0). **A.** Images of the ethidium bromide stained gels (Total) and membranes hybridized with RFP or ICP0 probes. To achieve comparable signal intensities, only 67% of sample was loaded for 0.5min. Normal and over-exposures (bottom panels) are shown for ICP0. **B.** Line graphs of the quantitated Southern blots presenting normalized levels of DNA against digestion time.

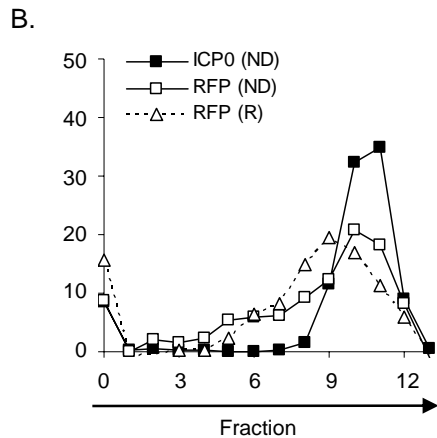
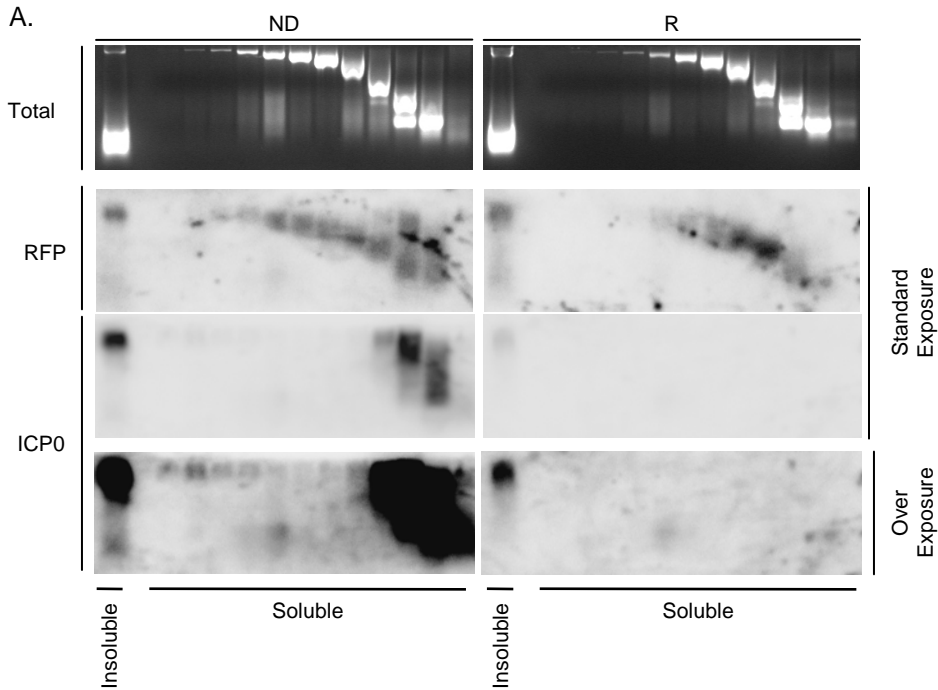


Figure 5.8. The effects of Rosco on accessibility are specific for the HSV-1 genome. Clone 57 cells were infected and treated with no drug (ND) or Rosco (R) and nuclei were harvested at 5hpi. Nuclei were then lysed and soluble and insoluble chromatin were fractionated. Insoluble chromatin was resuspended in MCN digestion buffer (0.05U MCN/ml), and subjected to serial MCN digestions. Supernatants were periodically removed and quenched, and the insoluble pellets were resuspended with fresh MCN. Soluble DNA-protein complexes were either pooled and further resolved on sucrose gradients. DNA from each fraction was analyzed by Southern blot with probes specific for genes driven by the ICP0 promoter recombined into the cellular genome (RFP) or in the native viral genome (ICP0). **A.** Images of the ethidium bromide stained gels (Total) and membranes hybridized with RFP or ICP0 probes. To achieve comparable signal intensities, only 50% of the soluble fractions were loaded. Normal and over-exposures (bottom panels) are shown. **B.** Line graph presenting DNA in each fraction as percent of DNA in the gradient. There was no detectable signal when probing the gradient from Rosco-treated cells with the ICP0 gene specific HSV-1 probe.

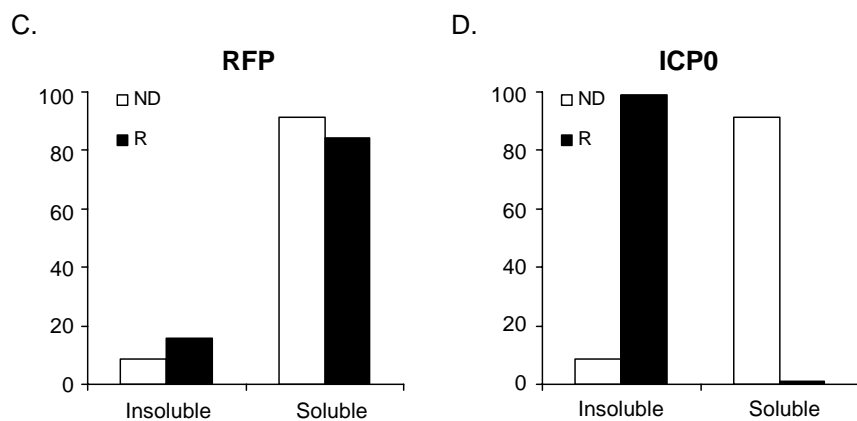


Figure 5.8. (continued) The effects of Rosco on accessibility are specific for the HSV-1 genome.

C and D. Bar graphs of the quantitated Southern blots from Fig 5.8A presenting the percentage of RFP (**C**) or ICP0 (**D**) DNA fractionating as the pellet (**Insoluble**) or supernatant (**Soluble**) following the serial MCN digestion

CHAPTER 6: PURINE AND NONPURINE PHARMACOLOGICAL CYCLIN-DEPENDENT KINASE INHIBITORS PREVENT INITIATION OF HSV-1 TRANSCRIPTION

This chapter contains published data from both

Diwan P., JJ. Lacasse*, and LM. Schang *Both of these authors contributed
equally to the published work.*

Journal of Virology 2004; 78(17): 9352-65

Lacasse, JJ, VMI. Provencher*, MD. Urbanowski, and LM Schang. *Both of
these authors contributed equally to the published work.*

Therapy 2005; 2(1): 77-90

6.1 Introduction

In the previous chapter, I showed that Rosco inhibits the activation, but not elongation, of HSV-1 transcription. This effect was specific to extrachromosomal DNA, in that transcription was inhibited from loci in HSV-1 genomes and transiently transfected plasmid DNA, but not the cellular genome. These results are consistent with a model in which Rosco inhibits a target required for maintaining extrachromosomal DNA in an accessible state whereby transcription proteins are able to activate HSV-1 transcription. Rosco is a highly specific inhibitor that selectively inhibits CDK 1, 2, 3, 5, 7, and 9, but not 295 other protein kinases (Appendix 1). I therefore next tested whether genome-specific

inhibition of transcription initiation from extrachromosomal HSV-1 genomes was common to other less selective PCIs.

6.2. Results

6.2.1. Less specific PCIs inhibit transcription directed by the ICP0 promoter in either HSV-1 or cellular genomes.

The specificity for HSV-1 genomes could be common to all PCIs or could be unique to Rosco, the PCI most specific for CDK1, CDK2, CDK5 and CDK7 (Vesely, Havlicek et al. 1994; Meijer, Borgne et al. 1997; Gray, Wodicka et al. 1998; Schang, Knockaert et al. 2002; Bain, McLauchlan et al. 2003). Thus, I compared the effects of Rosco with those of Purv (a purine PCI that is less specific for CDK1, CDK2, CDK5, and CDK7 than Rosco), and Flavo, (a flavonoid PCI that preferentially inhibits CDK9, but further inhibits all other tested CDKs, and many other protein kinases with comparable potencies).

Cells were infected in the presence of CHX and 0, 5, 10, 20, or 30 μ M Purv, or 0, 31.25, 62.5, 125, 250, or 500 nM Flavo. Thirty micromolar Purv inhibits HSV-1 replication in Vero cells completely (Schang, Knockaert et al. 2002), and 125 to 500 nM Flavo completely inhibit transcription of a variety of cellular and viral genes in vivo (Chao and Price 2001; Lam, Pickeral et al. 2001). Purv, which is less selective than Rosco, completely prevented transcription of ICP0 at 20 μ M, whereas it did not completely prevent transcription of RFP at 30 μ M. However, Purv prevented transcription of RFP more efficiently than Rosco (compare Fig. 6.1A with Fig 5.5A). Flavo, the least specific PCI tested, inhibited transcription of ICP0-driven

RFP at all concentrations tested (Fig. 6.1B). Interestingly, Flavo appears to prevent transcription of ICP0 promoter-regulated RFP from the cellular as, or perhaps even more, efficiently than transcription of ICP0 promoter-regulated ICP0 from the HSV-1 genome. No ICP0 or RFP transcripts were detected in the presence of any concentration of Flavo at 3hpi, and only low levels were detected in the presence of 31.25 or 62.5 nM at 9hpi in the experiments presented in Fig. 6.1B. However, very low levels of ICP0, but not of RFP, transcripts are occasionally detected at 3hpi in repeats of this experiment. In contrast, RFP mRNAs were detected at 3hpi at all concentrations of Rosco in all experiments, whereas almost no ICP0 transcripts were detected at 3, 6, or 9hpi in the presence of any concentration of Rosco in any experiment (Fig. 5.5A, top panels). Therefore, as the molecular specificity of the PCI decreases so does the specificity for inhibiting HSV-1 transcription.

6.2.2. Unrelated PCIs inhibit initiation of HSV-1 transcription

I have previously shown that Rosco prevents the initiation of, but does not inhibit ongoing, HSV-1 transcription. Therefore, I next evaluated whether this was a common mechanism for two PCIs that preferentially target CDKs involved in either transcription initiation (DRB) or elongation (Flavo). The effects on HSV-1 transcription were evaluated in the presence or absence of IE proteins, using a previously described CHX-release experimental design.

Briefly, Vero cells were infected in the presence of CHX with 20 PFU of HSV-1 per cell. After 5 h, cells were transferred to complete medium containing vehicle (DMSO), 50 μ g/ml CHX, 100 μ M Rosco, 150 μ M DRB, or 100nM Flavo.

Nuclei were isolated at 10hpi, and run-on assays were performed as described. As in Fig 5.1, I analyzed promoter specific (i.e., sense) and non-promoter specific (i.e., antisense) transcription by probing with single stranded DNA sense or antisense to selected HSV-1 genes.

Run-on transcription assays performed with nuclei of mock-infected cells (negative controls) resulted in only background levels of hybridization to HSV-1 genes. Run-on transcription assays performed with the nuclei of cells infected with HSV-1 in the absence of any drug (positive controls) resulted in abundant transcription of all HSV-1 genes, as expected (Fig. 6.2). As previously observed (Fig 5.1) most of the transcription was from the sense strand (promoter specific) but a small proportion was from the antisense strand (non-promoter-specific).

Run-on assays performed with nuclei of cells infected with HSV-1 and maintained in CHX resulted in transcription of the IE genes ICP4 and ICP27, albeit to varying levels (Fig. 6.2). However, since the concentrations of CHX required to efficiently reverse the effect of the drug do not completely inhibit protein synthesis, transcription of some E and L genes are therefore also observed under these conditions. Run-on assays performed with the nuclei of cells infected with HSV-1 for 5h in the presence of CHX and then further incubated for 5h with 100 μ M Rosco, 150 μ M DRB or 100nM Flavo resulted in almost complete inhibition of transcription of all tested HSV-1 genes (Fig. 6.2). All PCIs prevented promoter-specific and non-promoter-specific transcription. Flavo, which inhibits transcription elongation, also moderately inhibited transcription when it was present during the run-on transcription (Fig. 6.2). In contrast, DRB,

which acts primarily on transcription initiation, or Rosco, which acts primarily before transcription initiation, did not inhibit HSV-1 transcription when either of them was present during the run-on transcription (Fig. 6.2). These findings are consistent with the lack of effects of DRB on cellular run-on transcription, and of Rosco on HSV-1 run-on transcription, under similar circumstances. Therefore, the inhibition of initiation of HSV-1 gene transcription in the presence of IE proteins is common to at least three different PCIs.

6.3. References

- Bain, J., H. McLauchlan, et al. (2003). "The specificities of protein kinase inhibitors: an update." Biochem J **371**(1): 199-204.
- Chao, S. H. and D. H. Price (2001). "Flavopiridol inactivates p-TEFb and blocks most RNA polymerase II transcription in vivo." J Biological Chem **276**(34): 31793-31799.
- Gray, N. S., L. Wodicka, et al. (1998). "Exploiting chemical libraries, structure, and genomics in the search for kinase inhibitors." Science **281**(5376): 533-538.
- Lam, L., O. Pickeral, et al. (2001). "Genomic-scale measurement of mRNA turnover and the mechanisms of action of the anti-cancer drug flavopiridol." Genome Bio **2**(10): 0041.1-0041.11.
- Meijer, L., A. Borgne, et al. (1997). "Biochemical and cellular effects of roscovitine, a potent and selective inhibitor of the cyclin-dependent kinases cdc2, cdk2 and cdk5." Euro J Biochem **243**(1-2): 527-536.
- Schang, L. M., M. Knockaert, et al. (2002). "Pharmacological cyclin-dependent kinase inhibitors inhibit replication of wild type and drug-resistant strains of HSV and HIV-1 by targeting cellular, not viral proteins." J Virology **26**(15): 7884-7882.
- Vesely, J., L. Havlicek, et al. (1994). "Inhibition of cyclin-dependent kinases by purine analogues." Euro J Biochem **224**(2): 771-786.

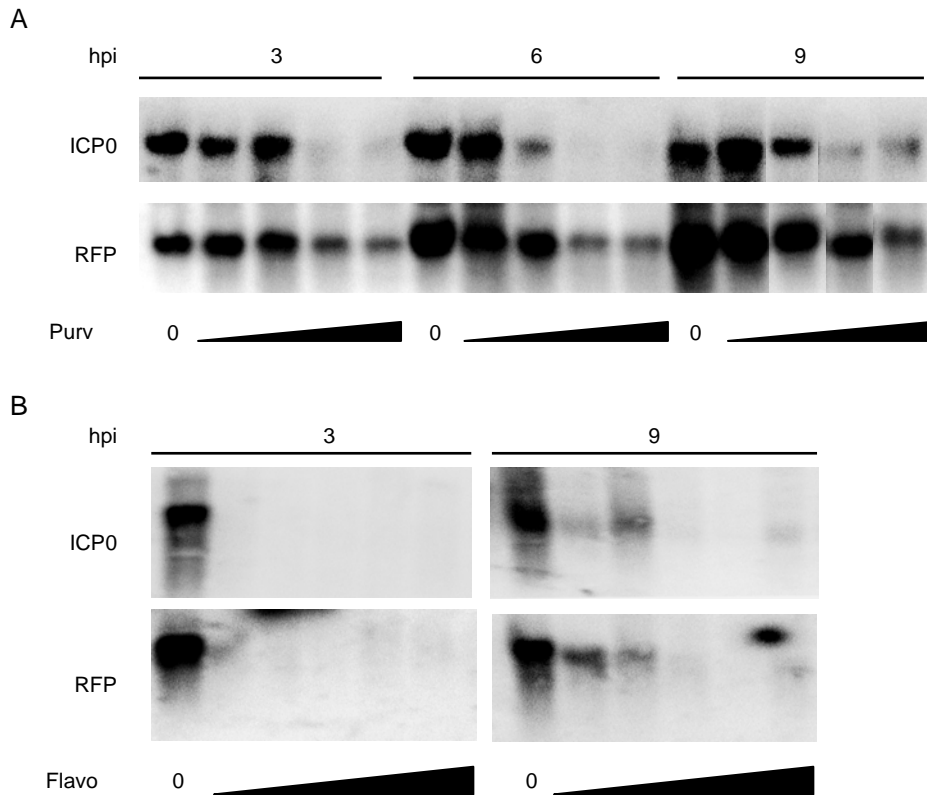
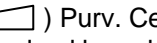
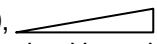


Figure 6.1. Less-specific PCIs, inhibit transcription directed by the ICP0 promoter in either the HSV-1 or cellular genomes.

A. Northern blot analyses of expression of ICP0 (ICP0 - top panels) and RFP (RFP - bottom panels) in Vero clone 57 cells infected with HSV-1 in the presence of CHX. Cells were infected with 5 PFU/cell and treated with CHX and 0, 5, 10, 20 or 30 μM (0, ) Purv. Cells were harvested at 3, 6, and 9 hpi (3, 6, 9), RNA was extracted, resolved by gel electrophoresis, and blotted to Nylon membranes. Membranes were then hybridized with RFP probe, stripped and re-hybridized with ICP0 probe. A composite picture is presented (the 10 and 20 μM samples at 9 hpi were switched in the original gel).

B. Northern blot analyses of expression of ICP0 (ICP0 - top panels) and RFP (RFP - bottom panels) in Vero clone 57 cells infected with HSV-1 in the presence of CHX. Cells were infected with 5 PFU/cell and treated with CHX and 0, 31.25, 62.5, 125, 250, or 500 nM (0, ) Flavo. Cells were harvested at 3 or 9 hpi (3, 9), RNA was extracted, resolved by gel electrophoresis, and blotted to Nylon membranes. Membranes were then hybridized with RFP probe, stripped and re-hybridized with ICP0 probe.

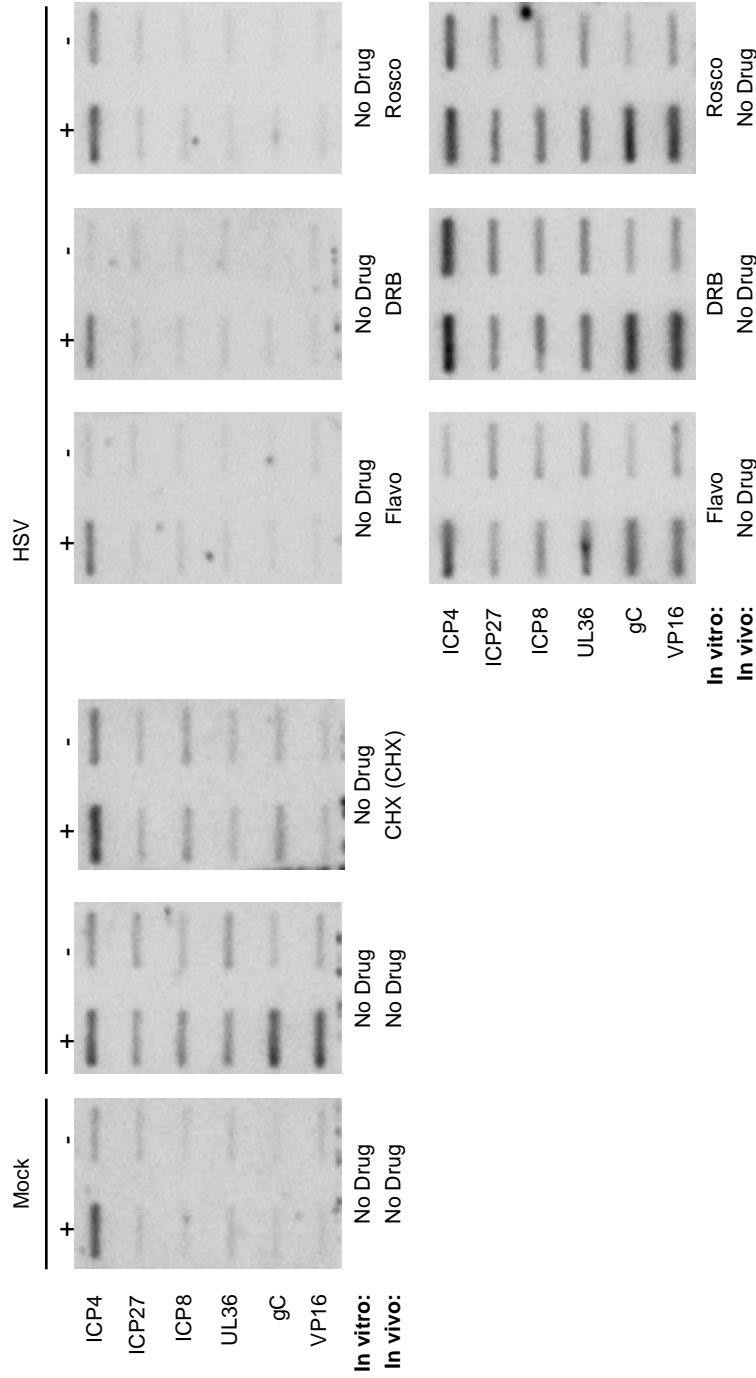


Figure 6.2. Unrelated PCIs inhibit initiation of HSV-1 transcription.

Nine membranes slot-blotted with single-stranded DNA complementary to (+), or same sense as (-), six HSV-1 genes and probed with RNA isolated from run-on transcription reactions. Cells were (**Mock**), or infected with HSV-1 (**HSV-1**) in the presence of CHX. Five hours later, cells were transferred to medium containing (**In vivo**) vehicle (**No Drug**), CHX (**CHX**), Flavo (**Flavo**), DRB (**DRB**), or Rosco (**Rosco**). Nuclei were isolated at 10 h post infection, and run-on transcription reactions were performed in the presence of (**In vitro**) vehicle (**No Drug**), Flavo (**Flavo**), DRB (**DRB**), or Rosco (**Rosco**). RNA was purified and probed with membranes containing single-stranded DNA complementary to (+), or same sense as (-), two immediate-early (**ICP4**, **ICP27**), two early (**ICP8**, **UL36**) and two late (**gC**, **VP16**) HSV-1 genes. The higher background in the ICP4 sense probe is consistently observed after CHX-treatments, and is most likely due to cross-hybridization with CHX-inducible cellular RNAs.

CHAPTER 7: DISCUSSION

The results presented in this thesis represent the first systematic characterization of the biophysical properties of HSV-1 DNA-containing complexes during lytic infection.

Prior to the results presented herein, the existence or properties of any intranuclear HSV-1 DNA nucleoprotein complexes during lytic infection was unclear. Primarily, the results obtained from classical studies (MCN digestions, trimethylsporolen photocrosslinking, and electron micrography), and those obtained from more recent ChIP assays, were most difficult to reconcile. Whereas classical evidence suggested HSV-1 DNA was primarily nucleosome-free, ChIP assays reported association of HSV-1 DNA with histones, and furthermore proposed that chromatin regulates HSV-1 transcription.

7.1. HSV-1 DNA during lytic infection

Classic studies concluded that HSV-1 DNA during lytic infection is mostly not in nucleosomes (Mouttet, Guetard et al. 1979; Leinbach and Summers 1980; Sinden, Pettijohn et al. 1982; Muggeridge and Fraser 1986). The conclusion was based primarily on using standard MCN digestions to probe the structure of intranuclear HSV-1 DNA. These reports showed that in contrast to DNA in cellular chromatin or in other nuclear DNA viruses such as polyoma-, papilloma-, and adenoviruses, which are digested to the typical nucleosome ladder, the majority of HSV-1 DNA was rapidly digested to heterogeneously sized fragments (Mouttet, Guetard et al. 1979; Leinbach and Summers 1980; Muggeridge and Fraser 1986;

Deshmane and Fraser 1989). Such a pattern is more reminiscent of protein-free DNA. In addition to the heterogeneously sized fragments, however, most groups also observed a minor percentage of HSV-1 DNA protected to nucleosome sizes (Leinbach and Summers 1980; Muggeridge and Fraser 1986; Deshmane and Fraser 1989). Muggeridge *et al.* therefore proposed that the minor percentage of HSV-1 DNA protected to nucleosome size may represent, i) a small number of chromatinized HSV-1 genomes, ii) the chromatinization of only parts of each of the HSV-1 genomes, or iii) the formation of complexes between HSV-1 DNA and non-histone proteins that are not as tightly associated as canonical nucleosomes and thus provide less protection than typical nucleosomes (Muggeridge and Fraser 1986). Evidence for coexistence of all three of the proposed arrangements of intranuclear HSV-1 DNA was supported by a previous study by Muller *et al.* in which nuclear spreads from HSV-1 infected cells were evaluated under the electron microscope (Muller, Schroder *et al.* 1980).

The structure of intranuclear HSV-1 DNA during lytic infection was also evaluated using trimethylpsoralen photocrosslinking (Sinden, Pettijohn *et al.* 1982). This study revealed that the accessibility of HSV-1 DNA increased following HSV-1 DNA replication, such that HSV-1 DNA became more accessible than DNA in most cellular chromatin. Furthermore, the accessibility of HSV-1 DNA resembled more that of non-nucleosomal DNA rather than that of standard chromatinized DNA, again suggesting that intranuclear HSV-1 DNA was mostly non-nucleosomal.

The lack of a role for chromatin in the regulation of HSV-1 gene expression during lytic infection was further supported by several reports showing that infecting HSV-1 genomes localized to nuclear domains adjacent to ND10s, domains which are devoid of cellular chromatin or histones (Ascoli and Maul 1991; Ishov and Maul 1996; Maul, Ishov et al. 1996). Also, HSV-1 replication compartments at late times post infection are partially depleted of histones (K.L. Conn PhD Thesis, University of Alberta 2010, Monier, Armas et al. 2000; Simpson-Holley, Colgrove et al. 2005).

For the 25 years following its initial characterization, HSV-1 DNA was therefore widely accepted to be nucleosome-free during lytic infections. More recently, however, ChIP assays have demonstrated that histones associate with HSV-1 DNA during lytic infections. These results have thus prompted a re-evaluation of the classic model (Herrera and Triezenberg 2004; Kent, Zeng et al. 2004; Huang, Kent et al. 2006; Narayanan, Ruyechan et al. 2007; Knipe and Cliffe 2008; Oh and Fraser 2008; Ferenczy and Deluca 2009; Kutluay, DeVos et al. 2009; Kutluay and Triezenberg 2009; Liang, Vogel et al. 2009; Placek, Huang et al. 2009).

Such ChIP assays have shown that histone H3 (Herrera and Triezenberg 2004; Kent, Zeng et al. 2004; Huang, Kent et al. 2006; Cliffe and Knipe 2008), as well as the other core histones H2A, H2B, and H4 (Kutluay and Triezenberg 2009), associate with HSV-1 DNA during lytic infections. These results are consistent with the presence of nucleosomes on the genomes of other herpesviruses, such as HCMV, EBV, and KSHV (Radkov, Touitou et al. 1999;

Chang and Liu 2000; Jenkins, Binne et al. 2000; Alazard, Gruffat et al. 2003; Deng, Chen et al. 2003; Knight, Lan et al. 2003; Lu, Zhou et al. 2003; Chau, Zhang et al. 2006; Day, Chau et al. 2007; Nitzsche, Paulus et al. 2008).

The activation domain of VP16 acts to recruit chromatin modifying proteins such as histone acetyl transferases, CBP (KAT3A) and P300 (KAT3B), as well as the ATP-dependent chromatin remodelers, Brg-1 and BRM, to HSV-1 IE promoters. However, all of these proteins were later shown to be dispensable for HSV-1 gene expression (Herrera and Triezenberg 2004; Kutluay, DeVos et al. 2009).

HCF-1 also acts to recruit both KMTs (Set1 and MLL) and KDM (LSD1) to IE promoters (Wysocka, Myers et al. 2003; Narayanan, Ruyechan et al. 2007; Liang, Vogel et al. 2009). This recruitment results in the accumulation of active (H3K4me3) chromatin marks and subsequent loss of repressive ones (H3K9me3) (Huang, Kent et al. 2006; Narayanan, Ruyechan et al. 2007). More recently, HCF-1-dependent recruitment of the KDM LSD1 was shown to be required for efficient IE gene expression (Liang, Vogel et al. 2009).

Considering these associations of histones and chromatin modifying proteins with HSV-1 DNA, most current models propose that chromatin regulates HSV-1 transcription in lytically infected cells. However, only a small percentage of HSV-1 DNA was found to consistently co-immunoprecipitate with histones in all (Herrera and Triezenberg 2004; Kent, Zeng et al. 2004; Huang, Kent et al. 2006; Kutluay, Doroghazi et al. 2008; Kutluay, DeVos et al. 2009; Kutluay and Triezenberg 2009; Placek, Huang et al. 2009) except one (Cliffe and Knipe 2008)

published paper, or to be protected from MCN in sizes corresponding to nucleosome DNA (Leinbach and Summers 1980; Muggeridge and Fraser 1986; Deshmane and Fraser 1989). It therefore remained unclear how histone association of only a small percentage of HSV-1 DNA could regulate HSV-1 transcription globally. Furthermore, the complexes containing histones and HSV-1 DNA remained uncharacterized. The objective of my doctoral thesis was therefore to evaluate the HSV-1 DNA containing complexes in lytically infected cells. Differing from all previous work, however, I used classical chromatin purification techniques. This approach led to most unexpected findings.

7.2. HSV-1 DNA is in complexes with the properties of unstable nucleosomes

For the initial characterization, I selected a single time point in the lytic cycle, 5hpi. At this time, all kinetic classes of HSV-1 genes are transcribed, HSV-1 DNA is replicated, and histones interact with HSV-1 DNA (Herrera and Triezenberg 2004; Kent, Zeng et al. 2004; Cliffe and Knipe 2008; Kutluay, DeVos et al. 2009; Kutluay and Triezenberg 2009; Placek, Huang et al. 2009).

Most current models propose that only a minor percentage of HSV-1 DNA is associated with histones. Therefore, they also predict that most HSV-1 DNA should fractionate as protein-free DNA. However, only 28% of detected nuclear HSV-1 DNA fractionated as such (Fig 3.1), indicating that the majority of nuclear HSV-1 DNA is in some sort of complex. Further analyses of these complexes after partial MCN digestion revealed that they fractionate as cellular mono- to dinucleosomes by differential centrifugation followed by sucrose gradients and then

size exclusion chromatography. However, these complexes differ from most cellular nucleosomes in three major aspects. First, the HSV-1 DNA in these complexes is far more accessible to MCN than DNA in most cellular chromatin (Fig 3.3, 3.8, 3.9) (Moultet, Guetard et al. 1979; Leinbach and Summers 1980; Sinden, Pettijohn et al. 1982; Muggeridge and Fraser 1986). Second, the interactions between the HSV-1 DNA complexes or between these complexes and cellular poly-nucleosomes are more unstable than the interactions between or within cellular nucleosomes (Figs 3.5 and 3.8). Such instability leads to the prompt dissociation of the HSV-1 DNA-containing complexes released into the soluble chromatin, allowing MCN access to the DNA within them, which is thus degraded. If digestion of the soluble fraction was prevented, however, then the unstable digestion intermediates were obvious (Fig 3.8). Third, the unstable HSV-1 DNA-containing complexes could be only partially stabilized from MCN redigestion by crosslinking. These unstable HSV-1 complexes are as unstable as the most unstable cellular nucleosomes (Fig 3.9).

The instability of the HSV-1 DNA containing complexes could be the result of weak HSV-1 DNA-protein or weak protein-protein interactions. Particularly unstable cellular nucleosomes have been characterized (Henikoff 2008). Jin *et al.* showed that such unstable cellular nucleosomes required crosslinking for stabilization (Jin and Felsenfeld 2007; Jin, Zang et al. 2009), similar to the unstable HSV-1 nucleosome-like complexes I characterize here (Fig 3.9). Instability within the cellular nucleosomes was attributed to the presence of histone variants such as H3.3. H3.3 is the H3 variant synthesized in G1, S, G2,

and G0 (Wu, Tsai et al. 1982) and assembled into nucleosomes via replication-independent pathways (Tagami, Ray-Gallet et al. 2004). H3.3 would therefore be the most likely H3 variant available to be assembled in nucleosomes with infecting HSV-1 genomes. Consistently, Berger *et al.* have shown by ChIP that H3.3 associates with infecting HSV-1 DNA (Placek, Huang et al. 2009). The association was observed from as early as 1hpi to as late as 10hpi (Placek, Huang et al. 2009). In contrast, association between HSV-1 DNA and the canonical H3 variant, H3.1, was not observed until 6hpi and was dependent on HSV-1 DNA replication (Placek, Huang et al. 2009), consistent with the normal replication-coupled deposition of H3.1 (Tagami, Ray-Gallet et al. 2004). Results from our lab show that the available pool of free H3.3 increases during HSV-1 infection (K.L. Conn PhD Thesis, University of Alberta 2010), suggesting a potential source of H3.3 available for its incorporation into unstable nucleosome-like complexes containing HSV-1 DNA.

The proposed unstable nucleosome-like complexes are consistent with the heterogeneously sized HSV-1 DNA fragments released by MCN digestion, which we and many others have observed (Fig 3.3 and refs. Leinbach and Summers 1980; Muggeridge and Fraser 1986; Lentine and Bachenheimer 1990; Kent, Zeng et al. 2004). HSV-1 DNA in unstable complexes would still remain randomly accessible to MCN. Such unstable complexes would by definition be dynamic, and therefore not expected to be tightly confined to 160bp of DNA. They would be expected to quickly change positions, by either unbinding and rebinding to, or by sliding through, the HSV-1 DNA. In contrast to DNA in most cellular

chromatin, therefore, MCN cleavage of HSV DNA would not be restricted by distinctly exposed (linker) or protected (core) sites.

If HSV-1 DNA was indeed in unstable nucleosomes, then histones must continuously bind and unbind to HSV-1 DNA and consequently should be mobilized in infected cells. Consistently, linker (Conn, Hendzel et al. 2008) and core (K.L. Conn PhD Thesis, University of Alberta 2010) histones are mobilized in infected cells at 4 and 7 hpi.

Our proposed model is also consistent with the otherwise intriguing distribution of the sizes of HSV-1 DNA fragments released by standard MCN digestions (Fig 3.3 and refs. Leinbach and Summers 1980; Muggeridge and Fraser 1986; Kent, Zeng et al. 2004). Besides the heterogeneously-sized fragments, only mono-, di-, and occasionally, tri- nucleosome-sized DNA fragments are visible, whereas tetra-, penta- or other poly-nucleosomes sized DNA are not. Each of the unstable nucleosome-like complexes has an equal and independent probability of dissociating in any given period. Therefore, the probability of detecting several adjacent complexes still together at any given time decreases exponentially. If each complex has a 75% chance of disassembling in a given period, for example, then the relative abundance of mono-, di-, tri-, and tetra- nucleosome-like complexes at any given digestion time would be 1:0.25:0.06:0.01, respectively, making the detection of tetra- or longer poly-nucleosome size DNA extremely difficult. Further consistent with the proposed model, the poly-nucleosome-sized HSV-1 DNA is obvious when the degradation of the unstable digestion intermediates is prevented by the modified MCN digestion protocol.

With only one exception (Cliffe and Knipe 2008), ChIP assays consistently show that a low and variable percentage of HSV-1, in comparison to cellular DNA, co-immunoprecipitates with histones (Herrera and Triezenberg 2004; Kent, Zeng et al. 2004; Huang, Kent et al. 2006; Kutluay, Doroghazi et al. 2008; Kutluay, DeVos et al. 2009; Kutluay and Triezenberg 2009; Placek, Huang et al. 2009). This low percentage has often been interpreted as low histone occupancy (Kutluay and Triezenberg 2009). However, the proposed unstable HSV-1 nucleosomes are also entirely consistent with such low percentages. Interactions between HSV-1 DNA and histones in unstable nucleosomes are transient by definition. Histones in unstable complexes therefore spend less of the time within crosslinking distance from DNA. At any given time, the probability of a given number of histones being crosslinked to DNA is lower, resulting in a low percentage of HSV-1 DNA co-immunoprecipitating with them (Jin, Zang et al. 2009). Jin *et al.* recently characterized highly unstable cellular nucleosomes (Jin and Felsenfeld 2007; Jin, Zang et al. 2009). Under standard conditions, histone variants H2A.Z and H3.3 could not be detected within the same nucleosomes by ChIP. When the interactions within these complexes were stabilized by crosslinking, however, then the nucleosomes containing both variants were easily detected (Jin, Zang et al. 2009).

ChIP results also show that although the occupancy appears to be low, the coverage throughout the entire HSV-1 genome appears to be relatively even (Herrera and Triezenberg 2004; Kent, Zeng et al. 2004; Cliffe and Knipe 2008; Kutluay and Triezenberg 2009; Placek, Huang et al. 2009). The most common

interpretation is that histones bind randomly through the entire HSV-1 genomes at low occupancy. However, it remained unclear how the association of histones with only a minority of HSV-1 DNA could regulate HSV-1 transcription globally. Through the modification of the MCN digestion protocol, however, I have quantitatively “trapped” most HSV-1 DNA in poly-nucleosome-like complexes, consistent with more or less regularly spaced nucleosomes (Fig 3.8). These results suggest that the entire HSV-1 genomes may instead be “regularly chromatinized”, albeit in unstable nucleosomes.

7.3. HSV-1 DNA is in unstable nucleosomes throughout the lytic replicative cycle

Most HSV-1 DNA in lytically infected cells is at 5hpi in complexes with the biophysical properties of highly unstable nucleosomes. However, it remained unknown whether HSV-1 DNA was in unstable nucleosomes at other times. My next objective was therefore to evaluate whether HSV-1 DNA was in such nucleosome-like complexes at other times during lytic infection. Using the serial MCN digestion, I showed that HSV-1 DNA was in nucleosome-like complexes throughout HSV-1 infection (Fig 4.2). The instability of the complexes isolated at 2, 7, and 9hpi however, was not directly evaluated as it was for 5hpi (by crosslinking and MCN redigestion, for example). However, the fact that HSV-1 DNA could be trapped in nucleosomes-like complexes only after serial MCN digestion is highly suggestive that these complexes are also unstable.

Standard MCN digestions revealed that HSV-1 DNA was 3.6-fold less accessible than at 2hpi than at 5hpi (Fig 4.1). Consistently, at 2hpi HSV-1 DNA was in larger, heavier, polynucleosome-like complexes than at 5hpi, as evaluated by serial MCN digestion (Fig 4.2). Most striking, however, was the differential accessibility of HSV-1 IE and L loci DNA. At 2hpi, HSV-1 IE, but not L, loci DNA was released in soluble chromatin, whereas at 5hpi both IE and L loci DNA were detectable to similar levels (Fig 4.2). Interestingly, this time coincides with the transition from transcription of IE, E, but not L genes (2hpi), to transcription of IE, E, and L genes, and the start of DNA replication (5hpi). Together these results suggested a relationship between HSV-1 transcription (or DNA replication) and accessibility of HSV-1 DNA to MCN. These results are also consistent with Leinbach *et al.*, who found that infecting (or parental) HSV-1 DNA was less accessible to MCN than replicated (progeny) HSV-1 DNA (Leinbach and Summers 1980).

Interestingly, Nitzsche *et al.* have recently evaluated the dynamics of histone and nucleosome occupancy on HCMV DNA during lytic infection using a time course MCN digestion (Nitzsche, Paulus et al. 2008). Consistent with the results presented herein, as well as with standard MCN digestions performed over the years (Leinbach and Summers 1980; Muggeridge and Fraser 1986; Deshmane and Fraser 1989), a percentage of HCMV DNA was protected to nucleosome size (Nitzsche, Paulus et al. 2008). This ranges from a very minor percentage at 2hpi to a far more substantial percentage at later times (48 and 96hpi). Importantly, the HCMV DNA digested to nucleosome size could only be detected as fragments

ranging from mono- to di- nucleosome in size. This suggests that during lytic infection, like HSV-1 DNA, HCMV DNA is most likely in unstable nucleosome-like complexes. The probability of detecting larger tri- and tetra- nucleosomes is therefore very low. Nitzche *et al.* also observed an increase in the accessibility of HCMV DNA as the infection progresses, very much like the data presented in Fig 4.1. Also consistent with the results presented in Fig 4.1, the majority of HCMV DNA was poorly accessible to MCN at early times post infection.

7.4. A percentage of nuclear HSV-1 DNA is poorly accessible to MCN

Both HSV-1 and HCMV DNA have populations that are poorly accessible to MCN. The poorly accessible HSV-1 DNA observed following standard MCN digestion is typically referred to as “resistant” HSV-1 DNA which is interpreted as encapsidated HSV-1 DNA (Leinbach and Summers 1980; Muggeridge and Fraser 1986; Deshmane and Fraser 1989; Nitzsche, Paulus et al. 2008). However, five lines of evidence suggest that most of the “resistant” HSV-1 DNA is not encapsidated. First, so-called “encapsidated” HSV-1 DNA is observed throughout HSV-1 infection, even at 5hpi (at a multiplicity of infection of 5PFU per cell) when most HSV-1 DNA is in replication intermediates and therefore decapsidated (Jacob and Roizman 1977). Second, the HSV-1 DNA that fractionates to the insoluble fraction after BamHI digestion is partially digested by BamHI (Fig 3.1, HSV-Nuclear, Insoluble). Therefore, the HSV-1 DNA in this fraction is still accessible to BamHI. Likewise, the HSV-1 DNA in the insoluble fraction after MCN digestion is also partially digested to heterogeneously sized

fragments (Fig 3.2, HSV-Insoluble). Third, the HSV-1 DNA migrating as a “resistant” band at the top of the agarose gel after standard MCN digestion is eventually digested by MCN, albeit to varying degrees dependent on the concentration of MCN (Fig 3.3, 4.1, 4.3, and 5.7). Fourth, in conditions under which HSV-1 is poorly accessible to MCN (Fig 4.1-2hpi, Fig 4.3-PAA, CHX, and Rosco), serial MCN digestions clearly show that HSV-1 DNA is in polynucleosome-like complexes (Fig 4.2 and 4.4). Finally, “resistant” HSV-1 DNA is most prominent following standard MCN digestion of nuclei from cells treated with PAA, CHX, or Rosco. In the presence of each of these drugs, all of the HSV-1 DNA detected following standard MCN digestion resolves as a “resistant” band at the top of the agarose gel. However, these drugs all inhibit different stages of HSV-1 replication. In fact, HSV-1 transcription is ongoing in both the presence of PAA (IE and E genes) and CHX (IE genes). Therefore, the MCN-resistant HSV-1 DNA is not likely encapsidated, but nonetheless less accessible to MCN.

7.5. The accessibility of lytic HSV-1 DNA depends on the transcriptional activation state

I next evaluated the relationship between the accessibility of HSV-1 DNA and transcription (or DNA replication), using PAA, CHX, and Rosco, which inhibit different stages of HSV-1 transcription. All three inhibitors largely decreased the accessibility of HSV-1 DNA (Fig 4.3 and 4.4). Interestingly, the extent to which they inhibited accessibility appeared to correlate with the extent to which they

inhibited HSV-1 transcription (Fig 4.3 and 4.4). For example, HSV-1 IE DNA was 2.5- and 1.5-fold less accessible in the presence of Rosco than in the presence of CHX or PAA, respectively. When evaluating HSV-1 L DNA, the decrease in accessibility increased to 4- and 2.5-fold, respectively. Consistently, Rosco also has the greatest effect on HSV-1 transcription. It inhibits the accumulation of HSV-1 IE, E, and L transcripts, as well as DNA replication (Schang, Rosenberg et al. 1999; Schang, Rosenberg et al. 2000). Taken together, these results suggest that accessibility of HSV-1 DNA may regulate transcription. Alternatively, changes in HSV-1 DNA accessibility may be a consequence of transcription.

7.6. The effects of Rosco on transcription and MCN accessibility are specific for extrachromosomal DNA

Consistent with a model in which Rosco inhibits transcription by decreasing access to HSV-1 DNA, I showed that Rosco prevents activation of, but does not inhibit ongoing, HSV-1 transcription (Fig 5.1). Furthermore, the effects were promoter-independent. Rosco prevented activation of transcription from otherwise unrelated HSV-1 IE and E promoters in the presence of their respective transcriptional activators (Fig. 5.1 and 5.6). Therefore, the functions targeted by Rosco participate in the activation of IE gene transcription by cellular proteins and HSV-1 structural proteins, as well as in the regulation of E gene transcription by HSV-1 IE proteins. In contrast, Rosco did not inhibit either the activation or the ongoing cellular transcription suggesting, that its effects were specific for the HSV-1 genome.

The genome-specific effects of Rosco were further evaluated using a recombinant cell line containing a reporter gene in which the ICP0 promoter drives the expression of RFP. In collaboration with Dr. Diwan, we showed that Rosco only inhibited transcription driven by the ICP0 promoter when in the context of extrachromosomal DNA. For example, Rosco strongly inhibited transcription driven by the ICP0 promoter in both the context of the native HSV-1 genome (Fig 5.5) and transiently transfected plasmid DNA (Fig 5.6). In both cases, the promoter and reporter gene were present as extrachromosomal DNA. In contrast, Rosco no longer inhibited transcription when the reporter gene driven by the ICP0 promoter was recombined into the cellular genome (Fig 5.5 and 5.6). Therefore, the effects of Rosco are genome-specific and promoter-independent.

Previous studies have shown that many promoters recombined into the HSV-1 genome are regulated as HSV-1 E promoters (in that they require activation by HSV-1 IE proteins) (Smiley, Smibert et al. 1987; Smibert and Smiley 1990). In contrast, HSV-1 promoters are typically regulated by similar mechanisms in HSV-1 or cellular genomes. For example, a variety of HSV-1 IE and E promoters recombined in a variety of cell lines still require activation by HSV-1 proteins (for examples, see Orberg and Schaffer 1987; Pasick and Smiley 1988). In fact, most early studies on the regulation of HSV-1 promoters were performed using HSV-1 promoters recombined in cellular genomes (for examples, see Mackem and Roizman 1982; Batterson and Roizman 1983). My results demonstrated that the transactivation of a given HSV-1 IE promoter requires different factors depending on whether the promoter is in its natural

location in the HSV-1 genome or recombined in the cellular genome. These results were therefore quite surprising. However, I was not the first to describe such a phenomenon. Nicholl *et al.* had previously shown that α -IFN treatment had similar genome-specific and promoter-independent effects. Similar to the effects of Rosco, α -IFN efficiently inhibited transcription driven by the ICP0 promoter in the context HSV-1 genome, but not by ICP0 promoters recombined in the genome (Nicholl and Preston 1996). In addition, Nicholl *et al.* also observed that α -interferon inhibited a heterologous promoter that was not responsive to the same cellular and HSV-1 structural proteins as when in the HSV-1 genome (Nicholl and Preston 1996).

Interestingly, one of the two most characterized functions of α -IFN is induction of cell-cycle arrest, resulting from an indirect inhibition of CDK activities. Two of the CDK activities inhibited by α -IFN are CDK1 and CDK2 (Bybee and Thomas 1992; Satomoto, Haisa et al. 1995; Sangfelt, Erickson et al. 1997; Mandal, Bandyopadhyay et al. 1998), which are also among the CDKs that are the most sensitive to inhibition by Rosco (Appendix 1, recently reviewed in Schang, St Vincent et al. 2006). The coincidences in the effects of Rosco and α -IFN and the genome-specific effects on transcription and MCN accessibility suggest that CDKs may be required to maintain extrachromosomal DNA in a transcriptionally active state.

7.7. The proposed mechanism for the role of chromatin in the regulation of HSV-1 gene expression during lytic infections

To summarize, one could envision a model in which incoming foreign DNA, whether extrachromosomal viral genomes (such as HSV-1) or plasmids (from transient transfections) is met by silencing efforts by the host cell. In the case of HSV-1, these silencing events would most likely involve an effort to chromatinize the infecting HSV-1 DNA (Fig. 7.1 A).

However, the poorly accessible nature of infecting (parental) HSV-1 genomes also suggests another possibility. Infecting HSV-1 DNA may remain complexed with the polyamines with which it was packaged in the capsid. HSV-1 DNA would then require histones to replace the polyamines, to enable the genomes to enter the replicative cycle. Such a model would be somewhat analogous to fertilization, during which packaging of the sperm DNA in the male pronucleus requires sequential replacement of core histones by small highly basic nuclear proteins called polyamines (Govin, Caron et al. 2004). Upon fertilization, the protamines are then displaced and maternal histones associate with the paternal DNA. The replication-independent H3 variant, H3.3, is required for this process. Interestingly, H3.3 has also been shown to be mobilized during HSV-1 infection (K.L. Conn PhD Thesis, University of Alberta 2010) and to associate with HSV-1 DNA as early as 1hpi (Placek, Huang et al. 2009). Regardless of the mechanisms whereby infecting HSV-1 DNA is maintained in an MCN-resistant state, escape from repression would result in an initial

mobilization of histones at early times post infection. These histones would likely come from the free pool or be mobilized from cellular chromatin.

This HSV-1 chromatin would then be locally de-repressed through the binding of Oct-1 to TAATGARAT sequences in IE promoters and subsequent recruitment of VP16 and HCF-1 (Fig 7.1B). This local de-repression would be mediated through the recruitment of chromatin modifying proteins (for example, LSD1) to modify the chromatin environment, and RNAPII to activate IE transcription (Fig 7.1C). This mechanism potentially prevents the formation of transcriptionally silent heterochromatin on HSV-1 DNA. Such a model is supported by decreased IE transcription, accumulation of histones occupying HSV-1 DNA, and the presence of histones bearing repressive chromatin marks (H3K9me3) in the absence of VP16 or HCF-1 (Kutluay and Triezenberg 2009; Liang, Vogel et al. 2009). However, VP16, KATs, chromatin remodelers, or removal of histones from HSV-1 DNA, have all been shown to be dispensable for IE transcription (Kutluay, DeVos et al. 2009; Kutluay and Triezenberg 2009). Therefore, the exact role histones and chromatin play in regulating HSV-1 IE gene expression still remain unclear.

The IE proteins ICP0 and ICP4 would then mediate a global de-repression of HSV-1 genomes resulting in the activation of E gene transcription (Fig 7.1D). Consistent with such a proposed role in de-repression, ICP0 and ICP4 both interact with chromatin modifying proteins and even disrupt chromatin. For example, ICP0 is an HSV-1 E3 ubiquitin ligase that promotes the degradation of the histone H3 variant CENP A (among many other proteins) (Everett, Earnshaw

et al. 1999; Lomonte, Sullivan et al. 2001; Lomonte and Morency 2007) and causes disruption of histone deacetylase (HDAC) complexes associated with transcriptional repression (Lomonte, Thomas et al. 2004; Gu, Liang et al. 2005; Gu and Roizman 2007). More recently, ICP0 has also been shown to interact with the p300/CBP association factor (PCAF) KAT complex stimulating the acetylation of histones on viral promoters (Li, Cun et al. 2009). In addition, ICP4, together with ICP0 disrupts silencing of cellular genes (Cheung, Panning et al. 1997).

I propose that the final stage of de-repression occurs during DNA replication of the HSV-1 genomes, which occurs after E proteins are expressed (Fig 7.1F). The passage of the replication machinery would de-repress the remainder of the HSV-1 genomes, exposing L gene promoters. Along with template amplification, L gene transcription would then be activated (Fig 7.1G).

One could therefore envision that blocking any of these proposed stages of de-repression, for example by the use of small molecule inhibitors, would prevent access to the HSV-1 promoters resulting in the inhibition of gene expression from HSV-1 genomes.

Future directions

By using a different approach than others, I have uncovered the molecular basis for a large literature of conflicting observations published during the last 20 years. The apparent association of only a small percentage of HSV-1 DNA with histones, the protection of only a small percentage of HSV-1 DNA to nucleosome

size, and the presence of so-called “encapsidated” HSV-1 DNA at 5hpi, are just a few of the observations that were difficult to reconcile based on our previous understanding of the intranuclear complexes formed by HSV-1 DNA during lytic infections. The results I present here as my Doctoral Thesis provide a potential explanation for these observations. Mainly, HSV-1 DNA is in complexes with the biophysical properties of unstable nucleosomes throughout lytic infections. However, this work is only the beginning of the characterization of the intranuclear HSV-1 DNA complexes during lytic infection. One of the first pressing questions concerns the nature of these unstable HSV-1 nucleosomes. This question can now be directly evaluated using the modified MCN digestion protocol described herein. Although the MCN digestion releases both cellular and HSV-1 DNA-containing complexes, the unstable nature of the HSV-1 complexes allows for their enrichment under conditions of limited digestions. Such enriched fractions are then amenable to further characterization, such as proteomic and structural analyses. Such studies could likewise be extended to the characterization of the poorly accessible population of HSV-1 DNA.

In addition, the relationship between DNA accessibility and transcription activation state described in Chapter 4 and 5 requires further examination. In collaboration with Dr. Stephanie Booth and Anna Majer at the University of Winnipeg, Canada, we are evaluating the HSV-1 DNA released as soluble chromatin in the presence of various HSV-1 replicative cycle inhibitors using an HSV-1 DNA microarray. By comparing the accessibility of the DNA of specific

HSV-1 genes released under different activation states we hope to further test our model of de-repression outline in Figure 7.1.

Finally, the observations that the effects of Rosco on accessibility and transcription are independent of promoter sequence and specific to extrachromosomal DNA are very intriguing. This observation implies that HSV-1 DNA is subject to a silencing mechanism that prevents transcription by decreasing DNA accessibility. Such mechanisms may globally regulate extrachromosomal DNA. Future studies should therefore be directed to identify the direct or indirect target of CDKs involved in the establishment of such a repressive state.

References

- Alazard, N., H. Gruffat, et al. (2003). "Differential hyperacetylation of histones H3 and H4 upon promoter-specific recruitment of EBNA2 in Epstein-Barr virus chromatin." *J Virol* **77**(14): 8166-72.
- Ascoli, C. A. and G. G. Maul (1991). "Identification of a novel nuclear domain." *J Cell Biol* **112**(5): 785-95.
- Batterson, W. and B. Roizman (1983). "Characterization of the herpes simplex virion-associated factor responsible for the induction of alpha genes." *J Virol* **46**(2): 371-377.
- Bybee, A. and N. S. Thomas (1992). "The synthesis of p58cyclin A and the phosphorylation of p34cdc2 are inhibited in human lymphoid cells arrested in G1 by alpha-interferon." *Biochim Biophys Acta* **1137**(1): 73-6.
- Chang, L. K. and S. T. Liu (2000). "Activation of the BRLF1 promoter and lytic cycle of Epstein-Barr virus by histone acetylation." *Nucleic Acids Res* **28**(20): 3918-25.
- Chau, C. M., X. Y. Zhang, et al. (2006). "Regulation of Epstein-Barr virus latency type by the chromatin boundary factor CTCF." *J Virol* **80**(12): 5723-32.
- Cheung, P., B. Panning, et al. (1997). "Herpes simplex virus immediate-early proteins ICP0 and ICP4 activate the endogenous human alpha-globin gene in nonerythroid cells." *J Virol* **71**(3): 1784-93.
- Cliffe, A. R. and D. M. Knipe (2008). "Herpes simplex virus ICP0 promotes both histone removal and acetylation on viral DNA during lytic infection." *J Virol* **82**(24): 12030-8.
- Conn, K. L., M. J. Hendzel, et al. (2008). "Linker histones are mobilized during infection with herpes simplex virus type 1." *J Virol* **82**(17): 8629-46.
- Day, L., C. M. Chau, et al. (2007). "Chromatin profiling of Epstein-Barr virus latency control region." *J Virol* **81**(12): 6389-401.
- Deng, Z., C. J. Chen, et al. (2003). "The CBP bromodomain and nucleosome targeting are required for Zta-directed nucleosome acetylation and transcription activation." *Mol Cell Biol* **23**(8): 2633-44.
- Deshmane, S. L. and N. W. Fraser (1989). "During latency, herpes simplex virus type 1 DNA is associated with nucleosomes in a chromatin structure." *J Virol* **63**(2): 943-7.
- Everett, R. D., W. C. Earnshaw, et al. (1999). "Specific destruction of kinetochore protein CENP-C and disruption of cell division by herpes simplex virus immediate-early protein Vmw110." *Embo J* **18**(6): 1526-38.
- Ferenczy, M. W. and N. A. Deluca (2009). "Epigenetic Modulation of Gene Expression from Quiescent Hsv Genomes." *J Virol*.
- Govin, J., C. Caron, et al. (2004). "The role of histones in chromatin remodelling during mammalian spermiogenesis." *Eur J Biochem* **271**(17): 3459-69.
- Gu, H., Y. Liang, et al. (2005). "Components of the REST/CoREST/histone deacetylase repressor complex are disrupted, modified, and translocated in HSV-1-infected cells." *Proc Natl Acad Sci U S A* **102**(21): 7571-6.

- Gu, H. and B. Roizman (2007). "Herpes simplex virus-infected cell protein 0 blocks the silencing of viral DNA by dissociating histone deacetylases from the CoREST-REST complex." Proc Natl Acad Sci U S A **104**(43): 17134-9.
- Henikoff, S. (2008). "Nucleosome destabilization in the epigenetic regulation of gene expression." Nat Rev Genet **9**(1): 15-26.
- Herrera, F. J. and S. J. Triezenberg (2004). "VP16-dependent association of chromatin-modifying coactivators and underrepresentation of histones at immediate-early gene promoters during herpes simplex virus infection." J Virol **78**(18): 9689-96.
- Huang, J., J. R. Kent, et al. (2006). "Trimethylation of histone H3 lysine 4 by Set1 in the lytic infection of human herpes simplex virus 1." J Virol **80**(12): 5740-6.
- Ishov, A. M. and G. G. Maul (1996). "The periphery of nuclear domain 10 (ND10) as site of DNA virus deposition." J Cell Biol **134**(4): 815-26.
- Jacob, R. J. and B. Roizman (1977). "Anatomy of herpes simplex virus DNA VIII. Properties of the replicating DNA." J Virol **23**(2): 394-411.
- Jenkins, P. J., U. K. Binne, et al. (2000). "Histone acetylation and reactivation of Epstein-Barr virus from latency." J Virol **74**(2): 710-20.
- Jin, C. and G. Felsenfeld (2007). "Nucleosome stability mediated by histone variants H3.3 and H2A.Z." Genes Dev **21**(12): 1519-29.
- Jin, C., C. Zang, et al. (2009). "H3.3/H2A.Z double variant-containing nucleosomes mark 'nucleosome-free regions' of active promoters and other regulatory regions." Nat Genet **41**(8): 941-5.
- Kent, J. R., P. Y. Zeng, et al. (2004). "During lytic infection herpes simplex virus type 1 is associated with histones bearing modifications that correlate with active transcription." J Virol **78**(18): 10178-86.
- Knight, J. S., K. Lan, et al. (2003). "Epstein-Barr virus nuclear antigen 3C recruits histone deacetylase activity and associates with the corepressors mSin3A and NCoR in human B-cell lines." J Virol **77**(7): 4261-72.
- Knipe, D. M. and A. Cliffe (2008). "Chromatin control of herpes simplex virus lytic and latent infection." Nat Rev Microbiol **6**(3): 211-21.
- Kutluay, S. B., S. L. DeVos, et al. (2009). "Transcriptional coactivators are not required for herpes simplex virus type 1 immediate-early gene expression in vitro." J Virol **83**(8): 3436-49.
- Kutluay, S. B., J. Doroghazi, et al. (2008). "Curcumin inhibits herpes simplex virus immediate-early gene expression by a mechanism independent of p300/CBP histone acetyltransferase activity." Virology **373**(2): 239-47.
- Kutluay, S. B. and S. J. Triezenberg (2009). "Regulation of histone deposition on the herpes simplex virus type 1 genome during lytic infection." J Virol **83**(11): 5835-45.
- Kutluay, S. B. and S. J. Triezenberg (2009). "Role of chromatin during herpesvirus infections." Biochim Biophys Acta **1790**(6): 456-66.
- Leinbach, S. S. and W. C. Summers (1980). "The structure of herpes simplex virus type 1 DNA as probed by micrococcal nuclease digestion." J Gen Virol **51**(Pt 1): 45-59.

- Lentine, A. F. and S. L. Bachenheimer (1990). "Intracellular organization of herpes simplex virus type 1 DNA assayed by staphylococcal nuclease sensitivity." *Virus Res* **16**(3): 275-92.
- Li, W., W. Cun, et al. (2009). "The transactivating effect of HSV-1 ICP0 is enhanced by its interaction with the PCAF component of histone acetyltransferase." *Arch Virol* **154**(11): 1755-64.
- Liang, Y., J. L. Vogel, et al. (2009). "Inhibition of the histone demethylase LSD1 blocks alpha-herpesvirus lytic replication and reactivation from latency." *Nat Med* **15**(11): 1312-7.
- Lomonte, P. and E. Morency (2007). "Centromeric protein CENP-B proteasomal degradation induced by the viral protein ICP0." *FEBS Lett* **581**(4): 658-62.
- Lomonte, P., K. F. Sullivan, et al. (2001). "Degradation of nucleosome-associated centromeric histone H3-like protein CENP-A induced by herpes simplex virus type 1 protein ICP0." *J Biol Chem* **276**(8): 5829-35.
- Lomonte, P., J. Thomas, et al. (2004). "Functional interaction between class II histone deacetylases and ICP0 of herpes simplex virus type 1." *J Virol* **78**(13): 6744-57.
- Lu, F., J. Zhou, et al. (2003). "Chromatin remodeling of the Kaposi's sarcoma-associated herpesvirus ORF50 promoter correlates with reactivation from latency." *J Virol* **77**(21): 11425-35.
- Mackem, S. and B. Roizman (1982). "Structural features of the herpes simplex virus alpha gene 4, 0, and 27 promoter-regulatory sequences which confer alpha regulation on chimeric thymidine kinase genes." *J Virol* **44**(3): 939-949.
- Mandal, M., D. Bandyopadhyay, et al. (1998). "Interferon-induces expression of cyclin-dependent kinase-inhibitors p21WAF1 and p27Kip1 that prevent activation of cyclin-dependent kinase by CDK-activating kinase (CAK)." *Oncogene* **16**(2): 217-25.
- Maul, G. G., A. M. Ishov, et al. (1996). "Nuclear domain 10 as preexisting potential replication start sites of herpes simplex virus type-1." *Virology* **217**(1): 67-75.
- Monier, K., J. C. Armas, et al. (2000). "Annexation of the interchromosomal space during viral infection." *Nat Cell Biol* **2**(9): 661-5.
- Mouttet, M. E., D. Guetard, et al. (1979). "Random cleavage of intranuclear herpes simplex virus DNA by micrococcal nuclease." *FEBS Lett* **100**(1): 107-9.
- Muggeridge, M. I. and N. W. Fraser (1986). "Chromosomal organization of the herpes simplex virus genome during acute infection of the mouse central nervous system." *J Virol* **59**(3): 764-7.
- Muller, U., C. H. Schroder, et al. (1980). "Coexistence of nucleosomal and various non-nucleosomal chromatin configurations in cells infected with herpes simplex virus." *Eur J Cell Biol* **23**(1): 197-203.
- Narayanan, A., W. T. Ruyechan, et al. (2007). "The coactivator host cell factor-1 mediates Set1 and MLL1 H3K4 trimethylation at herpesvirus immediate

- early promoters for initiation of infection." Proc Natl Acad Sci U S A **104**(26): 10835-40.
- Nicholl, M. J. and C. M. Preston (1996). "Inhibition of herpes simplex virus type 1 immediate-early gene expression by alpha interferon is not VP16 specific." J Virol **70**(9): 6336-9.
- Nitzsche, A., C. Paulus, et al. (2008). "Temporal dynamics of cytomegalovirus chromatin assembly in productively infected human cells." J Virol **82**(22): 11167-80.
- Oh, J. and N. W. Fraser (2008). "Temporal association of the herpes simplex virus genome with histone proteins during a lytic infection." J Virol **82**(7): 3530-7.
- Orberg, P. K. and P. A. Schaffer (1987). "Expression of herpes simplex virus type 1 major DNA-binding protein, ICP8, in transformed cell lines: complementation of deletion mutants and inhibition of wild-type virus." J Virol **61**(4): 1136-1146.
- Pasick, J. M. and J. R. Smiley (1988). "Regulated expression of stably transfected herpes simplex virus thymidine kinase genes in continuous cell lines expressing a temperature-sensitive mutant form of the immediate-early protein ICP4." Virology **162**(2): 490-493.
- Placek, B. J., J. Huang, et al. (2009). "The histone variant H3.3 regulates gene expression during lytic infection with herpes simplex virus type 1." J Virol **83**(3): 1416-21.
- Radkov, S. A., R. Touitou, et al. (1999). "Epstein-Barr virus nuclear antigen 3C interacts with histone deacetylase to repress transcription." J Virol **73**(7): 5688-97.
- Sangfelt, O., S. Erickson, et al. (1997). "Induction of Cip/Kip and Ink4 cyclin dependent kinase inhibitors by interferon-alpha in hematopoietic cell lines." Oncogene **14**(4): 415-23.
- Satomoto, K., M. Haisa, et al. (1995). "Cyclin A and Cdk2 kinase activity are suppressed by combined treatment with tumor necrosis factor-alpha and interferon-alpha." Biochem Biophys Res Commun **213**(3): 1115-21.
- Schang, L. M., A. Rosenberg, et al. (1999). "Transcription of herpes simplex virus immediate-early and early genes is inhibited by roscovitine, an inhibitor specific for cellular cyclin-dependent kinases." J Virol **73**(3): 2161-72.
- Schang, L. M., A. Rosenberg, et al. (2000). "Roscovitine, a specific inhibitor of cellular cyclin-dependent kinases, inhibits herpes simplex virus DNA synthesis in the presence of viral early proteins." J Virol **74**(5): 2107-20.
- Schang, L. M., M. R. St Vincent, et al. (2006). "Five years of progress on cyclin-dependent kinases and other cellular proteins as potential targets for antiviral drugs." Antivir Chem Chemother **17**(6): 293-320.
- Simpson-Holley, M., R. C. Colgrove, et al. (2005). "Identification and functional evaluation of cellular and viral factors involved in the alteration of nuclear architecture during herpes simplex virus 1 infection." J Virol **79**(20): 12840-51.

- Sinden, R. R., D. E. Pettijohn, et al. (1982). "Organization of herpes simplex virus type 1 deoxyribonucleic acid during replication probed in living cells with 4,5',8-trimethylpsoralen." Biochemistry **21**(18): 4484-90.
- Smibert, C. A. and J. R. Smiley (1990). "Differential regulation of endogenous and transduced beta-globin genes during infection of erythroid cells with a herpes simplex virus type 1 recombinant." Journal of Virology **64**(8): 3882-3894.
- Smiley, J. R., C. Smibert, et al. (1987). "Expression of a cellular gene cloned in herpes simplex virus: rabbit beta-globin is regulated as an early viral gene in infected fibroblasts." Journal of Virology **61**(8): 2368-2377.
- Tagami, H., D. Ray-Gallet, et al. (2004). "Histone H3.1 and H3.3 complexes mediate nucleosome assembly pathways dependent or independent of DNA synthesis." Cell **116**(1): 51-61.
- Wu, R. S., S. Tsai, et al. (1982). "Patterns of histone variant synthesis can distinguish G0 from G1 cells." Cell **31**(2 Pt 1): 367-74.
- Wysocka, J., M. P. Myers, et al. (2003). "Human Sin3 deacetylase and trithorax-related Set1/Ash2 histone H3-K4 methyltransferase are tethered together selectively by the cell-proliferation factor HCF-1." Genes Dev **17**(7): 896-911.

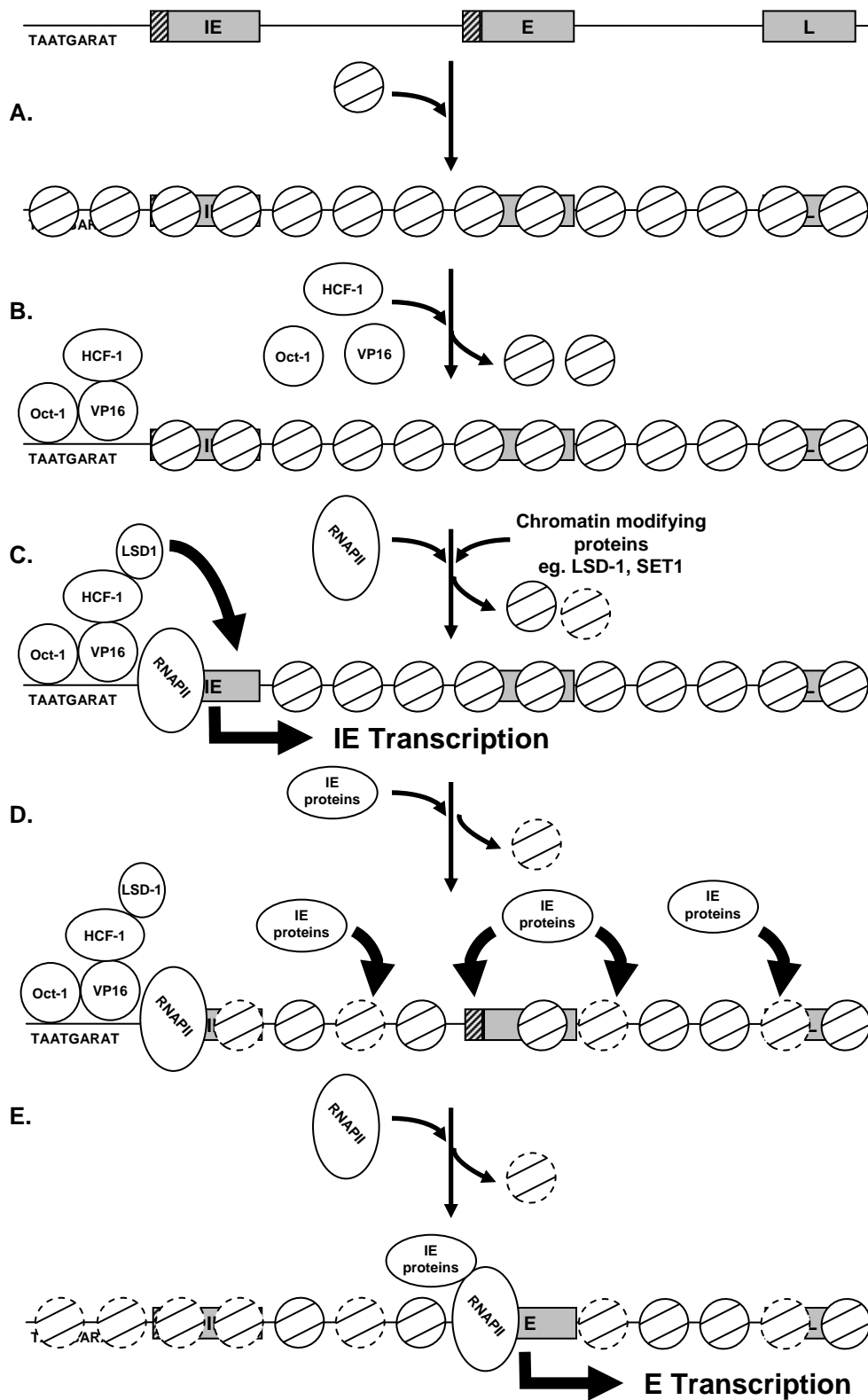


Figure 7.1. Model for the role of chromatin in the regulation of HSV-1 gene expression during lytic infections. See discussion for a description

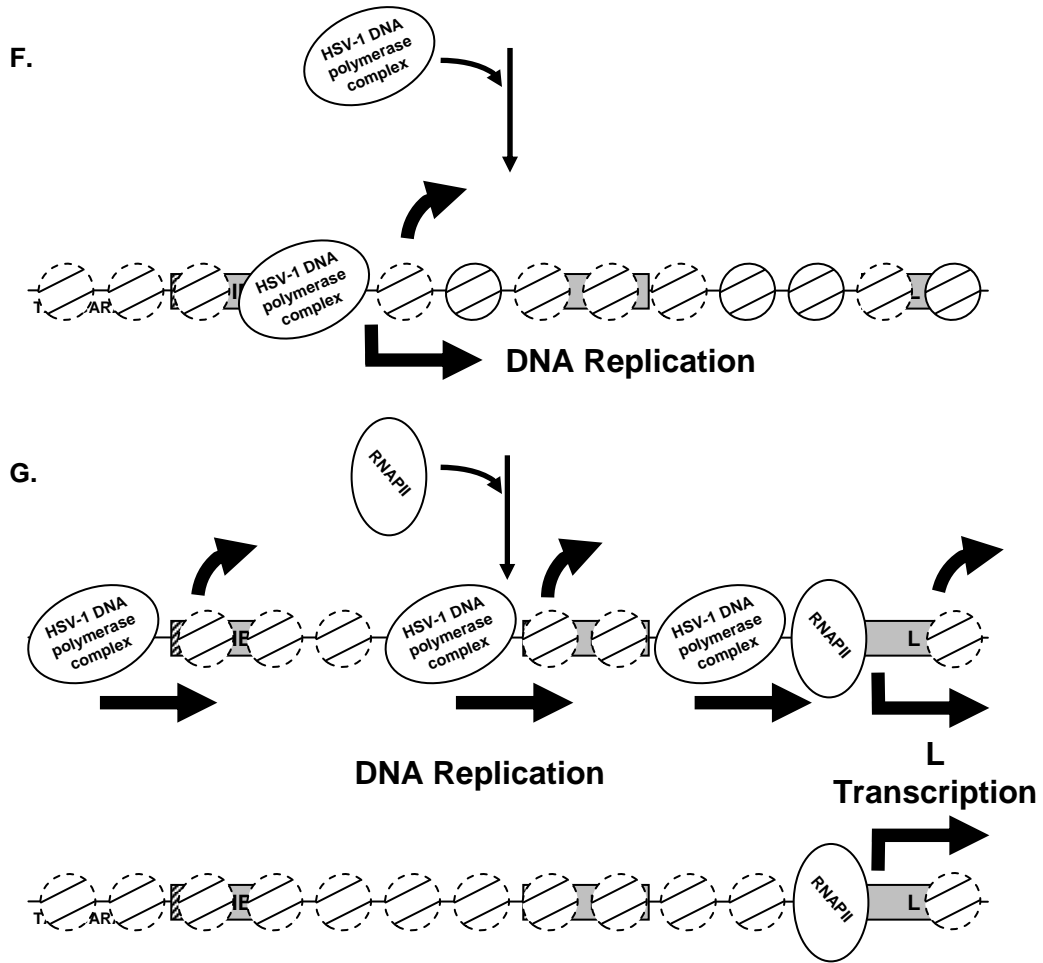


Figure 7.1. (continued) Model for the role of chromatin in the regulation of HSV-1 gene expression during lytic infections. See discussion for a description

APPENDICES

Appendix 1. Specificity profile of selected oligo- or pan-specific PCIs.

Appendix 1 is a modified version of Table 4 (Schang, St Vincent et al. 2006).

The activity or binding of two oligo-specific pharmacological cyclin-dependent kinase inhibitors (PCIs; Rosco, Purv A) and one pan-specific PCI (Flav) against all human protein kinases, several non-human protein kinases, and other selected enzymes or biomolecules are presented. The activities against each protein are presented as 50% inhibition concentrations (IC_{50} , in μM), degree of inhibition at $10\mu M$ of each drug (as percentage), or relative affinity (as K_d), n/t, not tested.

For roscovitine (Rosco), light gray represents $IC_{50} \geq 7 \mu M$, % inhibition < 80 and $K_d > 7 \mu M$, dark gray shading represents $0.7 \mu M \leq IC_{50} < 3.5 \mu M$, % inhibition ≥ 93 and $0.7 \mu M \leq K_d < 3.5 \mu M$, and bold and italicized figures represent $3.5 \mu M \leq IC_{50} < 7 \mu M$, $80 \leq \% \text{ inhibition} < 93$ and $3.5 \mu M \leq K_d < 7 \mu M$. For purvalanol A (Purv A), light grey represents $IC_{50} \geq 0.7 \mu M$ and % inhibition < 80 , dark grey represents $0.07 \mu M \leq IC_{50} < 0.35 \mu M$ and % inhibition ≥ 93 , and bold and italicized figures represent $0.35 \mu M \leq IC_{50} < 0.7 \mu M$ and $80 \leq \% \text{ inhibition} < 93$. For flavopiridol (Flav), light gray represents $IC_{50} > 1 \mu M$ and $K_d > 1 \mu M$, dark gray shading represents $0.1 \mu M \leq IC_{50} < 0.5 \mu M$ and $0.1 \mu M \leq K_d < 0.5 \mu M$, and bold and italicized figures represent $0.5 \mu M \leq IC_{50} < 1 \mu M$ and $0.5 \mu M \leq K_d < 1 \mu M$.

a, $250\mu M$ ATP (Kristjansdottir and Rudolph 2003); b, $15\mu M$ ATP (Gray, Wodicka et al. 1998); c, $15\mu M$ ATP (Meijer, Borgne et al. 1997); d, $15\mu M$ ATP (Vesely, Havlicek et al. 1994); e, ProQuinase, as quoted in (Bach, Knockaert et al.

2005); f, 100 μ M ATP (Bain, McLauchlan et al. 2003); g, 15 μ M ATP (Leclerc, Garnier et al. 2001); h, (Knockaert, Gray et al. 2000); i, 15 μ M ATP (Schang, Bantly et al. 2002); j, 15 μ M ATP (Knockaert and Meijer 2002); k, 144 μ M ATP (Wang, de la Fuente et al. 2001); l, 100 μ M ATP (McClue, Blake et al. 2002); m, 50 μ M ATP (Caligiuri, Becker et al. 2005); n, 10 μ M ATP; <http://www.upstate.com/img/pdf/KinaseProfiler.pdf>; o, 375 μ M ATP (Losiewicz, Carlson et al. 1994); p, 10 μ M ATP (Pinhero, Liaw et al. 2004); q, 400 μ M and 20 μ M ATP (CDK2 and CDK4, respectively, Carlson, Dubay et al. 1996); r, http://www.invitrogen.com/downloads/SelectScreen_Data_193.pdf; s, (Whittaker, Walton et al. 2004); t, (Whittaker, Walton et al. 2004; Fabian, Biggs et al. 2005); u, 15 μ M ATP (De Azevedo, Leclerc et al. 1997); v, 15 μ M ATP (Bach, Knockaert et al. 2005); w, 10 μ M ATP (Chao, Fujinaga et al. 2000); x, 15 μ M ATP (Tang, Li et al. 2005); y, 50 μ M ATP (Agbottah, de La Fuente et al. 2005); z, (Senderowicz and Sausville 2000); aa, 10 μ M ATP (Kawaguchi, Kato et al. 2003); ab, 144 μ M ATP (Heredia, Davis et al. 2005); ac, 100 μ M ATP (Zhou, Deng et al. 2004); ad, 1,000 μ M ATP (Kaiser, Nishi et al. 2001; Zhou, Deng et al. 2004); ae, (Oikonomakos, Schnier et al. 2000); af, (Schnier, Kaur et al. 1999); ag, (Hooijberg, Broxterman et al. 1999); ah, (Bible, Bible et al. 2000); ai, 15 μ M ATP (Hoessel, Leclerc et al. 1999); aj, 50 μ M ATP (Xie, Liu et al. 2004); ak, 5-50 μ M ATP (Bain, Plater et al. 2007); al (Karaman, Herrgard et al. 2008).

Definition of symbols and required formatting

\geq ; greater than or equal to, \leq ; lesser than or equal to, $>$; greater than, $<$; lesser than, IC_{50} ; where; IC in normal font, $_{50}$ in subscript

Oligo-specific

Pan-specific

| Group | Family | Kinase | Rosco | | | Purv A | | | Flavo | | |
|-------|--------|----------------------|-----------------------|-----------------------|-------------------------|-----------------------|-------------------------|-------------------------|-----------------------|----------------------------------|----------------------------------|
| | | | IC ₅₀ , μM | Inhibition at 10μM, % | Inhibition at 1μM, % ak | IC ₅₀ , μM | Inhibition at 10μM, % f | Inhibition at 1μM, % ak | IC ₅₀ , μM | K _d , μM ^l | K _d , μM ^l |
| AGC | AKT | AKT1/PKBα | >100 e | 2 r | <20 | nt | >10 | nt | >10 | nt | >10 |
| | | AKT2/PKBβ | >100 e | 0 r | <20 | nt | >10 | nt | >10 | nt | >10 |
| | | AKT3/PKBγ | >100 e | 0 r | nt | nt | >10 | nt | >10 | nt | >10 |
| DMPK | DMPK | DMPK2 | nt | nt | nt | nt | >10 | nt | >10 | nt | 0.65 |
| | | MRCka | nt | nt | nt | nt | >10 | nt | >10 | nt | 9.5 |
| | | MRCkb | nt | nt | nt | nt | >10 | nt | >10 | nt | 3.3 |
| | | ROCK2 | nt | <20 f | <20 | nt | nt | <20 | nt | nt | nt |
| | | ROCK1 | nt | 0 r | nt | nt | nt | nt | nt | nt | nt |
| | | CRIK | nt | 0 r | nt | nt | nt | nt | nt | nt | nt |
| | | BARK1, GRK2 | nt | 2 r | nt | nt | nt | nt | nt | nt | nt |
| | | BARK2, GRK3 | nt | 0 r | nt | nt | nt | nt | nt | nt | nt |
| | | GPRK4/GRK4 | nt | 0 r | nt | nt | nt | nt | nt | nt | nt |
| | | GPRK5/GRK5 | nt | 3 r | nt | nt | nt | nt | nt | nt | nt |
| MAST | MAST | GPRK6/GRK6 | nt | 6 r | nt | nt | nt | nt | nt | nt | nt |
| | | RHOK | nt | nt | nt | nt | nt | nt | nt | nt | nt |
| | | GPRK7/GRK7 | nt | 14 r | nt | nt | nt | nt | nt | nt | nt |
| | | MAST1, MAST2, MAST3, | nt | nt | nt | nt | nt | nt | nt | nt | nt |
| | | NDR1 | nt | nt | nt | nt | nt | nt | nt | nt | nt |
| | | LATS1 | nt | nt | nt | nt | nt | nt | nt | nt | nt |
| | | LATS2 | nt | nt | nt | nt | nt | nt | nt | nt | nt |
| | | NDR2/STK38L | nt | nt | nt | nt | nt | nt | nt | nt | nt |
| | | PKA | >50 ly | nt | 27 | nt | >10 | nt | 21ak | nt | >10 |
| | | PKAαβγ | >1000 c | <20 f | nt | nt | >10 | nt | <20 | nt | >10 |
| PKB | PKB | PKAα/PRKACA | nt | 7 r | nt | nt | >10 | nt | 145 o, 122 z | >10 | |
| | | PKACβ | nt | nt | nt | nt | >10 | nt | nt | >10 | |
| | | PKACγ | nt | nt | nt | nt | >10 | nt | nt | >10 | |
| | | PRKX | nt | 0 r | nt | nt | >10 | nt | nt | >10 | |
| | | PRKY | nt | nt | nt | nt | >10 | nt | nt | >10 | |
| | | PDK1 | nt | <20 f, n, 1 r | 20 | nt | >10 | nt | 21ak | >10 | |
| | | PKCα/PRKCA | >100 c, j | <20 f, n, 0 r | <20 | nt | nt | <20 | 6 o | nt | |
| | | PKCβ1/PRKCB1 | >100 c, j | <20 n, 0 r | nt | nt | >10 b | <20 | nt | nt | |
| | | PKCβ2 | nt | nt | nt | nt | >10 b | nt | nt | nt | |
| | | PKCγ | 100 c, j | <20 n, 15 r | nt | nt | >10 b | nt | nt | nt | |
| PKG | PKG | PKCδ/PRKCD | >1000 c | 3 r | nt | nt | >10 | nt | nt | 0.59 | |
| | | PKCε/PRKCE | >100 c | 0 r | nt | nt | >10 | nt | nt | 0.38 | |
| | | PKCη/PRKH | >100 c | 0 r | nt | nt | >10 | nt | nt | 0.35 | |
| | | PKCζ/PRKCZ | >1000 c | 0 r | <20 | nt | >10 b | nt | nt | nt | |
| | | PKCθ/PRKCQ | nt | 11 r | nt | nt | >10 | nt | nt | nt | |
| | | PKCi | nt | 0 r | nt | nt | >10 | nt | nt | nt | |
| | | PKG1/PRKG1 | >1000 c | 0 r | nt | nt | >10 | nt | nt | nt | |
| | | PKG2/PRKG2 | nt | 8 r | nt | nt | >10 b | nt | nt | nt | |
| | | PKN1/PRK1 | nt | 0 r | nt | nt | >10 | nt | nt | >10 | |
| | | PKN2/PRK2 | nt | <20 n | <20 | nt | >10 | nt | <20ak | nt | |
| RSK | RSK | PKN3/PRK3 | nt | nt | nt | nt | >10 | nt | nt | >10 | |
| | | MSK1/RPS6KA5 | nt | <20 f, 0 r | 22 | >10 | nt | <20ak | nt | 2 | |
| | | | nt | | | | | | | | |

Oligo-specific **Pan-specific**

| Group | Family | Kinase | Rosco | | | Purv A | | | Flavo | | | | |
|-------|--------|-------------------------|---------------|-----------------------------|-------------------------------|----------------------------|--|---------------|-------------------------------|-------------------------------|---------------|---------------------------------------|--|
| | | | IC50, μ M | Inhibition at 10 μ M, % | Inhibition at 1 μ M, % ak | K _d , μ M t | K _d , μ M ^{nl} | IC50, μ M | Inhibition at 10 μ M, % f | Inhibition at 1 μ M, % ak | IC50, μ M | K _d , μ M ^t | K _d , μ M ^{nl} |
| | | MSK2/RPS6KA4 | nt | 0 r | nt | nt | nt | nt | nt | nt | nt | nt | n-ter 1.3; c-ter >10 |
| | | p70S6K/S6K1/RPS6KB1 | 130 h | <20 f.n, 0 r | <20 | nt | nt | <20ak | 21 | <20ak | nt | nt | nt |
| | | p70S6kb | nt | nt | nt | nt | nt | nt | nt | nt | nt | nt | nt |
| | | RSK1/MAPKAP-K1a/RPS6KA1 | nt | 31 f, 22 r | <20 | nt | >10 | 26ak | 85 | 26ak | nt | nt | n-ter 2.3; c-ter 0.72 |
| | | RSK2/MAPKAP-K1b/RPS6KA3 | nt | 14 r | 29 | >10 | >10 | 29ak | nt | 29ak | nt | >10 | >10 |
| | | RSK3/MAPKAP-K1c/RPS6KA2 | nt | 24 r | nt | 3.2 | >10 | nt | nt | nt | nt | 1.6 | n-ter >10; c-ter 1.5 |
| | | RSK4/MAPKAP-K1d/RPS6KA6 | nt | nt | nt | nt | >10 | nt | nt | nt | nt | nt | n-ter >10; c-ter 0.8 |
| | | Sgk494 | nt | nt | nt | nt | nt | nt | nt | nt | nt | nt | nt |
| | RSKL | RSKL1, RSKL2 | nt | nt | nt | nt | nt | nt | nt | nt | nt | nt | nt |
| | SGK | SGK/SGK1 | nt | <20 f, 6 r | 25 | nt | nt | <20ak | <20 | <20ak | nt | nt | nt |
| | | SGK2 | nt | 3 r | nt | nt | nt | nt | nt | nt | nt | nt | nt |
| | | SGK3/SGKL | nt | 4 r | nt | nt | nt | nt | nt | nt | nt | nt | nt |
| | YANK | YANK1 | nt | nt | nt | nt | nt | nt | nt | nt | nt | nt | nt |
| | | YANK2 | nt | nt | nt | nt | >10 | nt | nt | nt | nt | nt | >10 |
| | | YANK3 | nt | nt | nt | nt | >10 | nt | nt | nt | nt | nt | >10 |
| | CAMK1 | CaMK1g | nt | nt | nt | >10 | >10 | nt | nt | nt | nt | nt | >10 |
| | | CaMK1a | nt | nt | <20 | >10 | >10 | <20ak | nt | <20ak | nt | nt | >10 |
| | | CaMK4 | nt | 4 r | nt | nt | >10 | nt | nt | nt | nt | nt | 3.2 |
| | | CaMK1d | nt | 1 r | nt | >10 | >10 | nt | nt | nt | nt | nt | >10 |
| | | CaMK1b | nt | nt | nt | nt | nt | nt | nt | nt | nt | nt | nt |
| | CAMK2 | CaMK2a | 32 h, >10 r | 2 r | nt | >10 | >10 | nt | nt | nt | nt | 1.3 | 1.7 |
| | | CaMK2b | nt | 9 r | nt | >10 | >10 | nt | nt | nt | nt | 2.6 | >10 |
| | | CaMK2y | nt | nt | nt | >10 | >10 | nt | nt | nt | nt | >10 | >10 |
| | | CaMK2b | nt | 9 r | nt | >10 | >10 | nt | nt | nt | nt | >10 | >10 |
| | CAMKL | CaMK2b | nt | <20 f.n | <20 | >10 | >10 | <20ak | 50 | <20ak | nt | 6.6 | >10 |
| | | AMPK α 1 | nt | <20 f.n | <20 | nt | >10 | 50 | 50 | <20ak | nt | nt | >10 |
| | | AMPK α 2 | nt | nt | nt | nt | >10 | nt | nt | nt | nt | nt | nt |
| | | BRSK | nt | nt | nt | nt | nt | nt | nt | nt | nt | nt | nt |
| | | BRSK2 | nt | nt | 21 | nt | nt | 24ak | nt | 24ak | nt | nt | nt |
| | | CHK1/CHEK1 | nt | <20 f.n, 5 r | <20 | nt | >10 | <20ak | 22 | <20ak | nt | nt | >10 |
| | | LKB1 | nt | nt | nt | nt | >10 | <20ak | nt | <20ak | nt | nt | >10 |
| | | HUNK | nt | nt | <20 | nt | >10 | nt | nt | nt | nt | nt | >10 |
| | | MARK1 | nt | nt | nt | >10 | >10 | nt | nt | nt | nt | nt | >10 |
| | | MARK2 | nt | nt | nt | >10 | >10 | nt | nt | nt | nt | nt | >10 |
| | | MARK3 | nt | nt | nt | >10 | >10 | nt | nt | nt | nt | nt | >10 |
| | | MARK4 | nt | nt | nt | >10 | >10 | nt | nt | nt | nt | nt | >10 |
| | | MELK | nt | nt | <20 | nt | >10 | 28ak | nt | 28ak | nt | nt | >10 |
| | | NIM1 | nt | nt | nt | nt | >10 | nt | nt | nt | nt | nt | nt |
| | | Nuak1/ISNARK | nt | nt | nt | nt | >10 | nt | nt | nt | nt | nt | 1.4 |
| | | Nuak2 | nt | nt | nt | nt | >10 | nt | nt | nt | nt | nt | nt |
| | | PASK | nt | 9 r | nt | nt | nt | nt | nt | nt | nt | nt | nt |

Oligo-specific **Pan-specific**

| Group | Family | Kinase | Rosco | | | Purv A | | | Flavo | | | | | |
|---------|---------|---|---------------|--------------------------------|-------------------------------|----------------------------|--|----------------------------|-------------------------------|-------------------------------|----------------------------|---------------------------------------|--|-----|
| | | | IC50, μ M | Inhibition at 10 μ M, % | Inhibition at 1 μ M, % ak | K _d , μ M t | K _d , μ M ^{nl} | IC ₅₀ , μ M | Inhibition at 10 μ M, % f | Inhibition at 1 μ M, % ak | IC ₅₀ , μ M | K _d , μ M ^t | K _d , μ M ^{nl} | |
| CAMK- | CASK | SIK/SNF1LK | nl | nl | nl | nl | >10 | nl | nl | nl | nl | >10 | >10 | |
| | | SIK2/SNF1LK2 | nl | nl | nl | nl | >10 | nl | nl | nl | nl | nl | >10 | |
| | | OSK, QIK, SNRK | nl | nl | nl | nl | nl | nl | nl | nl | nl | nl | nl | nl |
| | | VACAMKL, Sgk495, STK33 | nl | nl | nl | nl | >10 | nl | nl | nl | nl | nl | nl | 1.7 |
| CASK | DAPK | CASK | nl | nl | nl | nl | nl | nl | nl | nl | nl | nl | nl | nl |
| | | DAPK1 | nl | nl | nl | nl | >10 | nl | nl | nl | nl | nl | >10 | |
| | | DAPK2 | nl | nl | nl | nl | >10 | nl | nl | nl | nl | nl | >10 | |
| | | DRAK1/STK17A DRAK2/STK17B DAPK3/ZIPK | nl | nl | nl | nl | >10 | nl | nl | nl | nl | nl | 5.1 | >10 |
| DCAMKL | DCAMKL | DCAMKL1 | nl | nl | nl | nl | >10 | nl | nl | nl | nl | nl | 2.1 | |
| | | DCAMKL2 | nl | nl | nl | nl | >10 | nl | nl | nl | nl | nl | >10 | |
| | | DCAMKL3 | nl | nl | nl | nl | >10 | nl | nl | nl | nl | nl | 1.1 | |
| MAKKAPK | MAKKAPK | MAPKAPK2/IMK2 | nl | <20 f, 2 r | <20 | nl | >10 | nl | <20 | <20ak | nl | nl | >10 | |
| | | MAPKAPK3/3pk MAPKAPK5/PRAK MNK1/IMNK1 | nl | 1 r <20 f, 0 r | <20 | nl | nl | nl | 24 | <20ak | nl | nl | nl | nl |
| MLCK | MLCK | MNK2/IMNK2/GPRK7 smMLCK/IMYLK1 | nl | nl | <20 | nl | >10 | nl | nl | <20ak | nl | 1.9 | >10 | |
| | | caMLCK skMLCK/IMYLK2 | nl | 0 r | nl | nl | >10 | nl | nl | nl | nl | nl | nl | >10 |
| PHK | PHK | Sgk085 | nl | nl | nl | nl | >10 | nl | nl | nl | nl | nl | nl | |
| | | PHKg1 PHKg2 | nl | <20 f, 11 r | <20 | nl | >10 | nl | 64 | <20ak | nl | >10 | 2.2 | |
| PIM | PIM | PIM1 | nl | 0 r | >10 | nl | >10 | nl | nl | nl | nl | 2 | 2.9 | |
| | | PIM2 PIM3 | nl | 25 r 3 r | <20 | nl | >10 | nl | nl | <20ak | nl | 0.52 | 0.56 | |
| PKD | PKD | PKD1/PRKD1 PKD2/PRKD2 | nl | nl | <20 | nl | >10 | nl | nl | <20ak | nl | 0.65 | 0.77 | |
| | | PKD3/PRKCN/PRKD3 PSKH1, PSKH2 | nl | 0 r | <20 | nl | >10 | nl | nl | <20ak | nl | nl | 0.6 | |
| PSK | PSK | CHK2 | nl | nl | <20 | nl | >10 | nl | nl | <20ak | nl | nl | 0.52 | |
| | | Trb1, Trb2, Trb3 Trio, Trad, SPEG, Obscn | nl | 17 r | nl | nl | >10 | nl | nl | nl | nl | nl | 1.1 | |
| RAD53 | TSSK | TSSK1/STK22D TSSK2/STK22B | nl | 40 n, 13 r | <20 | nl | >10 | nl | nl | nl | nl | nl | 0.17 | |
| | | TSSK3 TSSK4, SSTK | nl | 4 r 0 r | nl | nl | >10 | nl | nl | nl | nl | nl | nl | |
| CK1 | CK1 | RLCK1 | nl | nl | nl | nl | >10 | nl | nl | nl | nl | nl | nl | |
| | | CK1 α /CSNK1A1 CSNK1A1L CK1 α 2 | nl | 100 v x (R); 120 v (S) 18 r | nl | nl | >10 | nl | >3.33 b | nl | <20ak | nl | nl | |
| CK1 | CK1 | CK1 β /CSNK1B CK1 δ | nl | nl | nl | nl | >10 | nl | nl | nl | nl | nl | nl | |
| | | CK1 ϵ /CSNK1D | nl | 17 f 47-50 f,i,r | 24 | nl | 0.26 | nl | 25 | <20ak | nl | nl | >10 | |

Oligo-specific

Pan-specific

| Group | Family | Kinase | Rosco | | | Purv A | | | Flavo | | | | |
|-------|------------------------------|------------------------------|-------------------------------------|-----------------------------|-------------------------------|----------------------------|--|---------------|-------------------------------|-------------------------------|---------------|---------------------------------------|--|
| | | | IC50, μ M | Inhibition at 10 μ M, % | Inhibition at 1 μ M, % ak | K _d , μ M t | K _d , μ M ^{nl} | IC50, μ M | Inhibition at 10 μ M, % f | Inhibition at 1 μ M, % ak | IC50, μ M | K _d , μ M ^t | K _d , μ M ^{nl} |
| CDKL | CLK | CDKL1, CDKL2, CDKL3, | <i>nt</i> | <i>nt</i> | <i>nt</i> | <i>nt</i> | <i>nt</i> | <i>nt</i> | <i>nt</i> | <i>nt</i> | <i>nt</i> | <i>nt</i> | |
| | | CLK1 | 35 r | <i>nt</i> | <i>nt</i> | 2.1 | 1.2 | <i>nt</i> | <i>nt</i> | <i>nt</i> | <i>nt</i> | 2.2 | 1.7 |
| CDC2L | CLK | CLK2 | 90 ^r | <i>nt</i> | <i>nt</i> | 0.47 | 0.7 | <i>nt</i> | <i>nt</i> | <i>nt</i> | <i>nt</i> | 1.4 | 2.2 |
| | | CLK3 | <i>nt</i> | <i>nt</i> | <i>nt</i> | >10 | >10 | <i>nt</i> | <i>nt</i> | <i>nt</i> | 7 | 1.6 | |
| | | CLK4 | <i>nt</i> | <i>nt</i> | <i>nt</i> | 4.5 | >10 | <i>nt</i> | <i>nt</i> | <i>nt</i> | >10 | >10 | |
| | | CDC2L1 | <i>nt</i> | <i>nt</i> | <i>nt</i> | >10 | >10 | <i>nt</i> | <i>nt</i> | <i>nt</i> | >10 | >10 | |
| DYRK | DYRK1A | CDC2L2 | <i>nt</i> | <i>nt</i> | <i>nt</i> | >10 | >10 | <i>nt</i> | <i>nt</i> | <i>nt</i> | <i>nt</i> | >10 | |
| | | DYRK1A | 85f | <20 | <i>nt</i> | <i>nt</i> | <i>nt</i> | 0.3 f | 94 | <20ak | <i>nt</i> | <i>nt</i> | |
| GSK | ASK- γ (plant GSK-3A) | DYRK1B | <i>nt</i> | <i>nt</i> | <i>nt</i> | 1.1 | <i>nt</i> | <i>nt</i> | <i>nt</i> | <i>nt</i> | <i>nt</i> | <i>nt</i> | |
| | | DYRK2 | <i>nt</i> | <20 | <i>nt</i> | <i>nt</i> | <i>nt</i> | <i>nt</i> | <i>nt</i> | <i>nt</i> | <i>nt</i> | 0.084 | |
| | | DYRK4 | 0 r | <20 | <i>nt</i> | <i>nt</i> | <i>nt</i> | <i>nt</i> | <i>nt</i> | <i>nt</i> | <i>nt</i> | <i>nt</i> | |
| | | DYRK3 | 0 r | <20 | <i>nt</i> | <i>nt</i> | <i>nt</i> | <i>nt</i> | <i>nt</i> | <i>nt</i> | <i>nt</i> | <i>nt</i> | |
| | | HIPK1, HIPK2, HIPK3 | <i>nt</i> | <i>nt</i> | <i>nt</i> | <i>nt</i> | <i>nt</i> | <i>nt</i> | <i>nt</i> | <i>nt</i> | <i>nt</i> | <i>nt</i> | |
| | | HIPK2 | <i>nt</i> | <20 | <i>nt</i> | <i>nt</i> | <i>nt</i> | <i>nt</i> | <i>nt</i> | <i>nt</i> | <i>nt</i> | <i>nt</i> | |
| | | HIPK3 | <i>nt</i> | <20 | <i>nt</i> | <i>nt</i> | <i>nt</i> | <i>nt</i> | <i>nt</i> | <i>nt</i> | <i>nt</i> | <i>nt</i> | |
| | | HIPK4, PRP4 | <i>nt</i> | <i>nt</i> | <i>nt</i> | <i>nt</i> | <i>nt</i> | <i>nt</i> | <i>nt</i> | <i>nt</i> | <i>nt</i> | <i>nt</i> | |
| | | ASK- γ (plant GSK-3A) | 220 c | <i>nt</i> | <i>nt</i> | <i>nt</i> | <i>nt</i> | <i>nt</i> | <i>nt</i> | <i>nt</i> | <i>nt</i> | <i>nt</i> | <i>nt</i> |
| | | GSK3A | <i>nt</i> | 24 r | <i>nt</i> | <i>nt</i> | <i>nt</i> | <i>nt</i> | <i>nt</i> | <i>nt</i> | <i>nt</i> | <i>nt</i> | 1.3 |
| MAPK | Erk2/3/6 | GSK3B | 130 g, 32.2 y | <20 f,n, 7 r | 24 | <i>nt</i> | >10 | >10 b, 13 g | <20 | 21ak | 0.45 g | <i>nt</i> | 0.73 |
| | | p44mpk | <i>nt</i> | <i>nt</i> | <i>nt</i> | <i>nt</i> | <i>nt</i> | <i>nt</i> | <i>nt</i> | <i>nt</i> | <i>nt</i> | <i>nt</i> | <i>nt</i> |
| | | GST-erk1 | 30 c | <i>nt</i> | <20 | <i>nt</i> | <i>nt</i> | <i>nt</i> | <i>nt</i> | <i>nt</i> | <i>nt</i> | <i>nt</i> | <i>nt</i> |
| | | His-tagged erk1 | <i>nt</i> | <i>nt</i> | <i>nt</i> | <i>nt</i> | <i>nt</i> | <i>nt</i> | <i>nt</i> | <i>nt</i> | <i>nt</i> | <i>nt</i> | <i>nt</i> |
| | | Erk1/3/6 | 34 c,h; 25 v (R); 16 v (S) | 14 r | <i>nt</i> | <i>nt</i> | <i>nt</i> | >10 | 9 b | <i>nt</i> | <i>nt</i> | <i>nt</i> | >10 |
| | | Erk2/3/6 | 14 c,h; 1.17 l; 20 v,x (R); 13v (S) | <20-45 f,n,r | <20 | <i>nt</i> | >10 | <i>nt</i> | <i>nt</i> | 74 | <20ak | <i>nt</i> | >10 |
| | | Erk3 | <i>nt</i> | <i>nt</i> | <i>nt</i> | <i>nt</i> | <i>nt</i> | >10 | <i>nt</i> | <i>nt</i> | <i>nt</i> | <i>nt</i> | >10 |
| | | Erk4 | <i>nt</i> | <i>nt</i> | <i>nt</i> | <i>nt</i> | <i>nt</i> | >10 | <i>nt</i> | <i>nt</i> | <i>nt</i> | <i>nt</i> | >10 |
| | | Erk5 | <i>nt</i> | <i>nt</i> | <i>nt</i> | <i>nt</i> | <i>nt</i> | >10 | <i>nt</i> | <i>nt</i> | <i>nt</i> | <i>nt</i> | >10 |
| | | Erk7 | <i>nt</i> | <i>nt</i> | <i>nt</i> | <i>nt</i> | <i>nt</i> | >10 | <i>nt</i> | <i>nt</i> | <i>nt</i> | <i>nt</i> | 0.62 |
| RCK | SRPK | Erk8 | <i>nt</i> | 60 | <i>nt</i> | <i>nt</i> | >10 | <i>nt</i> | <i>nt</i> | 30ak | <i>nt</i> | 0.33 | |
| | | JNK1/SAPK1c | <20 f,n | <20 | <20 | >10 | >10 | >1 b | <20 | <20ak | >10 | >10 | |
| | | JNK2 | <20 n | <20 | <20 | >10 | >10 | <i>nt</i> | <i>nt</i> | <20ak | >10 | >10 | |
| | | JNK3 | <i>nt</i> | <i>nt</i> | <i>nt</i> | >10 | >10 | <i>nt</i> | <i>nt</i> | <20ak | >10 | >10 | |
| | | NLK | <i>nt</i> | <i>nt</i> | <i>nt</i> | >10 | >10 | <i>nt</i> | <i>nt</i> | <i>nt</i> | >10 | >10 | |
| | | p38/SAPK2a/3/6/11 | <20 f,n, 14 r | <20 | <20 | >10 | >10 | <i>nt</i> | <i>nt</i> | <20ak | >10 | >10 | |
| | | p38 β /SAPK2b/3/6/11 | <20 f, 0 r | <20 | <20 | >10 | >10 | <i>nt</i> | <20 | <20ak | >10 | >10 | |
| | | p38 γ /SAPK3/6/11 | <20 f,n, 8 r | <20 | <20 | >10 | >10 | <i>nt</i> | <20 | <20ak | >10 | >10 | |
| | | p38 δ /SAPK4/6/11 | <20 f,n, 2 r | <20 | <20 | <i>nt</i> | <i>nt</i> | <i>nt</i> | <20 | <20ak | >10 | >10 | |
| | | MAK, ICK, MOK | <i>nt</i> | <i>nt</i> | <i>nt</i> | <i>nt</i> | <i>nt</i> | <i>nt</i> | <i>nt</i> | <i>nt</i> | <i>nt</i> | <i>nt</i> | <i>nt</i> |
| RGC | SRPK | SRPK1 | <i>nt</i> | <20 | <i>nt</i> | <i>nt</i> | >10 | <i>nt</i> | <i>nt</i> | <i>nt</i> | <i>nt</i> | >10 | |
| | | SRPK2 | 32 r | <i>nt</i> | <20 | <i>nt</i> | >10 | <i>nt</i> | <i>nt</i> | <i>nt</i> | <i>nt</i> | >10 | |
| | | MSSK1 | <i>nt</i> | <i>nt</i> | <i>nt</i> | <i>nt</i> | <i>nt</i> | <i>nt</i> | <i>nt</i> | <i>nt</i> | <i>nt</i> | <i>nt</i> | |
| | | ANPa, ANPb, CYGD, CYGF, HSER | <i>nt</i> | <i>nt</i> | <i>nt</i> | <i>nt</i> | <i>nt</i> | <i>nt</i> | <i>nt</i> | <i>nt</i> | <i>nt</i> | <i>nt</i> | <i>nt</i> |

Oligo-specific

Pan-specific

| Group | Family | Kinase | Rosco | | | Purv A | | | Flavo | | | |
|-------|--------|------------------|---------------|-----------------------------|-------------------------------|----------------------------|--|----------------------------|-------------------------------|-------------------------------|----------------------------|---------------------------------------|
| | | | IC50, μ M | Inhibition at 10 μ M, % | Inhibition at 1 μ M, % ak | K _d , μ M t | K _d , μ M ^{nl} | IC ₅₀ , μ M | Inhibition at 10 μ M, % f | Inhibition at 1 μ M, % ak | IC ₅₀ , μ M | K _d , μ M ^t |
| Alk | Alk | ALK | nt | 57 r | nt | nt | 2.3 | nt | nt | nt | nt | 0.67 |
| | | LTK | nt | nt | nt | >10 | >10 | nt | nt | nt | nt | 2.2 |
| Axl | Axl | AXL | nt | nt | nt | nt | >10 | nt | nt | nt | nt | nt |
| | | MER/MER/MERTK | nt | 14 r | nt | nt | >10 | nt | nt | nt | nt | 3.5 |
| CCK4 | CCK4 | TYRO3/JRSE | nt | 11 r | nt | nt | >10 | nt | nt | nt | nt | 6.8 |
| | | CCK4 | nt | nt | nt | nt | >10 | nt | nt | nt | nt | >10 |
| Csk | Csk | CTK/HL/MATK | nt | <20 f, 10 r | <20 | >10 | >10 | 80 | <20ak | nt | >10 | >10 |
| | | DDR1 | nt | 0 r | nt | nt | >10 | nt | nt | nt | nt | >10 |
| EGFR | EGFR | DDR2 | nt | nt | nt | nt | nt | nt | nt | nt | nt | nt |
| | | EGFR/ErbB1 | nt | 8 r | nt | >10 | >10 | nt | nt | nt | nt | >10 |
| Eph | Eph | HER2/ErbB2 | nt | 0 r | nt | >10 | >10 | nt | nt | nt | nt | >10 |
| | | HER3/ErbB3 | nt | nt | nt | nt | nt | nt | nt | nt | nt | nt |
| Eph | Eph | HER4/ErbB4 | nt | 8 r | nt | nt | >10 | nt | nt | nt | nt | >10 |
| | | EphA1 | nt | 0 r | nt | nt | >10 | nt | nt | nt | nt | >10 |
| Eph | Eph | EphA2 | nt | 8 r | nt | nt | >10 | nt | nt | nt | nt | >10 |
| | | EphA3 | nt | 12 r | nt | nt | >10 | nt | nt | nt | nt | >10 |
| Eph | Eph | EphA4 | nt | 19 r | nt | nt | >10 | nt | nt | nt | nt | >10 |
| | | EphA5 | nt | 0 r | nt | nt | >10 | nt | nt | nt | nt | 2.5 |
| Eph | Eph | EphA8 | nt | 0 r | nt | nt | >10 | nt | nt | nt | nt | 3.3 |
| | | EphB1 | nt | 9 r | nt | nt | >10 | nt | nt | nt | nt | >10 |
| Eph | Eph | EphB2 | nt | 14 r | nt | nt | >10 | nt | nt | nt | nt | >10 |
| | | EphB3 | nt | 16 r | nt | nt | >10 | nt | nt | nt | nt | >10 |
| Eph | Eph | EphB4 | nt | 15 r | nt | nt | >10 | nt | nt | nt | nt | >10 |
| | | EphB6 | nt | 7 r | nt | nt | >10 | nt | nt | nt | nt | >10 |
| Eph | Eph | EphA7 | nt | 6 r | nt | nt | >10 | nt | nt | nt | nt | >10 |
| | | EphA10 | nt | 4 r | nt | nt | >10 | nt | nt | nt | nt | >10 |
| Fak | Fak | EphA6 | nt | nt | nt | nt | nt | nt | nt | nt | nt | nt |
| | | FAK/PTK2 | nt | nt | nt | nt | nt | nt | nt | nt | nt | nt |
| Fer | Fer | FAK2/PTK2B/PYK2 | nt | nt | nt | nt | nt | nt | nt | nt | nt | nt |
| | | FER | nt | 12 r | nt | nt | >10 | nt | nt | nt | nt | >10 |
| FGFR | FGFR | FES/FPS | nt | 16 r | nt | nt | >10 | nt | nt | nt | nt | >10 |
| | | FGFR1 | nt | 39 r | nt | nt | >10 | nt | nt | nt | nt | >10 |
| FGFR | FGFR | FGFR2 | nt | 6 r | nt | nt | >10 | nt | nt | nt | nt | >10 |
| | | FGFR3 | nt | 10 r | nt | nt | >10 | nt | nt | nt | nt | >10 |
| InsR | InsR | FGFR4 | nt | 13 r | nt | nt | >10 | nt | nt | nt | nt | >10 |
| | | IGF1R | nt | 0 r | nt | nt | >10 | nt | nt | nt | nt | >10 |
| InsR | InsR | INSR | nt | 13 r | nt | nt | >10 | nt | nt | nt | nt | >10 |
| | | IRR/INSRR | nt | 17 r | nt | nt | >10 | nt | nt | nt | nt | >10 |
| JAKA | JAKA | JAK1 | 70 c | 16 r | nt | nt | >10 | 5 b | nt | nt | >10 | |
| | | JAK2 | nt | 0 r | nt | nt | >10 | nt | nt | nt | >10 | |
| JAKA | JAKA | JAK3 | nt | 13 r | nt | nt | >10 | nt | nt | nt | >10 | |
| | | TYK2 | nt | nt | nt | nt | >10 | nt | nt | nt | >10 | |
| Lmr | Lmr | LMR1, LMR2, LMR3 | nt | nt | nt | nt | nt | nt | nt | nt | nt | >10 |
| | | MET/cMET | nt | 12 r | nt | nt | >10 | nt | nt | nt | nt | >10 |
| Met | Met | RON/MST1R | nt | 42 r | nt | nt | >10 | nt | nt | nt | nt | >10 |
| | | MUSK | nt | 20 r | nt | nt | >10 | nt | nt | nt | nt | >10 |

Oligo-specific **Pan-specific**

| Group | Family | Kinase | Rosco | | | Purv A | | | Flavo | | | | | |
|-------|--------|-----------------------|---------------|-----------------------------|-------------------------------|----------------------------|--|---------------|-------------------------------|-------------------------------|---------------|---------------------------------------|--|----|
| | | | IC50, μ M | Inhibition at 10 μ M, % | Inhibition at 1 μ M, % ak | K _d , μ M t | K _d , μ M ^{nl} | IC50, μ M | Inhibition at 10 μ M, % f | Inhibition at 1 μ M, % ak | IC50, μ M | K _d , μ M ^t | K _d , μ M ^{nl} | |
| PDGFR | | FMS | nt | 2 r | nt | >10 | nt | nt | >10 | nt | nt | >10 | nt | |
| | | FLT3 | nt | 16 r | nt | >10 | nt | nt | >10 | nt | nt | >10 | nt | |
| | | KIT | nt | 7 r | nt | >10 | nt | nt | >10 | nt | nt | >10 | nt | |
| | | PDGFR α | nt | 6 r | nt | >10 | nt | nt | >10 | nt | nt | >10 | nt | |
| | | PDGFR β | nt | 6 r | nt | >10 | nt | nt | >10 | nt | nt | >10 | nt | |
| | | RET | nt | 0 r | nt | >10 | nt | nt | >10 | nt | nt | >10 | nt | |
| | | ROR1, ROR2 | nt | nt | nt | nt | nt | nt | nt | nt | nt | nt | nt | nt |
| | | Ryk | nt | nt | nt | nt | nt | nt | nt | nt | nt | nt | nt | nt |
| | | Sev | nt | nt | nt | nt | nt | nt | nt | nt | nt | nt | nt | nt |
| | | Src | nt | nt | nt | nt | nt | nt | nt | nt | nt | nt | nt | nt |
| | | BRK/PTK6 | >100 e | 0 r | nt | >10 | nt | nt | >10 | nt | nt | >10 | nt | |
| | | FGR/p55fgR/TPK-III/Q1 | nt | 4 r | nt | >10 | nt | nt | >10 | nt | nt | >10 | nt | |
| | | LCK/p56lck | nt | 7 r | nt | >10 | nt | nt | >10 | nt | nt | >10 | nt | |
| | | LYN/p56lyn/TPK-IIIa | nt | 3 r | nt | >10 | nt | nt | >10 | nt | nt | >10 | nt | |
| | | SRC/c-src | nt | 10 r | 24 | >10 | nt | nt | >10 | nt | nt | >10 | nt | |
| | | YES/YES1 | nt | 10-30 f,n,r | 24 | >10 | nt | nt | >10 | nt | nt | >10 | nt | |
| | | FRK/PTK5 | 250c | 11 r | nt | >10 | nt | nt | >10 | nt | nt | >10 | nt | |
| | | SRM | nt | <20 n, 11 r | <20 | >10 | nt | nt | >10 | nt | nt | >10 | nt | |
| | | SYK | nt | 7 r | nt | >10 | nt | nt | >10 | nt | nt | >10 | nt | |
| | | ZAP70 | nt | 4 r | nt | >10 | nt | nt | >10 | nt | nt | >10 | nt | |
| | | BTK | nt | 3 r | nt | >10 | nt | nt | >10 | nt | nt | >10 | nt | |
| | | ITK | nt | 21 r | nt | >10 | nt | nt | >10 | nt | nt | >10 | nt | |
| | | TEC | nt | 12 r | nt | >10 | nt | nt | >10 | nt | nt | >10 | nt | |
| | | TXK | nt | 0 r | nt | >10 | nt | nt | >10 | nt | nt | >10 | nt | |
| | | BMX | nt | 8 r | nt | >10 | nt | nt | >10 | nt | nt | >10 | nt | |
| | | TIE2/TEK | nt | nt | nt | >10 | nt | nt | >10 | nt | nt | >10 | nt | |
| | | TIE1 | nt | 0 r | nt | >10 | nt | nt | >10 | nt | nt | >10 | nt | |
| | | SuRTK106 | nt | 9 r | nt | >10 | nt | nt | >10 | nt | nt | >10 | nt | |
| | | TRK/NTRK1 | nt | nt | nt | >10 | nt | nt | >10 | nt | nt | >10 | nt | |
| | | TRK/NTRK2 | nt | 5 r | nt | >10 | nt | nt | >10 | nt | nt | >10 | nt | |
| | | TRK/NTRK3 | nt | 13 r | nt | >10 | nt | nt | >10 | nt | nt | >10 | nt | |
| | | FLT1/VEGFR1 | nt | 5 r | nt | >10 | nt | nt | >10 | nt | nt | >10 | nt | |
| | | FLT4/VEGFR3 | nt | 10 r | nt | >10 | nt | nt | >10 | nt | nt | >10 | nt | |
| | | KDR/VEGFR2 | nt | 9 r | nt | >10 | nt | nt | >10 | nt | nt | >10 | nt | |
| | | IRAK1, IRAK2 | nt | 14 r | nt | >10 | nt | nt | >10 | nt | nt | >10 | nt | |
| | | IRAK3 | nt | nt | nt | >10 | nt | nt | >10 | nt | nt | >10 | nt | |
| | | IRAK4 | nt | nt | nt | >10 | nt | nt | >10 | nt | nt | >10 | nt | |
| | | LIMK1 | nt | 27 t | nt | >10 | nt | nt | >10 | nt | nt | >10 | nt | |
| | | LIMK2 | nt | nt | nt | >10 | nt | nt | >10 | nt | nt | >10 | nt | |
| | | TESK1 | nt | nt | nt | >10 | nt | nt | >10 | nt | nt | >10 | nt | |
| | | TESK2 | nt | nt | nt | >10 | nt | nt | >10 | nt | nt | >10 | nt | |
| | | LRRK1, LRRK2 | nt | nt | nt | >10 | nt | nt | >10 | nt | nt | >10 | nt | |
| | | DLK | nt | nt | nt | >10 | nt | nt | >10 | nt | nt | >10 | nt | |
| | | HH498, ILK, LZK | nt | nt | nt | >10 | nt | nt | >10 | nt | nt | >10 | nt | |
| | | MLK1/MAP3K9 | nt | nt | nt | >10 | nt | nt | >10 | nt | nt | >10 | nt | |
| | | | nt | 7 r | nt | >10 | nt | nt | >10 | nt | nt | >10 | nt | |
| | | | nt | nt | nt | >10 | nt | nt | >10 | nt | nt | >10 | nt | |
| | | | nt | nt | nt | >10 | nt | nt | >10 | nt | nt | >10 | nt | |
| | | | nt | nt | nt | >10 | nt | nt | >10 | nt | nt | >10 | nt | |
| | | | nt | nt | nt | >10 | nt | nt | >10 | nt | nt | >10 | nt | |

Oligo-specific

Pan-specific

| Group | Family | Kinase | Rosco | | | Purv A | | | Flavo | | | | | | |
|----------|------------|---|---|-----------------------------|-------------------------------|----------------------------|--|----------------------------|-------------------------------|-------------------------------|----------------------------|---------------------------------------|--|-----|----|
| | | | IC50, μ M | Inhibition at 10 μ M, % | Inhibition at 1 μ M, % ak | K _d , μ M t | K _d , μ M ^{nl} | IC ₅₀ , μ M | Inhibition at 10 μ M, % f | Inhibition at 1 μ M, % ak | IC ₅₀ , μ M | K _d , μ M ^t | K _d , μ M ^{nl} | | |
| Atypical | TKL-Unique | MLKL | MLK2 | nt | nt | nt | >10 | nt | nt | nt | nt | nt | 5.2 | | |
| | | | MLK3 | nt | nt | nt | >10 | nt | nt | nt | nt | nt | >10 | | |
| | | | MLK4, TAK1 | nt | nt | nt | nt | nt | nt | nt | nt | nt | nt | nt | |
| | | | ZAK | nt | nt | nt | >10 | nt | nt | nt | nt | nt | nt | >10 | |
| | | | cRAF/RAF1 | nt | <20 n, 41 r | nt | >10 | >1 b | nt | nt | nt | nt | nt | >10 | |
| | | | ARAF | nt | nt | nt | nt | nt | nt | nt | nt | nt | nt | nt | |
| | | | BRAF | nt | 39 r | nt | nt | nt | nt | nt | nt | nt | nt | nt | |
| | | | KSR1, KSR2 | nt | nt | nt | nt | nt | nt | nt | nt | nt | nt | nt | |
| | | | RIPK1 | nt | nt | nt | >10 | nt | nt | nt | nt | nt | nt | >10 | |
| | | | RIPK2 | nt | nt | nt | >10 | nt | nt | nt | nt | nt | nt | >10 | |
| STKR | | RIPK3, ANKRD3, Sgk288 | nt | nt | nt | nt | nt | nt | nt | nt | nt | nt | nt | | |
| | | ALK1, ALK2, ALK7 | nt | nt | nt | nt | nt | nt | nt | nt | nt | nt | nt | | |
| | | ALK4 | nt | 4 r | nt | nt | nt | nt | nt | nt | nt | nt | nt | | |
| | | BMPR1A, BMPR1B, BMPR2, MISR2 | nt | nt | nt | nt | nt | nt | nt | nt | nt | nt | nt | | |
| Other | | ADCK3 ADCK4 EF2K RIOK1 RIOK3 BUBR1, BUB1, PRPK/BUD32/pid261, Haspin, IKK α , IRE1, IRE2, MOS, NEK3, NEK4, NEK8, NEK10, NEK11, Sgk069, Sgk110, SBK, PINK1, Sgk223, Sgk269, CLIK1L, CLIK1, Sgk307, Sgk424, NRBP1, NRBP2, Sgk483, Sgk496, Sgk071, Sgk196, Sgk396, KIS, RNAsel, PEK, PKR, HRI, SCYL1, SCYL2, SCYL3, Siob, TBCK, PBK, ULK1, ULK2, ULK4, PIK3R4, Wee1B, Wnk1, Wnk2, Wnk3, Wnk4 | ADCK3 | nt | nt | nt | >10 | nt | nt | nt | nt | nt | >10 | | |
| | | | ADCK4 | nt | nt | nt | >10 | nt | nt | nt | nt | nt | >10 | | |
| | | | EF2K | nt | nt | <20 | nt | nt | nt | <20ak | nt | nt | nt | nt | |
| | | | RIOK1 | nt | nt | nt | >10 | nt | nt | nt | nt | nt | nt | >10 | |
| | | | RIOK3 | nt | nt | nt | >10 | nt | nt | nt | nt | nt | nt | >10 | |
| | | | BUBR1, BUB1, PRPK/BUD32/pid261, Haspin, IKK α , IRE1, IRE2, MOS, NEK3, NEK4, NEK8, NEK10, NEK11, Sgk069, Sgk110, SBK, PINK1, Sgk223, Sgk269, CLIK1L, CLIK1, Sgk307, Sgk424, NRBP1, NRBP2, Sgk483, Sgk496, Sgk071, Sgk196, Sgk396, KIS, RNAsel, PEK, PKR, HRI, SCYL1, SCYL2, SCYL3, Siob, TBCK, PBK, ULK1, ULK2, ULK4, PIK3R4, Wee1B, Wnk1, Wnk2, Wnk3, Wnk4 | nt | nt | nt | nt | nt | nt | nt | nt | nt | nt | nt | nt |
| | | | BUBR1, BUB1, PRPK/BUD32/pid261, Haspin, IKK α , IRE1, IRE2, MOS, NEK3, NEK4, NEK8, NEK10, NEK11, Sgk069, Sgk110, SBK, PINK1, Sgk223, Sgk269, CLIK1L, CLIK1, Sgk307, Sgk424, NRBP1, NRBP2, Sgk483, Sgk496, Sgk071, Sgk196, Sgk396, KIS, RNAsel, PEK, PKR, HRI, SCYL1, SCYL2, SCYL3, Siob, TBCK, PBK, ULK1, ULK2, ULK4, PIK3R4, Wee1B, Wnk1, Wnk2, Wnk3, Wnk4 | nt | nt | nt | nt | nt | nt | nt | nt | nt | nt | nt | nt |
| | | | BUBR1, BUB1, PRPK/BUD32/pid261, Haspin, IKK α , IRE1, IRE2, MOS, NEK3, NEK4, NEK8, NEK10, NEK11, Sgk069, Sgk110, SBK, PINK1, Sgk223, Sgk269, CLIK1L, CLIK1, Sgk307, Sgk424, NRBP1, NRBP2, Sgk483, Sgk496, Sgk071, Sgk196, Sgk396, KIS, RNAsel, PEK, PKR, HRI, SCYL1, SCYL2, SCYL3, Siob, TBCK, PBK, ULK1, ULK2, ULK4, PIK3R4, Wee1B, Wnk1, Wnk2, Wnk3, Wnk4 | nt | nt | nt | nt | nt | nt | nt | nt | nt | nt | nt | nt |
| | | | BUBR1, BUB1, PRPK/BUD32/pid261, Haspin, IKK α , IRE1, IRE2, MOS, NEK3, NEK4, NEK8, NEK10, NEK11, Sgk069, Sgk110, SBK, PINK1, Sgk223, Sgk269, CLIK1L, CLIK1, Sgk307, Sgk424, NRBP1, NRBP2, Sgk483, Sgk496, Sgk071, Sgk196, Sgk396, KIS, RNAsel, PEK, PKR, HRI, SCYL1, SCYL2, SCYL3, Siob, TBCK, PBK, ULK1, ULK2, ULK4, PIK3R4, Wee1B, Wnk1, Wnk2, Wnk3, Wnk4 | nt | nt | nt | nt | nt | nt | nt | nt | nt | nt | nt | nt |
| | | | BUBR1, BUB1, PRPK/BUD32/pid261, Haspin, IKK α , IRE1, IRE2, MOS, NEK3, NEK4, NEK8, NEK10, NEK11, Sgk069, Sgk110, SBK, PINK1, Sgk223, Sgk269, CLIK1L, CLIK1, Sgk307, Sgk424, NRBP1, NRBP2, Sgk483, Sgk496, Sgk071, Sgk196, Sgk396, KIS, RNAsel, PEK, PKR, HRI, SCYL1, SCYL2, SCYL3, Siob, TBCK, PBK, ULK1, ULK2, ULK4, PIK3R4, Wee1B, Wnk1, Wnk2, Wnk3, Wnk4 | nt | nt | nt | nt | nt | nt | nt | nt | nt | nt | nt | nt |

| Group | Family | Kinase | Rosco | | | | Purv A | | | | Flavo | | | |
|---------------|--------|---------------------------------------|---------------------|------------------------------------|--------------------------------------|----------------------------------|--|---------------------|--------------------------------------|--------------------------------------|---------------------|---|--|--|
| | | | IC50, μM | Inhibition at 10 μM , % | Inhibition at 1 μM , % ak | K _d , μM t | K _d , μM ^{nl} | IC50, μM | Inhibition at 10 μM , % f | Inhibition at 1 μM , % ak | IC50, μM | K _d , μM ^t | K _d , μM ^{nl} | |
| | | AurC/AURKC/AuroraC/AIEZ/STK13 | >100e | nt | <20 | >10 | >10 | nt | <20ak | nt | >10 | >10 | | |
| | | AurB/AURKB/AuroraB/STK12/STK5 | >100e | 0 r | <20 | nt | >10 | nt | <20ak | nt | nt | >10 | | |
| | | Aur/AURKA/Aurora2/STK6/STK15 | 600b, >100e | 0 r | nt | >10 | >10 | nt | nt | nt | >10 | >10 | | |
| | | CaMKK2 | nt | nt | 29 | >10 | nt | nt | 40ak | nt | 0.32 | 0.43 | | |
| | | CaMKK1 | nt | nt | 27 | >10 | nt | nt | 24ak | nt | 0.019 | 0.079 | | |
| | | CARK/TNNI3K | nt | nt | nt | nt | >10 | nt | nt | nt | nt | 0.055 | | |
| | | CDC7/DBF4 | >1000 m | nt | nt | nt | nt | nt | nt | nt | nt | nt | | |
| | | CIT | nt | nt | nt | >10 | >10 | nt | nt | nt | nt | >10 | | |
| | | CK2 | nt | <20 f, n | <20 | nt | >10 b | <20 | <20ak | nt | nt | >10 | | |
| | | CK2 α 1/CSNK2A1 | >1000 c | 3 r | nt | >10 | >10 | nt | nt | nt | nt | >10 | | |
| | | CK2 α 2/CSNK2A2 | nt | 0 r | nt | >10 | >10 | nt | nt | nt | nt | >10 | | |
| | | CSF1R | nt | nt | nt | >10 | >10 | nt | nt | nt | nt | 2.8 | | |
| | | IKK β /IKKB | nt | 0 r | 20 | nt | nt | nt | <20ak | nt | nt | nt | | |
| | | TBK1 | nt | 1 r | nt | nt | nt | nt | nt | nt | nt | nt | | |
| | | GAK | nt | nt | nt | >10 | >10 | nt | nt | nt | 1.1 | 0.37 | | |
| | | GCN2 (Kin. Dom. S808G) | nt | nt | nt | >10 | >10 | nt | nt | nt | >10 | >10 | | |
| | | AAK1 | nt | nt | nt | >10 | >10 | nt | nt | nt | >10 | 5.3 | | |
| | | IKK ϵ | nt | nt | nt | >10 | >10 | nt | nt | nt | >10 | 3.1 | | |
| | | MPSK1/STK16 | nt | nt | nt | >10 | >10 | nt | nt | nt | >10 | >10 | | |
| | | BIKE | nt | nt | nt | >10 | >10 | nt | nt | nt | >10 | >10 | | |
| | | NEK1 | nt | 0 r | nt | >10 | >10 | nt | nt | nt | >10 | >10 | | |
| | | NEK2 | nt | 0 r | <20 | >10 | >10 | nt | <20ak | nt | >10 | >10 | | |
| | | NEK5 | nt | nt | nt | >10 | >10 | nt | nt | nt | >10 | >10 | | |
| | | NEK6 | nt | nt | <20 | >10 | >10 | nt | <20ak | nt | >10 | >10 | | |
| | | NEK7 | nt | nt | <20 | >10 | >10 | nt | <20ak | nt | >10 | >10 | | |
| | | NEK9 | nt | nt | nt | >10 | >10 | nt | nt | nt | >10 | >10 | | |
| | | PKR | nt | nt | nt | >10 | >10 | nt | nt | nt | >10 | 5.2 | | |
| | | PLK1 | nt | 9 r | <20 | >10 | >10 | nt | <20ak | nt | >10 | >10 | | |
| | | PLK3 | nt | 3 r | nt | >10 | >10 | nt | nt | nt | >10 | >10 | | |
| | | PLK4/STK18/SAK | nt | nt | nt | >10 | >10 | nt | nt | nt | 3.1 | >10 | | |
| | | PLK2 | nt | 2 r | nt | nt | nt | nt | nt | nt | nt | >10 | | |
| | | TGFBR1 | nt | nt | nt | >10 | >10 | nt | nt | nt | nt | >10 | | |
| | | TGFBR2 | nt | nt | nt | >10 | >10 | nt | nt | nt | nt | 5.6 | | |
| | | TLK1 | nt | nt | nt | >10 | >10 | nt | nt | nt | nt | >10 | | |
| | | TLK2 | nt | nt | nt | >10 | >10 | nt | nt | nt | nt | >10 | | |
| | | TTK | nt | nt | nt | >10 | 1.6 | nt | nt | nt | >10 | >10 | | |
| | | dnmFused/hsSTK36 | nt | nt | nt | >10 | 2.1 | nt | nt | nt | >10 | >10 | | |
| | | ULK3 | nt | nt | nt | >10 | >10 | nt | nt | nt | >10 | >10 | | |
| | | MYT1/PKMYT1 | nt | 47 a | nt | >10 | >10 | nt | nt | nt | >10 | >10 | | |
| | | Wee1 | nt | 0 a | nt | nt | nt | nt | nt | nt | nt | >10 | | |
| Other kinases | | Nucleotide diphosphate kinase/NDPK | nt | nt | nt | nt | nt | nt | nt | nt | nt | nt | | |
| | | Phosphoinositide 3-kinase/PI3K/PIK3CA | >50 s | nt | nt | >10 | >10 | nt | nt | nt | nt | >10 | | |

| Group | Family | Kinase | Oligo-specific | | | | Pan-specific | | | |
|--|---|-------------------------|---|--|---|--|---|--|---|--|
| | | | Rosco | Purv A | Flavo | Rosco | Purv A | Flavo | | |
| Viral kinases | | PIP5K1A | IC50, μM <i>nt</i> | Inhibition at 10 μM , % <i>nt</i> | K _d , μM t <i>nt</i> | K _d , μM m ^l >10 | IC ₅₀ , μM <i>nt</i> | Inhibition at 10 μM , % f <i>nt</i> | K _d , μM t <i>nt</i> | K _d , μM m ^l >10 |
| | | PIP5K2B | <i>nt</i> | <i>nt</i> | <i>nt</i> | >10 | <i>nt</i> | <i>nt</i> | <i>nt</i> | <i>nt</i> |
| | | Pyridoxal Kinase/PDXK | binds v,x >26 aa | <i>nt</i> | <i>nt</i> | <i>nt</i> | <i>nt</i> | <i>nt</i> | <i>nt</i> | <i>nt</i> |
| | | HSV-1 UL13 VZV ORF47 | not inhibited ak | <i>nt</i> | <i>nt</i> | <i>nt</i> | <i>nt</i> | <i>nt</i> | <i>nt</i> | <i>nt</i> |
| | Multidrug resistance protein 1/MRP-1 | <i>nt</i> | <i>nt</i> | <i>nt</i> | <i>nt</i> | <i>nt</i> | <i>nt</i> | activated ag | <i>nt</i> | <i>nt</i> |
| | Glycogen Phosphorylase a/Gpa | <i>nt</i> | <i>nt</i> | <i>nt</i> | <i>nt</i> | <i>nt</i> | <i>nt</i> | 2.5 ad | <i>nt</i> | <i>nt</i> |
| | Glycogen Phosphorylase b/GPb | <i>nt</i> | <i>nt</i> | <i>nt</i> | <i>nt</i> | <i>nt</i> | <i>nt</i> | 1 ad, 15.5 ae | <i>nt</i> | <i>nt</i> |
| | Aldehyde Dehydrogenase/ALDH | <i>nt</i> | <i>nt</i> | <i>nt</i> | <i>nt</i> | <i>nt</i> | <i>nt</i> | binds but no inhibition af | <i>nt</i> | <i>nt</i> |
| Other molecule | | Duplex DNA | <i>nt</i> | <i>nt</i> | <i>nt</i> | <i>nt</i> | <i>nt</i> | binds ah | <i>nt</i> | <i>nt</i> |
| Rosco; Roscovitine; Purv A, Purvalanol A; Flavo, Flavopiridol | | | | | | | | | | |
| Rosco | | | IC ₅₀ \geq 7 μM ; % inhibition <80; K _d >7 μM | | | | | | | |
| | | | 3.5 μM IC ₅₀ <7 μM ; 80% % inhibition <93; 3.5 μM K _d <7 μM | | | | | | | |
| | | | 0.7 μM IC ₅₀ <3.5 μM ; % inhibition \geq 93; 0.7 μM K _d <3.5 μM | | | | | | | |
| Purv A | | | IC ₅₀ \geq 0.7 μM ; % inhibition <80 | | | | | | | |
| | | | 0.35 μM IC ₅₀ <0.7 μM ; 80% % inhibition <93 | | | | | | | |
| | | | 0.07 μM IC ₅₀ <0.35 μM ; % inhibition \geq 93 | | | | | | | |
| Flavo | | | IC ₅₀ >1 μM ; K _d >1 μM | | | | | | | |
| | | | 0.5 μM IC ₅₀ <1 μM ; 0.5 μM K _d <1 μM | | | | | | | |
| | | | 0.1 μM IC ₅₀ <0.5 μM ; 0.1 μM K _d <0.5 μM | | | | | | | |

References

- Agbottah, E., C. de La Fuente, et al. (2005). "Antiviral activity of CYC202 in HIV-1-infected cells." *J Biol Chem* **280**(4): 3029-42.
- Bach, S., M. Knockaert, et al. (2005). "Roscovitine targets, protein kinases and pyridoxal kinase." *J Biol Chem* **280**(35): 31208-19.
- Bain, J., H. McLauchlan, et al. (2003). "The specificities of protein kinase inhibitors: an update." *Biochem J* **371**(Pt 1): 199-204.
- Bain, J., L. Plater, et al. (2007). "The selectivity of protein kinase inhibitors: a further update." *Biochem J* **408**(3): 297-315.
- Bible, K. C., R. H. Bible, Jr., et al. (2000). "Flavopiridol binds to duplex DNA." *Cancer Res* **60**(9): 2419-28.
- Caligiuri, M., F. Becker, et al. (2005). "A proteome-wide CDK/CRK-specific kinase inhibitor promotes tumor cell death in the absence of cell cycle progression." *Chem Biol* **12**(10): 1103-15.
- Carlson, B. A., M. M. Dubay, et al. (1996). "Flavopiridol induces G1 arrest with inhibition of cyclin-dependent kinase (CDK) 2 and CDK4 in human breast carcinoma cells." *Cancer Res* **56**(13): 2973-8.
- Chao, S. H., K. Fujinaga, et al. (2000). "Flavopiridol inhibits P-TEFb and blocks HIV-1 replication." *J Biol Chem* **275**(37): 28345-8.
- De Azevedo, W. F., S. Leclerc, et al. (1997). "Inhibition of cyclin-dependent kinases by purine analogues: crystal structure of human cdk2 complexed with roscovitine." *Eur J Biochem* **243**(1-2): 518-26.
- Fabian, M. A., W. H. Biggs, 3rd, et al. (2005). "A small molecule-kinase interaction map for clinical kinase inhibitors." *Nat Biotechnol* **23**(3): 329-36.
- Gray, N. S., L. Wodicka, et al. (1998). "Exploiting chemical libraries, structure, and genomics in the search for kinase inhibitors." *Science* **281**(5376): 533-8.
- Heredia, A., C. Davis, et al. (2005). "Indirubin-3'-monoxime, a derivative of a Chinese antileukemia medicine, inhibits P-TEFb function and HIV-1 replication." *Aids* **19**(18): 2087-95.
- Hoessel, R., S. Leclerc, et al. (1999). "Indirubin, the active constituent of a Chinese antileukaemia medicine, inhibits cyclin-dependent kinases." *Nat Cell Biol* **1**(1): 60-7.
- Hooijberg, J. H., H. J. Broxterman, et al. (1999). "Potent interaction of flavopiridol with MRP1." *Br J Cancer* **81**(2): 269-76.
- Kaiser, A., K. Nishi, et al. (2001). "The cyclin-dependent kinase (CDK) inhibitor flavopiridol inhibits glycogen phosphorylase." *Arch Biochem Biophys* **386**(2): 179-87.
- Karaman, M. W., S. Herrgard, et al. (2008). "A quantitative analysis of kinase inhibitor selectivity." *Nat Biotechnol* **26**(1): 127-32.
- Kawaguchi, Y., K. Kato, et al. (2003). "Conserved protein kinases encoded by herpesviruses and cellular protein kinase cdc2 target the same

- phosphorylation site in eukaryotic elongation factor 1delta." J Virol **77**(4): 2359-68.
- Knockaert, M., N. Gray, et al. (2000). "Intracellular targets of cyclin-dependent kinase inhibitors: identification by affinity chromatography using immobilised inhibitors." Chem Biol **7**(6): 411-22.
- Knockaert, M. and L. Meijer (2002). "Identifying in vivo targets of cyclin-dependent kinase inhibitors by affinity chromatography." Biochem Pharmacol **64**(5-6): 819-25.
- Kristjansdottir, K. and J. Rudolph (2003). "A fluorescence polarization assay for native protein substrates of kinases." Anal Biochem **316**(1): 41-9.
- Leclerc, S., M. Garnier, et al. (2001). "Indirubins inhibit glycogen synthase kinase-3 beta and CDK5/p25, two protein kinases involved in abnormal tau phosphorylation in Alzheimer's disease. A property common to most cyclin-dependent kinase inhibitors?" J Biol Chem **276**(1): 251-60.
- Losiewicz, M. D., B. A. Carlson, et al. (1994). "Potent inhibition of CDC2 kinase activity by the flavonoid L86-8275." Biochem Biophys Res Commun **201**(2): 589-95.
- McClue, S. J., D. Blake, et al. (2002). "In vitro and in vivo antitumor properties of the cyclin dependent kinase inhibitor CYC202 (R-roscovitine)." Int J Cancer **102**(5): 463-8.
- Meijer, L., A. Borgne, et al. (1997). "Biochemical and cellular effects of roscovitine, a potent and selective inhibitor of the cyclin-dependent kinases cdc2, cdk2 and cdk5." Eur J Biochem **243**(1-2): 527-36.
- Oikonomakos, N. G., J. B. Schnier, et al. (2000). "Flavopiridol inhibits glycogen phosphorylase by binding at the inhibitor site." J Biol Chem **275**(44): 34566-73.
- Pinhero, R., P. Liaw, et al. (2004). "A uniform procedure for the purification of CDK7/CycH/MAT1, CDK8/CycC and CDK9/CycT1." Biol Proced Online **6**: 163-172.
- Schang, L. M., A. Bantly, et al. (2002). "Pharmacological cyclin-dependent kinase inhibitors inhibit replication of wild-type and drug-resistant strains of herpes simplex virus and human immunodeficiency virus type 1 by targeting cellular, not viral, proteins." J Virol **76**(15): 7874-82.
- Schang, L. M., M. R. St Vincent, et al. (2006). "Five years of progress on cyclin-dependent kinases and other cellular proteins as potential targets for antiviral drugs." Antivir Chem Chemother **17**(6): 293-320.
- Schnier, J. B., G. Kaur, et al. (1999). "Identification of cytosolic aldehyde dehydrogenase 1 from non-small cell lung carcinomas as a flavopiridol-binding protein." FEBS Lett **454**(1-2): 100-4.
- Senderowicz, A. M. and E. A. Sausville (2000). "Preclinical and clinical development of cyclin-dependent kinase modulators." J Natl Cancer Inst **92**(5): 376-87.
- Tang, L., M. H. Li, et al. (2005). "Crystal structure of pyridoxal kinase in complex with roscovitine and derivatives." J Biol Chem **280**(35): 31220-9.
- Vesely, J., L. Havlicek, et al. (1994). "Inhibition of cyclin-dependent kinases by purine analogues." Eur J Biochem **224**(2): 771-86.

- Wang, D., C. de la Fuente, et al. (2001). "Inhibition of human immunodeficiency virus type 1 transcription by chemical cyclin-dependent kinase inhibitors." J Virol **75**(16): 7266-79.
- Whittaker, S. R., M. I. Walton, et al. (2004). "The Cyclin-dependent kinase inhibitor CYC202 (R-roscovitine) inhibits retinoblastoma protein phosphorylation, causes loss of Cyclin D1, and activates the mitogen-activated protein kinase pathway." Cancer Res **64**(1): 262-72.
- Xie, Y., Y. Liu, et al. (2004). "Indirubin-3'-oxime inhibits c-Jun NH2-terminal kinase: anti-apoptotic effect in cerebellar granule neurons." Neurosci Lett **367**(3): 355-9.
- Zhou, M., L. Deng, et al. (2004). "Coordination of transcription factor phosphorylation and histone methylation by the P-TEFb kinase during human immunodeficiency virus type 1 transcription." J Virol **78**(24): 13522-33.